Tectonic Variation and Structural Evolution of the West Greenland Continental Margin

Sulaiman Lafi Alsulami

Submitted in accordance with the requirements for the degree of
Degree of Philosophy

The University of Leeds
School of Earth and Environment

November, 2014

Declaration

I confirm that this study submitted is my own and that appropriate credit was given where reference has been made to the work of others.

Acknowledgements

I thank Allah for a successful completion of the PhD. A special thanks to my family. Words cannot express how grateful I am to my mum, wife and children (Rayan and Renad) for all of the sacrifices that they made on my behalf.

I would like to express my special appreciation and thanks to my advisors Dr. Douglas Paton at the University of Leeds, Dr. David Cornwell at the Aberdeen University, you have been of tremendous help to me. I express my profound gratitude to my sponsor Saudi Aramco Company (Exploration Organization, Career and Development Department), for providing the grant to undertake the PhD. I would especially like to thank GEUS and TGS for supplying the datasets for the study.

I would also like to thank all of my colleagues at IGT and BSG, in particular thanks goes to Dr. Christopher Green for his continuous help and pieces of advice on gravity and magnetic modelling. I enjoyed both the professional and mutual interaction. Finally, I would like to express my gratitude to the technical staff of the School of Earth and Environment for their support throughout the PhD.

Abstract

The study sets out to unravel the tectonic evolution and lateral structural variation of the West Greenland (Baffin Bay, Davis Strait and Labrador Sea) and to consider its hydrocarbon potential in light of this new evaluation. The study follows a multidisciplinary approach by using 2D seismic, gravity, magnetic, depth-dependent stretching data combined with heat flow and petroleum system modelling.

The Western Greenland margin evolved through a complex combination of processes that included multiple phases of extension, varying degrees of subsidence and margin uplift. Basin fill architecture indicates that the margin changes dramatically laterally along the margin. Two rift events were recognized based on architecture of syn-rift sediments. The complex structural variation along the margin is revealed by: the presence of a clear magnetic lineament indicating formation of oceanic crust in Labrador Sea at Chron 31; a good correlation between gravity anomalies in areas of oceanic crust where the extinct spreading axis between Canada and Greenland was identified; areas of continental crust with greater uncertainty in the structure of the continental lithosphere; and greater extension accommodated by the lithosphere in its entirety, rather than by the upper crust alone as indicated by depth-dependent stretching along the margin

This study therefore demonstrates that understanding the complex processes involved in multiple-rifting and depth-dependent stretching is important to constraining hydrocarbon potential of passive margin basins.

Table of Contents

List of Tables

List of Figures

Chapter 1

Introduction

1.1 Rationale

One of the most significant controls in the development of a passive continental margin is the nature in which the continental lithosphere thins prior to break up into a continental margin over the last 45 years, many models have been developed to describe ways continental lithosphere thins and promotes continental break up during extension. Published models include the pure shear model, simple shear model, and combined pure shear-simple shear model (Lister et al., 1986), have described how crustal attenuation, followed by thermal subsidence and isostatic compensation have played the key roles in lithospheric and mantle geodynamics.

The development of lithosphere stretching models has contributed notably to our understanding of the evolution of extensional basin (Davis and Kusznir, 2004; Fletcher et al., 2013; Franke, 2013; Kusznir et al., 1995; Nestola et al., 2013; Philippon et al., 2014). Due to the acknowledged variability in rift basins formation and geometries, no single model can serve as the standard for all basins. Nonetheless, we test these models in this thesis by integrating geophysical data to understand the processes observed during the formation of West Greenland margin and to consider their influence on hydrocarbon potential.

1.2 Aim and objectives

The aims of this thesis are to better understand the nature of continental break up between Greenland and North America plates and to constrain the structural evolution and regional tectonic processes during the opening of the West Greenland margin. These aims are achieved through following objectives:

- Derive a tectono-statigraphic study to constrain basin architecture (2D seismic interpretation and borehole seismic data).
- Investigate deeper crustal structures of the margin (gravity and magnetic models
- Constrain the extensional style of the margin (pure shear, simple shear or depth-dependent stretching modelling).
- Undertake heat flow and petroleum system modelling

The objective is to provide additional knowledge on the processes of lithospheric stretching and continental breakup especially in what the influence of heat flow on hydrocarbon prospectivity of rifted continental margins is concerned.

1.3 Location of the study area

The study area is located on the West margin of Greenland (Figure 1.1), and is divided into the Baffin Bay to the northwest of the study area, the David strait and the Labrador Sea on its central and southwest regions respectively.

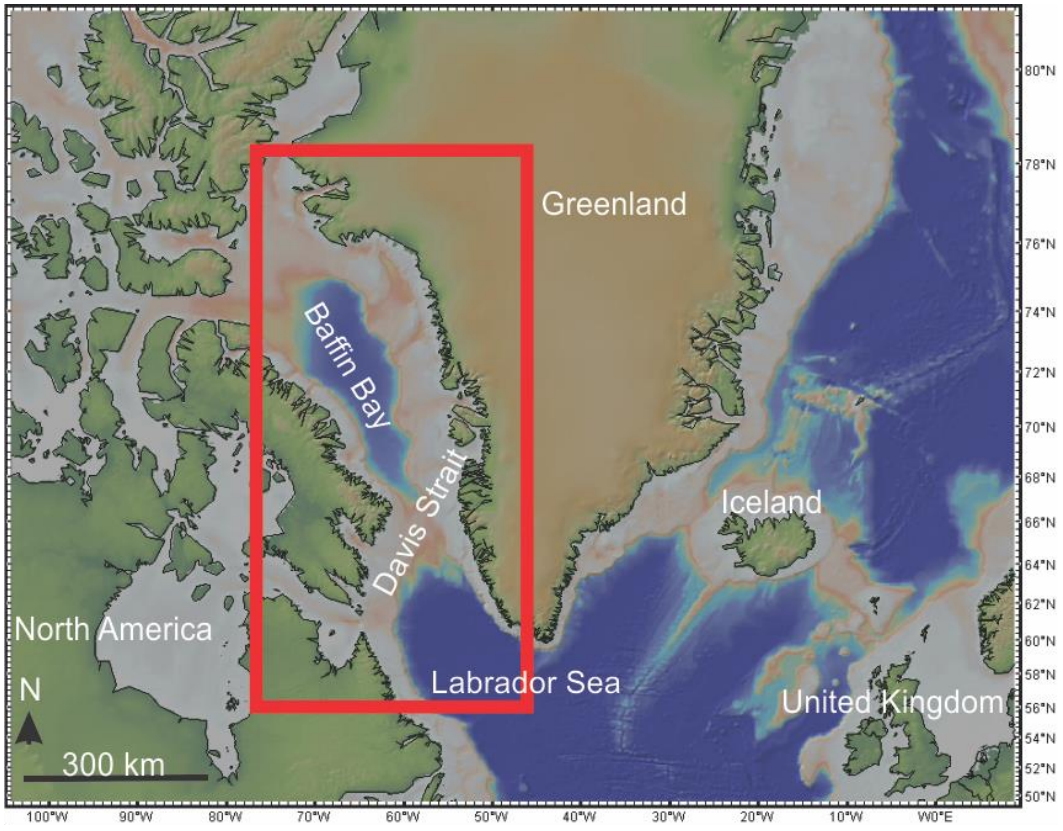

Figure 1.1: Location of the study area highlighting the main basins interpreted and modelled in this study.

The West Greenland margin was formed by the northward propagation of continental rifting and seafloor spreading associated with the continental breakup of North America from Europe during the Late Cretaceous and Early Tertiary periods. The margin of West Greenland was formed by rifting of the Labrador Sea in late Mesozoic to early Cenozoic time (Schenk, 2011; Balkwill et al., 1990; Chalmers et al., 1993; Chalmers, 1991). Apart from the three basins previously mentioned, the margin of West Greenland is characterised by several sub-basins (Figure 1.2). The major sub-basins of Baffin Bay include Melville and Kivioq Bay. In the Davis Strait, these sub-basins include the Aasiaa and Sisimiut Basins. The Sisimiut Basin is

bounded to the west, northwest and north by the Ikermiut Fault Zone (Figure 1.2).

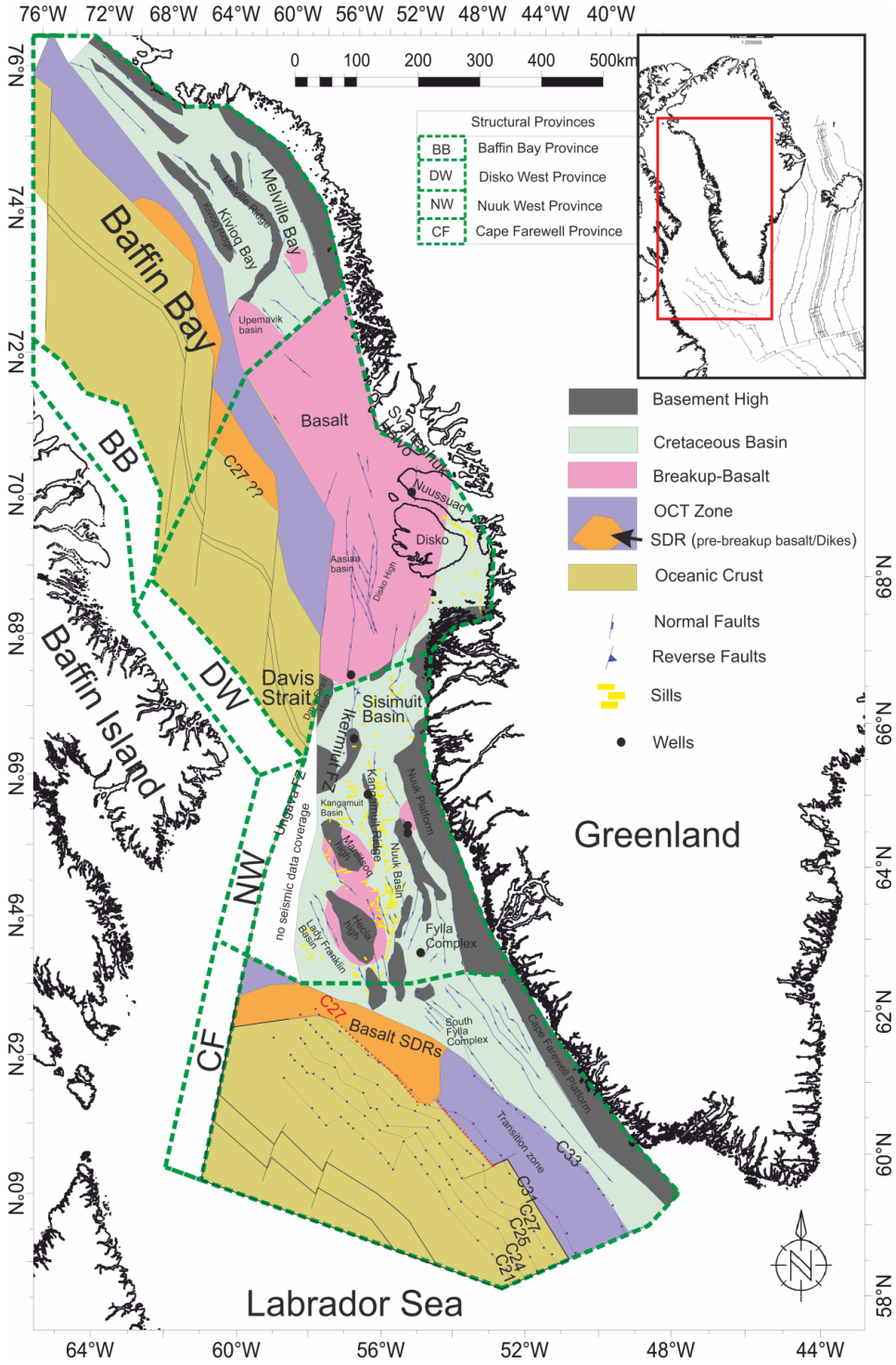

Figure 1.2: Regional tectonic framework of the West Greenland study area. The map is generated by data integration of Seafloor bedrock age from Müller, 2008. The structural Provinces are defined after Knutsen et al., 2012.

West of the Ikermiut Fault Zone is a shallow basin exhibiting synclinal folding in similarity to the Davis Strait High (Chalmers, 2012), which probably consists of continental basement at or near the seabed. To the southeast of the Sisimiut Basin is the Nukik Platform, an area of shallow basement and volcanics drilled by the Nukik-1 and Nukik-2 wells. The northern Nuuk Basin is flanked to the east by the Nukik Platform and to the west by a shallow basement/volcanic complex here termed as the Maniitsoq Rise (Figure 1.2).

In the Labrador Sea, the southern limit of the Nukik Platform is at approximately 65°N, south of which is an area of fault-blocks of the Atammik Structural Complex (Figure 1.2). Southwest of the Atammik Structural Complex, and partly separated from it by an area of shallow basement, is the Fylla Structural Complex. A major SSW–NNE-trending fault separates the Atammik and Fylla Structural Complexes from the Nuuk Basin to the west (Figure 1.2). The southern part of the Nuuk Basin is bordered to its west by the shallow basement and volcanic Hecla Rise (Tucholke and Fry, 1985). The West part of the Hecla Rise consists of large fault-blocks that step down to the Lady Franklin Basin (Figure 1.2).

1.4 Layout of Thesis

The thesis is comprised of eight chapters (Table 1.1). In Chapter 1, an introduction is given on the importance or rationale of this study, its aims, together with an overview of the study area and its basins. In the final section of chapter 1, a breakdown of the entire thesis is provided. Chapter 2

include a review of literature and previous works on lithospheric stretching and continental breakup and also on the tectonic and stratigraphic composition of the West Greenland margin. This is followed by a detailed description of the datasets used in Chapter 3. The methods used for Chapter 4 are presented in Chapter 3 while the methods used for Chapters 5, 6 and 7 are presented within each chapter. The data chapters include Chapters 4, 5, 6 and 7. The thesis is written in a manner where the data Chapters are presented as separate chapters. The last chapter is a synthesis of the data chapters and aims to compare the results of this study with published data from other margins.

Table 1.1: The layout of the thesis

Chapters	**Content**
Chapter 1	An introduction; aims and background of the study.
Chapter 2	Regional Setting of the West Greenland margin and comparison with adjacent margins.
Chapter 3	Data used in this study
Chapter 4	Tectonic evolution of West Greenland from Seismic interpretation of the multiple 2D lines
Chapter 5	Modelling of continental extension on the West Greenland margin
Chapter 6	Gravity and Magnetic modelling of crustal development of the margin
Chapter 7	Heat flow, hydrocarbon maturation on the West Greenland margin
Chapter 8	Discussion and Conclusion chapter in which the results from chapters 4 to 7 was integrated

Chapter 2

Geological Setting

2.1 Abstract

The purpose of this chapter is to provide a regional geological background to this study. The first part provides a review of the current understanding of the processes involved in lithospheric extension. The second part considers the regional geological setting of the Western Greenland margin. The tectonic evolution of the margin and adjacent basins is reviewed, prior to a summary of existing stratigraphic understanding and an appraisal of petroleum system.

2.2 Continental rifting and lithospheric extension

Continental rifting involves thinning and stretching of the lithosphere, ultimately leading to the rupture of the continent and the formation of a mid-oceanic ridge and sea-floor spreading (Brun, 1999; Corti, 2003; Merle, 2011; Ziegler, 1992).

The rifting process may or may not lead to the formation of new oceanic crust, as some rifts become inactive upon commencement of rifting leading to a failed rift system or aulacogen (Ziegler and Cloetingh, 2004). Lithospheric extension is thus a fundamental process of plate tectonics,

controlling the collapse of mountain belts, the break-up of continents and the formation of new oceanic basins (Rosenbaum et al., 2008). The thinning of the lithosphere may be driven by one of two mechanisms: a) horizontal extension associated with far-field stresses b) the impingement of a mantle plume beneath the lithosphere (Merle, 2011).

Based on the processes driving lithospheric extension and on the role of volcanism during lithospheric stretching, continental rifting can be classified as a) “Active” rifting, when rifting is controlled by the effect of a mantle plume heating up the base of the lithosphere, leading to stretching and formation of rift margins (e.g. Burke and Dewey, 1973; Condie, 1982; Sengör and Burke, 1978) or b) passive rifting, which produces thinning and upwelling of the hot asthenosphere followed by subsidence driven thermal decay (Mc Kenzie, 1978).

The schematic representation of these two types of rifting is shown in Figures 2.1 to 2.5. Furthermore, depending on the volumes of extension-related magmatism two end-member passive margin types can be defined either as volcanic or magma-poor (Figures 2.3 to 2.5; Franke, 2013; Watts et al., 2013).

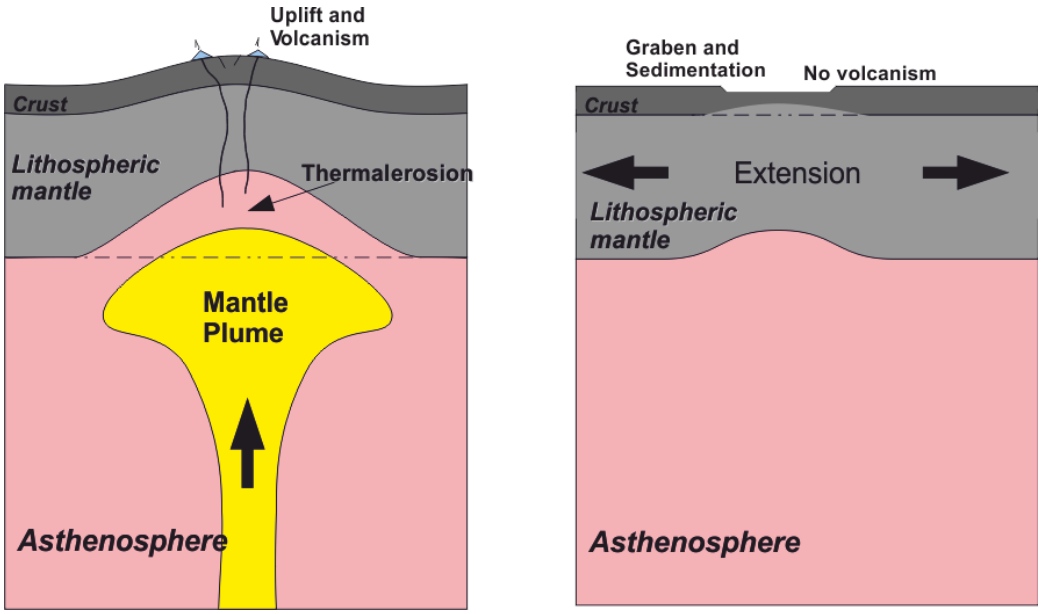

Figure 2.1: “Active” rifting is characterised by lithospheric uplift and volcanism resulting from thermal erosion at the base of the lithosphere. “Passive” rifting displays graben formation and sedimentation without volcanism as a result of horizontal extension of the lithosphere. Modified from Merle (2011).

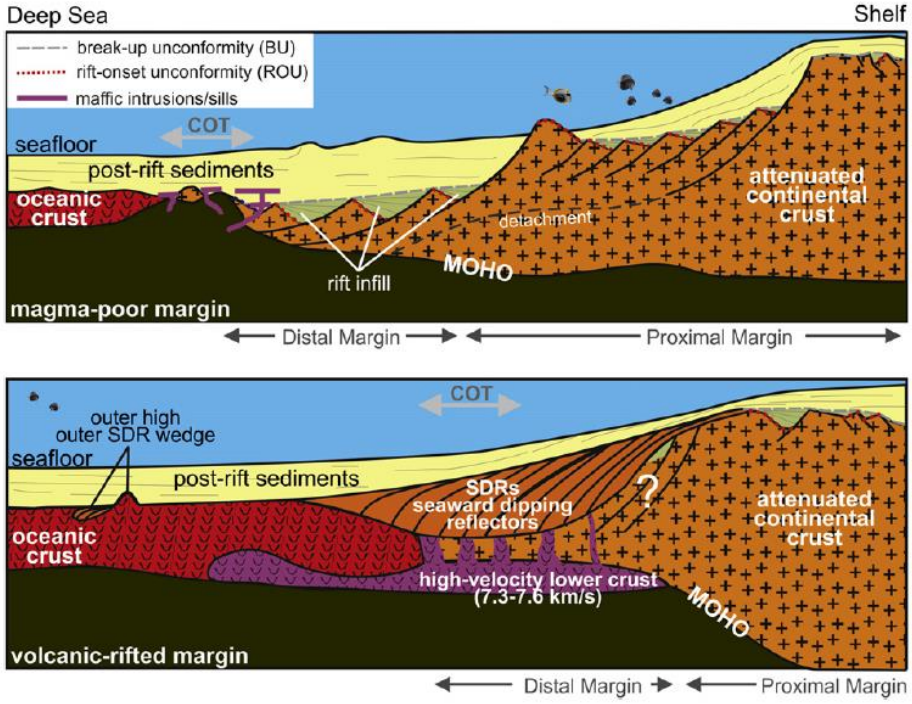

Figure 2.2: A simplified schematic through the layout of volcanic and no-volcanic continental margins (Franke, 2013)

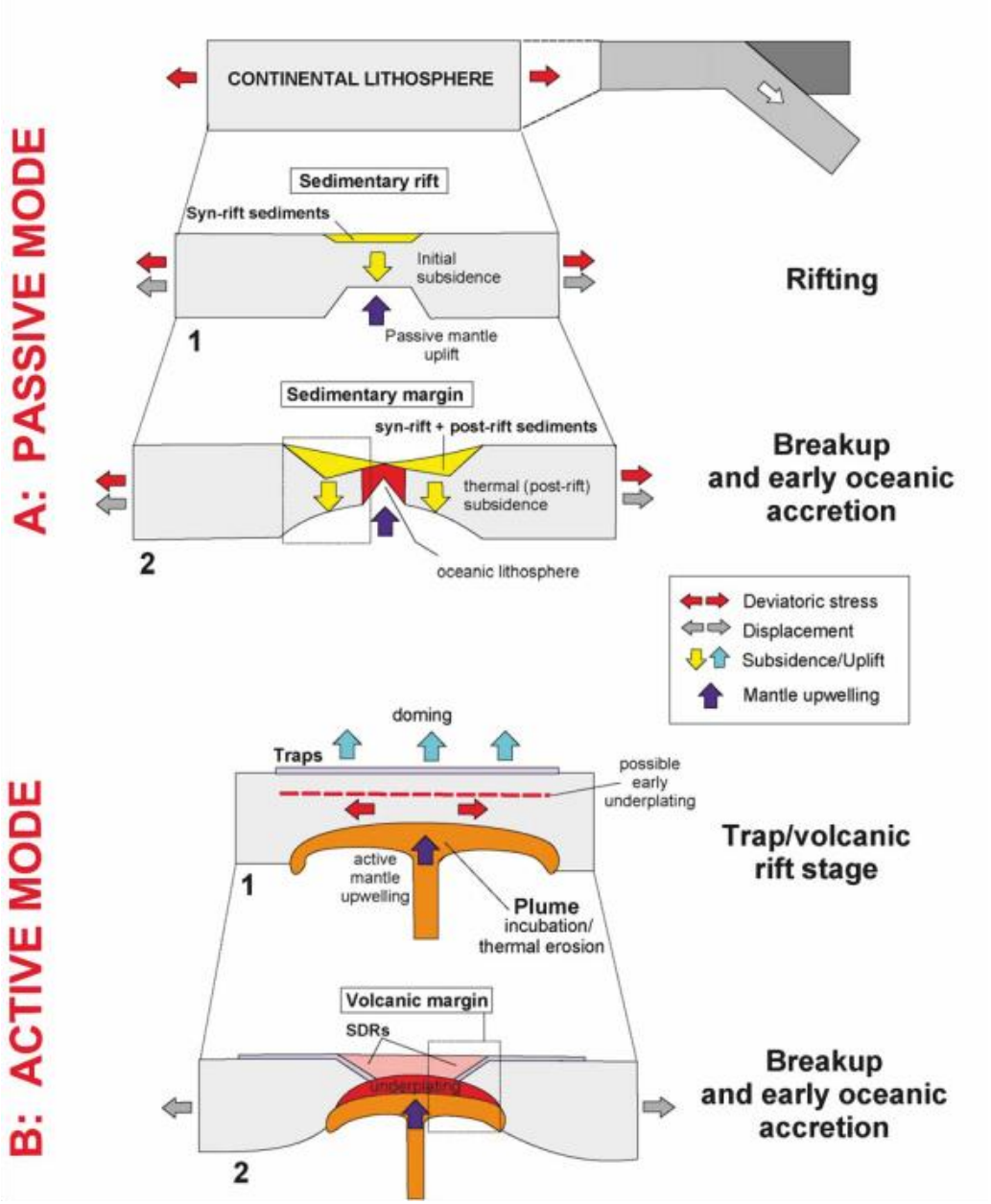

Figure 2.3: Mechanism of passive and active rifting during continental breakup (Laurent, 2005).

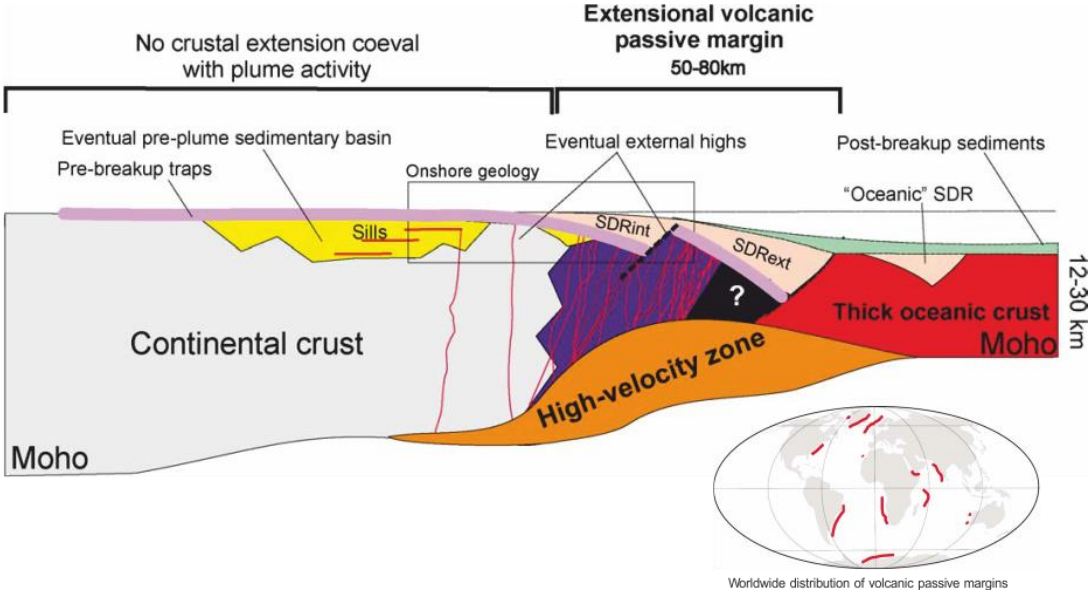

Figure 2.4: Across-strike section of a volcanic passive margin, (Laurent, 2005)

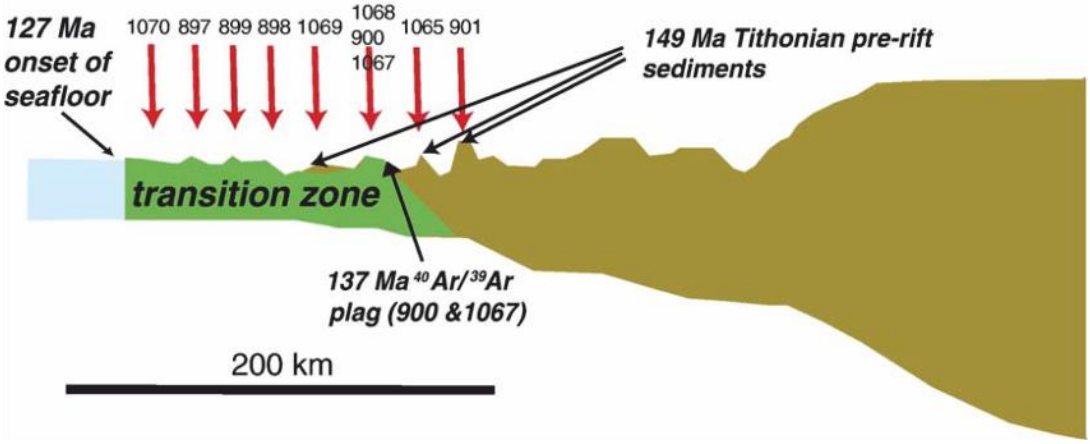

Figure 2.5: Non volcanic schematic cartoon of the Iberia Abyssal Plain (Pérez-Gussinyé et al., 2006)

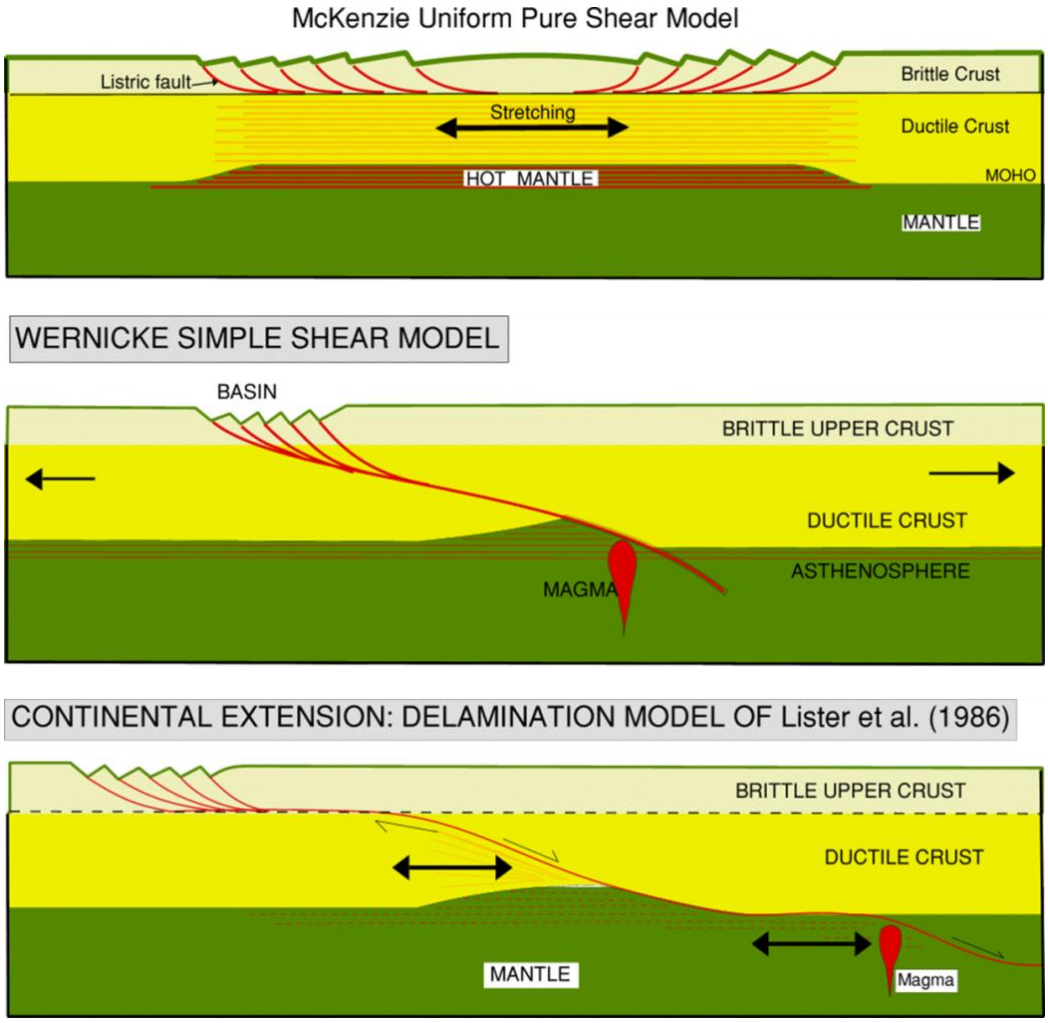

Figure 2.6: Three models for continental extension, (Lister et al., 1986)

2.2.1 Models of lithospheric stretching

Despite the large number of studies on continental rifts and rifted continental margins, Prosser (1993); Steel, 1993; Notvedt et al. (1995, 2000); Ravnås and Steel et al. (1998), there is still a lack of a unified understanding of the mechanical and thermal processes that control their extensional geometry (Huismans and Beaumont, 2007, Fletcher et al., 2013; Nestola et al., 2013; Scotchman et al., 2010). The common models for lithospheric stretching are reviewed in this section.

McKenzie (1978) introduced a simple ID (pure shear model) that assumes a uniform extension model. According to the model (Figure 2.6), the first event during rifting consists of a rapid stretching of the continental lithosphere, which produces thinning and passive upwelling of the hot asthenosphere. This stage is associated with block faulting and subsidence. Mantle upwelling of the hot asthenosphere causes crust attenuation. The continental plate then cools and returns to its original thermal equilibrium (Thermal subsidence). The slow subsidence and heat flow depends only on the amount of stretching, which can be estimated from these quantities and from the change in thickness of the continental crust formed by extension.

In contrast to McKenzie 1978, Lister et al., (1986); Wernicke, (1985); Wernicke and Burchfiel (1982), suggest that movement on a low angle detachment zone has penetrated the entire crust and lithosphere to accommodate major lithospheric extension. According to Lister et al (1986), this mode of stretching is not uniform and is characterised by an asymmetrical geometry (Figure 2.6). Based on geophysical studies of the Basin and Range Province, that extend eastward beneath the west margin of the Colorado Plateau and the Rocky Mountain regions, Lister et al (1986) argues that lithospheric stretching is accomplished by displacement on a large scale of normal simple shear of the crust. Detachment faults may occur in all major extension basins, accommodating extension and playing a significant role in controlling their structural evolution.

In contrast to the latter work, Rosenbaum et al. (2008) suggest that the prominent role of detachment faults implies that depth-dependent stretching should be the rule rather than the exception. The model Rosenbaum et al. (2008) suggests that basins are stretched asymmetrically by a large scale detachment fault extending from the upper crust to the asthenosphere. Lister et al. (1986); Kusznir et al. (1995), Roberts et al. (1998) and Davis and Kusznir (2004) also observed that extension is mainly an asymmetric process resulting in the formation of conjugate passive margins that are quite different in character. The upper plate occupies the hanging wall of the master detachments and the lower plate margin consists of the detachment footwall, commonly including highly faulted and extended segments of the upper plate.

2.2.2 Atlantic-type rift margin

Passive continental margins represent one facet of a successful rift separation. The term passive refers to the general assumption that most tectonism has ceased along such a margin. The evolution of rift margins can be divided into an early, rift-related phase and a later, drift-related phase (Figure 2.2). Earlier structures are predominantly associated with basement block faulting; later phase deformation is concentrated in the overlying sedimentary wedge. Sedimentation typically begins with coarse, syntectonic, nonmarine clastics (alluvial fan, fan delta, braided stream), possibly interbedded with fine-grained, organic lacustrine shales. These sediments are commonly intruded by, and interbedded with, volcanic material, mostly of

mafic composition on volcani margins (Laurent, 2005). This sequence accumulates in half-grabens between major fault blocks, as well as within the central rift. It is then progressively faulted, tilted, and rotated as extension continues (e.g. Harris and Whiteway, 2011; Franke 2013; Japsen et al., 2012).

On some rifted margins, evaporites mark the earliest stages of marine incursion, as the rift expands to form an ocean basin. These evaporites may also occur at the top of the rifting section, if marine incursion occurs during continentnal breakup. Thicknesses of salt may therefore be confined to half-grabens, or may occur as more extensive sheets overlapping local basins.

2.3 Tectonic development of the Western Greenland margins

A tectonic development of West Greenland records complex, multiphase episodes of rifting from early Jurassic extension to the opening of Baffin Bay and onset of seafloor spreading, to the opening of the north Atlantic that resulted in the cessation of ocean spreading and co-eval inversion (Schenk, 2011; Balkwill et al., 1990; Rowley and Lottes, 1988; Roest and Srivastava, 1989; Chalmers et al., 1993).

The margins of Western Greenland were formed by continental rifting and northward propagation of seafloor spreading associated with the breakup of North America from Europe during the Late Cretaceous and early Tertiary (Nielsen et al., 2002). The separation and movement of the Greenland and

Canada cratons were strongly influenced by the migration of a mantle plume that caused thermal uplift, extension and subsequent plate movements (Harrison et al., 1999). A possible scenario describing the plume dynamics under Greenland involves the movement of a small upper mantle plume horizontally on encountering the base of the lithosphere (Larsen et al., 1999; Nielsen et al., 2002).

The first and earliest recorded rifting event probably occurred in the Early Cretaceous (140 to 130 Ma) or Late Jurassic as a consequence of the extension between Africa and North America to the South and uplift associated with the thermal doming induced by the Thulean mantle plume which was located in central Greenland (Harrison et al., 1999). A second rifting event of Late Cretaceous and early Palaeogene age culminated in thermal subsidence and subsequent passive margin sedimentation at magnetic Chron 27 and c. 61 Ma (Dam et al., 2000; Larsen and Pulvertaft, 2000).

The Early Cretaceous rifting event is recorded by the deposition of siliciclastics materials in half grabens and grabens in the Kitsissut and Appat sequences on the West Greenland margin (Figure 1.2). Typical sedimentary facies include alluvial fan, fluvial, fan-delta, deltaic and shallow lacustrine sandstones and mudstones of the Kome and Atane Formations, from Nuussuaq basin (Schenk, 2011; Dam et al., 2000; Balkwill et al., 1990). Subsequently, the Kangeq sequences were deposited during a period of thermal subsidence/sag phase succeeding the earliest rifting phase

(Bojesen-Koefoed et al., 1999). Coarse-grained clastics deposited during this stage include marginal marine sandstones of the Fylla complex (Dalhoff et al., 2003; Dam and Sønderholm, 1994). Palaeocene to Oligocene strata chiefly comprise fine-grained clastics typical of slope fan systems (Schenk, 2011; Dalhoff et al., 2003; Dam et al., 2000).

Seafloor spreading started earlier in the south of the Labrador Sea and opening was orientated in an ENE direction during the Palaeogene (Chalmers, 1991). The second phase of seafloor spreading is associated with the emergence of the Ungava transform fault zone and the oceanic basins that underlie Baffin Bay. These have been inferred to have been generated during Magnetic Chrons 24–13, about 56–33 Ma (Figure 1.2). The oceanic crust of Labrador Sea and Baffin Bay are separated by the Ungava transform fault zone in the Davis Strait. The Ungava transform fault zone is characterized by complex structures that were initially extensional; these structures were subsequently affected by both transtension and transpression processes as the Ungava fault zone evolved into a transform zone (Sørensen, 2006; Skaarup et al., 2006). Current theories of the development of this area centres on whether the ocean opening propagated northwards forming the oceanic crust in the central west (Davis Strait) and northwest (Baffin Bay) or if magma-starved spreading occurred and the Icelandic plume drove the opening of the margin (Schenk, 2011; Roest and Srivastava, 1989; Chalmers et al., 1993; Chalmers, 1991).

The rift stage is characterized by NW propagation of the rift axis during the collision of the Greenland with northern Canada. This collision resulted in the development of compressional structures north of Greenland during the Tertiary Eureka orogeny (Schenk, 2011). The tectonic development of Western Greenland did not occur as a simple rift to drift phase. Instead the evolution of the margin witnessed significant emplacement of extrusive rocks. The Paleocene was a time of widespread volcanic activity in the central part of the Western Greenland (Larsen and Pulvertaft, 2000; Pedersen and Larsen, 2006), a period that coincided with the eruption of several kilometres of plume-related volcanic rocks at a regional scale (Schenk, 2011).

Initial continental rifting of the Labrador Sea is characterized by substantial volcanism, as evidenced by voluminous emplacement of picrites and basalts that result from the influence from the Iceland plume at c.62 Ma (Larsen and Saunders, 1998). The largest area covered by volcanic rocks is located north of 68^0N, partly covering the Nuussuaq Basin. The Maniitsoq and Hecla Rises along with Nukik Platform are also important volcanic areas (Bonow et al., 2006). Svartenhuk Halvø, Nuussuaq and Disko basins contain the volcanic rocks formed during the Palaeogene time. In all cases, the rocks extend offshore to the NW from this volcanic region towards the Kivioq and Melville Bay Basins in southern Baffin Bay (Rolle, 1985). Recent geochemical and geochronological data on Palaeocene flood basalts from West Greenland, SE Greenland and the British Isles show that volcanic activity at these widely separated locations commenced nearly

simultaneously at 61–62 Ma (Schenk, 2011; Roest and Srivastava, 1989; Chalmers et al., 1993).

2.4 Stratigraphy of Western Greenland

The Precambrian bedrock of the West Greenland area consists of Achaean and Proterozoic crystalline rocks characterized by numerous complex terranes and suture zones (Hoffman, 1988; Oakey and Chalmers, 2012). Unconformably overlying the basement is the Appat sequence of west Greenland connected with the extension and subsequent development of the rift system in a present day Labrador Sea and Baffin Bay and also dyke intrusion along the west Greenland margin (Figure 2.7; Larsen, 2006, Umpleby, 1979).

The Kitsissut and Appat sequences reflect clastic deposition in grabens and half-grabens deposited when Greenland separated from Canada. Rift facies include alluvial fan, fluvial, fan-delta, deltaic and shallow lacustrine sandstones and mudstones. These deposits are materialised by the Bjarni Formation in the Canadian Labrador shelf (Balkwill et al., 1990) and by the Kome and Atane Formations in Nuussuaq, West Greenland (Dam et al., 2000; Larsen and Pulvertaft, 2000).

The Kangeq Formation is composed of mudstones and sandstones at a main depocentres. Subsequently, deposition in the margin included channelized sediments of the Nuusanq Basin (Chalmers et al., 1999;

Chalmers and Pulvertaft, 2001). The West Greenland volcanic margin area was subjected to regional uplift in the Danian (65–61Ma) prior the extrusion of pre-breakup volcanic Formations such as the Ikermiut Formation, Nukik Formation and the Kangamint Formation (Abdelmalak et al., 2012). The Kangeq sequence include is Campanian–Maastrichtian in age and is composed of largely fine grained marginal marine sandstones to deep marine slope and fan sandstones. Palaeogene strata are largely fine-grained, but include several slope and fan sandstones (Dam et al., 2000; Dalhoff et al., 2003).

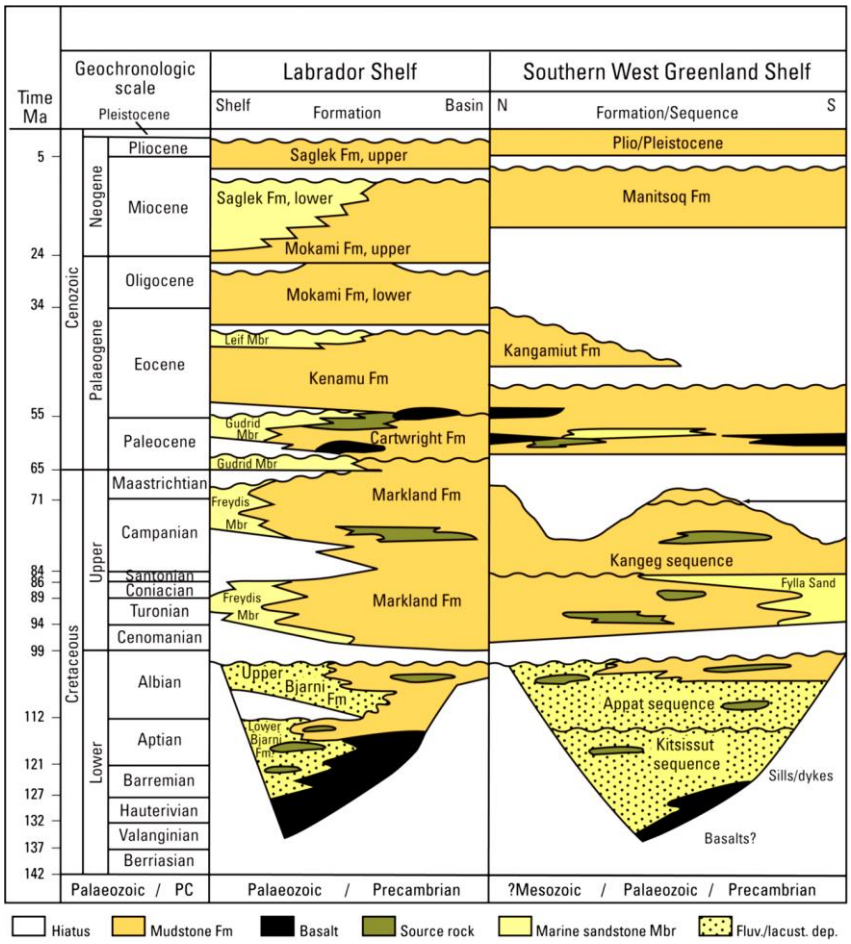

Figure 2.7: Stratigraphic column for the West Greenland–East Canada Province modified from Sørensen, 2006. N.B: Potential source–rock intervals shown in green.

2.5 Regional geodynamic setting (North Atlantic margins)

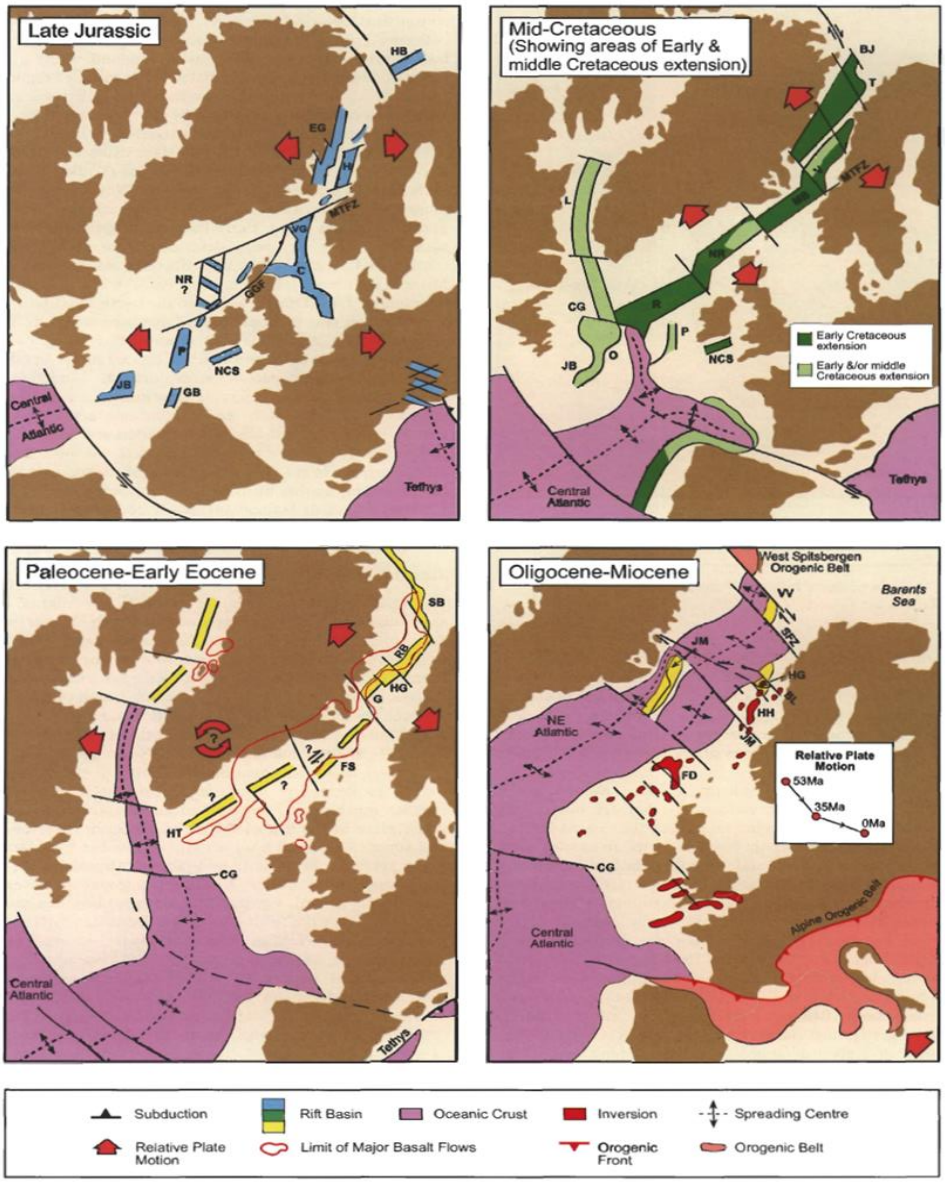

Figure 2.8: Plate reconstructions - Jurassic, Cretaceous, Paleocene and Cenozoic, indicating relative plate motion, contemporaneous rifts and areas of inversion (Doré et al., 1999).

Several basins formed and developed along the continental margins of the North Atlantic such as, the Scotia margin in south-eastern Canada and the Moroccan margin in northwest Africa which were formed in the Late Triassic when North America separated from Africa (Figure 2.8). The North America

continent separated from Iberia to form the southern Newfoundland margin before chron M3 (125 Ma); Louden, (2002). The rift initiated with extension in NW-SE direction and began in Late Jurassic to Early Cretaceous with deposition of red beds and evaporites in the form of stratigraphic sequences that are similar to those on the Scotian margin and South Newfoundland (Grand Banks) and the variation in sediment geometries and thicknesses of the Iberia margin reveals a relative westward migration of major subsiding areas during continental extension prior to breakup (Pereira and Alves, 2011).

The Triassic-Jurassic transition in the North Atlantic regions saw a change to rift tectonics associated with ocean floor spreading in the Tethys to the southeast and in the Proto-Central Atlantic to the southwest (Doré et al., 1999). Based on the seismic data interpretation reconstructions and the extension of the lithosphere obtained from the subsidence history modeling of this region. Srivastava et. al. (1988) estimates a pole of rotation observed at the time of the initial opening in the region between the Flemish Cap and the Charlie-Gibbs Fracture Zone spreading between the British Isles and Newfoundland.

Doré et al. (1999) suggests that the Late Jurassic to Early Cretaceous rifting in Northwest Europe was less influenced by seafloor spreading than by the Northwest Atlantic (Labrador Sea). Hall and White (1994) also observe that subsidence occurred at the beginning of the Tertiary Palaeogene within a large number of Mesozoic rift basins on the shelves of the proto - North

Atlantic margin (e.g. Porcupine basin, North Sea). These authors proposed that anomalous increases in subsidence close to major mantle plumes may be caused by the presence of basaltic magmas trapped at depths of greater than 50 km.

2.6 Igneous provinces and influence of the plume in Eastern and Western Greenland.

The Tertiary volcanism of the North Atlantic region (Figure 2.9) provides the best described magmatic record of the interaction between plume interaction and the continental lithosphere (Gill et al., 1995; Torsvik et al., 2001). The plume was located under West Greenland at 60 Ma, then at 50 Ma the westerly direction of the movement of North America and the spreading ridges had moved the Norwegian Sea Ridge by approximately 200 km to the plume head and had moved the Labrador Sea 300-400 away from the plume in the west direction.

Early picrites of west Greenland are similar to sub-aerial Icelandic basalts and are formed by processes similar to melting of their source mantle (Holm et al., 1993). However, Gill et al. (1995) suggest that the volcanic eruption of the West Greenland picrites occurred 5 to 6 Myrs earlier than the start of volcanism in East Greenland. This is supported by Parkin et al. (2007) who estimated the temperature of the Icelandic mantle plume decreased by 50 °C over the first 5 Myrs following continental breakup, and then oscillated by 25 °C over a c.3 Myrs period.

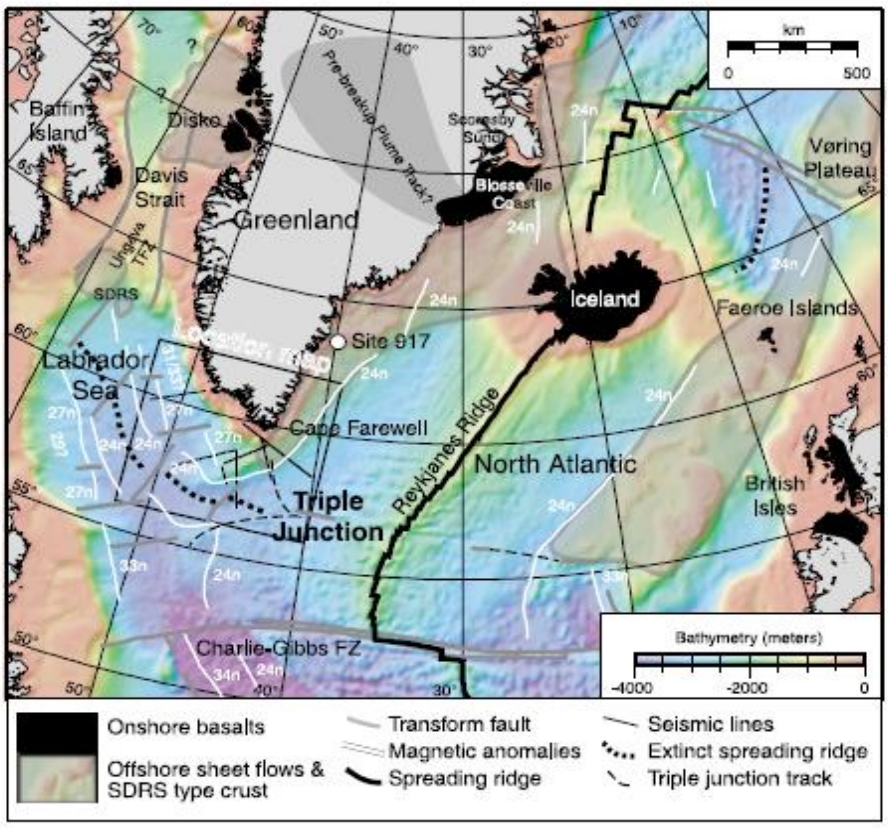

Figure 2.9: Distribution of early Paleogene (53-61 Ma) continental flood basalts and onshore volcanic rocks in the NAIP including the main seaward-dipping reflection sequence (Nielsen et al., 2002).

A possible scenario describing the plume dynamics under Greenland at c. 62 Ma involves a small, fast moving upper mantle plume that rapidly spreads out horizontally on encountering the base of the lithosphere (Larsen et al., 1999; Nielsen et al., 2002). Palaeomagnetic reconstructions in the hotspot by Torsvik et al., (2010) suggest that mantle and crust processes are linked, but the NW directional change in the North Atlantic path broadly corresponds to the oldest known magnetic anomaly from the Labrador Sea. This event was the deciding factor in establishing the position of the Icelandic plume at the eastern trailing edge of the NE Atlantic in the Tertiary period.

Chapter 3

Data and Methods

3.1 Overview

This chapter presents a detailed overview of the methods used throughout the thesis.These can be divided into: seismic interpretation, depth-dependent modelling, gravity and magnetic modelling, and heat flow modelling. The methods for Chapters 5, 6 and 7 are not presented in this section because they represent standalone methodologies and are best suited to the individual Chapters.

3.2 Data

Hydrocarbon exploration started in the Arctic region in the late sixties with the collection of gravity, magnetic, seismic and drilled borehole data. During the last 50 years existing information has been substantially enriched by a series of completed 3D seismic surveys and a significant amount of 2D seismic data. However no major hydrocarbon discoveries have been made.

3.2.1 Seismic and Well data

Access to c. 30,000 km of 2D migrated seismic reflection data was provided by GEUS and TGS for this study (Figure 3.1). Further details of the acquisition and processing of the seismic is provided in Appendix I. In

addition, information from seven published wells (Dalhoff et al., 2003), was used to create synthetic seismograms to tie well data to the seismic data (Figure 3.8). As discussed below, lithological constraints were provided by seven published wells some reaching a depth of 2363 m to 3874 m. These wells include Hellefisk-1, Ikermiut-1, Kangâmiut-1, Nukik-1, Nukik-2, Qulleq-1 and GEO-3 (Table 3.1). The location of the wells is shown in Figure 3.1.

3.2.2 Gravity and Magnetic data

The global data sets used are:

- Global Multi Resolution Topography (GMRT)
- Free Air Gravity (Sandwell and Smith v18.1)
- NASA Elevation Model (USA 10m, World 30m, Ocean 900m)
- Seafloor Bedrock Age (Müller 2008)
- Topography (Smith and Sandwell 2009)

The description of the gravity, magnetic and topographic data are given below: - The Free Air Gravity (Sandwell and Smith v18.1) (Figure 3.2) and magnetic data (Figure 3.3) are compilations obtained from NOAA “Geophysics of North America”.

1. The Free Air Gravity values were extracted from the latest public domain version of the satellite altimetry with a spatial resolution of 1-min (1 nautical mile) of Sandwell and Smith, 2009; Figure 3.2. The

obtained free-air gravity was correlated with prominent bathymetric features in the region.

2. DNAG Magnetic Field, Geophysics of North America: The magnetic dataset the total magnetic field of North America sampled every 2 kilometres (Figure 3.3). The data in this grid can be recovered from the indices of a grid point. https://catalog.data.gov/dataset/aeromagnetic-regional-grid-data)

3. Topography (Smith and Sandwell, 2009) data (See Figure 3.4).

Table 3.1: Total of seven wells were used in this study

Well Name	Latitude	Longitude	TD (MD)
GRO-3	70°27'45.89"N	54°05'13.63"W	2996
HELLEFISK-1	67°52'37.10"N	56°44'2.49"W	3201
IKERMIUT-1	66°56'7.99"N	56°35'8.62"W	3619
KANGÂMIUT-1	66°08'57.07"N	56°11'6.96"W	3874
NUKIK-1	65°31'32.10"N	54°45'20.86"W	2363
NUKIK-2	65°37'50.30"N	54°45'43.58"W	2694
QULLEQ-1	63°48'48.02"N	54°27'6.59"W	2973

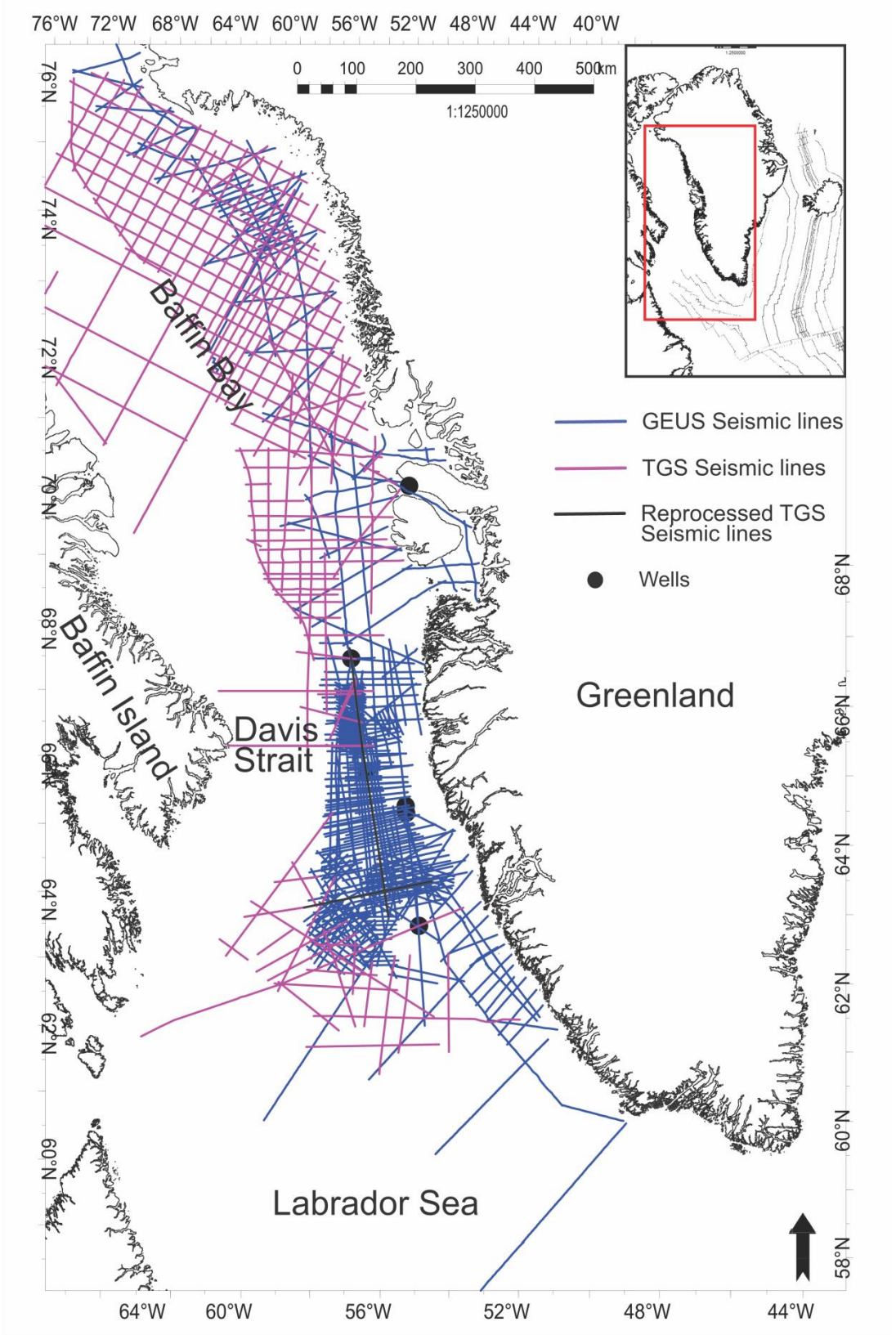

Figure 3.1: Map showing the layout of the seismic lines used for the thesis.

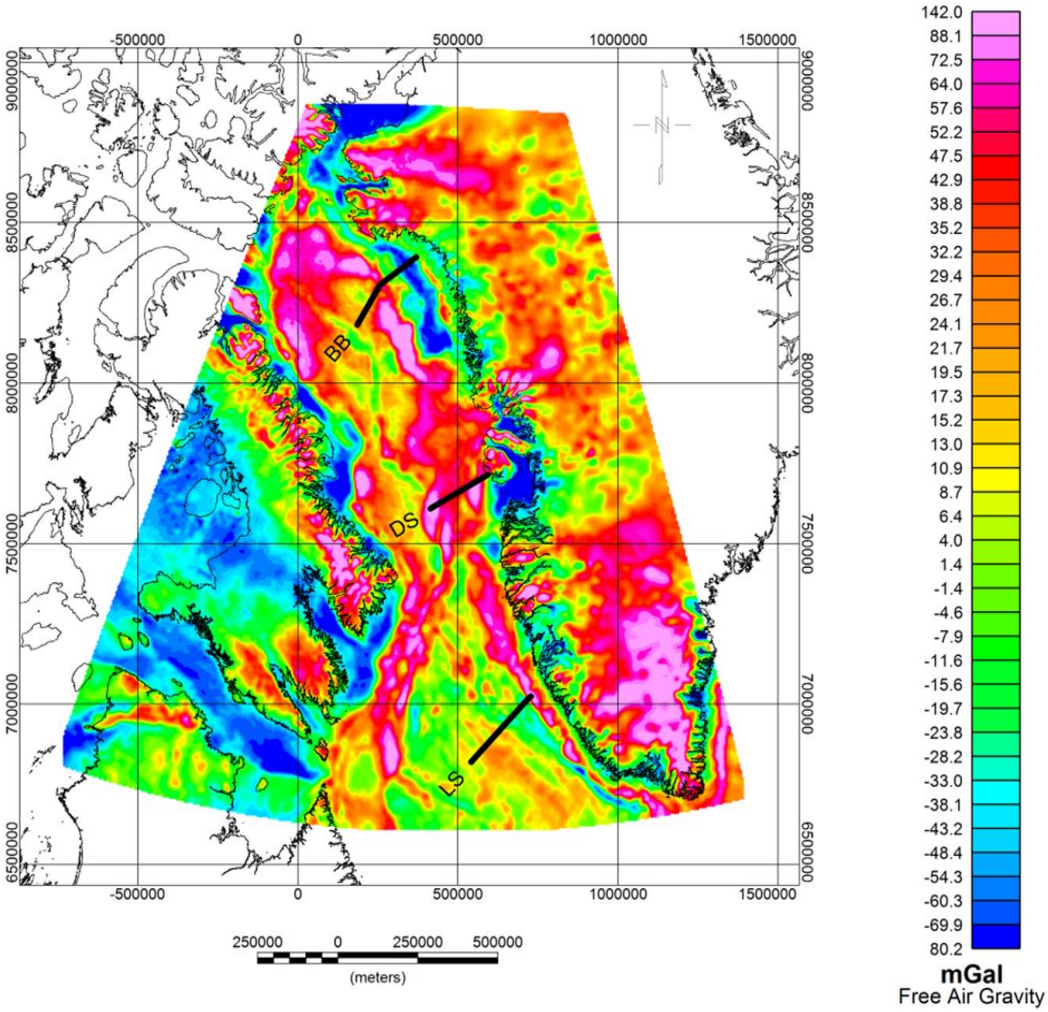

Figure 3.2: The Free Air Gravity (Sandwell and Smith v18.1) map used for the thesis from www.noaa.gov. The black lines show the location of the representative seismic profiles used in chapter 4 and 5 respectively.

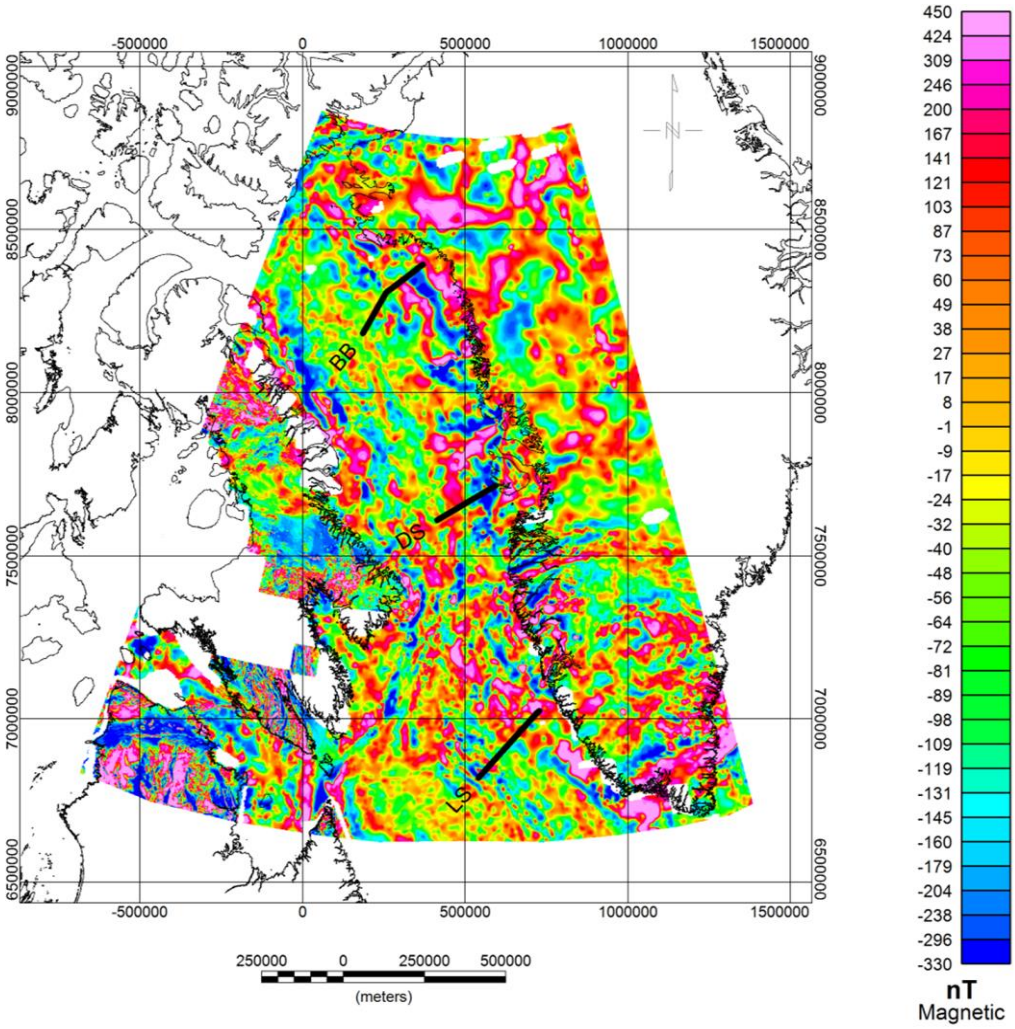

Figure 3.3: The DNAG Magnetic Field map, the total magnetic field of North America sampled at 2 kilometres

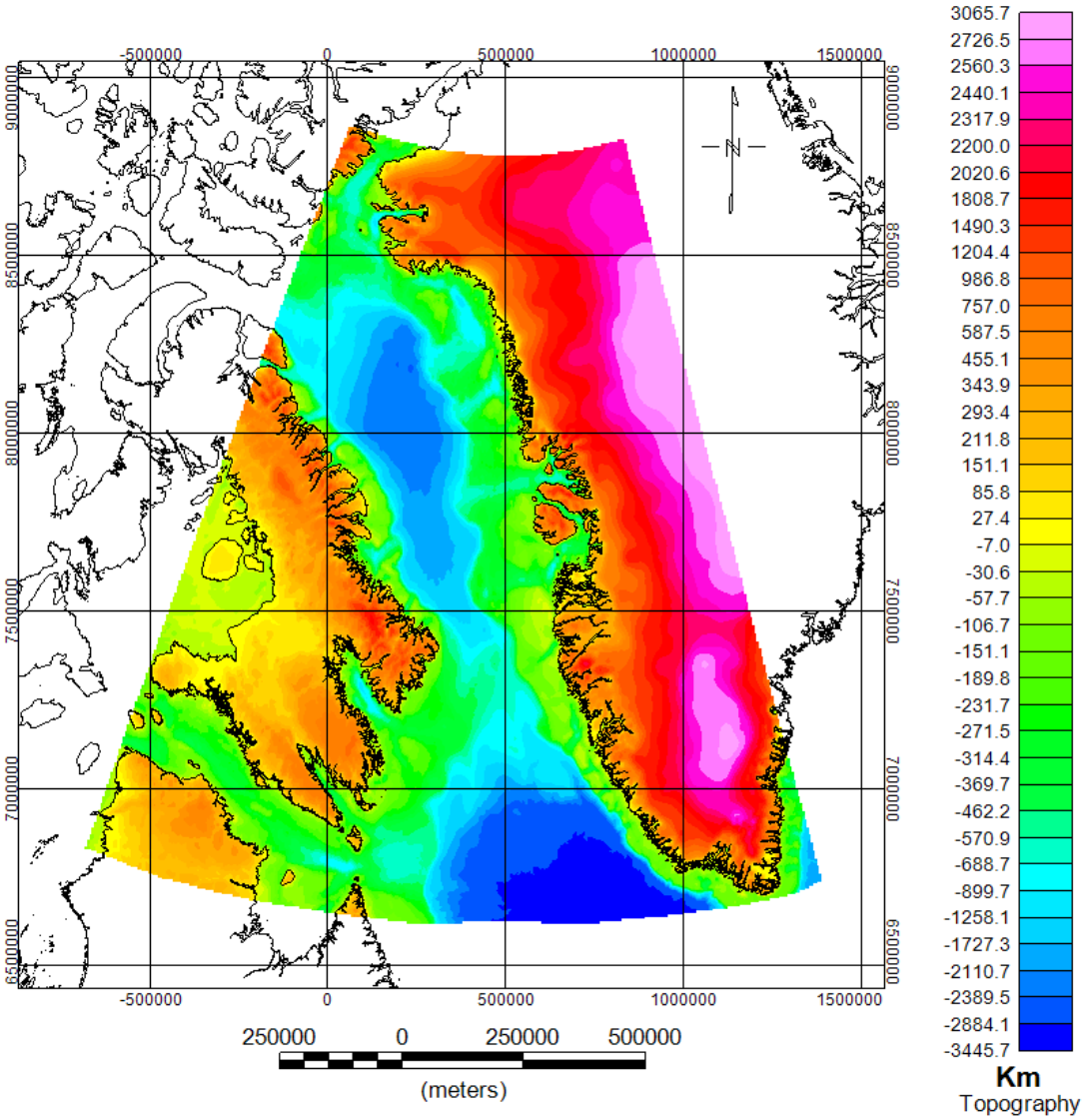

Figure 3.4: Topography map of the western Greenland margin. The deepest basin is located in the Labrador Sea south of the study area.

3.3 Seismic Interpretation

3.3.1 Synthetic seismogram

Published well logs (Gamma Ray, Density and Sonic) (Figure 3.5 and 3.6) were first scanned using Engauge Digitizer which scans well logs and saves them in text (ASCII files). The files were imported into Kingdom Suite ®, with logs being later converted and saved in LAS format to be imported into Petrel ®.

The synthetic seismograms were generated in both Kingdom suite ® and Petrel ®. All synthetic seismograms generated for all wells are shown in Figure 3.5. A correlation and integration panel for all integrated data used is shown in Figure 3.6.

The well ties were used to constrain both the age of key seismic intervals and the lithology. As some of the wells are not exactly on the seismic lines, these wells were processed and projected where appropriate. Wells are approximately 160, 130 and 250 km from the seismic lines of Cape Farewell, Disko West and Baffin Bay provinces respectively. The exception is Nuuk West provice distance between wells and lines are (0-7 km), stratigraphic interpretation away from the wells was done by correlating key horizons with the stratigraphic chart of Sørensen (2006).

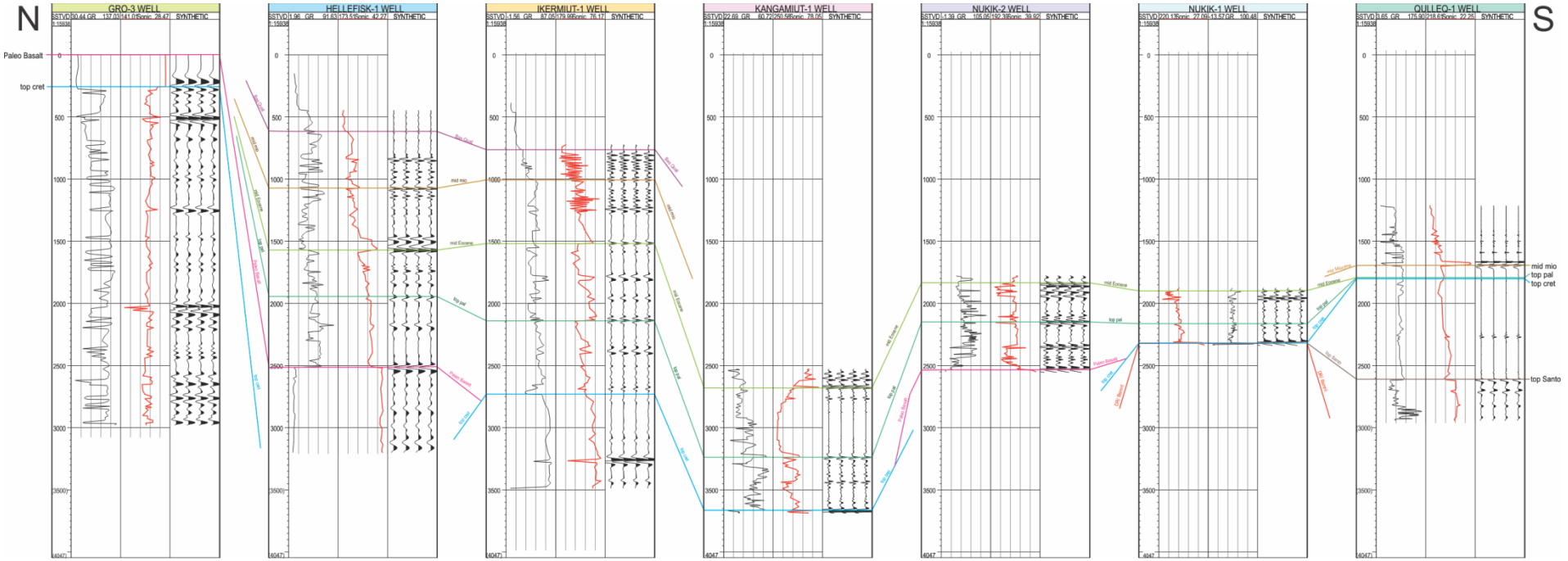

Figure 3.5: Wells cross section showing the generated well synthetics

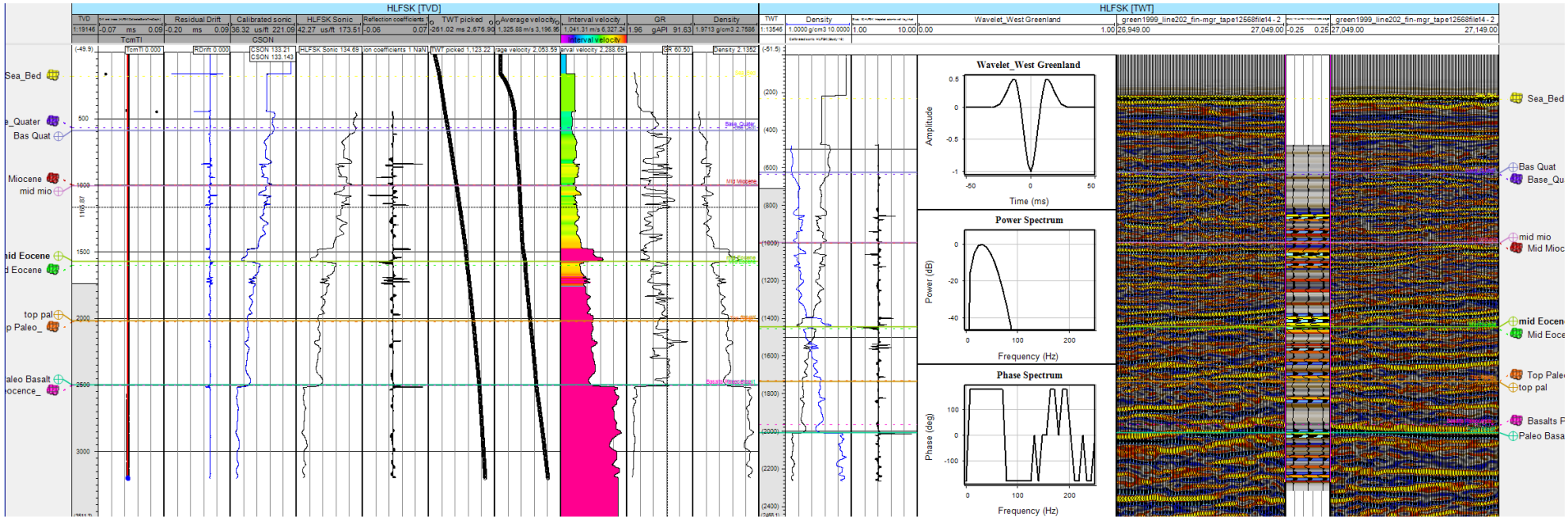

Figure 3.6: Example of Well data used for the study. Synthetic seismogram was generated to tie the well data with seismic.

3.3.2 Horizon Mapping

The European SEG convention was used for interpreting the horizons. If the signal arises from a reflection that indicates an increase in acoustic impedance, the polarity is, by convention, positive and is displayed as a trough for a zero-phase wavelet. If the signal comes from a reflection that indicates a decrease in acoustic impedance, the polarity is negative and is displayed as a peak (Figure 3.7). An increase in acoustic impedance with depth was considered to be a trough. The troughs were displayed as blue while the troughs as red (Figure 3.7). In addition to defining the seismic convention, seismic facies parameters were used to further constrain the horizons. These include amplitude, continuity, frequency variation, and reflection terminations (Figure 3.9 and 3.10).

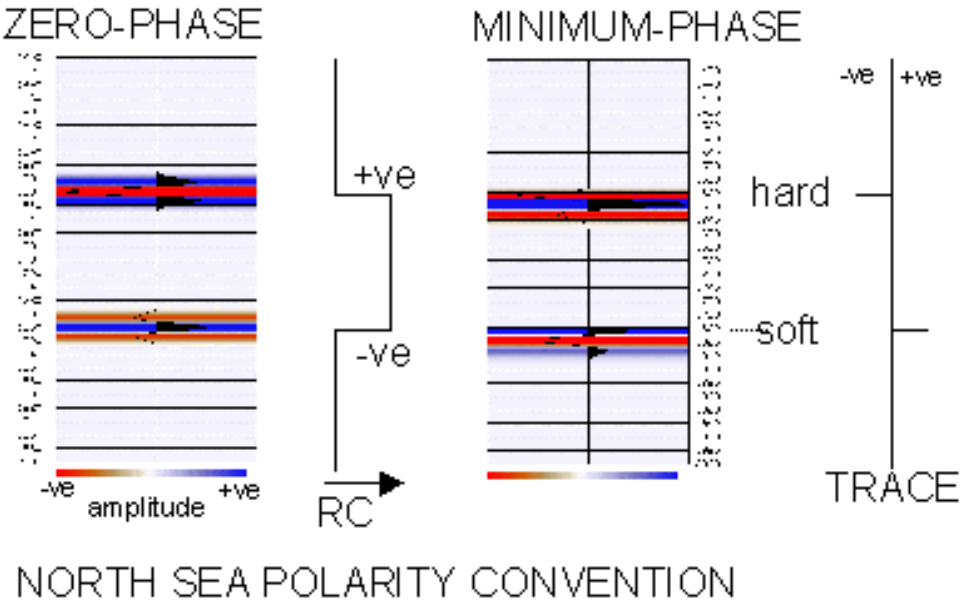

Figure 3.7: The European SEG convention was used for interpreting the seismic data. The data is zero-phased; hence an increase in acoustic impedance with depth was considered a trough.

Reflection terminations (e.g. onlap, down lap, erosional truncation) were used to identify major sequence boundaries /unconformities on seismic sections (Figure 3.9). Reflection packages were categorised as pre-rift, syn-rift, and post-rift. Furthermore, seismic facies used to discriminate megasequences include the high amplitude reflections, continuity, frequency variation and lap geometries (e.g. Mitchum Jr et al., 1977).

An onlap is a baselap in which an initially inclined surface laps out against a surface of greater initial inclination geometries (Figure 3.9; Mitchum Jr et al., 1977). Toplap is lapout at the upper boundary of a depositional sequence; it is a form of offlap. Initially inclined strata such as foreset beds and clinoforms may show this relationship. On seismic sections, the resolution may be such that the toplap lapout is too thin to be resolved and the reflections appear to truncate against the upper surface at a low angle (Badley, 1985).

From the initial seismic interpretation, nine main megasequences were identified (Table 3.2) based on differences in the seismic reflection characteristics. These include the Sea bed (SB), Base Quaternary (BQ), Mid-Miocene Unconformity (MMU), Mid-Eocene Unconformity (MEU), Top Palaeocene (TP), Palaeocene Basalt (PB), Top Cretaceous (TC), Mid-Early Cretaceous (MEC) and the Acoustic Basement (Bs) (Figure 3.6). These units were defined and correlated to the regional stratigraphic column of Sørensen (2006).

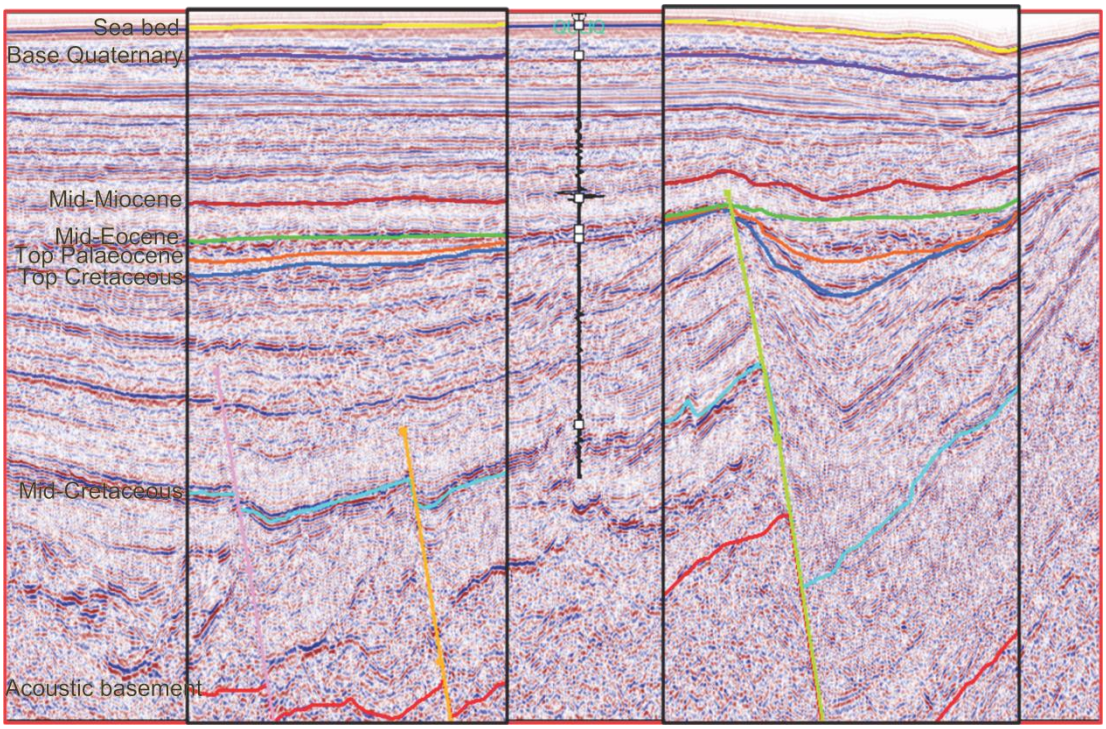

Figure 3.8: A seismic well tie integrated with seismic interpretation to ensure consistent interpretation. The use of correlation panel enhanced interpretation of horizon across the seismic lines.

3.3.3 Fault Mapping

Faults are shown as breaks or truncations of seismic reflections (Figure 3.8). They were picked concurrently with the horizons and were characterized as low amplitude zones where there is offset/truncation of reflection. Names were assigned to the major faults and were modified under the section fault management.

Fault planes were manually mapped on fault normal seismic profiles. The faults were displayed as polygons in map-view (Figure 4.1). Even with a high spacing between 2D seismic lines (8 km in Nuuk west province, 50 km in Cape Farewell, 20 to 25 km in Disko West and Baffin Bay respectively), it was possible to recognize and link major faults based on their geometries,

dip direction and the amount of displacement. Multiple lines were used to connect the faults in order to create fault array maps and constrain the geological sense of regional faults trends along the margin.

3.3.4 TWTT thickness maps

Time differences between particular horizons have been calculated to generate isochron maps, which were used to describe the regional time-thickness distribution of the packages. Two way travel time (TWTT) thickness maps can reveal (a) relative stratigraphic thickness trend (b) zones affected by faulting, and (c) general architecture of the basin. Seven isochron maps have been generated to delineate the sedimentary thickness variations of syn- and post-rift packages. These maps provide sufficient trends of the sedimentary variations to enable the basin evolution to be established. TWTT thickness maps are affected by lateral changes in seismic velocity common with changes in lithology, diagenesis and compaction, and these uncertainties have to be consider while interpreting the maps.

3.3.5 Depth Conversion

Depth conversion for the interpreted horizons was conducted using two velocity models:

1. The interval velocity obtained from the wells.
2. The stacking velocity derived from the processing algorithm.

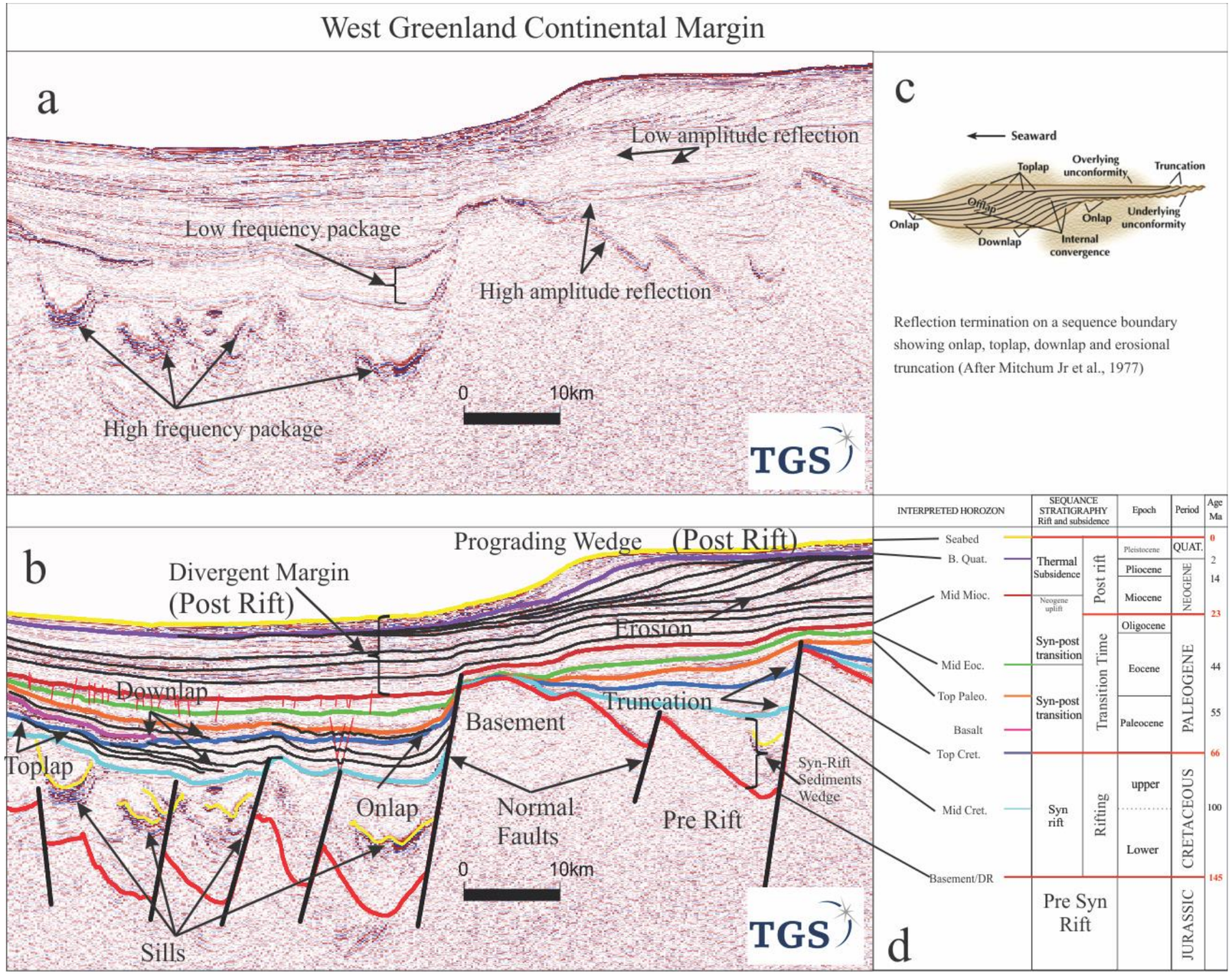

Figure 3.9: A) an examples of reflection terminations used for the seismic interpretation in (this study). Reflection attributes include continuity, amplitude, frequency/spacing (Modified after Badley, 1985). B) Interpreted seismic examples from the study area showing applied reflection termination on a sequence boundary showing onlap, toplap, downlap and erosional truncation © (After Mitchum Jr et al., 1977). D) Chronostratographic interpretation in this study.

See Appendix I for further details on the depth conversion procedure. With the aid of the Dix equation (Dix, 1955), stacking velocities were converted into interval velocities. In order to describe stacking velocities the vertical variation of velocity and inclination of subsurface beds are the two most commonly employed parameters. The stacking velocities, Vs, were obtained by using of a seismic event hyperbola. The results were used to define the room mean square velocity, Vrms. These techniques are described in Robinson and Durrani (1986), Sheriff and Geldart (1995) and Chalmers et al. (1999).

Table 3.2 Nine main stratigraphic units were identified based on differences in the seismic reflection characteristics (from youngest to oldest).

HORIZON	**SEISMIC FACIES CHARACTER**
Sea bed	Strong reflection, high amplitude
Base Quaternary	Weak reflection, low amplitude
Mid-Miocene Unconformity	Weak-discontinuous to fair reflection, low amplitude
Mid-Eocene Unconformity	Good to fair reflection with low to medium amplitude
Top Palaeocene	Strong reflection with very low amplitude
Paleocene Basalt	Continuous strong reflection, relatively high amplitude
Top Cretaceous	Strong to good reflection with low to medium amplitude
Mid Cretaceous	Good to fair reflection, low to high amplitude
Basement/Deeper Reflection	Fair reflection with variable amplitude and continuity

Chapter 4

Rift-Drift Evolution of the West Greenland Basin during the late Cretaceous and early Tertiary Break-up

4.1 Abstract

Due to its geographic extent of over 2500 km, the West Greenland margin provides a much understudied example of a divergent continental margin, both with respect to hydrocarbon exploration and academic studies. A seismic interpretation study of representative 2D reflection profiles from the Labrador Sea, Davis Strait and Baffin Bay was undertaken to identify sedimentary and structural components to elucidate the tectonic development of the margin. Nine megasequences were interpreted from six representative seismic lines in the area. Margin-scale tectono-stratigraphy was derived from isochore maps, the geometry of mappable faults and their associated stratal architecture.

Rifting began in Early to Late Cretaceous at c.145 -130 Ma, which was followed by two pulses of volcanism in Eocene and Palaeocene ages. The

transition to the drift stage includes a typical subsidence phase but also erosion, uplift and deposition of Neogene post-rift packages. The shift in the position of depocentres in the Davis Strait and the Labrador Sea during Palaeocene and Miocene times is evidence for structural modification of the basin bounding faults. Drift stage deformation suggests a possible anticlockwise rotation in the orientation of the spreading axis in Baffin Bay culminating in an ultraslow seafloor spreading.

Seafloor spreading on the West Greenland margin started in the south at 70 Ma (Chron 31) in the Labrador Sea and propagated northward into the Baffin Bay by 60 Ma (Chron 26). Prospective petroleum systems include thick Cretaceous age strata, with structural traps provided by grabens and inversion structures. Our structural model provides insight into margin that is highly variable in its structural configuration, further modified by other processes such as magma-assisted rifting.

4.2 Introduction

Although there has been considerable interest, over a number of decades, in the evolution of sedimentary basins associated with lithospheric stretching (e.g. McKenzie, 1978; Wernicke, 1985; Lister, 1986), recent studies have made significant advances in our understanding of the processes involved. These studies have greatly expanded our understanding on the variability of margins, in particular: the differences between volcanic and non-volcanic margins (e.g. Reston and Perez-Gussinye, 2007; Franke, 2013); the role of depth dependent stretching and multiple rift stages (e.g. Huismans &

Beaumont, 2011; Soares et al., 2012); and the influence of mantle plumes (White and McKenzie, 1989; Clift and Turner, 1995; Corti, 2009; Lundin and Doré, 2011). These studies commonly focus on portions of margins, or their equivalents on the conjugate margins. The aim of this study is to consider the lateral variability of a single margin. We chose the West Greenland Margin because of the interplay amongst a number of the key factors including: the presence of a mantle plume; the existence of volcanic and non-volcanic areas on the margin; and changes in extension orientations. Furthermore, the absence of salt enables us to understand margin architecture without the limitations of either sub-salt imaging or salt tectonics.

The West Greenland Margin includes the Labrador Sea, Davis Strait and Baffin Bay (Figure 4.1). The margin is considered to have formed by the northward propagation of continental rifting and seafloor spreading associated with the breakup of North America from Europe during the late Cretaceous and early Tertiary periods (Balkwill et al., 1990; Chalmers, 1991, 2000, 2012; Chalmers and Pulvertaft, 2001; Chalmers et al., 1993; Nielsen et al., 2002; Roest and Srivastava, 1989; Rowley and Lottes, 1988; Schenk, 2011).

The aim of this study is to consider the interplay amongst processes involved along an entire margin during lithospheric rifting and drifting. We describe the basin development along the West Greenland continental margin and consider the implication of this on hydrocarbon exploration. By

doing so, we quantify the overall basin fill and architecture during the different phases of basin growth. We demonstrate that the timing of initiation and cessation of rifting together with the duration of sea floor spreading are critical to improving the evolutionary models for the West Greenland margin.

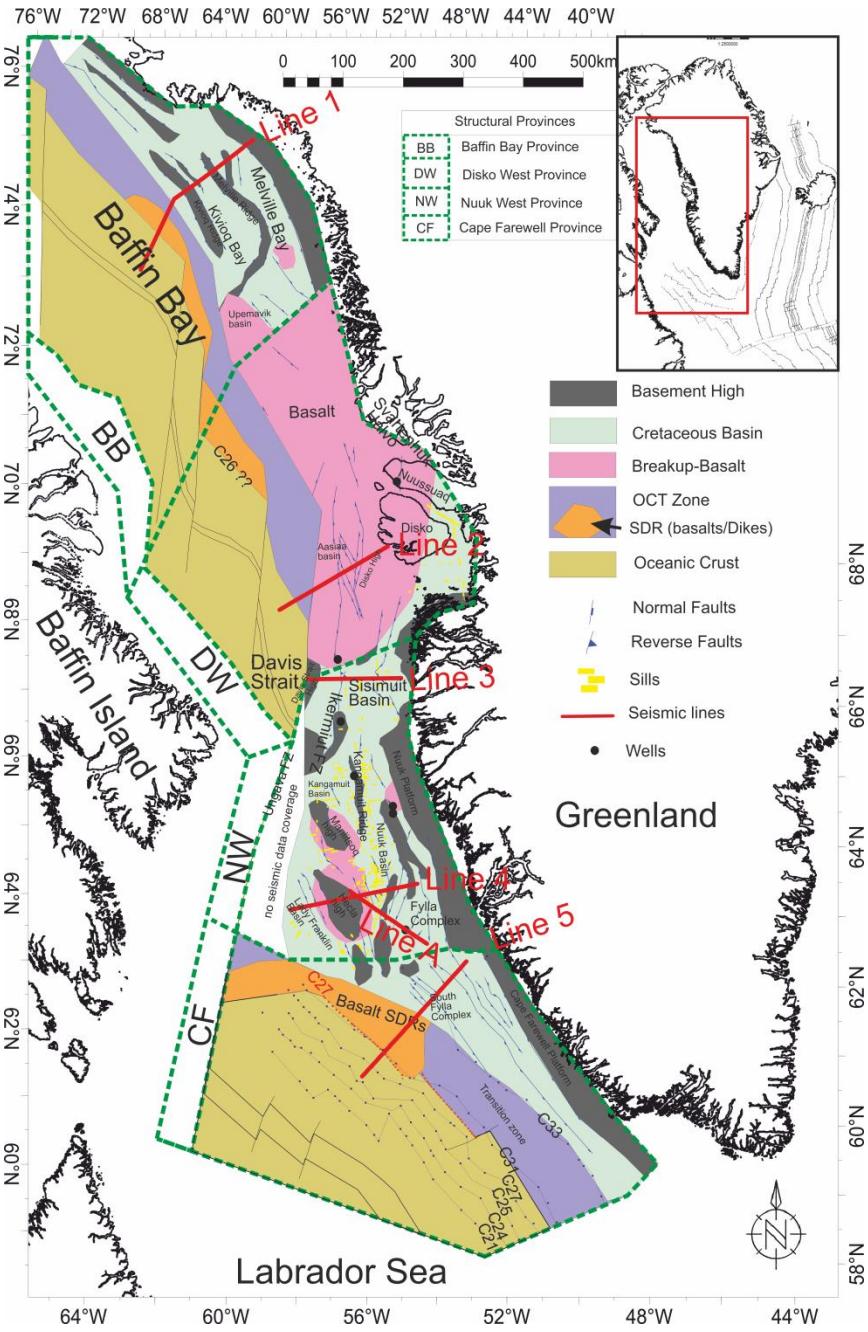

Figure 4.1: Regional tectonic framework of the west Greenland study area. Generated by data integration of, 2D seismic data (GEUS and TGS), Structural Provinces after Knutsen et al., (2012) . Global Seafloor Fabric and Magnetic chrons from Roest & Srivastava 1989; and Chalmers and Laursen (1995). Seafloor from Müller 2008 which has been modified to fit data seismic, gravity and magnetic characteristics. New COT boundaries have been interpreted based on multidisciplinary data integration of seismic reflection, refraction interpretation, gravity, magnetic 2D modelling and backstripping thermal subsidence modelling.

4.3 Tectonic and Geological settings of the Western Greenland basin

The earliest rifting event probably occurred in the Early Cretaceous (c.145 - 130 Ma) or Late Jurassic periods (Schenk, 2011; Harrison et al., 1999). A second rifting event of Late Cretaceous and early Palaeogene age culminated in thermal subsidence and subsequent passive margin sedimentation at ~ 60 Ma (Dam et al., 2000).

The Early Cretaceous rifting event is evidenced by deposition of clastic sediments in half grabens and graben basins, such as the Kitsissut and Appat sequences (Chalmers and Pulvertaft, 2001). Sedimentary facies within this area includes alluvial fan, fluvial, fan-delta, deltaic and shallow lacustrine sandstones and mudstones of the Kome and Atane Formations from Nuussuaq basin (Balkwill et al., 1990; Chalmers and Pulvertaft, 2001; Dam et al., 2000).

A Late Cretaceous unconformity separates deltaic deposits of the upper Albian-lowermost Campanian Atane Formation from fully marine deposits of the lower-middle Campanian Itilli formation (Dam et al., 2000). This

Campanian Formation is equivalent to the Fylla sandstone, which is overlain by Kangeq Formation offshore West Greenland. The Kangeq seismic sequences in West Greenland basin were probably deposited into a thermally subsiding basin (Chalmers et al., 1993; Chalmers and Pulvertaft 2001). The oldest Mesozoic sediments in the Baffin Bay region are Aptian to Lower Albian sandstones of the Quqaluit Formation, described by (Burden and Langille, 1990).

The Aptian-Albian mudstone units of the upper Bjarni Formation on the Canadian Labrador shelf are equivalent to the Appat Formation of Greenland. Similarly, the lower Bjarni Formation is equivalent to the Kitsissut Formation of West Greenland (Chalmers et al. 1993, 2012). An unconformity is present between the Cretaceous and early Paleocene mudstones (Nøhr-Hansen and Dam, 1997). Early Palaeocene mudstones were deposited above the Kangeq Formation (Chalmers and Pulvertaft 2001).

The onset of the second rifting event took place in the early Tertiary (Chron 27, *c*. 61 Ma) and was probably associated with seafloor spreading along the West Greenland margin (Oakey and Chalmers, 2012). Extrusion of plateau basalts in both offshore and onshore West Greenland took place in the late Palaeocene and Eocene and is overlain by the fluvio-deltaic and marine sediments of early Palaeogene age (Chalmers, 2012). Offshore basalts drilled in the Hellefisk-1 and Nukik-2 wells have been interpreted in the Hecla and Maniitsoq Highs (Chalmers et al., 1993, Rolle, 1985). Basalt layers in the southern part of Baffin Bay represent the northernmost

extension of the volcanic rocks found in the Davis Strait and were possibly expanded equivalents of sea-floor spreading in Baffin Bay (Whittaker, 1997; Rolle, 1985).

The Labrador Sea and Baffin Bay regions are connected by the Ungava transform fault zone in the Davis Strait area (Figure 4.1). The Ungava transform fault zone is characterized by complex structures that were initially extensional. These structures were subsequently affected by both transtension and transpression processes as the Ungava fault zone evolved into a transform zone (Skaarup et al., 2006; Sørensen, 2006). A Mid-Eocene unconformity was then developed (Nøhr-Hansen and Dam, 1997) as a result of strike slip movement across the margin as well as the Ikermiut flower structure (Chalmers et al., 1999).

From mid-Eocene times, the West Greenland Basin subsided without further obvious evidence of tectonism, until late Neogene times (Chalmers and Pulvertaft 2001; Green et al., 2011). Strata of largely fine-medium grained clastics were deposited as slope and fan sandstones as a result of the second post-rift subsidence phase (Dalhoff et al., 2003; Schenk, 2011)

Neogene uplift in the central part of the West Greenland margin is recorded by 2-3 km uplift in the Nuussuaq Basin (Chalmers, 2000, Chalmers and Pulvertaft, 2001). Offshore evidence on seismic can be seen in the uplift of the eastern Sisimiut Basin (Dalhoff et al., 2003). In the Northwest end of Baffin Bay channel erosion is observed which is probably related to

Neogene uplift in the Jones Sound, southern Nares Strait and Lancaster Sound (Harrison et al., 2011). The cause of Neogene uplift is still unknown. Although, subsidence analysis of the margin reveals that Neogene uplift is unrelated to subsidence in offshore areas (McGregor et al., 2012).

4.4 Tectonostratigraphy

The nine megasequences interpreted include sea bed (SB); base Quaternary (BQ); Mid-Miocene Unconformity (MMU); Mid-Eocene unconformity (MEU); top Palaeocene (TP); Palaeocene basalt (PB); top Cretaceous (TC): Mid-Early Cretaceous (MEC); and acoustic basement (Bs). The high amplitude (peak) and continuous nature of the SB, MMU, MEU, TP, and MEC reflections provided a high confidence interpretation whereas the moderate to discontinuous (trough) reflector character of TC, PB, BQ and Bs reflections resulted in some uncertainty in the interpretation. The Acoustic Basement (Bs), Mid Cretaceous and Top Cretaceous reflectors were not mapped in Disko West as they have been masked by the overlying Palaeocene basalt

The main structural domains of the margin are Baffin Bay, Davis Strait and the Labrador Sea. These major basins define the West Greenland margin and are characterised by a large variety of complex structures including grabens, half-grabens, horsts, flower structures, and thrust faults. These structures, and the associated sedimentary packages within the basin fill, represent a multi-phase evolution of the margin. At the margin scale, this complex evolution can be simplified into four phases of deformation rifting,

transition, seafloor spreading and Neogene uplift (Figure 4.2). The pre-rift strata are characterised by parallel reflectors that can extend down to the acoustic basement.

Syn-rift packages display characteristic sediments wedging geometry across basin-scale faults. The earliest rift phase is of Lower Cretaceous to Late Cretaceous in age and defines the main graben structures. The transition period from rifting to drift stage is interpreted to be of Early Palaeocene to Mid Eocene age. Post-rift phases, in which no fault controlled thickening is observed occur above the mid-Miocene unconformity. There is significant erosional truncation and uplift in a number of areas of the margin in particular at Mid Eocene and Mid-Miocene level. Neogene uplift also affected the margins.

4.4.1 Structure and History of the Individual Basins

Recent studies have sub-divided the margin into four structural provinces namely, Cape Farewell, Nuuk West, Disko West and Baffin Bay basins (e.g. Knutsen et al., 2012; Figure 4.1). We describe the main structures and basin fill within these provinces using interpreted 2D seismic lines to compare and contrast the variation in stratigraphic and structural configurations along the margin (Figure 4.2). We focus on the main basins in each province, which include Kivioq and Melville Bays and the Upernavik basin in Baffin Bay province, the Aaisaa basin in the Disko West province; the Lady Franklin, Kangamuit, Sisimuit and Fylla complex Basins in Nuuk West province; the

south Fylla complex basin and the Cape Farewell basin in Cape Farewell province (Figure 4.1).

4.4.2 Baffin Bay Province (BB)

The structure of Baffin Bay province is characterised by two NW-SE trending grabens (Kivioq and Melville Bays) that are separated by the intervening Melville Ridge (Figure 4.4). The two grabens, which are broadly asymmetric, comprise features that are approximately 50 km wide and over 310 km long with sediment thickness of up to 5.0 second TWTT in the Melville Bay area (Figure 4.5). The Kivioq Basin is 200 km long and 25 km wide; whereas the Umberk Basin is 80 km long by 50 km wide (Table 1). The Melville Ridge has minor sediment accumulation on top of it (~0.1 second or less) suggesting that it remained a structural high throughout most of the evolution of the margin (Figure 4.4).

The graben-controlling faults are commonly planar structures with displacements of up to 4.5 second TWTT, and are correlatable along trend as a single fault (Figure 4.5) in excess of 310 km in length in the interior of the Baffin Bay Basin (Figure 4.1). In addition to the graben forming structures, a number of intra-basin faults with the same orientation as the basin bounding faults are observed with displacements of up to 1.0 second TWTT. As would be expected, these latter faults have shorter lengths compared to the boundary faults.

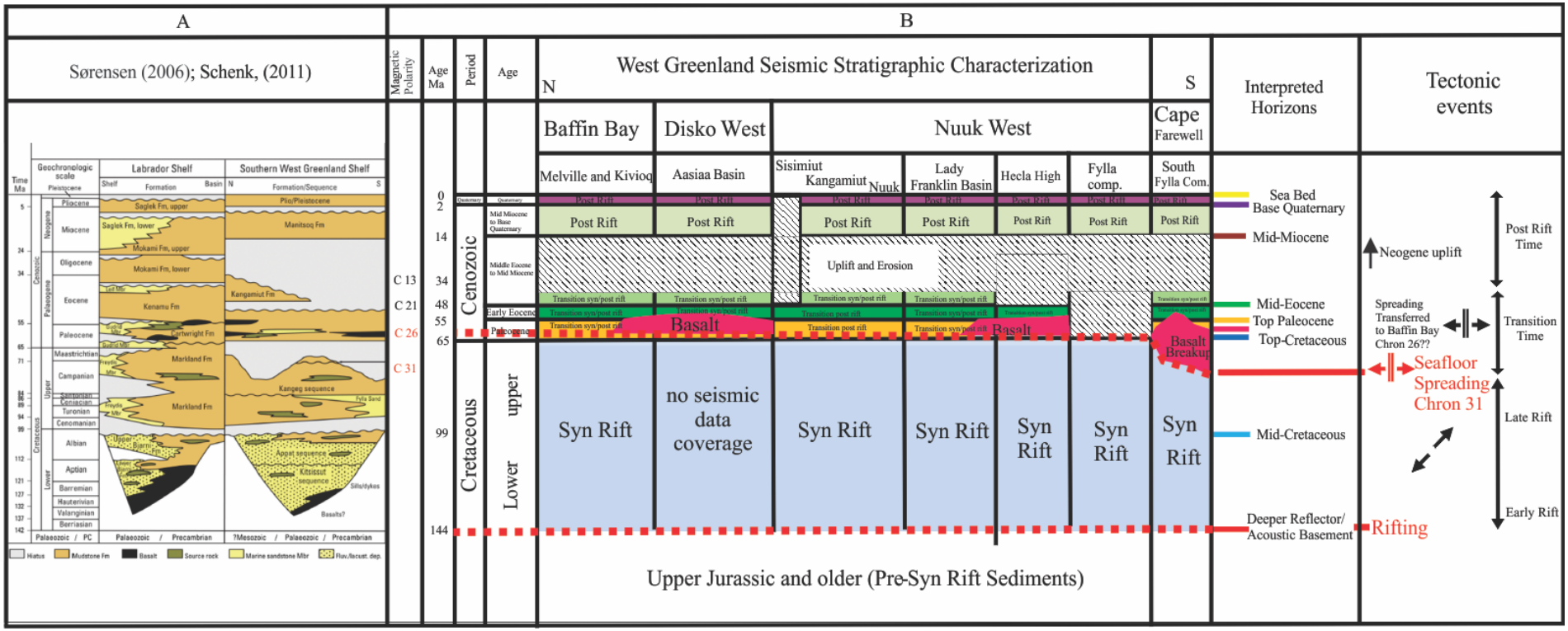

Figure 4.2: Correlation of stratigraphic columns: A) southwest Greenland generalized stratigraphy after Sørensen (2006) and Schenk (2011). B) Whole provinces of west Greenland margin stratigraphy (this paper) differential subsidence and uplift among these basins have been established.

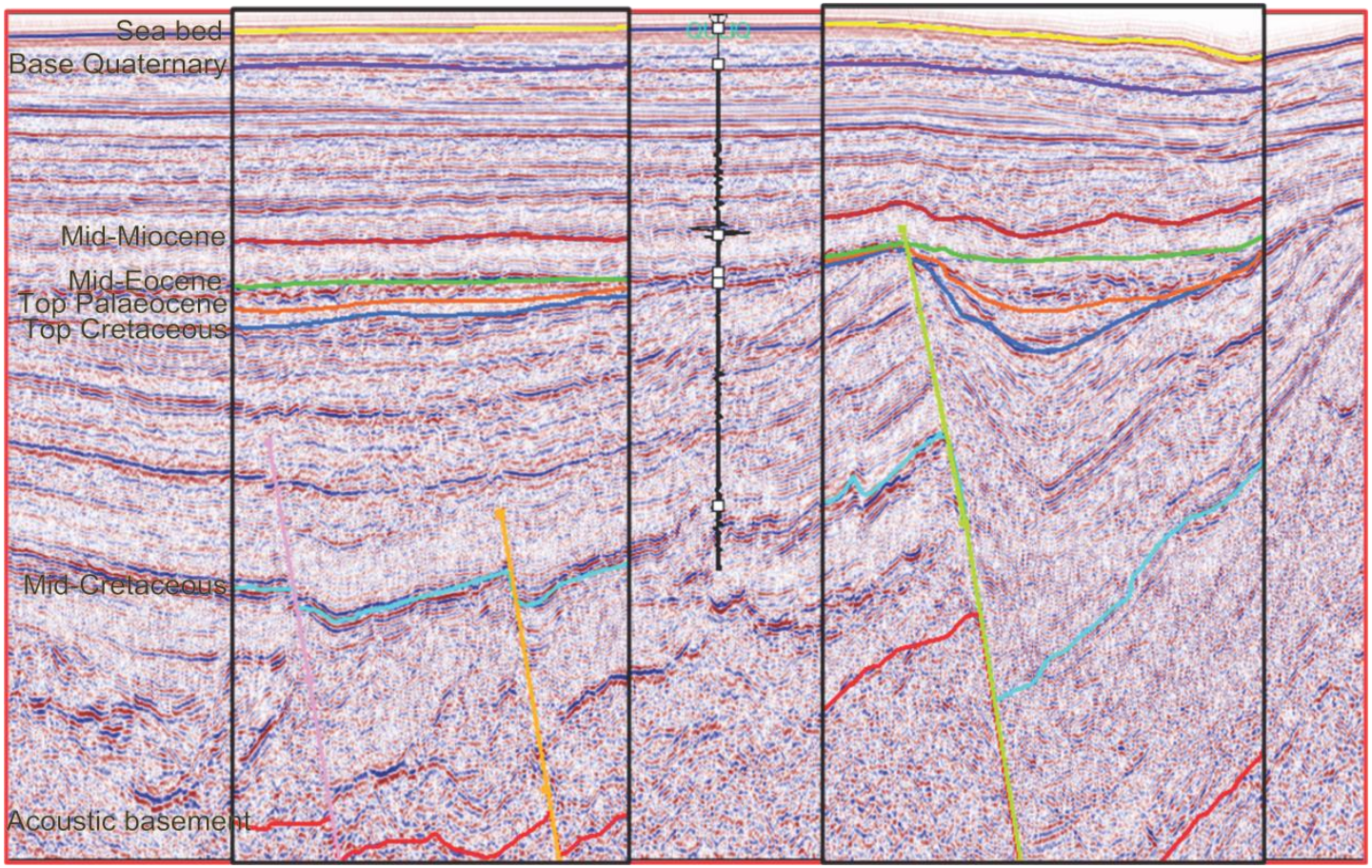

Figure 4.3: Seismic profile of Line A showing Well information tied to the seismic reflection and interpreted seismic Megasequences (line position in Figure 4.1).

Despite the distance from Baffin Bay to the closest well tie-point of 800 km away from the representative seismic line, the continuous nature of the principal mega-sequence reflections allows the correlation of the packages into the province with some degree of confidence. The rift phase in Baffin Bay Province is Lower Cretaceous and was controlled by many of the main basin bounding faults, e.g. the Melville Platform fault. However, not all the faults were active during the earliest stages of rifting, with much of the regional vertical displacement being accommodated on a master fault that is now in the middle of the Kivioq Basin. These dominant faults became inactive before the cessation of rifting (Figure 4.4). Instead, the majority of thickening (often sediments thickness up to 0.5 second TWTT) during the late stage of rifting is localised onto the graben bounding faults (Figure 4.5) such as the Northern Kivioq Ridge Fault, the Northern and Southern Melville Ridge Fault and the Southern Melville Platform fault (Figures 4.7, 4.8 and 4.11).

During the transition phase from early Palaeocene to mid Miocene, sediments are characterised by wedging and thickening towards the faults, are truncated against Kivioq Ridge fault and are thinner than Cretaceous syn-rift sediments. The post-rift package from mid Miocene to present thins towards the South which is likely to be a reflection of a reduction in sediment supply from the margin towards the north and differential compaction (See Figures 4.12, 4.13 and 4.14).

As noted, the Baffin Bay province is dominated by a series of grabens demarcated to the south by the Kivioq Ridge (Figure 4.4). Across the ridge there is a rapid transition over 20 km from continental crust across the gravity high and into a transition zone (Figure 4.4). The continental region as a whole is characterized by large rotated basement blocks composed of seaward dipping faults and a deep syn-rift basin. The central area of Baffin Bay is bounded by a collapsed structure created by an inclined West limb and a sub-horizontal to gently dipping eastern limb (Figure 4.4). The transition zone is characterized by thinner syn-rift sediments, basalts and seaward dipping reflectors (SDR) that separates rotated continental basement faulted blocks from the oceanic crust. The oceanic crust is interpreted in the southwest part of Baffin Bay and evident as a chaotic reflection occurring at depth of ~4800 ms TWTT.

The most common fault geometry observed includes horst and graben structures resulting from NW-SE normal faults that divide the Baffin Bay basin into NW-SE structural domains. A NE-SW fault also divides the Kiviog Basin from the Upermavik Basin (Figure 4.1). These NE-SW faults, ridges and sub-basins were initiated during the earliest phases of rifting (Figure 4.4). Deposition of Cretaceous sediments in Baffin Bay was into an extensive basin in Kivioq and Melville Bay basin (Figures 4.5) which is at least 5.0 second TWTT thick. The Melville Ridge is a topographic high on the NE part of the bay (Figure 4.1). The total thicknesses in Melville and Kivioq sub-basins are approximately 5.0 second to 4 seconds TWTT respectively (Figures 4.4 and 4.5).

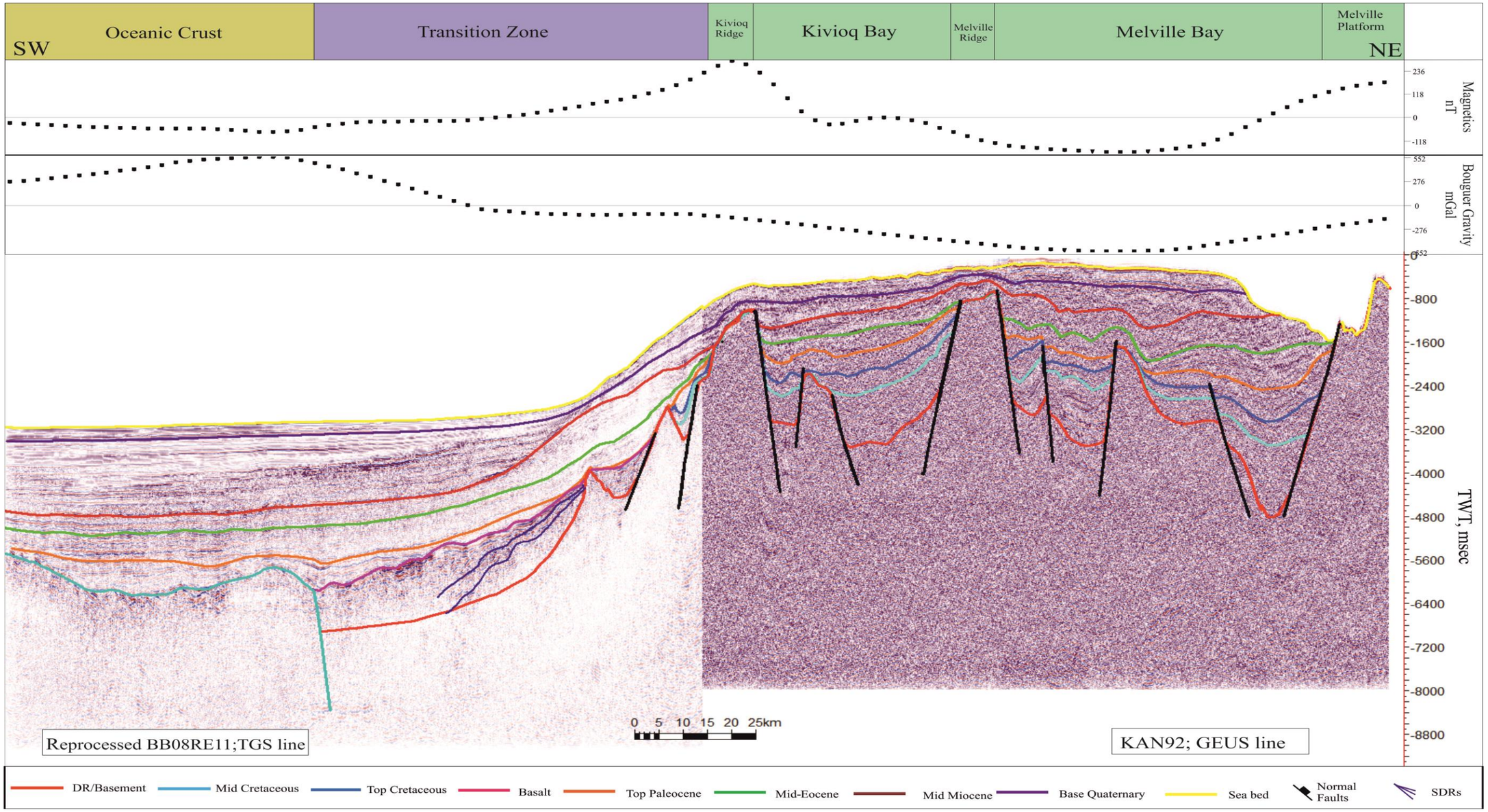

Figure 4.4: Seismic profile line 1 (line position in Figure 4.1) showing the interpreted sedimentary units in north Baffin Bay Province. Syn-rift sediments of lower and upper Cretaceous in Melville Bay and Kivioq basins. Transition zone sediments include the Paleocene and early Eocene sediments and post-rift sediments from mid-Miocene to present. The oceanic crust exposed at c. (6.0 second TWTT) southwest of Kivioq ridge. A transition zone at c. (4.5 Second TWTT) between the oceanic and continental crust and charecterised by SDRs and basalt. Half right part is Kan92 of (GEUS) seismic data and other half on the right is reprocessed BB08RE11 (TGS) seismic data.

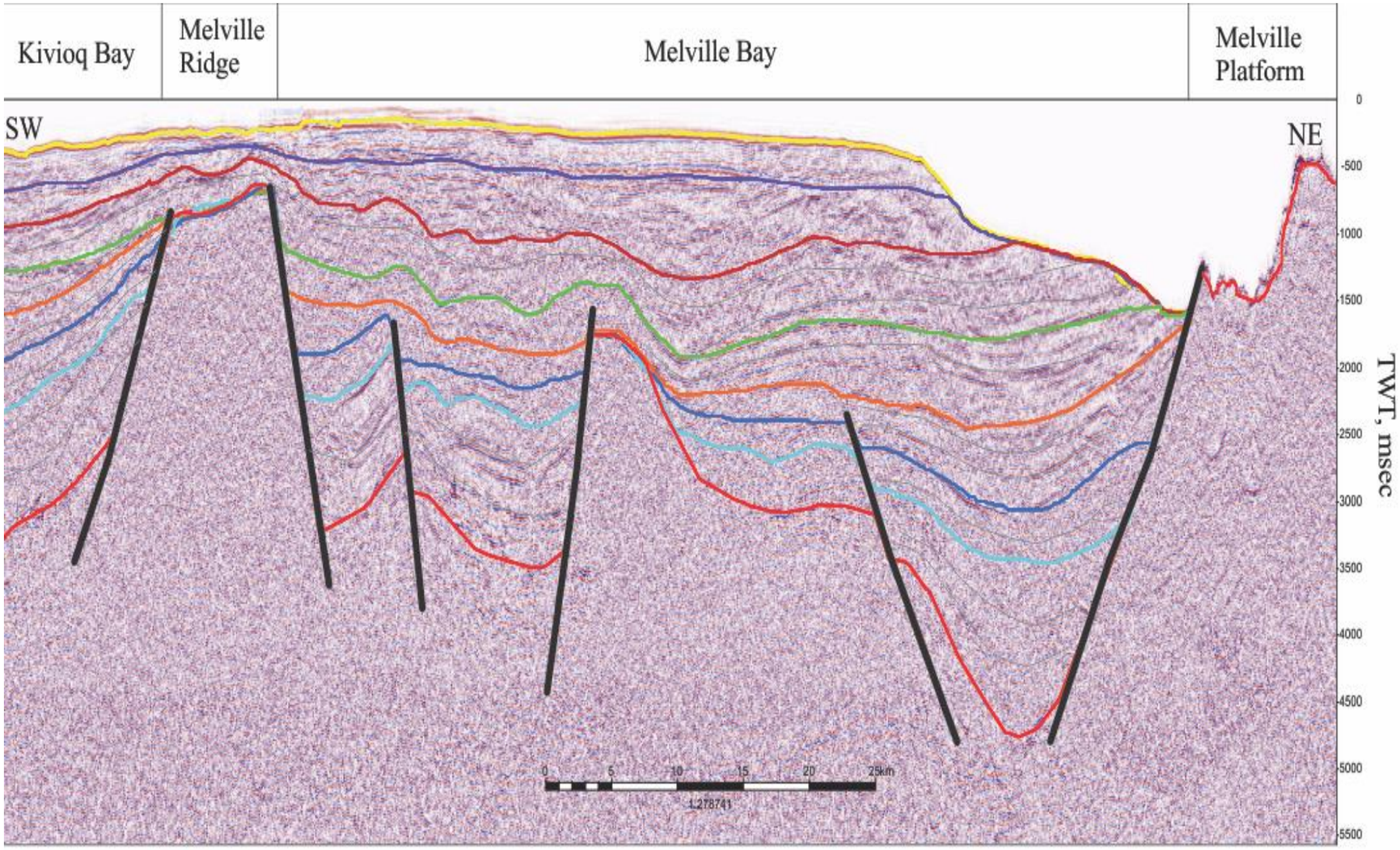

Figure 4.5: Zoomed in section of (Figure 4.4) in Baffin Bay Province showing Horst and Graben structures. Syn-rift sediments wedges of lower and upper cretaceous in addition to the Paleocene and Eocene sediments in Melville bay. post-rift sediments include the Mid- Miocene to present time. All sediments deposited in the isolated Melville Bay. The Bay is bounded by Melville platform on the right hand side (sediments wedges and onlapping) and Melville ridge on the left hand side (sediments truncating).

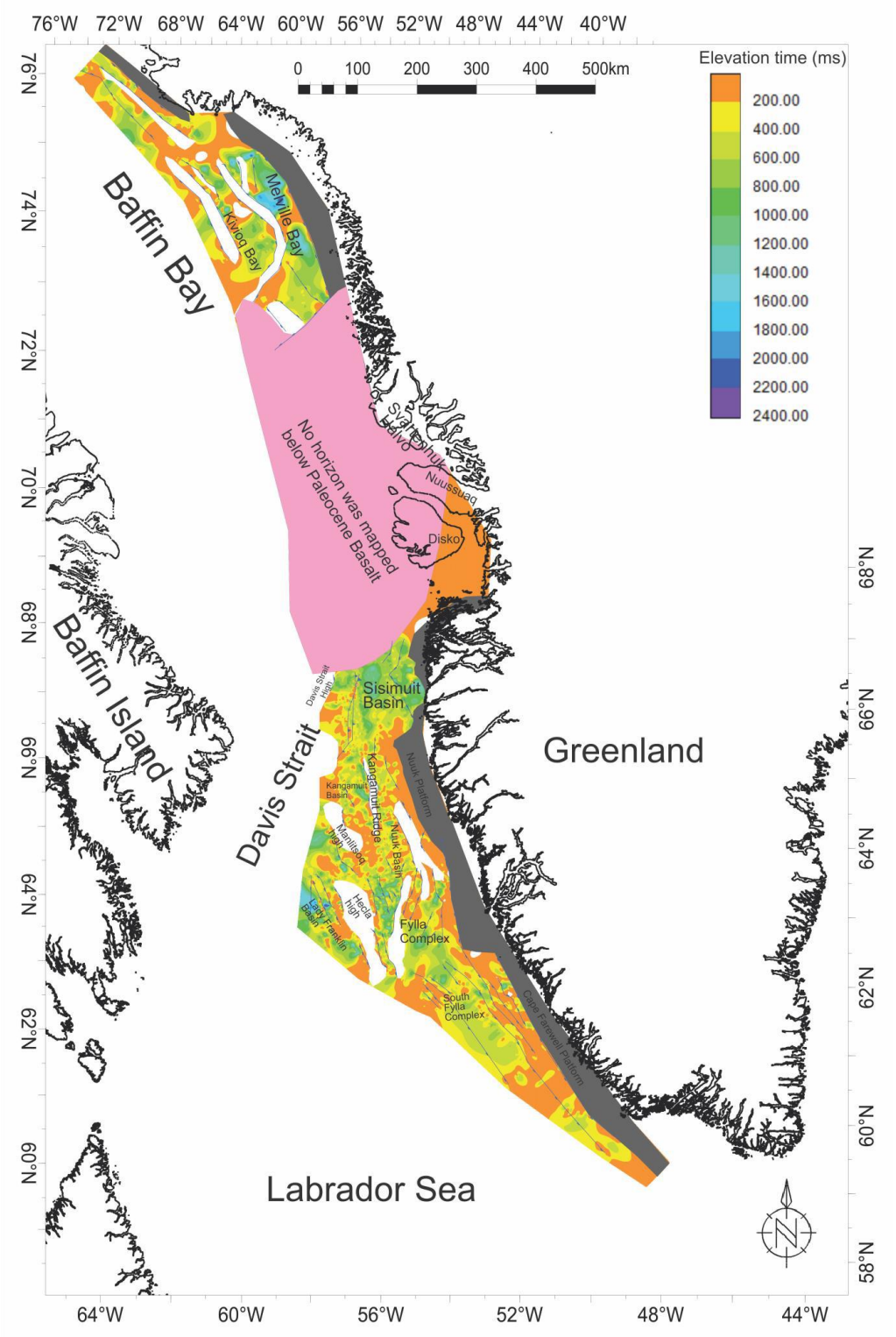

Figure 4.6: Mid-Cretaceous to Acoustic Basement isochron map

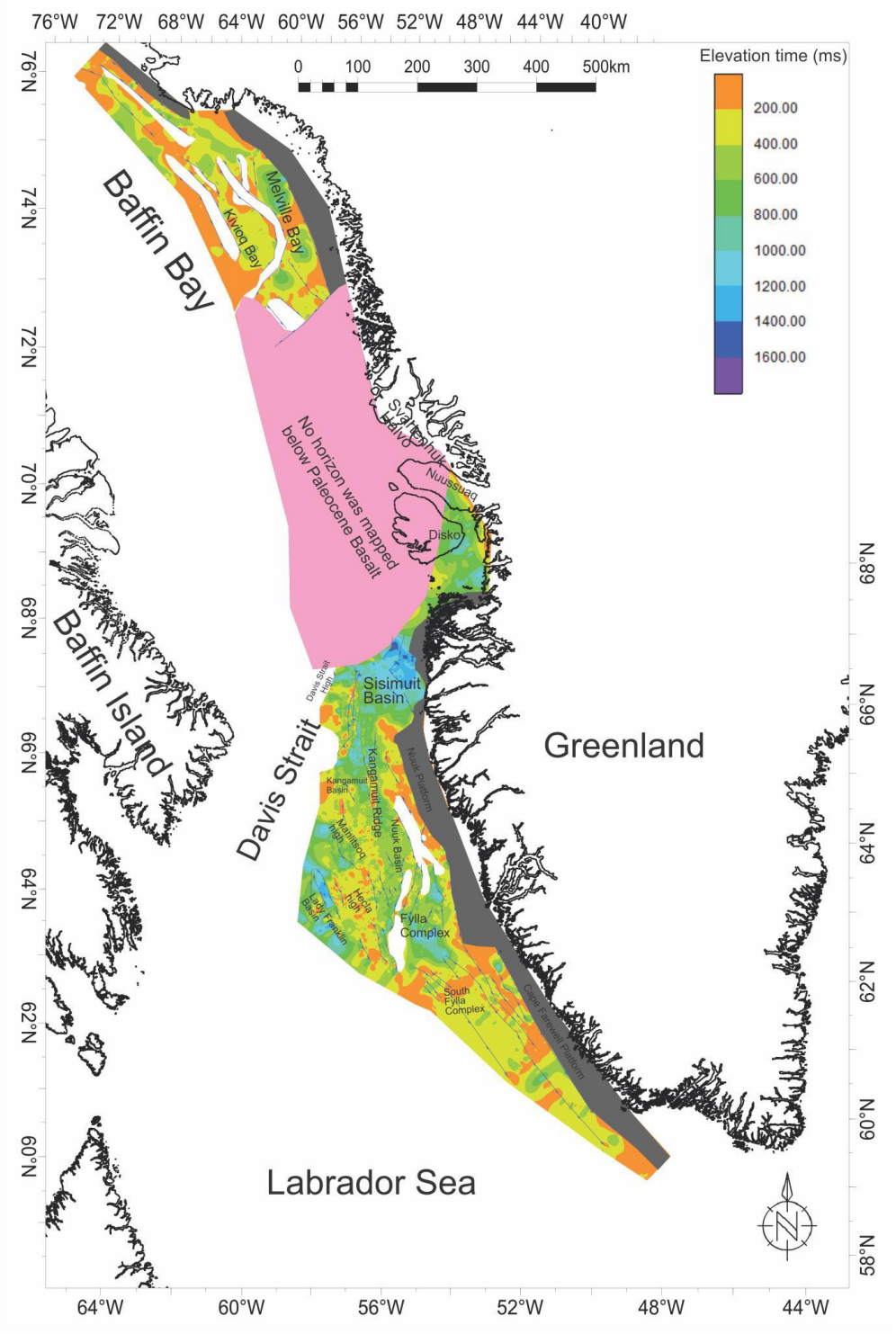

Figure 4.7: Top Cretaceous to Mid-Cretaceous isochron map

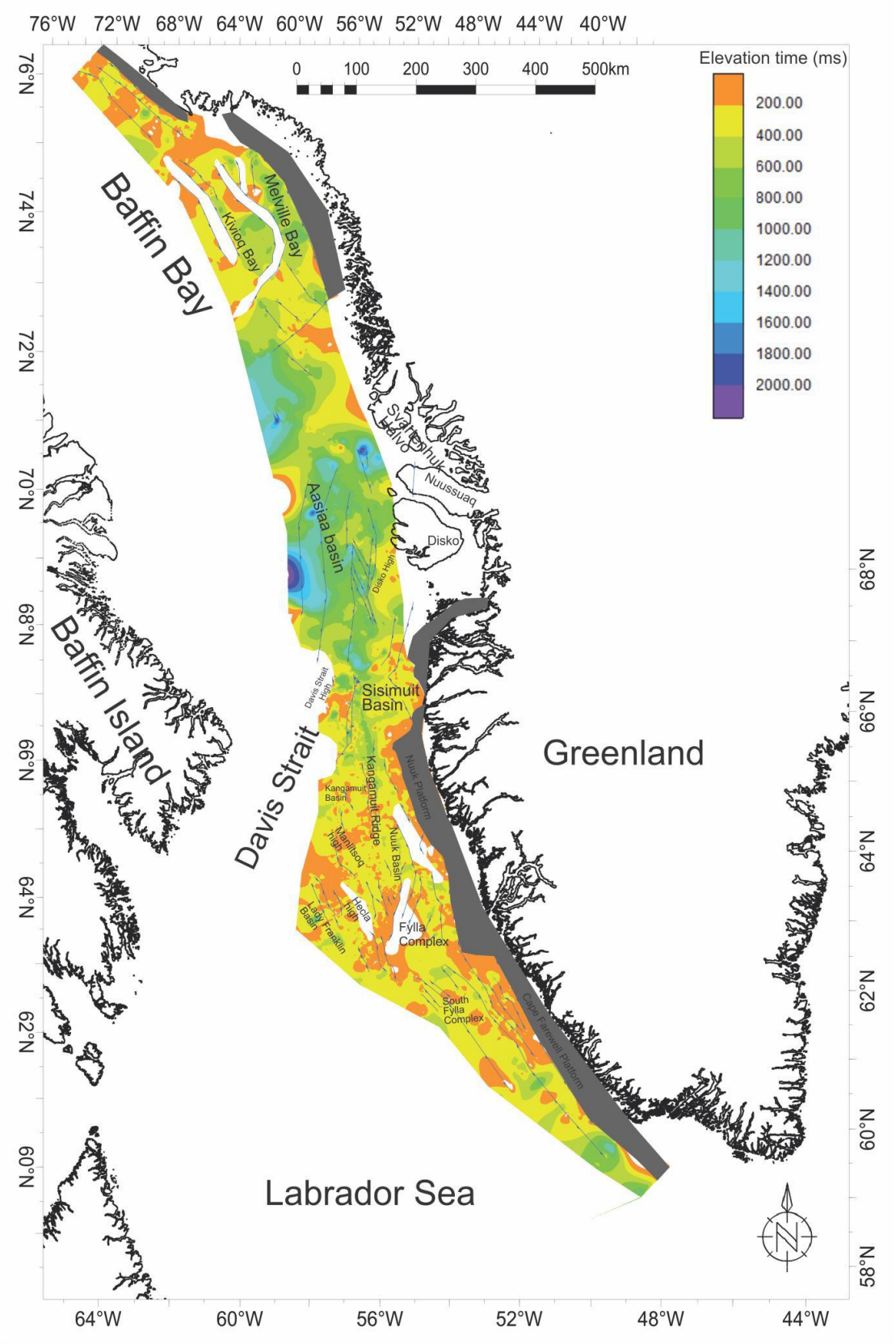

Figure 4.8: Top Palaeocene to Top Cretaceous isochore map

4.4.3 Disko West Province (DW)

The deepest reflection that is imaged in the Disko West province is the Paleocene Basalt (PB), which is identified as a high-amplitude reflection and is mappable both across the margin and along the Aasiaa Basin. The Aasiaa Basin is 350 km long and 30 to 110 km wide and the Disko High is 280 km long and 40 to 60 km wide (Figure 4.1 and 4.8). The Nussuaq basin is 130 km long and 60 km wide (Table 1). This indicates that the volcanic rocks cover an area of ~150,000 km^2 (Figure 4.1). Evidence from boreholes, seismic reflection and refraction data located both west and east of Disko Island indicate the presence of thick clastics sediments of Cretaceous age implying that the area is underlain by Cretaceous strata (Chalmers et al., 1999; Dam et al., 2009, Funck et al., 2012; Suckro et al., 2013 and 2012). This is supported by the presence of similarly aged stratigraphy that is found in the east of the Disko West province that has not been covered by basalt (Figure 4.1). Although the basalt geometry is not imaged, the basalt reflection package is remarkably continuous.

In Disko West Province, the faults are dominated by steeply dipping normal faults with a series of half grabens with lengths of up to 350 km and widths of 110 km (Figures 4.9). The faults show clear thickening of up to 0.6 second TWTT during the Top Cretaceous-Top Paleocene package (Figures 4.8 and 4.10). In contrast to the basin bounding faults in Baffin Bay, these faults (N-S and NW-SE) are present in sigmoidal plan view geometry and most likely resembles fault within a pull-apart basin. This is supported by the presence of strike-slip faults within the area. Towards the southwest, post-basalt

faulting is very limited. The exception is a few relatively small normal faults on the eastern flank and a normal fault on the northern edge of the Davis Strait High (Figure 4.1). However, mapping of gravity and magnetic anomalies suggest that oceanic crust is present with a probably age of 60 Ma (~chron 26; Oakey and Chalmers, 2012). Reflections above the oceanic crust clearly show significant thickening of post-rift wedge (Figures 4.9 and 4.10) from approximately 0.1 second TWTT in the northeast nearshore to 1.5 second TWTT in the southwest. This thickening is most evident in the Mid-Miocene to Quaternary packages (Figures 4.13 and 4.14). The thickness variation is unrelated to rifting but deposition of post-rift packages into topography created by the emplacement of the basalt.

4.4.4 Nuuk West Province (NW)

The Nuuk West Province has a number of strike-slip structures that trend broadly in a NE-SW orientation and are associated with the Ungava transform fault (Figures 4.15 and 4.16). In terms of this province length, the Nuuk West province is about 550 km long from the Fylla complex structure to the Sisimut Basin and has a width of 150 km in the North and 260 km in the South (Table 1). The geometry in the South of the Nuuk West Province is remarkably different from that to the North. Instead of a relatively unfaulted flexure, the South is dominated by a number of basement highs (Hecla, Manlitsoq, Kangamuit, Fylla) separated by grabens and half-grabens, different from the faulted north.

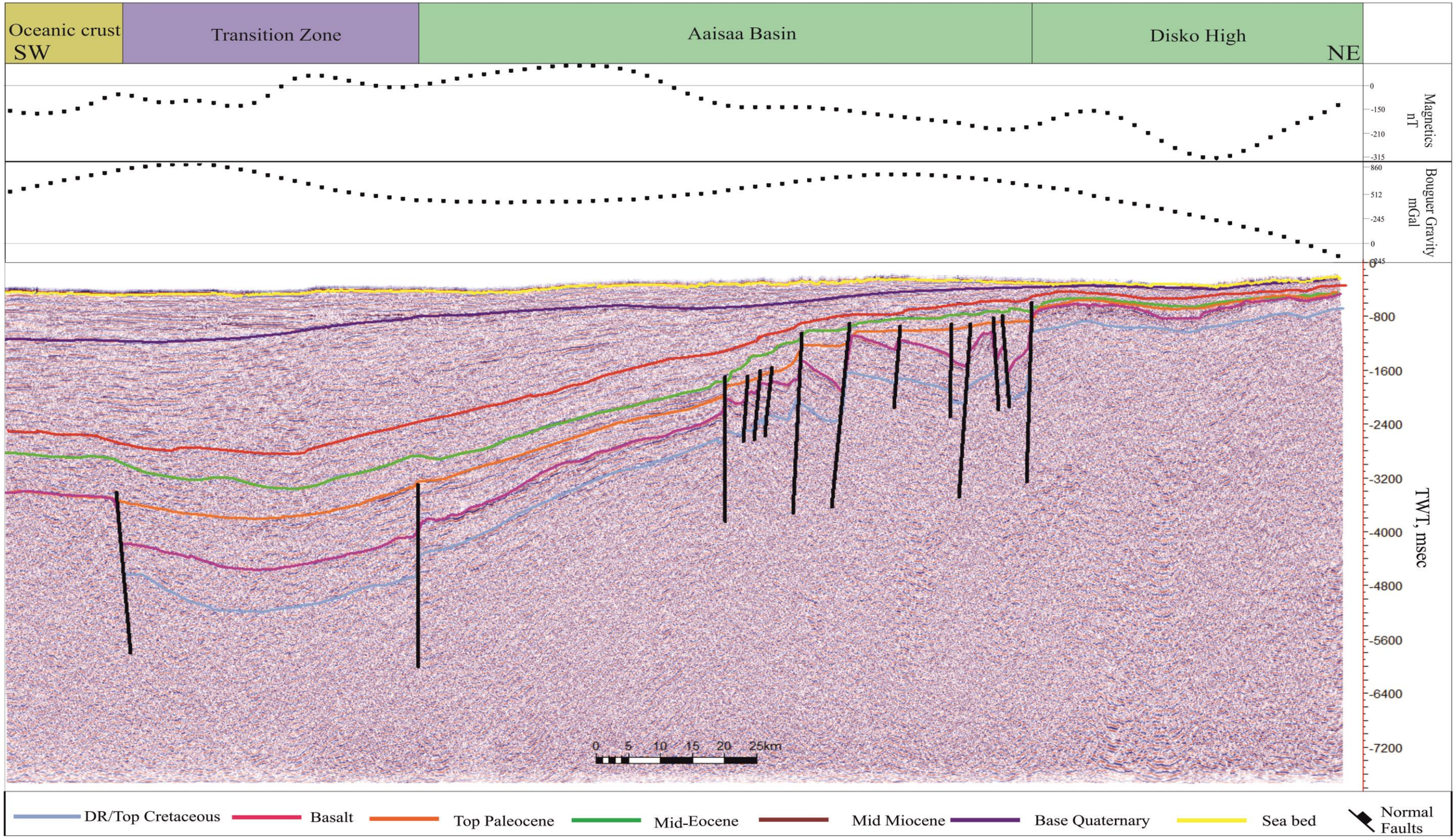

Figure 4.9: Seismic profile line 2 (line position in Figure 4.1) showing the interpreted sedimentary units of syn-rift in the Disko West Province including Basalt, Paleocene and early Eocene sediments. Post-rift from mid- Miocene to present sediments. Cretaceous Syn rift sediments masked by a basalt layer. The approximate position of transition zone to continental crust which occurs at c. (4.5 second TWTT). The oceanic crust exposed at c. (3.8 second TWTT) southwest of Aaisaa basin

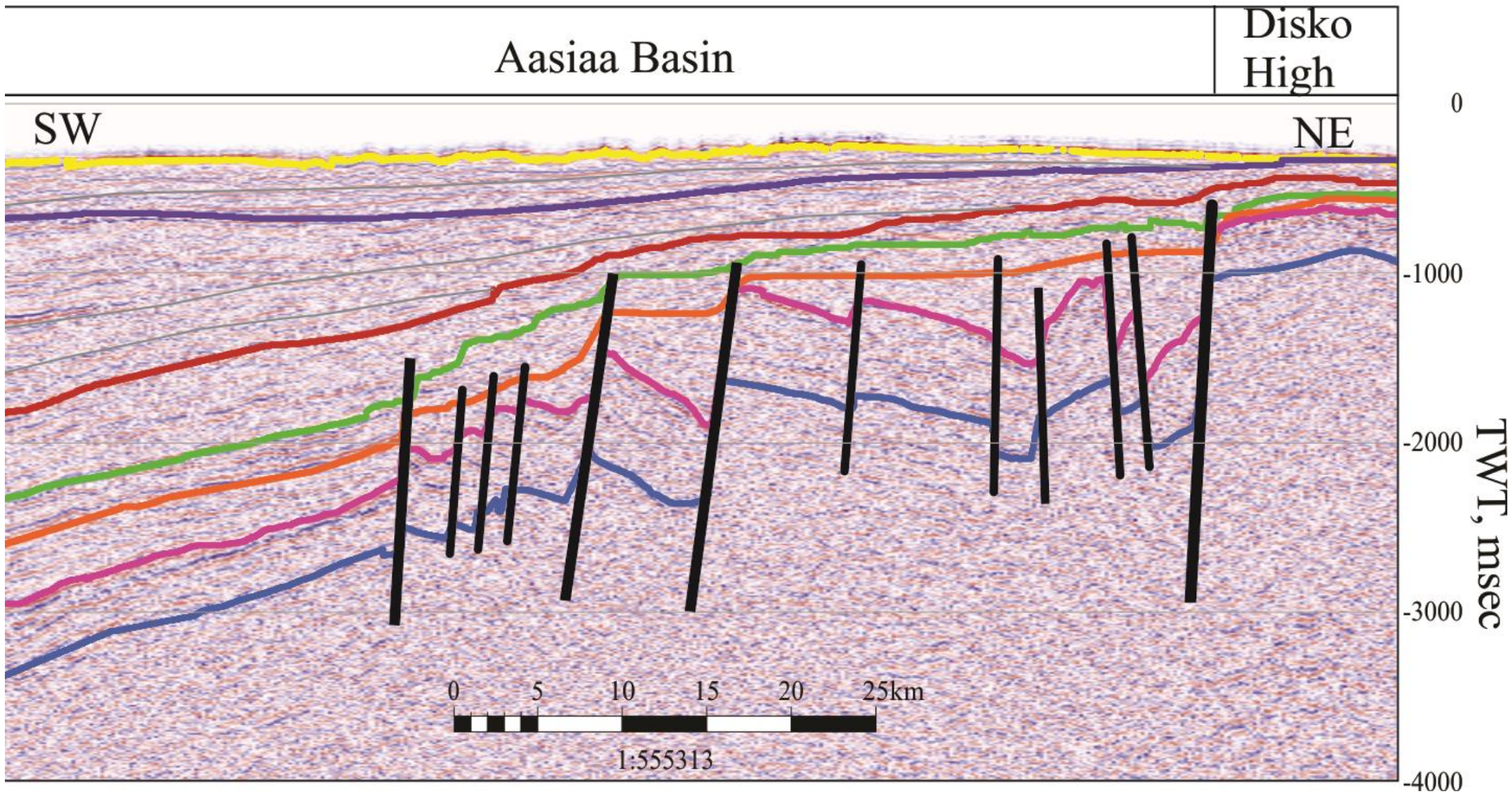

Figure 4.10: Zoomed in section from (Figure 4.9) showing the interpreted sedimentary units of the Disko West province. Half Graben pull apart like structure was active during the Paleocene Basalt, Paleocene and Eocene syn-rift sediments. Post-rift sediments include Mid- Miocene to present, sediments are onlapping Mid-Miocene and Base Quaternary unconformities. Syn -rift sediments of Cretaceous masked by thick Paleocene basalt and not interpreted.

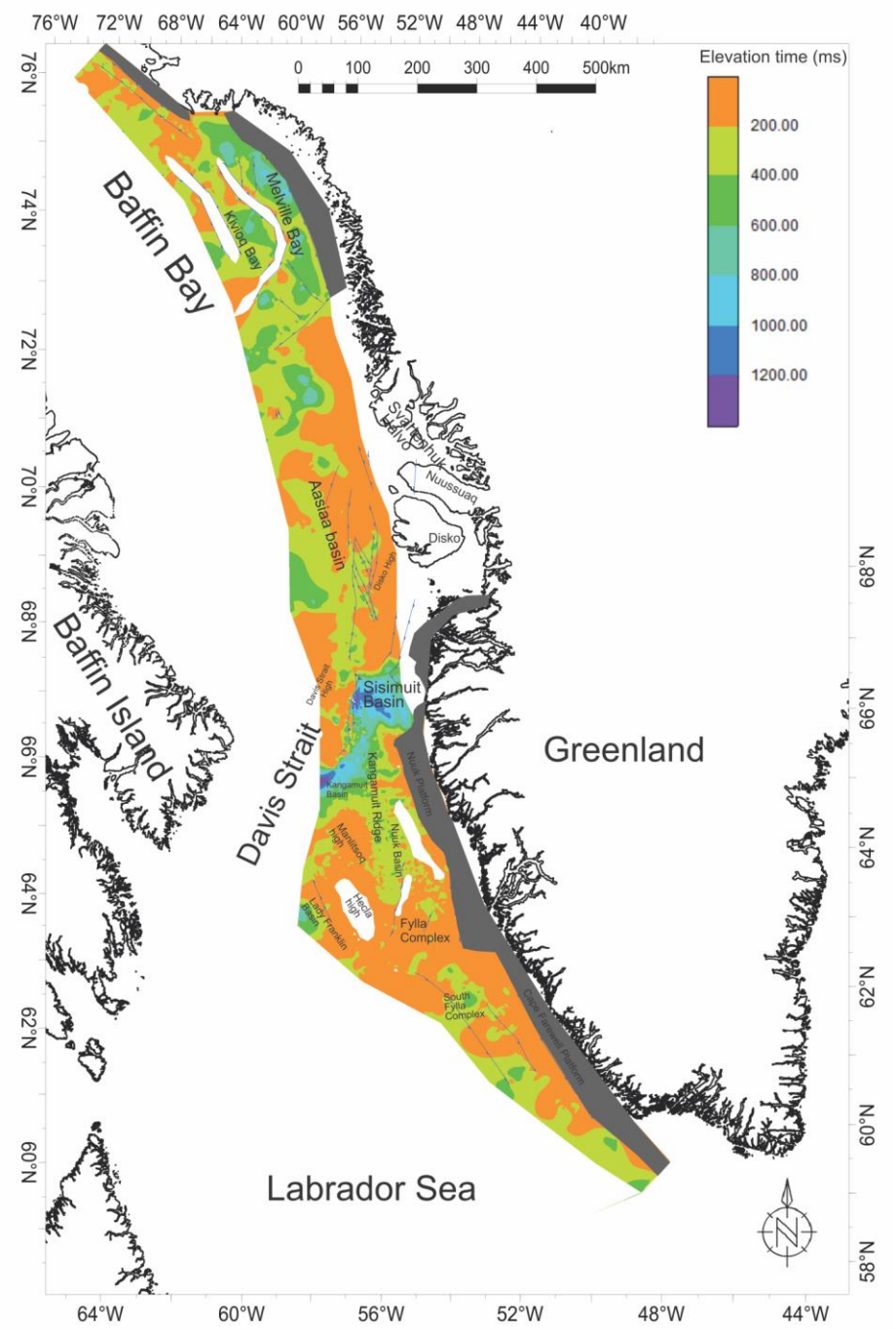

Figure 4.11: Mid-Eocene to Top Paleocene isochron map

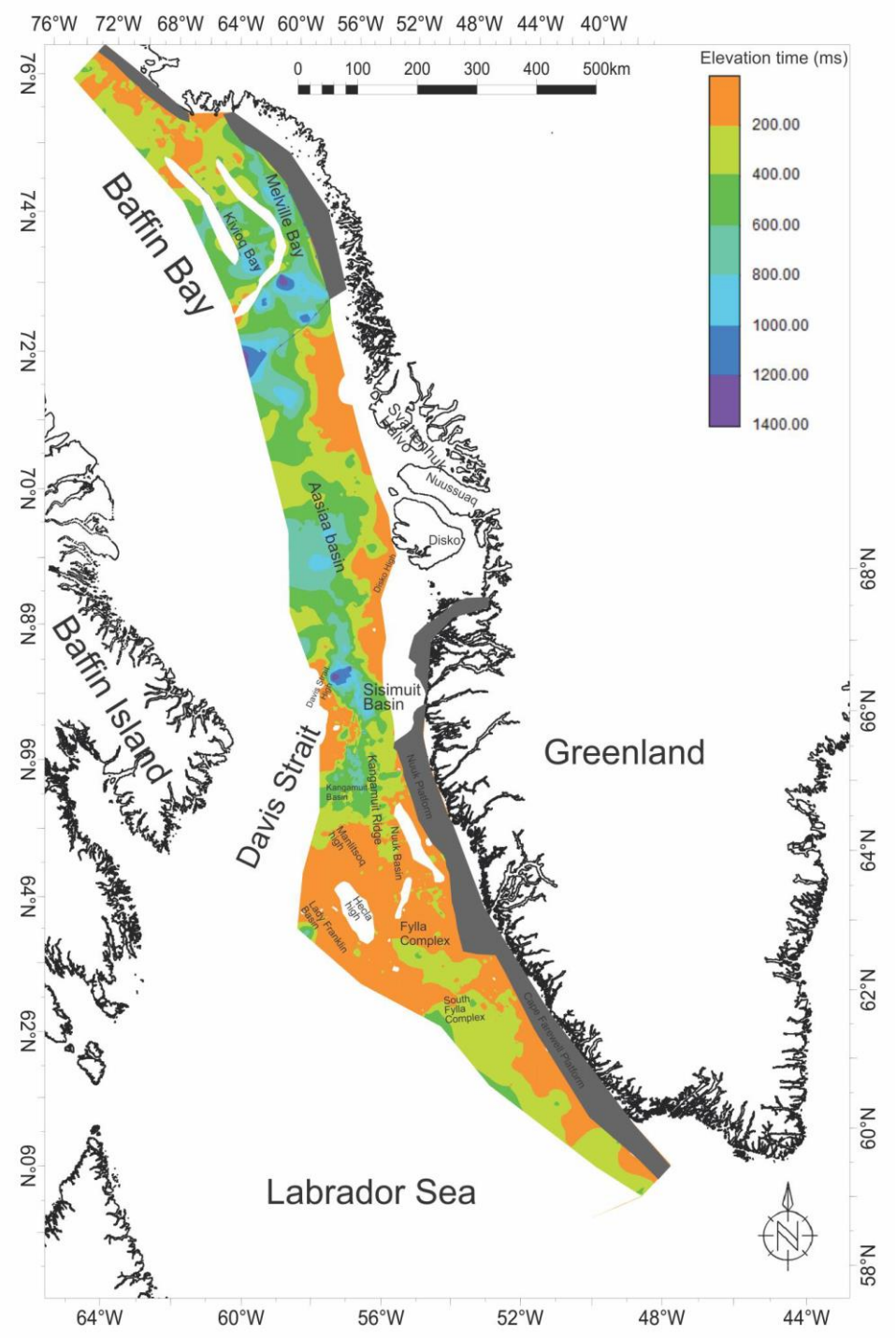

Figure 4.12: Mid-Miocene to Mid-Eocene isochron map

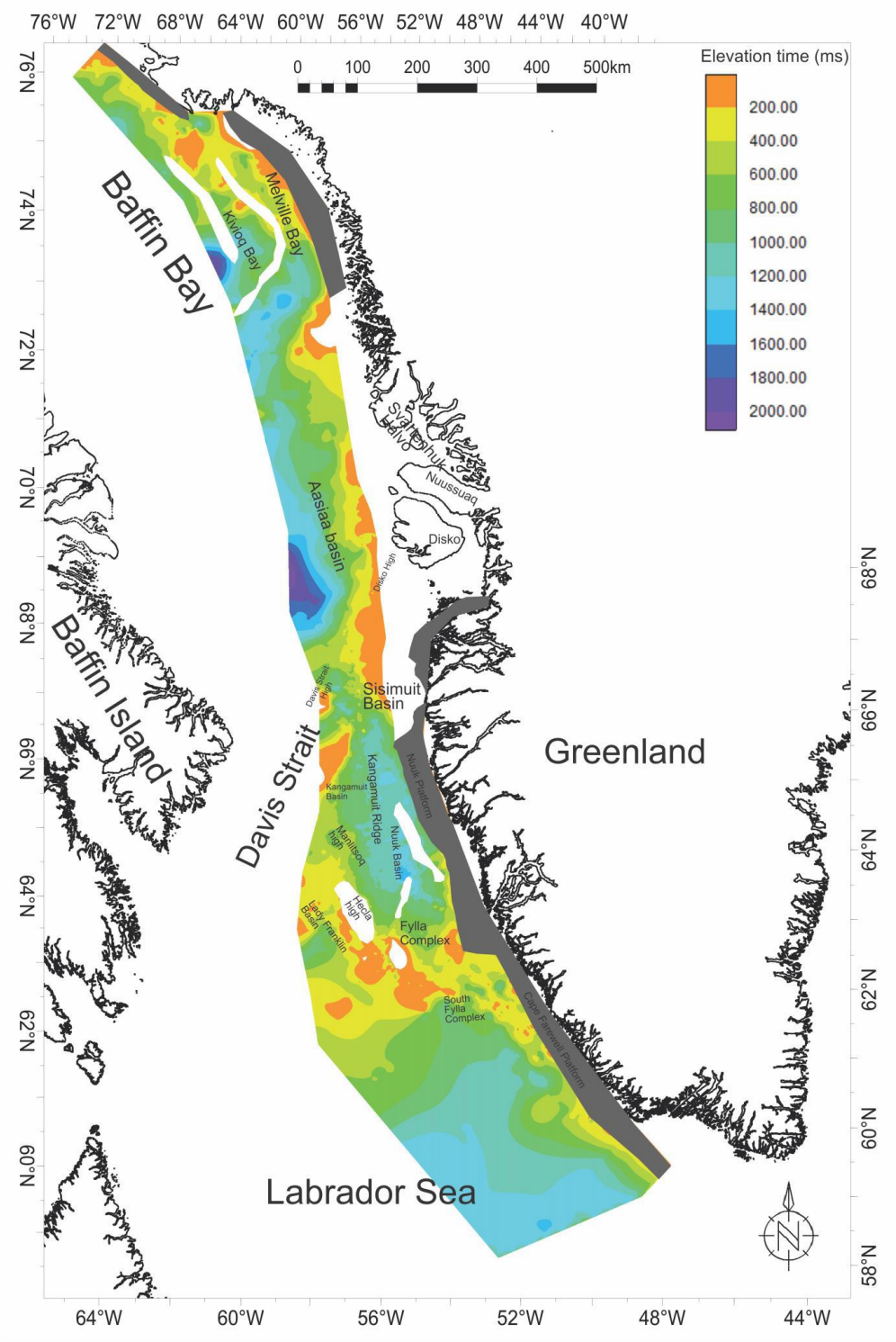

Figure 4.13: Base Quaternary to Mid-Miocene isochron map

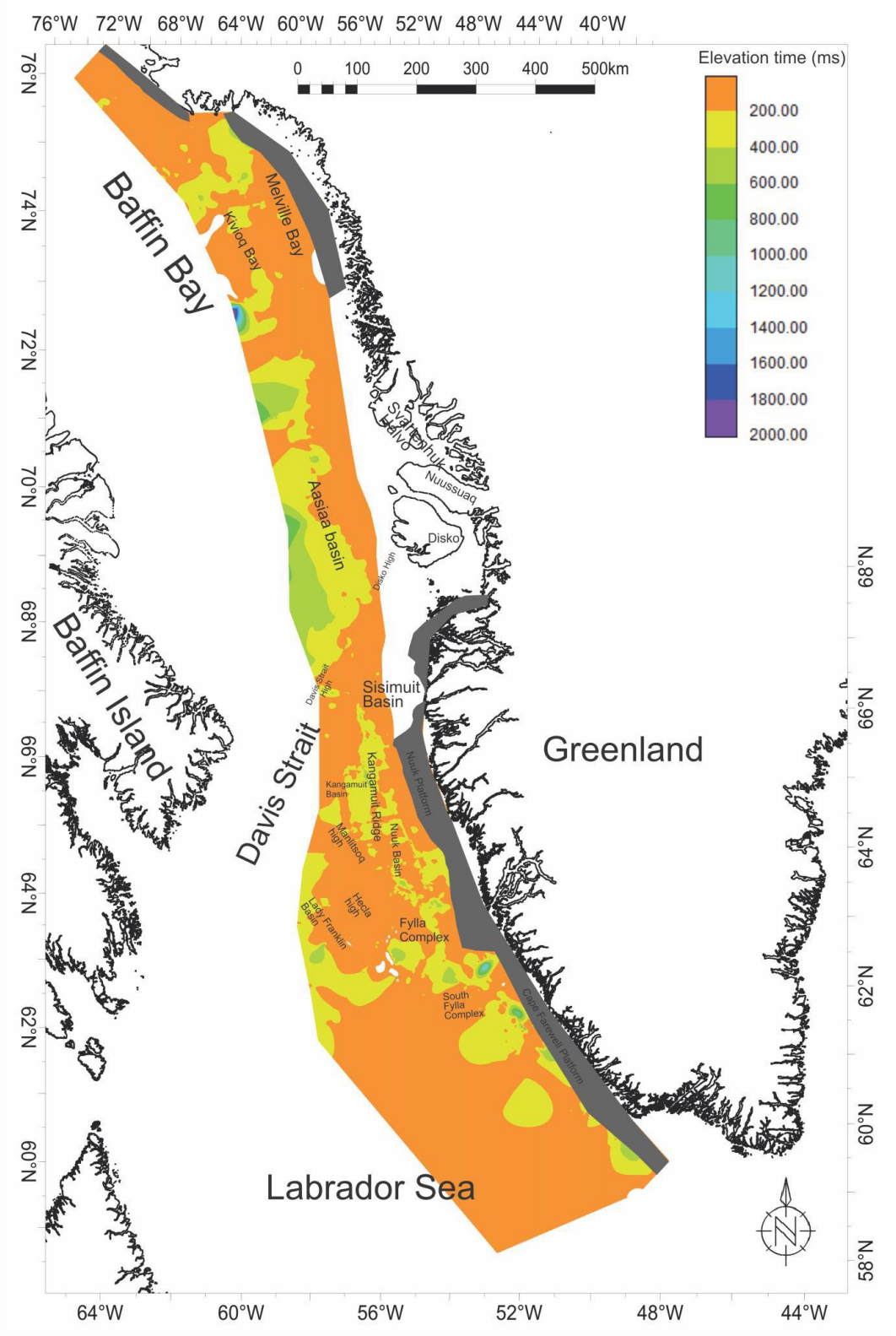

Figure 4.14: Sea bed to Base Quaternary isochron map

The absence of the Paleocene basalt in this area (except on the Hecla and Maniisoq Highs) allows the identification of top acoustic basement with greater certainty. Cretaceous rifting is again interpreted in this region and the interpretation in this work suggests a series of isolated, large (> 7 km) rift basins during this phase (Figure 4.6). The late Cretaceous package is more uniformly distributed and is mappable across at least some of the basement highs suggesting post rift sediments in most of the margin (Figure 4.7). The nature of this unit however is rather variable. Within the Lady Franklin (Figure 4.17), Sisimiut (Figure 4.15) Nuuk (Figure 4.17) and Sputh Fylla complex (Figure 4.19) Basins there is demonstrable thickening of strata into rift faults typical of syn-rift intervals.

In contrast, many of the basin faults within the Cretaceous grabens (e.g. Cape Farewell) show no thickening (Figure 4.19). This may be an indication of how extension was progressively localised onto a limited number of faults during the rift episode. Thick basalts are deposited on both flank of the Hecla High and a flower structure is interpreted within the Sisimiut Basin (Figure 4.8). Sediments of post-rift package were probably deposited during thermal subsidence resulting in onlapping of sediments onto the topography highs. In the Hecla High, post-rift strata are thin and post Mid- Miocene in age in contrast to the thick (~1.0 second TWTT) post-rift packages of the Fylla structures complex (Figure 4.12, 4.13 and 4.14).The post-rift sediments are thicker (~2.0 second TWTT) in the Sisimiut and Kangamiut Basins than in the Fylla and Hecla Basins (Gregersen and Skaarup, 2007). In addition, the eastern side of Sisimiut Basin is characterised by non-deposition of sediment resulting in the absence of mid Miocene to present day (Figure 4.15).

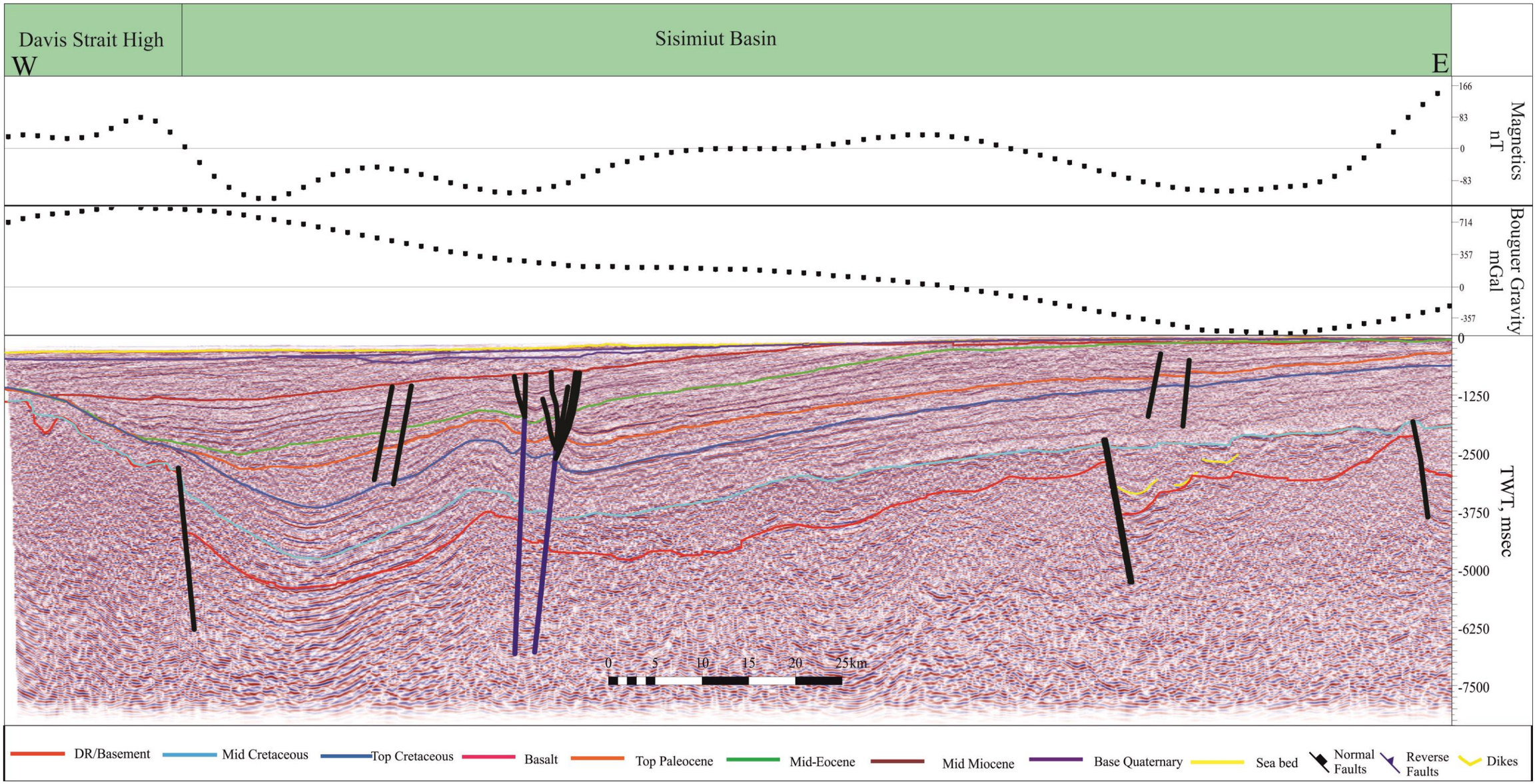

Figure 4.15: Seismic profile line 3 (line position in Figure 4.1) showing the interpreted sedimentary units in the Nuuk West Province. Syn-rift sediments of lower and upper Cretaceous in sisimint Basin. Transition zone sediments include the Paleocene and early Eocene sediments and post-rift sediments from mid- Miocene to present. The basin characterized by flower structures as part of the Ungava transform fault and tertiary sills in the lower cretaceous sediment.

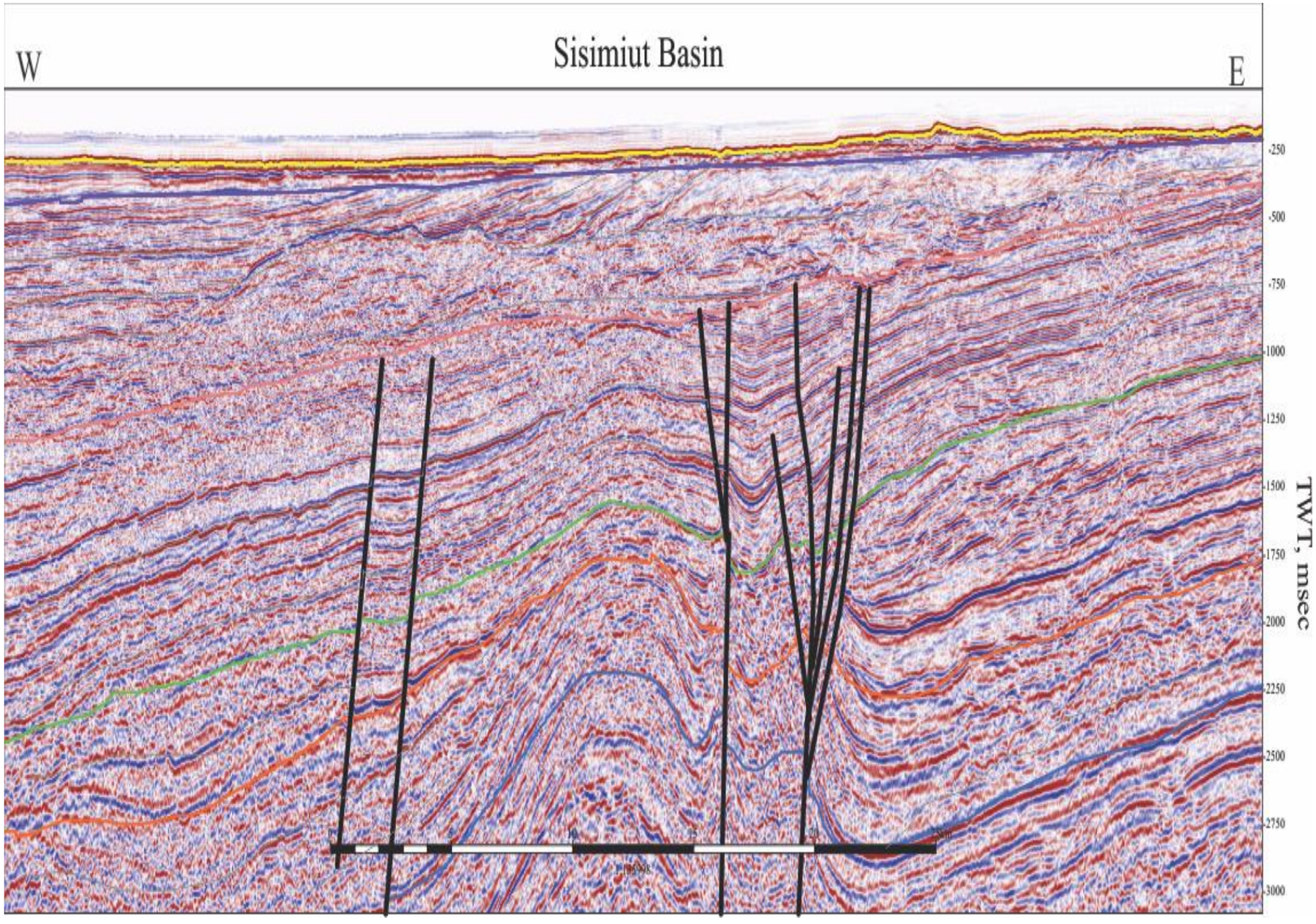

Figure 4.16: Zoomed in section of (Figure 4.15) showing the interpreted sedimentary units in the northern side of Nuuk West Province. Late Cretaceous to early Tertiary Syn-rift sediments showing the development of flower structure and indicating strike slip movement and transformation of seafloor spreading from Labrador Sea towards Baffin Bay to form Ungava Fault Zone.

4.4.5 Cape Farewell Province (CF)

The Cape Farewell province shows faults up to 200-400 km in length and typical throws of 0.5 seconds TWTT (Figures 4.1 and 4.19). The south Fylla Complex is 400 km long and 100 km wide, whereas the Cape Farewell is approximately 400 km long and 200 km wide (Table 1). One of the faults has a throw of 1.5 second TWTT that may be the result of reactivation during the late stage of rifting in late Cretaceous (Figure 4.19). The Cape Farewell province also marks a significant narrowing in the width of the continental margin as the transition from attenuated continental crust into full oceanic crust occurs over ~80 km (rather than >250 km as is the case further north). On the continental crust the rifting geometry is dominated by relatively planar faults and rotated faults blocks (Figures 4.1 and 4.19). The imaging of the footwall cut-offs suggest faults remain planar and show no evidence of a listric geometry with depth. From stratal thickening it is evident that the faults were active during the Cretaceous, similarly to basins in the North. However, the fault throws are significantly smaller (maximum observed throws are <0.5 second TWTT) in contrast to reactivated faults with throws of 1.5 second TWTT. This difference in fault geometry is also reflected in a change of fault orientation. Faults in the southern Nuuk province are dominated by a broadly north-south orientation whereas in Cape Farewell they have a NW-SE orientation.

In the more distal portion of the basin, the lower section is characterised by low amplitude reflectivity suggestive of oceanic crust at ~ 8 seconds TWTT (Figure 4.19). In addition, the presence of ~ 80 km wide magnetic chron 31

(70 Ma) and chron 27 (60 Ma) at the south and north respectively further justifies the presence of the oceanic crust (*cf*. Chalmers and Laursen 1995; Figures 4.1 and 4.19). The seismic character of the area between the attenuated continental crust containing the rift faults and the oceanic crust is rather enigmatic and may be either Seaward Dipping Reflector (SDR), basaltic intrusions; this is interpreted as the transition zone (Figure 4.19). It is onlapped by the Upper Cretaceous unit and then overlain by Paleocene basalts that are attributed to break-up related magmatism. These volcanic rocks appear to mask all internal reflections at a transition zone of c. 80 km observed between the oceanic and continental crust. The west section of the transition zone has high amplitude reflectors that may be seaward dipping reflections (Figure 4.19), and this, coupled to a positive gravity anomaly above it, suggests that it is a late stage volcanic event that may have been the pre-cursor to break-up. Overlying the entire section (Figure 4.19), including the oceanic and continental crust, is a post rift sequence with a rather constant thickness of ~1.3 second TWTT, reflecting a uniform subsidence across the margin. The exceptions are post-rift packages of Palaeocene to Eocene ages, which show local onlap onto both the margin to the east and a volcanic edifice on the ocean crust.

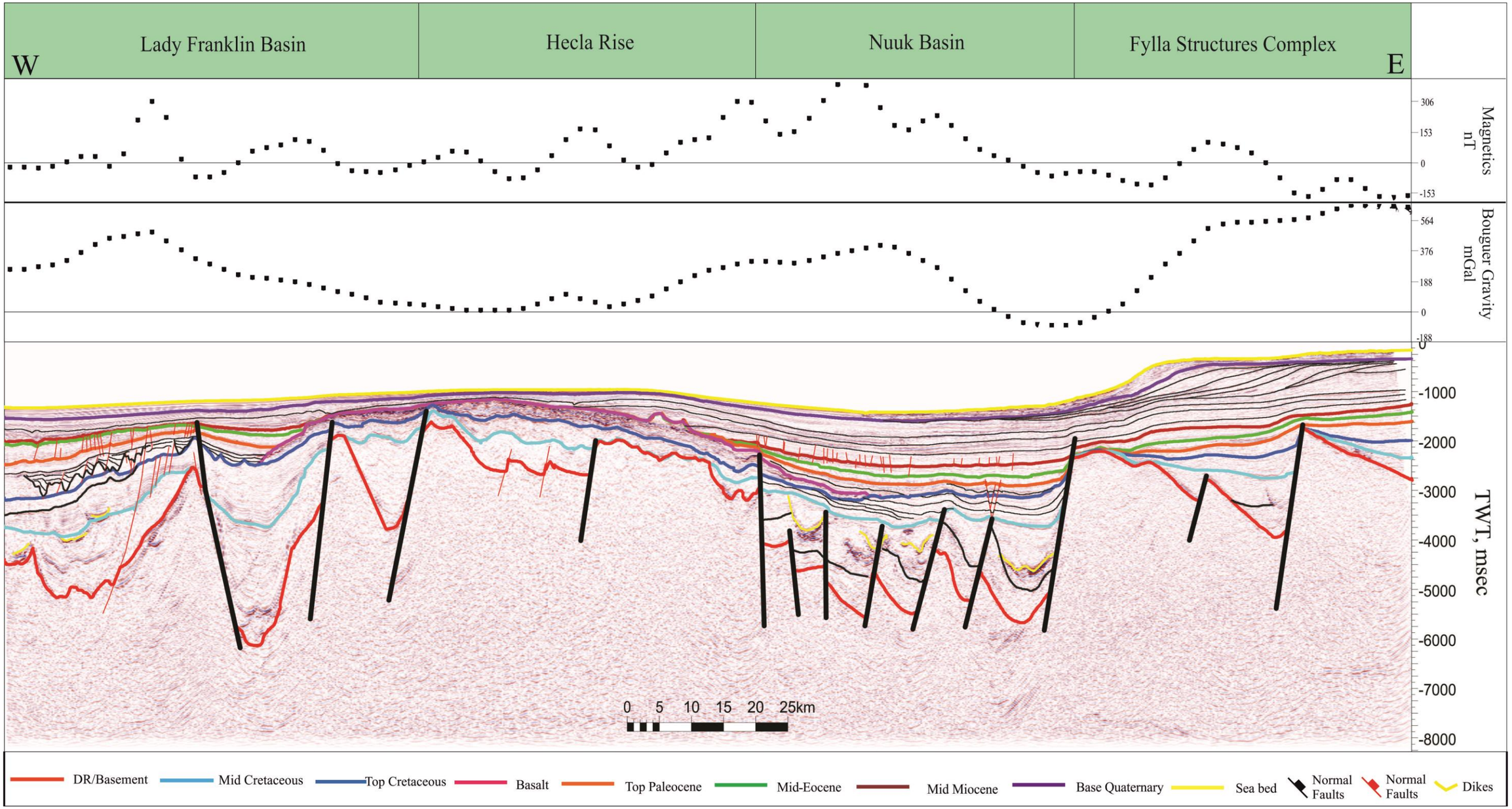

Figure 4.17: Seismic profile line 4 (line position in Figure 4.1) showing the interpreted sedimentary units in the Nuuk West Province. Syn-rift sediments of lower and upper Cretaceous in Nuuk and Lady Franklin Basins. Transition zone sediments include the Paleocene and early Eocene sediments and post-rift sediments from mid- Miocene to present. Tertiary sills in the lower cretaceous sediment.

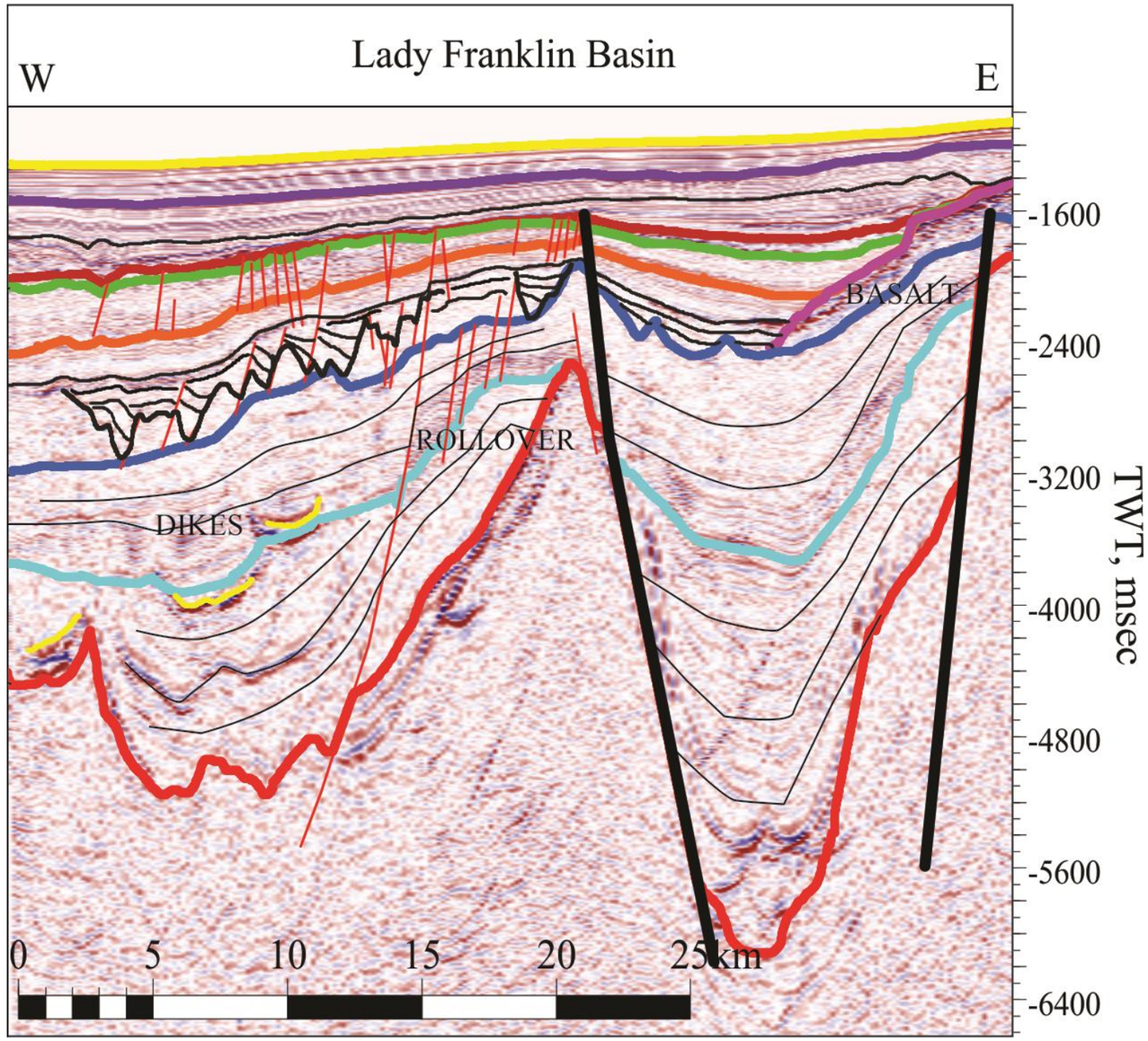

Figure 4.18: The western most part of (Figure 4.17). Syn-rift sediments wedges of lower and upper cretaceous in addition to the Paleocene and Eocene sediments in Lady Franklin Basin. Compressional deformation is notably within the lower and middle Cretaceous strata as these sediments have rolled over. Post-rift sediments from the Mid- Miocene to present time.

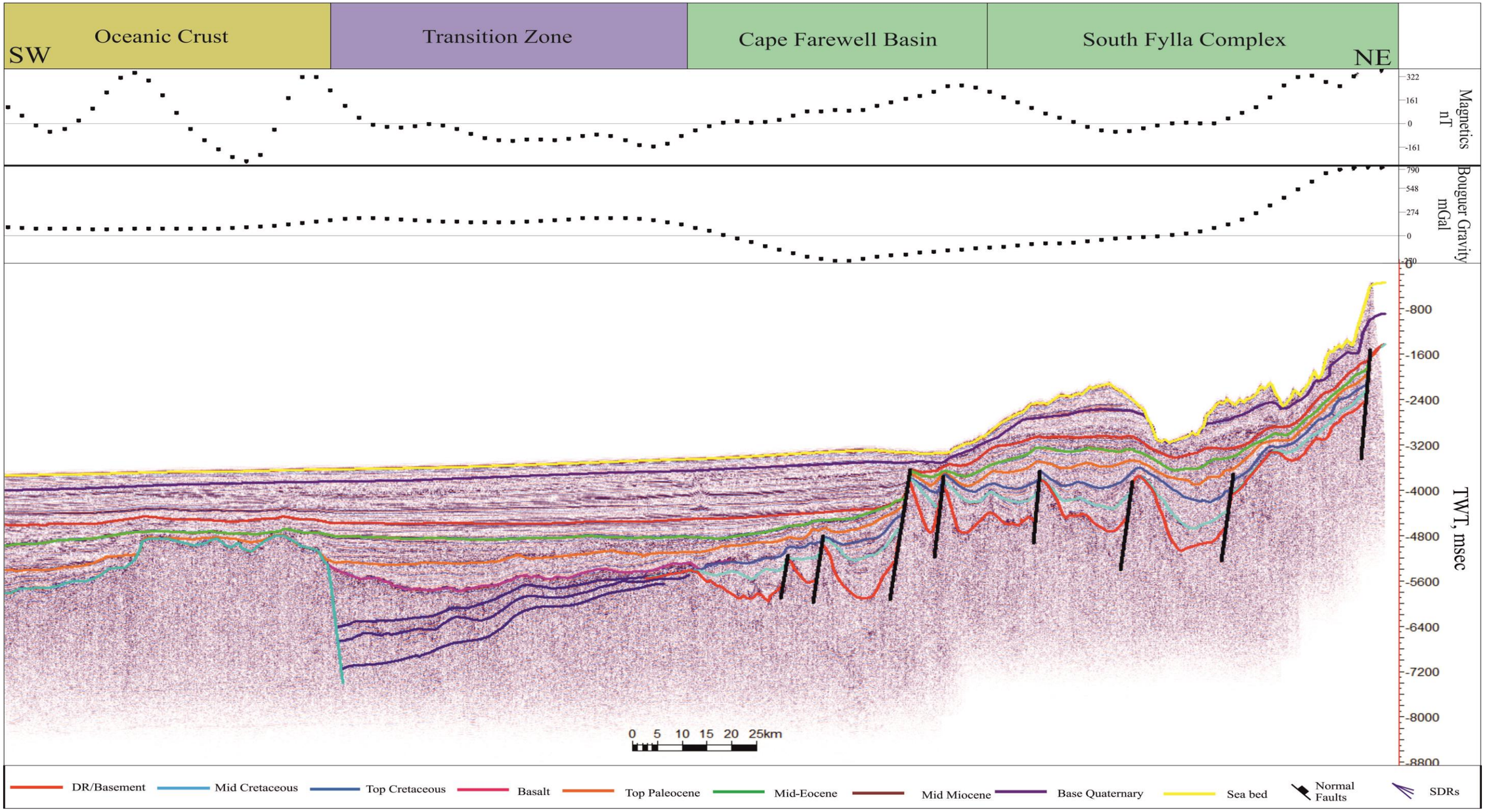

Figure 4.19: Seismic profile line 5 (line position in Figure 4.1) showing the interpreted sedimentary units in Cape Farewell Province. Syn-rift sediments of lower and upper Cretaceous in (south Fylla complex structures). Transition zone sediments include the basalt of early Paleocene to mid-Miocene. Post-rift sediments from mid- Miocene to present as well as oceanic crust formation. The oceanic crust is flanked by high amplitude reflections which might be a transition zone. This transition zone occurs at c. (6.0 second TWTT).

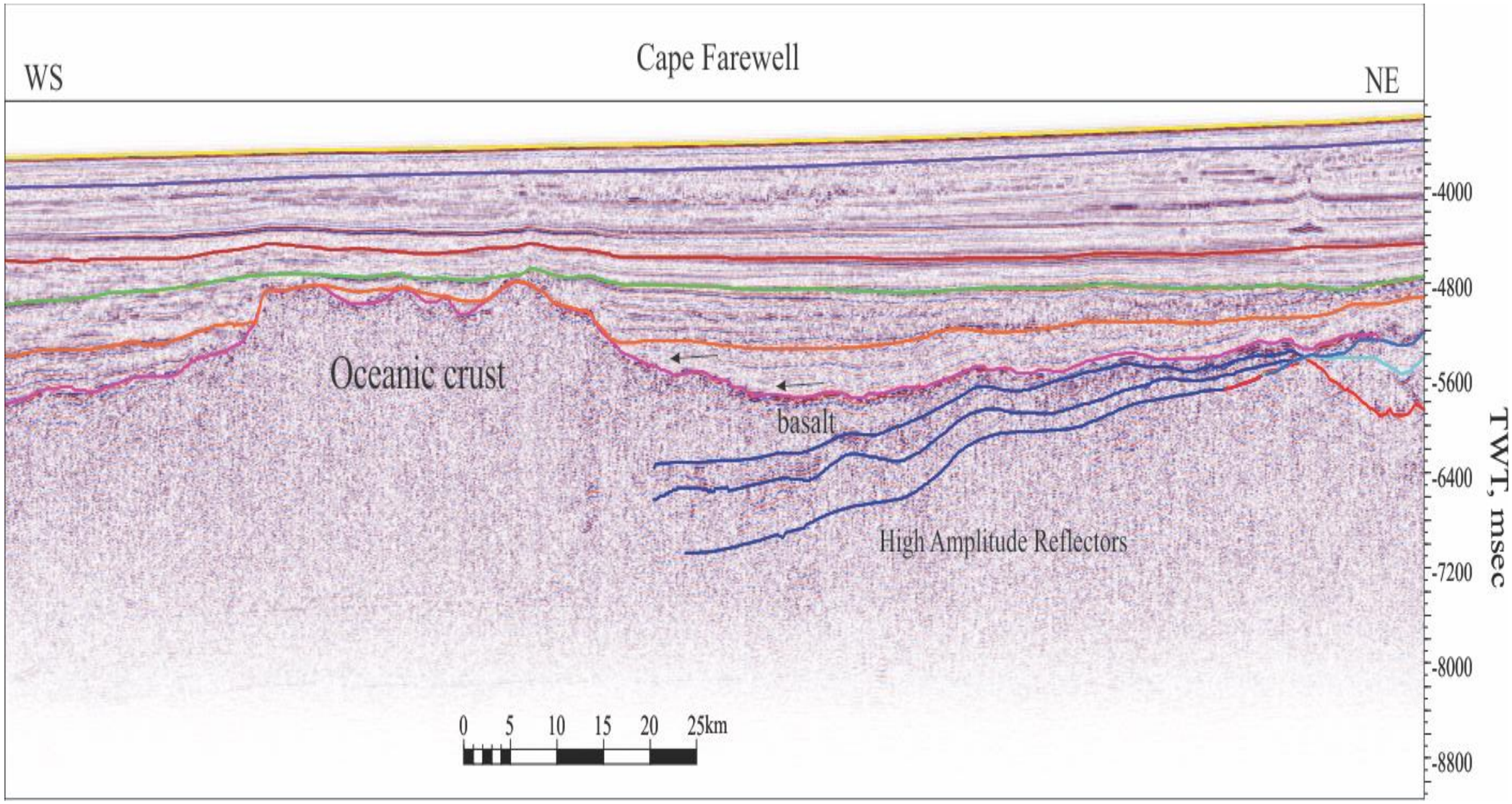

Figure 4.20: Zoomed in section of (Figure 4.19) showing the oceanic crust is flanked by high amplitude reflections (SDRs) of a transition zone. Syn-rift include the Paleocene and early Eocene sediments in which are onlapping both sides of oceanic crust. Post-rift sediments from the Mid Miocene to present time.

Table 4.1: summarising the major basins geometries and thicknesses of west Greenland continental margin

West Greenland provinces	Basins geomentry			Rift I, sediments thicknesses		Rift II, sediments thicknesses	
	Basin Name	Length, km	Width, km	Syn-rift 1 SR1 TWTT,s	Post-rift 1 PR1 thickness TWTT,s	Syn-rift 2 SR2 thickness TWTT,s	Post-rift 2 PR2 thickness TWTT,s
Baffib Bay province	Melville	310	50	2.1	0.4	1.25	1.3
	Kivioq	200	25	1.11	0.378	0.9	2.1
	Umberk	80	50	0.65	0.337	1.0s (lower 0.350s basalt)	2.15
Disko West Province	Aasiaa	30-100	350	n	n	1.8s (lower 0.7s basalt)	2
	Disko high	40-60	280	n	0.166	0.5s (lower 0. 25s basalt)	0.14
	Nussuaq basin	130	60	0.4	0.56	n	n
				0	0		
Nuuk West Province	Sisimiut	120	100	1.2	1.2	1.3	1.1
	Ikimurt	120	40	1.1	1.02	1.14	0.9
	Kangamuit	110	50	1.9	0.24	1.21	1.1
	Maniisoq high	80	60	0.8	0.22	0.22s basalt	0.75
	Nuuk west	200	80	2	0.535	0.8	1.2
	Lady franklin	180	80	2.4	1.27	1.5	0.75
	Fylla complex	110	100	0.9	0.65	0	0.72
	Helca high	120	55	1.5	0.37	0.3s (basalt)	0.35
							0
Cape Fairwell Province	South Fylla complex	400	100	0.65	0.4	0.75	0.95
	Cape Fairwell	400	200	0.5	0.3	0.76	1.3

4.5 Discussion

4.5.1 Models for Tectonic Development of the Western Greenland margin

The development of the West Greenland margin involved deposition of thick sediment wedges during rifting, faulting of the rift sequence, and erosion of fault scarps that formed during early lithospheric extension by post-rift sedimentation. The regional erosion during the latter stage is revealed by Mid-Eocene and Early Miocene unconformities. The rift event interpreted in this study area occurred intermittently with the emplacement of volcanic rocks during the Palaeocene and Eocene. Categorically, the pre-rift packages are flanked by an irregular dome structure in Cape Farewell; the dome is interpreted as a remnant of the oceanic crust or serpentine zone (Figure 4.21) , and it is shown as chaotic and high-amplitude reflection at a deeper stratigraphic level on the seismic data (Figure 4.20). Furthermore, we surmise that the boundaries of the oceanic crust are delimited by a probably zone of SDRs developed prior the initial opening of the oceanic crust. Neogene uplift, post seafloor spreading are dated ~11-10 Ma and 7-2 Ma (cf. Chalmers, 2000; Green et al., 2011; Japsen et al., 2006). These observations all suggest a rather complex and variable margin evolution.

We propose a tectonic model that integrates the seismic interpreted faulting and overall basin geometry with the key stage of tectonic development (Figure 4.21):

I. Rifting stage (145-130 Ma): NE-SW extension across the West Greenland margin. This rift produced rotated fault blocks that formed horsts and grabens in the Cape Farewell, Baffin Bay and Nuuk West Provinces. The basin geometry in Disko West Province at this stage is not covered by the available seismic data. However, deposition of Cretaceous age strata onshore suggests that the province was affected by this rift stage. Late stage rifting comprises an early magmatic pulse during which the margin was intruded by dykes in Nuuk West and probably Disko West.

II. Magma-poor phase (80-70 Ma): recorded as the development of a continental-ocean transition zone that presumably includes attenuated continental crust in the Cape Farewell and Baffin Bay provinces or serpentinised zone. Possible thermal subsidence occurs on other areas across the West Greenland margin. The margin underwent post-rift thermal subsidence as materialised by the marine mudstones of Kangeq sequence, which show little evidence of extension prior to the onset of seafloor spreading at 60 Ma (Chalmers 2012).

III. Seafloor spreading (70-60 Ma): Seafloor spreading started in the south of Cape Farewell province (Chron 31, 70 Ma) and is likely to have propagated to the northwest of Cape Farewell province (Chron 27, 61 Ma) and then transferred to Baffin Bay via the Ungava fault zone to form oceanic crust at (Chron 26, 60 Ma) (See figures 4.4 and 4.21). The presence of a Magnetic high suggests uniform stretching of the lithosphere in Cape Farewell. Disko West and Baffin Bay

showed magnetic low implying slow seafloor spreading on an underlying strongly extended continental crust and/or serpentinised mantle (Reid and Jackson, 1997). We propose that the cessation of seafloor spreading occurred during chron 21 (48 Ma) and at chron 13 (33 Ma) in Cape Farewell and Baffin Bay provinces respectively, corroborating the works of Chalmers and Pulvertaft (2001) and Oakey and Chalmers (2012). The shift in spreading axis was from NNE in Palaeocene to NNW in Eocene in Baffin Bay (See also Oakey and Chalmers, 2012). This is attributed to an anticlockwise rotation of spreading axis by the oceanic crust or a shift in magmatic intrusion from West to East Greenland. Hence, the margin subsided after the breakup in the Davis Strait in Palaeocene to Late Eocene times, supporting the model of post rift subsidence reported onshore Disko and Nuussuaq basins (cf. Green et al., 2011).

4.5.2 Magmatism and influence of the mantle plume

For the study area, there continues to be a debate whether the Eocene and Palaeocene volcanism events are the product of multiple mantle plumes or a single mantle plume. The separation and movement of the Greenland and Canada cratons were probably influenced by the migration of a mantle plume that may have caused transient thermal uplift, extension and subsequent plate movements (Harrison et al., 1999). Several authors favoured a single plume hypothesis for the emplacement of all the volcanic provinces (Larsen et al., 1999; Nielsen et al., 2002; Storey et al., 1998; Torsvik et al., 2001). The geochemistry of early picrites of West Greenland

are similar to subaerial Icelandic basalts and are formed by similar greater degrees of melting of their source mantle than their Icelandic counterparts (Holm et al., 1993). The volcanic eruption of the West Greenland picrites occurred ~5-6 Ma earlier than the start of volcanism in eastern Greenland (Gill et al., 1995). A possible scenario describing the plume dynamics under West Greenland is that the ~ 60 Ma events involves volcanism from a fast moving upper mantle plume that rapidly spreads out horizontally on encountering the base of the lithosphere (*cf.* Larsen et al., 1999; Nielsen et al., 2002). Palaeomagnetic reconstructions show that mantle and crust processes are linked via complex and enigmatic cause-and-effect relationships (Torsvik et al., 2001).

Our data analysis supports the notion that the West Greenland plume formed at ~60 Ma as suggested by earlier workers (e.g. Storey et al, 1998). Critically, there was early rifting along the whole margin during a magma-poor phase with more extension recorded in the south. The evidence is for a plume that is present at the transfer zone rather than at the area of greatest extension. Subsequently, the plume played a minor role in rift initiation and development. Therefore, we suggest that the role of the plume was less significant than proposed by previous authors. The plume may have contributed to the cessation of rifting in the study area. Our model proposes that the West-Greenland volcanic margin developed after a period of amagmatic extension during the Cretaceous in accord with the work of Abdelmalak et al. (2012). Consequently, the area was subjected to regional uplift in the Danian (65–60Ma) before the extrusion of pre-breakup magmatic rocks.

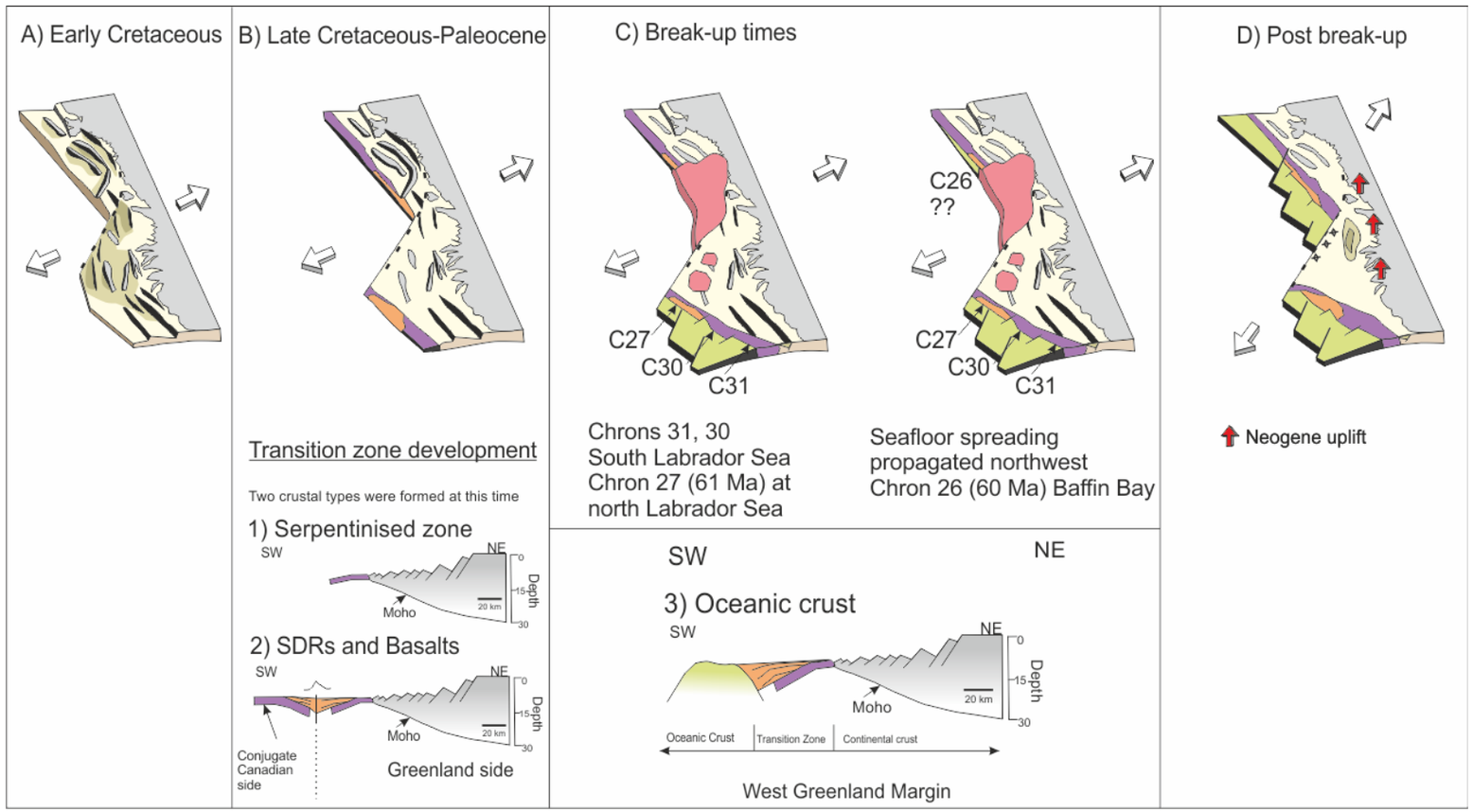

Figure 4.21: Conceptual model for the evolution of the West Greenland margin as discussed in the text.

4.5.3 Contribution to understanding of lithospheric stretching

Based on the model defined in section 4.1, we propose a) multiphase extension and continental breakup for the West Greenland margin and that b) individual basins within West Greenland comprise both magma-poor and rich basins. The seismic stratigraphic division from this work is consistent with the classification of Schenk (2011). As the transition from rifting to drifting is marked by the breakup unconformity (BU) of Falvey (1974) and Franke (2013); the BU in this study is the mid-Miocene horizon. Angular unconformities with erosional truncation on seismic profiles were interpreted as the Rift Onset Unconformity (ROU) in line with the definition of Falvey, (1974). In the study area, the ROU is the top Cretaceous Horizon. The nature and position of the Ocean-Continent Transition (OCT) is marked by the presence of Seward Dipping Reflectors (SDR). Structurally, the interpretation of compressional and inversion structures accompanied by strike-slip faulting and local transtensional faults and flexures are expression of the Eurekan orogeny (Gregersen et al., 2013). However, the identification of the transition between syn-rift and post-rift settings may not always be reflected by a simple breakup unconformity (Alves et al., 2009; Soares et al., 2012). These authors show that the “breakup unconformity” is a Lithospheric Breakup Surface (LBS) that is not always developed as an unconformity and that the entire lithosphere is involved in the breakup process, not only the continental crust. The complex nature of the transition phase, which is stratigraphically between the demonstrable syn-rift and post-rift phases, in this study is a reflection that the simple concept of the breakup unconformity

is not applicable. Hence, the mid-Miocene (BU) may only indicate basinward shift of the extensional locus and not the end of rifting processes along West Greenland margins (Falvey 1974; Soares et al., 2012).

Our model offers supporting evidence for the occurrence of a passive continental margin comprised of both magma-rich and magma-poor lithospheric extension. Since most passive margins develop in response to lithospheric extension, passive margins can be classified into two end-members depending on the volume of extension-related magmatism (Franke, 2013). Baffin Bay and Labrador Sea are magma-rich margins characterized by SDRs at their ocean-continent transition. Keen et al (2012) showed that the Labrador Sea is exemplified by the presence of excess magmatism, SDRs, and volcanic plateau and thick igneous crust. This agrees with the classification of Funck et al (2007) and Gerlings et al (2009). In contrast, Skaarup et al (2000) proposed that the Labrador Sea is a non-volcanic margin. From this work, the Davis Strait is interpreted as a magma-poor margin that is defined by a wide area of highly attenuated crust where the upper crust is deformed by planar faults. Unlike other magma-poor passive margins, the detachment over which the fault soles was not interpreted. Therefore, the West Greenland to the north and south are magma-rich margins while centrally it is magma-poor margin. This highlights that single margins can be highly variable and these simple end members are not always applicable.

The role of mantle plumes in the evolution of magma-rich margins has been a subject of debate. Crustal rifting can evolve in conjunction with a plume head as: a) where the plume head triggers the rift evolution by a circular uplift in which the earliest and widest rift is expected to be close to the plume head and the width of the rift decreases away from the plume; and b) where the rift starts farther from the plume with a consistently decreasing width of the rift toward the plume (Franke, 2013). Examples include Iberia–Newfoundland, the Equatorial Atlantic Ocean, and East Antarctica–Australia. We have shown that extension along the West Greenland was less dependent on the mantle plume and that continental extension and break-up is not always associated with large amounts of volcanism.

The evolutionary model presented in this paper has implications for all aspects of hydrocarbon prospectivity in West Greenland. Reservoir intervals are likely to be present in syn-rift strata deposited in the observed half grabens of substantial size as well as post-rift clastic deposits (Table 1). These intervals include the fluvio-deltaic sandstones of the Cretaceous Atane Formation in the Nuussuaq Basin, the mid-Cretaceous to Paleocene marine slope channel sandstones and the marine canyon sandstones equivalent to the incised valley fill sandstones of the Paleocene Quikavsak Member (Dam et al., 2009; Dam et al., 1998). The deposition of these intervals, and the facies variations within them, will be intimately controlled by the basin and fault architecture that we have presented (Figure 4.21). Of equal importance as reservoir distribution is the trapping mechanisms, which within our interpretation are likely to include both structural and stratigraphic plays. Early rotated faults blocks, grabens and their horsts are important

structural trap forming three-way closure. Additional trapping mechanism may include Upper Cretaceous compressional structures and rollover four-way closures formed by syn-rift packages (Figure 4.18).

The Paleocene was a time of widespread volcanic activity in the central part of the province (Larsen and Pulvertaft, 2000; Pedersen and Larsen, 2006), when several kilometres of plume-related volcanic rocks were extruded regionally. Consequently, basalts extruded into Cretaceous strata are going to alter both reservoir and basin scale heat flow scenarios. The syn-volcanic strata of the Baffin Bay province may be of interest for hydrocarbon exploration activity (Pedersen et al., 2002) with the stratigraphic position of volcanic rocks is playing a role on reservoir scale source rock maturation. Volcanic activity from regional and widespread magma source may result in elevated regional heat flow which has considerable impact on hydrocarbon maturation. Further constraining the implications of heat flow associated with volcanic activities in comparison to that associated with lithospheric stretching will be critical in future exploration. The Neogene was a time of widespread clastic input along North Atlantic passive margins, indicative of Neogene uplift that has been documented from many onshore locations around the Arctic and North Atlantic (Japsen et al., 2005; Japsen and Chalmers, 2000). The implications of such uplift are poorly constrained on other margins but are likely to influence sediment supply, geometry of stratigraphic traps and may also alter regional heat flows (Paton et al., 2008).

4.6 Conclusions

We present a new structural framework for the West Greenland margin. This reveals a long and complex evolution, and in particular demonstrates:

- Rifting margin in early Cretaceous with syn-rift packages intercalated with volcanic sills. The Palaeocene basalt occurred in the Disko West, South Baffin Bay and the North Cape Farewell provinces. These extrusive rocks are connected with the breakup stage during the development of the West Greenland margin.
- The architecture of faults in the Davis Strait High suggests continuity between the structures of Labrador Sea and Baffin Bay. Strike-slip faults in the Davis Strait acted as transfer zones for displacement during seafloor spreading during and after volcanic activity.
- Incipient rifting on the West Greenland margin was unaffected by the mantle plume. Seafloor spreading started in the Cape Farewell, propagated to the North West and later slowly to Baffin Bay where the underlying continental crust is strongly extended over a probable serpentinised mantle.
- The sub-basins on the West Greenland margin such as the Sisimiut, Kangamiut and Melville Bay Graben have significant potential for hydrocarbon reservoir and seal in thick Cretaceous strata. Structural traps include half grabens and grabens with further potential in possibly inverted structures.
- The West Greenland margin is characterised by magma-rich and –poor basins.

- In conclusion, tectono- stratigraphic packages studied from seismic reflection and borehole data interpretation has permitted the basin architecture to be established and allowed us to construct a model for the tectonic development of West Greenland basins. The West Greenland margin shows complex tectono-stratigraphy and the along margin variability, in particular the variation of magma-poor to magma-rich margin, the relatively small influence of plume emplacement, and the significant variation in rift architecture along the margin is highly applicable to our understanding of other passive continental margins.

Chapter 5

Gravity and Magnetic Modelling of the Deeper Crustal Structure

5.1 Abstract

This chapter investigates the crustal structure of the Western Greenland margin by integrating gravity and magnetic modelling with the seismic reflection data interpretation presented in Chapter Four. The aim is to provide an understanding of crustal architecture along the margin.

The interpretation from seismic reflection data revealed the presence of a transition zone from oceanic to continental crust in the Baffin Bay and Davis Strait. The calculated gravity provides a close match to the observed where the oceanic and continental crusts are present.

Aeromagnetic data over the study area reveals NW-SE magnetic lineaments that are inferred to be parallel to an extinct spreading axis located between Canada and Greenland. The lineaments are interpreted into onshore areas where older NNW-SSE lineament of c.27 chron were interpreted. The absence of obvious magnetic anomalies in the Baffin Bay indicates the existence of serpentinised mantle underneath continental crust, and

ultraslow seafloor spreading in this region. The similarity of the crustal structure derived from gravity modelling and seismic data implies that the Moho corresponds to a major density jump and is unarguably the boundary between crust and mantle.

This chapter provides additional information on the nature of the ocean-continent transition zone and the overall crustal structure along the western Greenland margin. In detail, the continental crust is thinner and the width of extension is greater in the Davis Strait compared to Baffin Bay and Labrador Sea. Hence, the geometry of the crust along the western suggest that rifting and seafloor spreading commenced from Labrador Sea in the south to Baffin Bay in the north.

5.2 Introduction

The nature of the crust and the position of the oceanic-continent transition zone boundary in western Greenland remains a subject of ongoing controversy. Despite recently collected geophysical data, and studies to understand the nature of the plate boundary between North America and Greenland plates, the geodynamic evolution of the West Greenland continental margin is very complex and still poorly understood. For example, until recently the opening of Labrador Sea was considered to be of Late Cretaceous age (Roest and Srivastava, 1989, Oakey, 2008). New evidence, however, using wide-angle seismic velocity analysis, gravity, magnetic and single Euler rotation pole models, proposed the onset of seafloor spreading

to be Palaeocene in age, justifying Eocene motion of the Greenland Plate relative to North America (Chian and Louden, 1994; Chalmers and Laursen, 1995; Oakey and Chalmers, 2012). In addition, the West Greenland margin is categorized as non-volcanic on it Southwest section and volcanic to the North (Keen et al., 2012). Other models include the presence of oceanic crust in Davis Strait and southern Baffin Bay. A 250 km long oceanic crust and c.6 to 9-km thick transition is estimated from a 450 km long seismic refraction (Funck et al., 2012). Other issues related to the geodynamic evolution of the Western Greenland margin include the presence of 20 km thick igneous crust underlain by 4 km thick layer of unknown affinity and the tectonic significance of the Ungava transform fault zone (Funck et al., 2007; Funck et al., 2012). On the northern Baffin Bay, the transition zone to oceanic crust is characterised by a high gravity anomaly and magnetic anomalies dated as Eocene at N27-25N and 24N-13N (Whittaker et al., 1997; Oakey and Chalmers, 2012).

The aim of this chapter is to investigate the nature of the crustal structure offshore West Greenland and relate it to the overall margin evolution. To achieve these purposes, we apply gravity and magnetic modelling to the seismic interpretation in this thesis and validate the nature of COB in three representative seismic profiles in the Baffin Bay, Davis Strait and Labrador Sea. In this chapter we show that the West Greenland margin is characterised by a complex crustal architecture, as revealed by the variation in depth and length of the oceanic and continental crusts. This chapter also provides additional evidence for the propagation and migration of the rift axis

during the breakup of North America and Europe. In the concluding section, it is shown how the model fits the structure observed onshore and offshore Greenland.

5.3 Methods

The gravity and magnetic datasets were transformed from Canadian Lambert coordinates into UTM 21 zone with a WGS 84 datum. Section lines from the gravity and magnetic maps were extracted from Figures 3.2 and 3.3 respectively. The sections were set to +30 km and -30 km in order to minimise the side effect of the gravity modelling and the depth-converted seismic lines were imported as bitmap background images, the horizons and structural interpretations were digitized.

Furthermore, densities of the different stratigraphic units were calculated as a function of velocities using four different methods (Figure 5.4, 5.5 and 5.6) and checked against published seismic refraction studies such as Chalmers et al., (1995), Funck et al. (2007, 2012), and Suckro et al. (2012, 2013). A comparison of the velocity versus density relationship of Gardner et al (1974), Nafe–Drake curve (Ludwig et al., 1970), Christensen and Mooney, (1995) and Godfrey et al. (1997) was attained and plotted in Figures 5.4, 5.5 and 5.6. The serpentinite zone from Nafe–Drake polynomial curve was interpreted in Baffin Bay, Davis Strait and Labrador Sea by comparing density versus velocity relations using the method of Brocher (2005) (Figure 5.4, 5.5 and 5.6). The density values were assigned to the digitized seismic images.

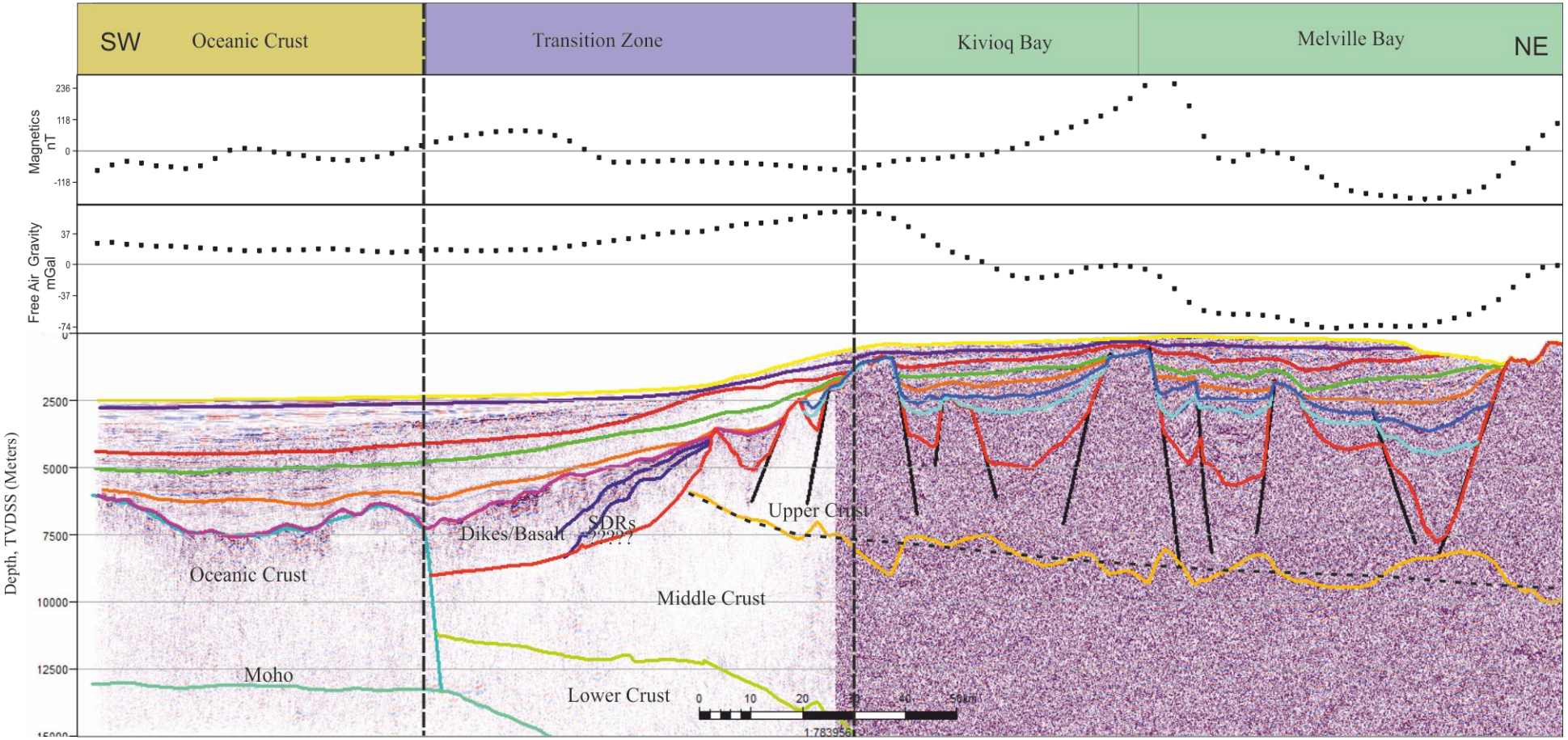

Figure 5.1: Depth-converted seismic line across the Baffin Bay. The principal sub-basins identified include Kivioq and Melville Bay. The oceanic crust is interpreted SW of Baffin Bay with the Moho discontinuity inferred at approximately 12.5 km depth.

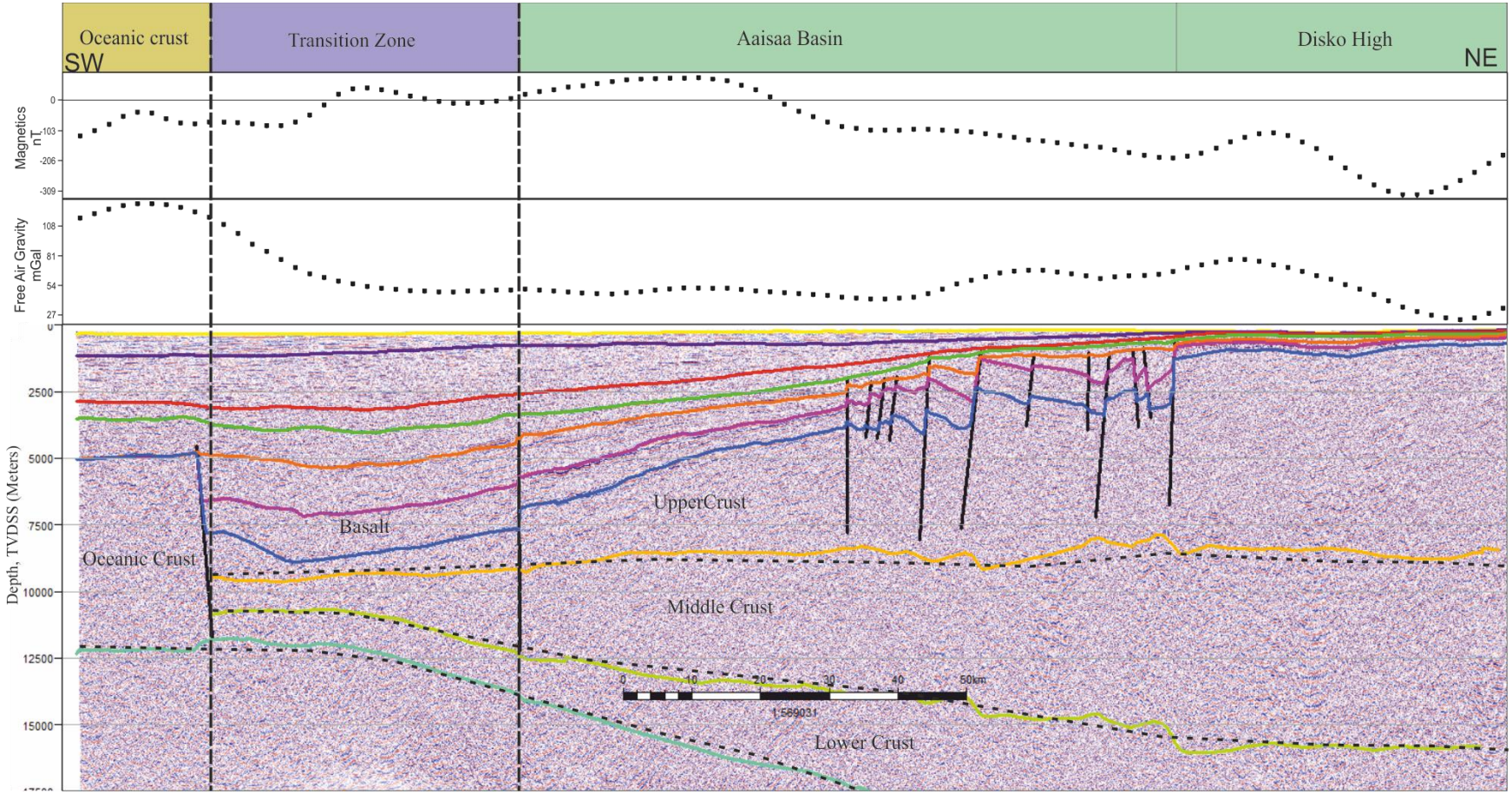

Figure 5.2: Depth-converted seismic line across the Davis Strait. The oceanic crust is interpreted SW of the area at depth of 5.0 km with the Moho discontinuity inferred at c.12.5 km depth. Faults in Davis Strait include half graben and graben intercepting the syn-rift packages.

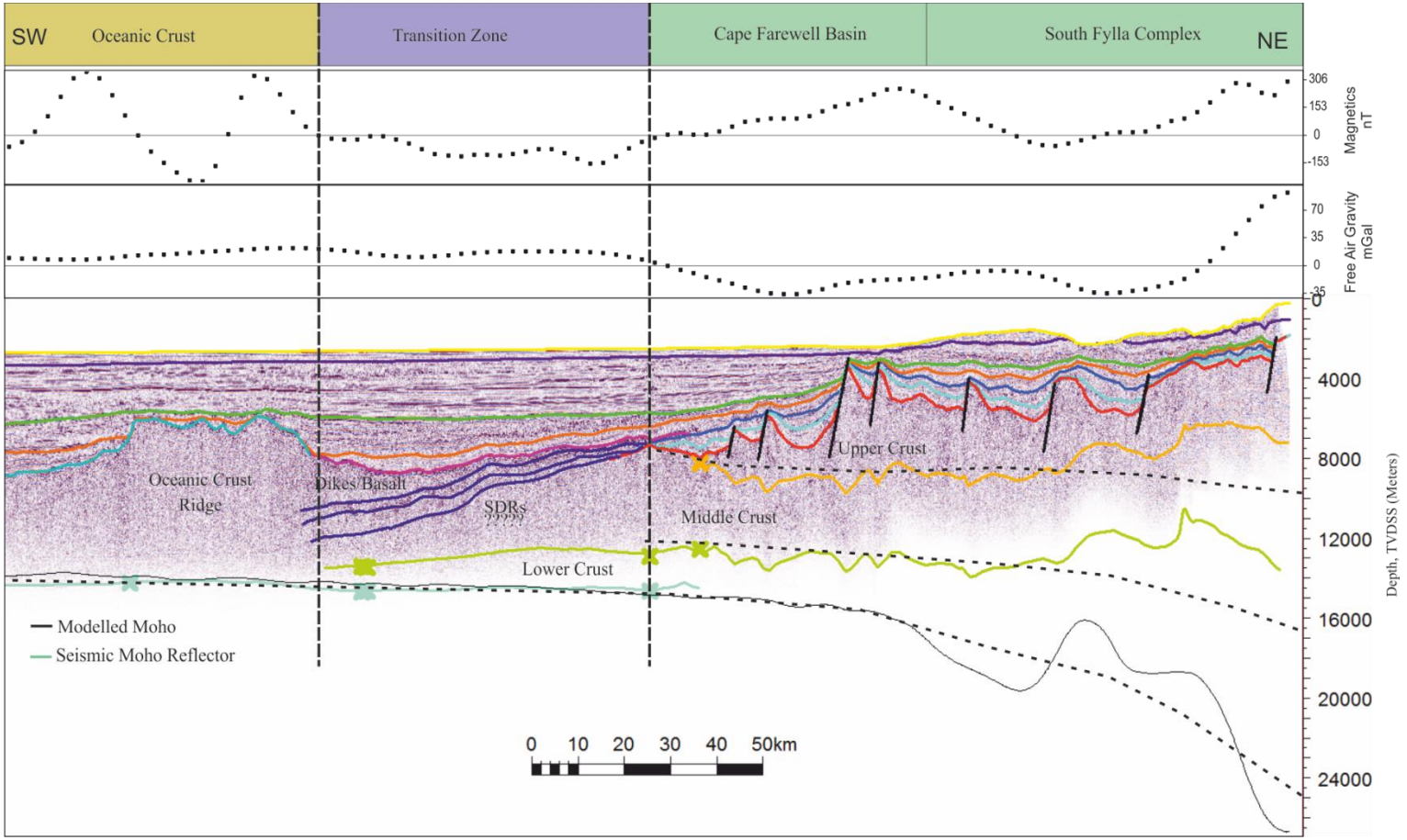

Figure 5.3: Depth-converted seismic line across the Labrador Sea. The transition from continental to oceanic crust is marked by the presence of SDRs. The seismic Moho is buried a depth of c.12.5 km in the SW part of the Strait. There is a good to close match between the seismic and modelled Moho in this area.

The first stage of the 2D modelling estimated Moho depths derived from isostatic modelling. The result shows that the Moho estimation was poor (Figure 5.8). As an alternative, published Moho refraction and Free Air Gravity (Sandwell and Smith v18.1) were used in the 2D gravity modelling (Figure 3.2). After completing the gravity modelling, continental crust, transition and oceanic crust were interpreted in plan view and 3D in order to assess lateral crustal variations, and to integrate results from this Chapter with those of Chapter Four (3D model resulted from seismic interpretation).

The 2D magnetic modelling started with Euler deconvolution (Figure 5.7) as a way to estimate depth to the source body location (Durrheim and Cooper, 1998). Using data filtering such as vertical gradient, a potential field can be described as the convolution of a source distribution with a function of the degree of the structural indices and the window size. The Structural Index (SI) then provides a means of determining the geometry of the source. A default parameter of the window size was used as well as structures indices of 0.05 and 1, (Reid et al.,1990) (Table 5.1). Structural Index of 1 was used to calculate and assign magnetic susceptibility to match the observed magnetic anomalies for the dikes.

Table 5.1: Structural indices for different geological structures (after Reid et al. 1990)

Structural Index	Geological Structure
0	Contact
1	Sill/Dike
2	Vertical Pipe
3	Sphere

The structural indexes (SI=1) from the magnetic Euler deconvolution modelling were used to locate and map dikes (blocks), then magnetic susceptibility was assigned to these blocks (red cycles in Figure 5.7). In our analyses, the assigned susceptibility for upper crust blocks areas failed to match observed magnetic anomaly. Therefore, the Euler deconvolution indexing technique may not represent dikes in all cases. As a result, the mapped blocks assigned magnetic susceptibility were removed across the entire profile and 2D gravity modelling was used instead. Consequently, the 2D gravity modelling (Modelling run 2; See figures 5.14, 5.17 and 5.20) for the mantle, top lower crust and top middle crust were modelled based on published seismic refraction (Figure 5.8), which resulted in little variation between modelled and calculated gravity anomalies.

5.4 Gravity and Magnetic Forward 2D Modeling

In this section, the results of the modeling are presented from transects across the basins forming the West Greenland margin. In order to simplify the observation and discussion, the subsections are divided into profiles based on seismic, gravity, velocity and magnetic modellng results. First, we summarise the crustal structure from seismic and compared their velocity, gravity and magnetic properties.

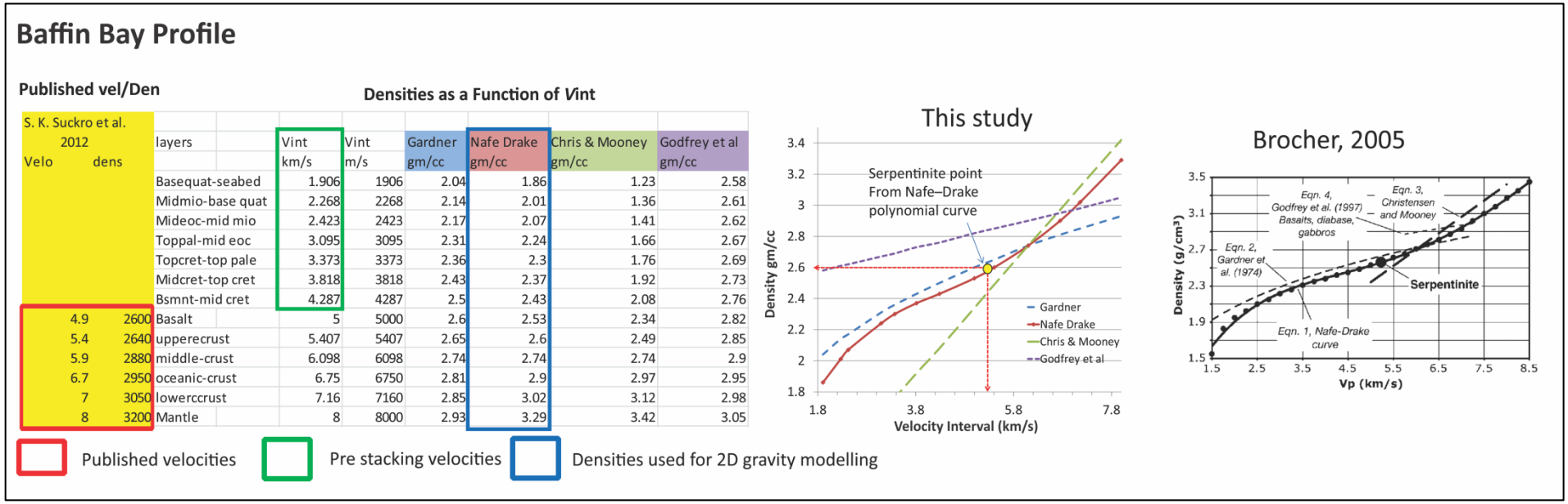

.

Figure 5.4: Baffin Bay velocity vs density comparison chart. Densities were then calculated as a function of velocities using four different methods and in comparison with published data of Chalmers et al., (1995), Funck et al. (2007, 2012), and Suckro et al. (2012, 2013). Serpentinite zone from Nafe–Drake polynomial curve was interpreted in Baffin Bay, Davis Strait and Labrador Sea in accord with the work of Brocher 2005.

Davis Strait Profile

Published vel/Den

Densities as a Function of *Vint*

FUNCK ET AL 2012 velo	den	layers	Vint km/s	Vint m/s	Gardner gm/cc	Nafe Drake gm/cc	Chris & Mooney gm/cc	Godfrey et al gm/cc
		Basequat-seabed	2.239	2239	2.13	2	1.35	2.61
		Midmio-base quat	2.435	2435	2.18	2.07	1.42	2.62
		Mideoc-mid mio	2.827	2827	2.26	2.18	1.56	2.65
		Toppal-mid eoc	4.044	4044	2.47	2.4	2	2.74
		basalt-Toppal	4.642	4642	2.55	2.48	2.21	2.79
5.1	2575	basalt	5.127	5127	2.62	2.55	2.39	2.83
5.8	2700	upperecrust	5.763	5763	2.7	2.67	2.62	2.88
6.4	2795	Oceanic-crust	6.35	6350	2.76	2.8	2.83	2.92
6.7	2855	middle-crust	6.6	6600	2.79	2.86	2.92	2.94
7	2940	lower-crust	6.75	6750	2.81	2.9	2.97	2.95
7.9	3300	Mantle	8	8000	2.93	3.29	3.42	3.05

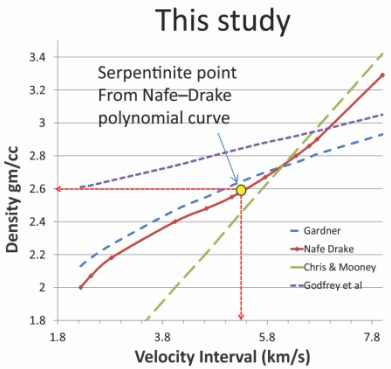

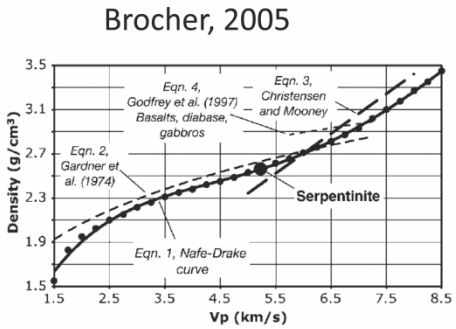

Published velocities Pre stacking velocities Densities used for 2D gravity modelling

Figure 5.5: Davis Strait velocity vs density comparison chart. Densities were then calculated as a function of velocities using four different methods and in comparison with published data of Chalmers et al., (1995), Funck et al. (2007, 2012), and Suckro et al. (2012, 2013). Serpentinite zone from Nafe–Drake polynomial curve was interpreted in Baffin Bay, Davis Strait and Labrador Sea in accord with the work of Brocher 2005.

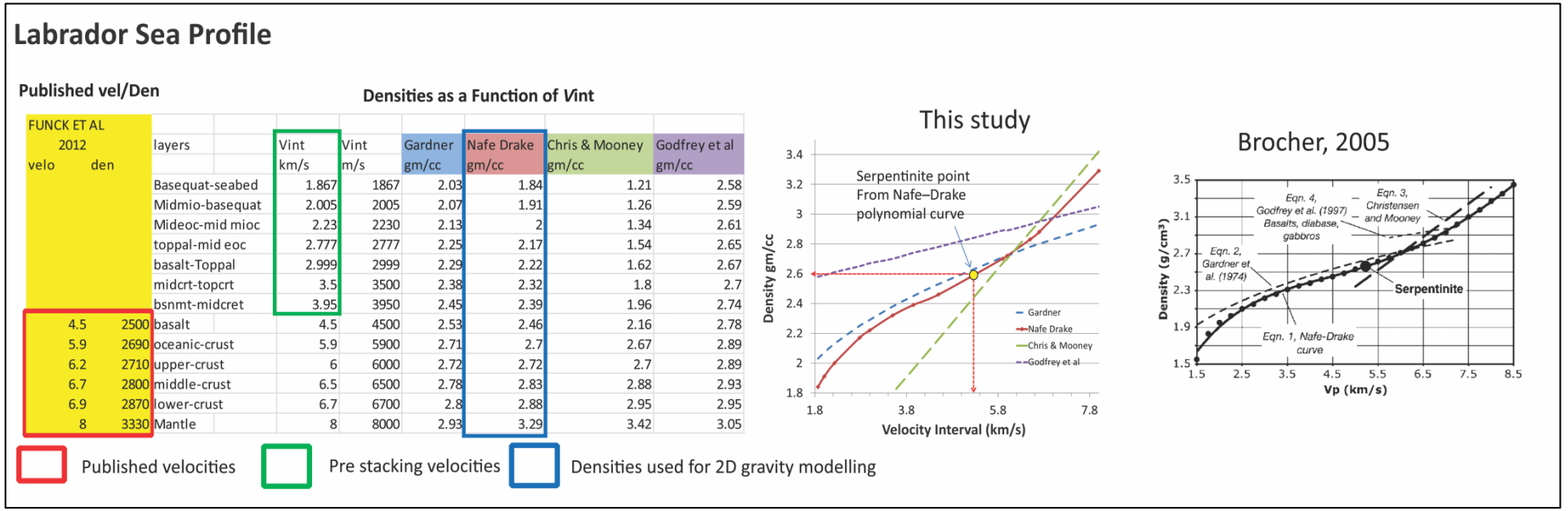

Figure 5.6: Labrador Sea Baffin Bay velocity vs density comparison chart. Densities were then calculated as a function of velocities using four different methods and in comparison with published data of Chalmers et al., (1995), Funck et al. (2007, 2012), and Suckro et al. (2012, 2013). Serpentinite zone from Nafe–Drake polynomial curve was interpreted in Baffin Bay, Davis Strait and Labrador Sea in accord with the work of Brocher 2005.

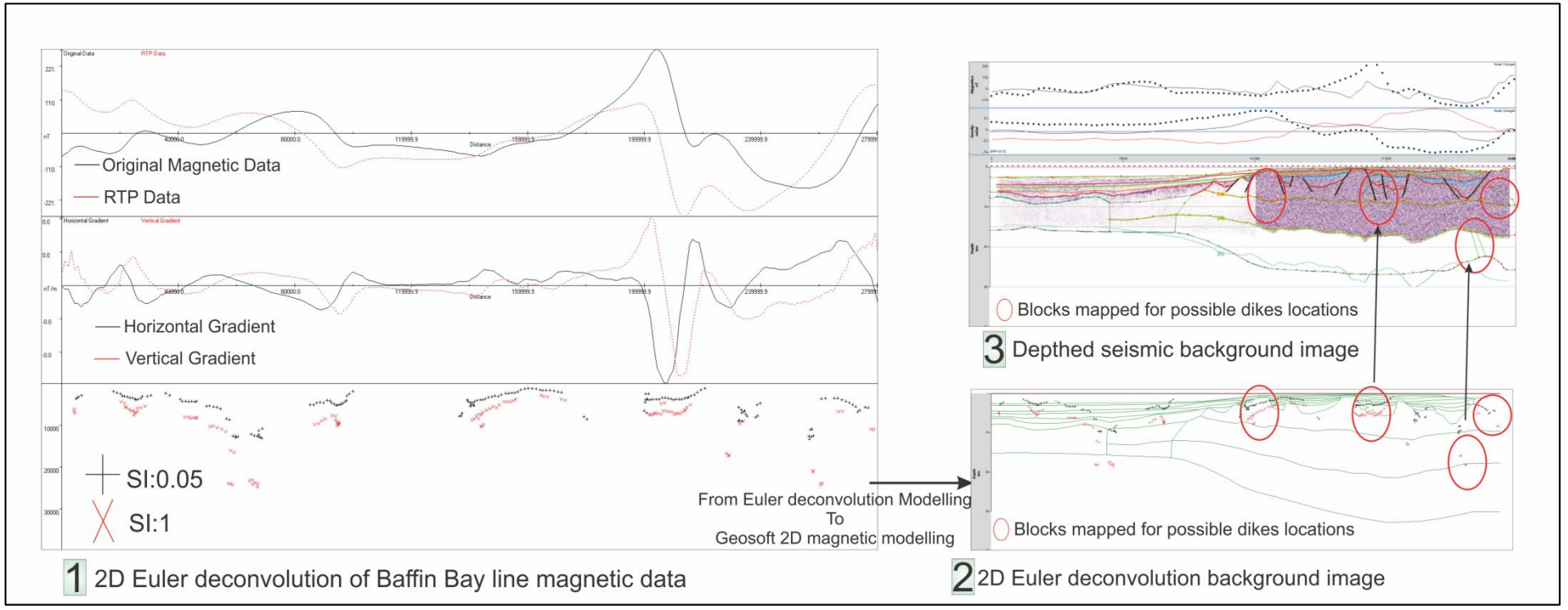

Figure 5.7: Showing Euler deconvolution and blocked assigned magnetic susceptibility used for magnetic modelling

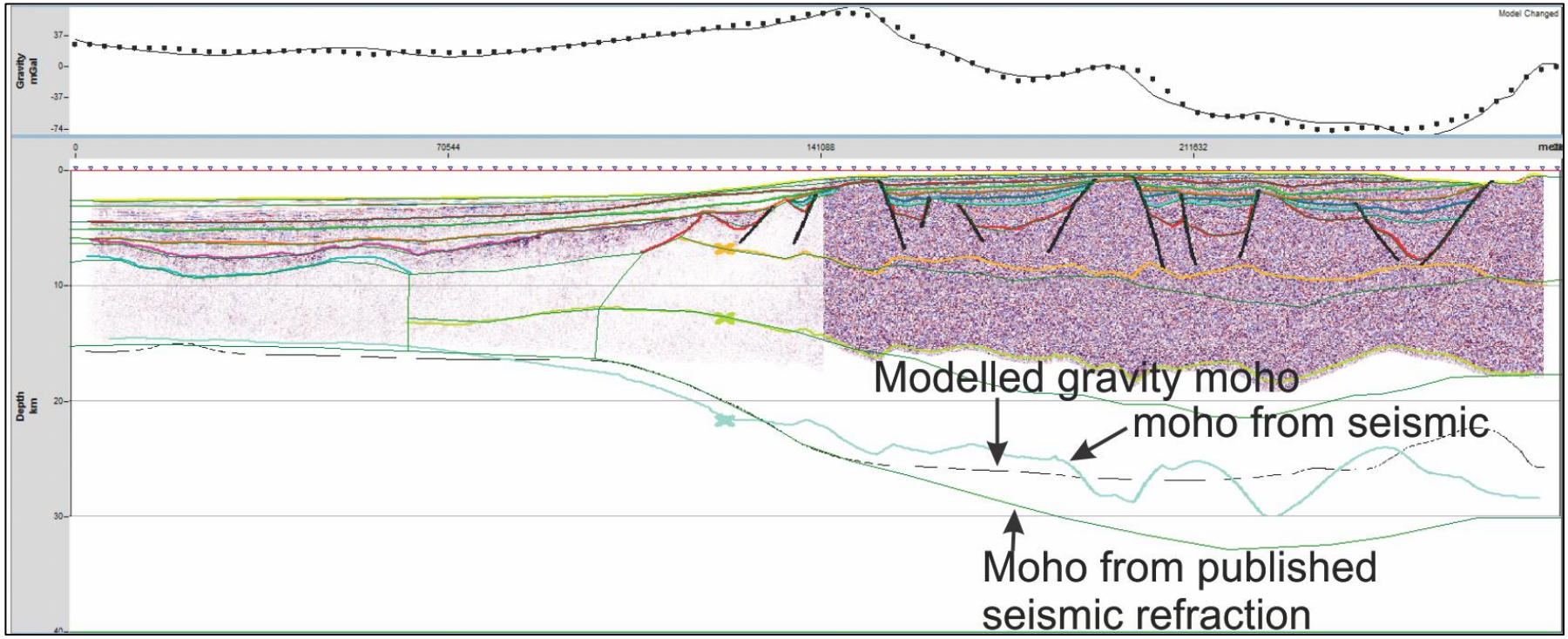

Figure 5.8: Showing the first trial for Moho modelled from isostatic gravity, the Moho mapped in seismic reflection (no control reflection) and the final modelled Moho based on seismic refraction Funck et al., 2012; Suckro et al., 2013.

5.4.1 Baffin Bay

The Baffin Bay seismic profile is 280 km long (Figure 5.1) and shows sediment thickness of *c*.5.6 km in Kivioq Bay, and *c*.7 km in both Melville Bay and Southwest Kivioq ridge. The depth to the Moho was based on published seismic refraction data, indicating a range between *c*.22 km and *c*.27 km for continental crust (Chalmers et al., (1995), Funck et al. (2007, 2012), and Suckro et al. (2012, 2013). The transition zone between the oceanic and continental crust has as a depth to the Moho ranging from *c*.22-15 km to *c*.15 km.

Very minor differences are recorded between observed and calculated gravity anomalies (< 10 mGal; Figure 5.9) in the Kivioq and Melville Bays, at the ocean-continent transition zone and on oceanic crust (Figure 5.14). The gravity model predicts that the westernmost60 km is oceanic crust, out of the 280 km section. The oceanic crust occurs at depth of *c*.7 to 15 km (8 km thick) southwest of Kivioq Ridge (Figure 5.14) and is charecterised by a positive Free Air gravity anomaly (20 mGal). Continental crust is *c*.143 km wide, extend from the Melville Platform in the northeast to the Kivioq Ridge in the middle of the section. Here, continental crust is characterised by negative FA gravity anomalies (-74 mGal in Melville Bay and -20 mGal in Kivioq Bay). A transition zone of *c*.77 km between oceanic and continental crust is observed and characterised by positive FA gravity anomaly decreasing gradually from 74 mGal over Kivioq Ridge to 25 mGal southwest of Kivioq Ridge.

Interval velocities obtained from pre-stacking velocities were used for seismic layers spanning the seabed to acoustic basement, (Figure 5.4 and 5.12). Observed velocities range from 1.9 to 4.2 km/s. Published seismic refraction velocities (e.g Suckro et al, 2012) were used for the layers observed from the acoustic basement to mantle, where interval velocities range reach 5 to 8 km/s (Figure 5.4).

The average densities of modeled crustal structures in the Baffin Bay region are 1.8 to 2.4 gm/cc for the sedimentary cover, 2.5 gm/cc for basalt, 2.6, 2.7 and 3.0 gm/cc for upper, middle and lower crusts respectively, an oceanic crust density of 2.9 gm/cc and 3.3 gm/cc for the mantle (Figure 4.5 and 5.13).

The magnetic profile shows positive and high magnetic anomalies recorded in the Melville Ridge that are attributed to magmatism on the ridge (Figure 5.9). The magnetic anomaly is c.228 nT, a value that contrasts with the high negative magnetic anomaly recorded in the adjacent Melville Bay (Figure 5.9). The SW portion of Baffin Bay is characterized by a negative magnetic anomaly correlated to the oceanic crust (Figure 5.9). The variation between observed and modeled magnetic anomalies is noted to the SW of the transition zone and at the boundary between the Kivioq and Melville Bays (Figure 5.9). At the transition zone, the dikes were mapped and modelled whereas the upper crust is exposed close to the surface at the boundary between Kivioq and Melville Bay.

5.4.2 Davis Strait

The seismic profile modelled in the Davis Strait is approximately 209 km long (Figure 5.2). An inferred overburden thickness has been assumed to be *c.*2 km and *c*.6 km in the Disko High and Aaisaa Basin, respectively. The depth to the Moho as interpreted on seismic refraction (Suckro et al, 2012) is *c*.25-18 km below the continental crust, 18-15 km deep at the transition zone and c.15 km in the oceanic crust.

Differences between the observed and calculated FA gravity anomaly values are very low in the Disko High and Aaisaa Basin (< 20 mGal). The gravity model implies the existence of a 18 km long oceanic crust. The oceanic crust occurs at a depth of *c*.7 to 15 km i.e. 8 km thick Southwest of Aaisaa Basin (Figure 5.17) and is characterised by a positive FA gravity anomaly (135 mGal). Continental crust is *c*.150 km, extending from the Disko High in the Northeast to the centre of the Aaisaa Basin, and is characterised by a positive FA gravity anomalies (27-81 mGal in the Disko High and 54-81 mGal in the Aaisaa Basin). A transition zone of 41 km between the oceanic and continental crust is observed and characterised by a positive FA gravity anomaly (81 mGal).

Published seismic refraction velocities for rocks observed between the acoustic basement and the top of the mantle ranges from 5.1 to 7.9 km/s (Suckro et al, 2012, Figure 5.5). The average densities of modeled crustal structures in the Davis Strait region are 2.0 to 2.5 g/cc for sedimentary cover, 2.55 g/cc for basalt, 2.6, 2.8 and 2.9 g/cc for upper, middle and lower

crusts respectively, an oceanic crust density of 2.8 g/cc and 3.3 gm/cc for the mantle (Figure 5.5 and 5.16).

The magnetic profile across the Davis Strait displays a positive amplitude over the Aaisaa Province (Figure 5.10). The transition zone between the oceanic and continental crust is characterized by a very low amplitude magnetic anomaly. There is a significant difference between the modelled and observed anomalies at the transition zone and in the SW part of the Aaisaa Basin. This variation is attributed to the presence of a thick basalt layer underneath the transition zone which thins to the northeastern part of Disko High. A thin sedimentary cover was interpreted from the transition zone to the NE part of the seismic section (Figure 5.10).

5.4.3 Labrador Sea

The Labrador Sea seismic profile is approximately 277 km in length (Figure 5.3). Overburden thickness varies from 1 to 6 km in the Cape Farewell basin and 1 to 4 km in the South Fylla complex. Depth to Moho is 16 km and 27 km below the continental crust. The transition zone has a Moho depth approaching 15 km and 14 km at oceanic crust.

Differences in the modelled and observed FA gravity anomalies are in the range of <15 mGal, as noted in Cape Farewell and the South Fylla complex. The gravity models revealed a 70 km wide oceanic crust

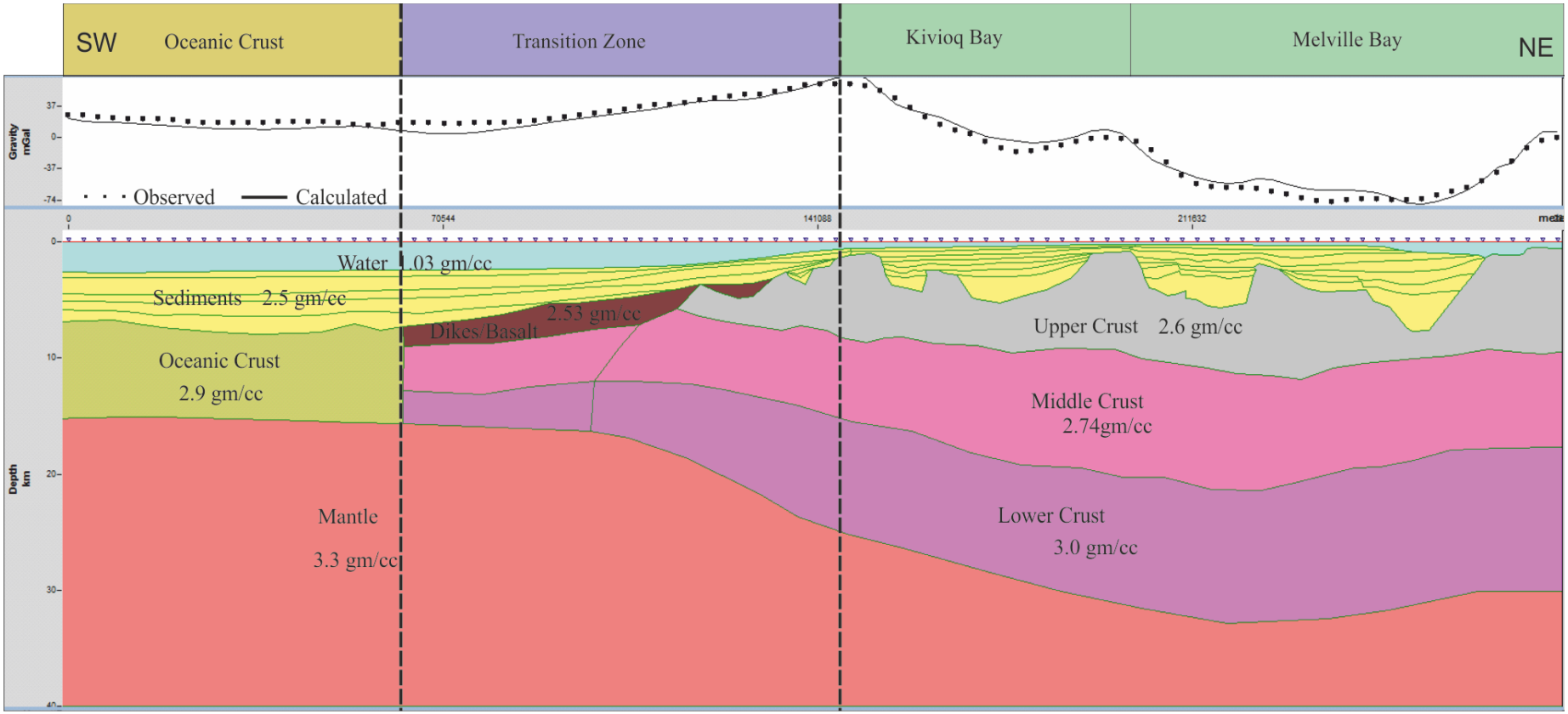

Figure 5.9: Showing the modelled gravity and magnetic for Baffin Bay (Model run 1)

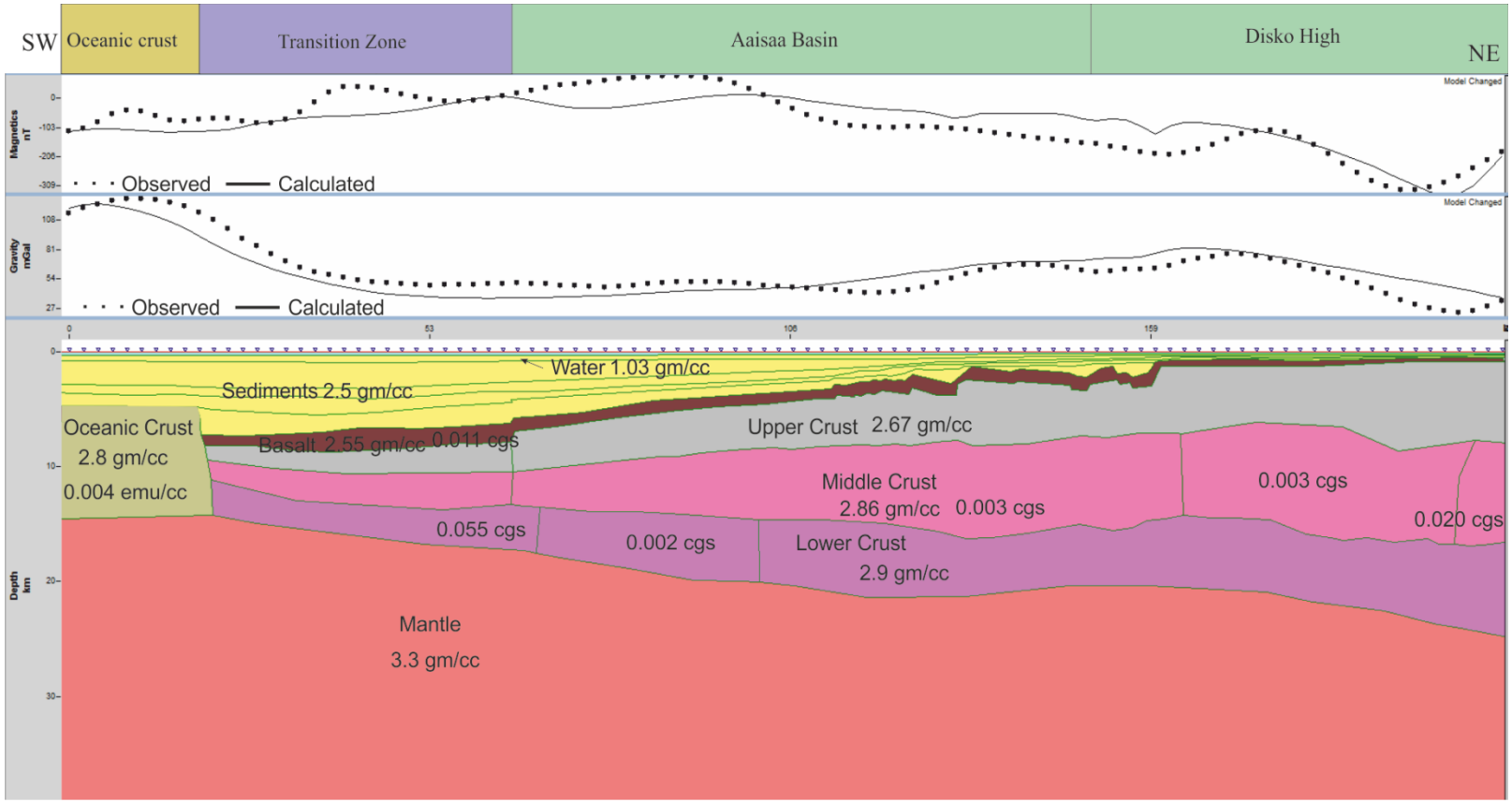

Figure 5.10: Showing the modelled gravity and magnetic for Davis Strait (Model run 1)

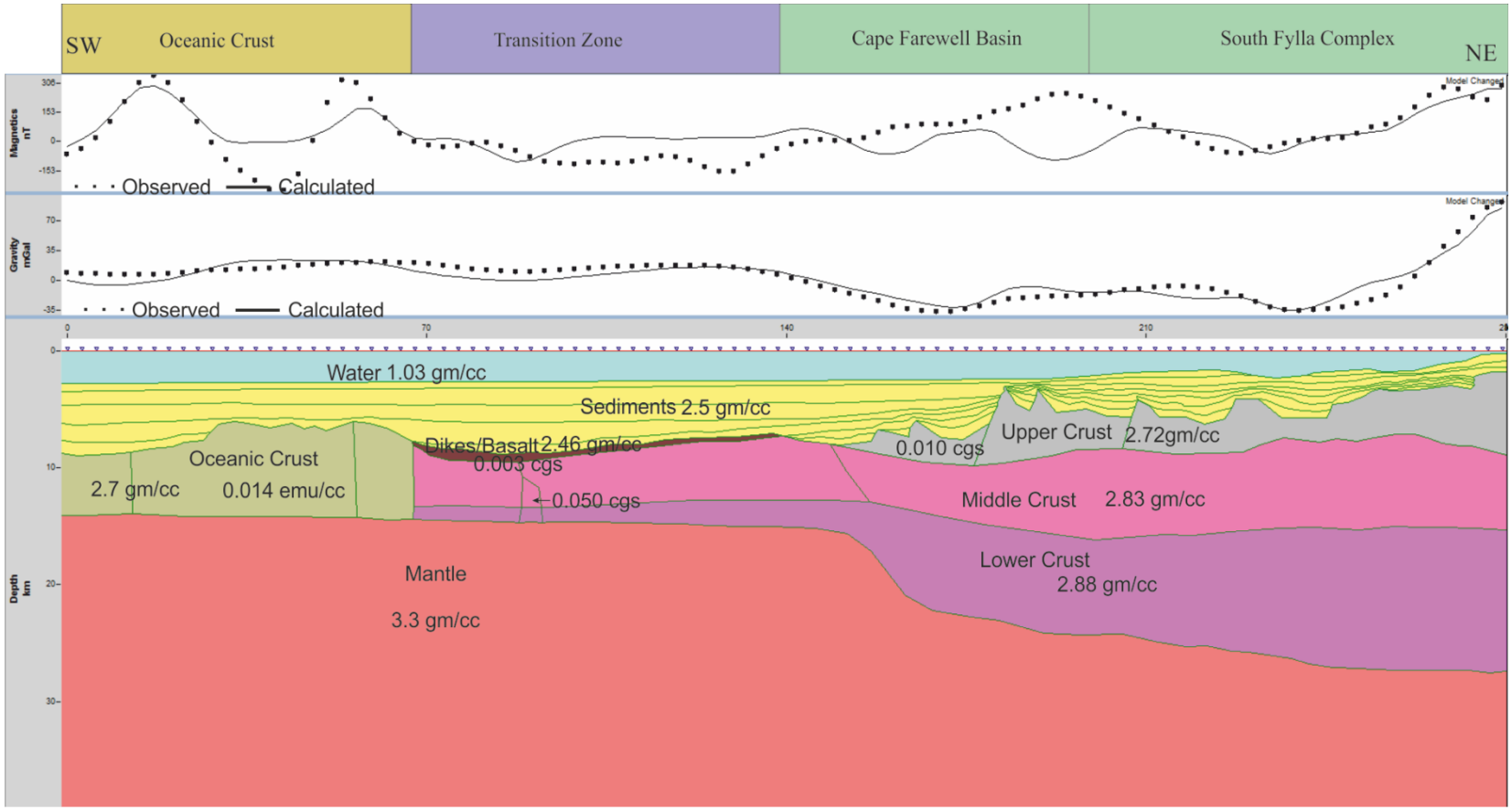

Figure 5.11: Showing the modelled gravity and magnetic for Labrador Sea (Model run 1)

The crust reaches a depth of 7 to 14 km (7 km thick) Southwest of Cape Farewell (Figure 5.20) and is characterised by a positive FA gravity anomaly (15-20 mGal). The continental crust is nearly 127 km wide, extending from the South Fylla complex in the northeast to the middle of Cape Farewell Basin. It is characterised by both positive and negative FA gravity anomalies (105 to -35 mGal in South Fylla complex and 20 to -35 mGal in Cape Farewell Basin). A transition zone of about 80 km wide is modelled between the oceanic and continental crust, being characterised by a positive FA gravity anomaly (20 mGal).

For the Labrador Sea, the internal velocities used are 1.8 to 3.9 km/s (Funck et al, 2012). Average densities are 1.8 to 2.3 g/cc for sedimentary cover, 2.5 g/cc for basalt, 2.7, 2.8 and 2.88 g/cc for upper, middle and lower crusts respectively and an oceanic crust density of 2.7 g/cc and 3.3 g/cc for the mantle (Figure 5.6 and 5.19).

Positive magnetic amplitudes are observed Southwest of Cape Farewell and South Fylla complex (Figure 5.11). This area of high magnetic amplitudes is 70 km wide and 7.5 km thick, and is interpreted to be oceanic crust. The observed anomalies are higher than the modelled anomaly at the boundary between Cape Farewell Basin and South Fylla Complex. However, smaller differences in amplitude are observed between these anomalies at the ocean-continent transition zone. The upper crust is exposed at the boundary between Cape Farewell Basin and South Fylla Complex. This area also presents very thin sedimentary cover (Figure 5.11).

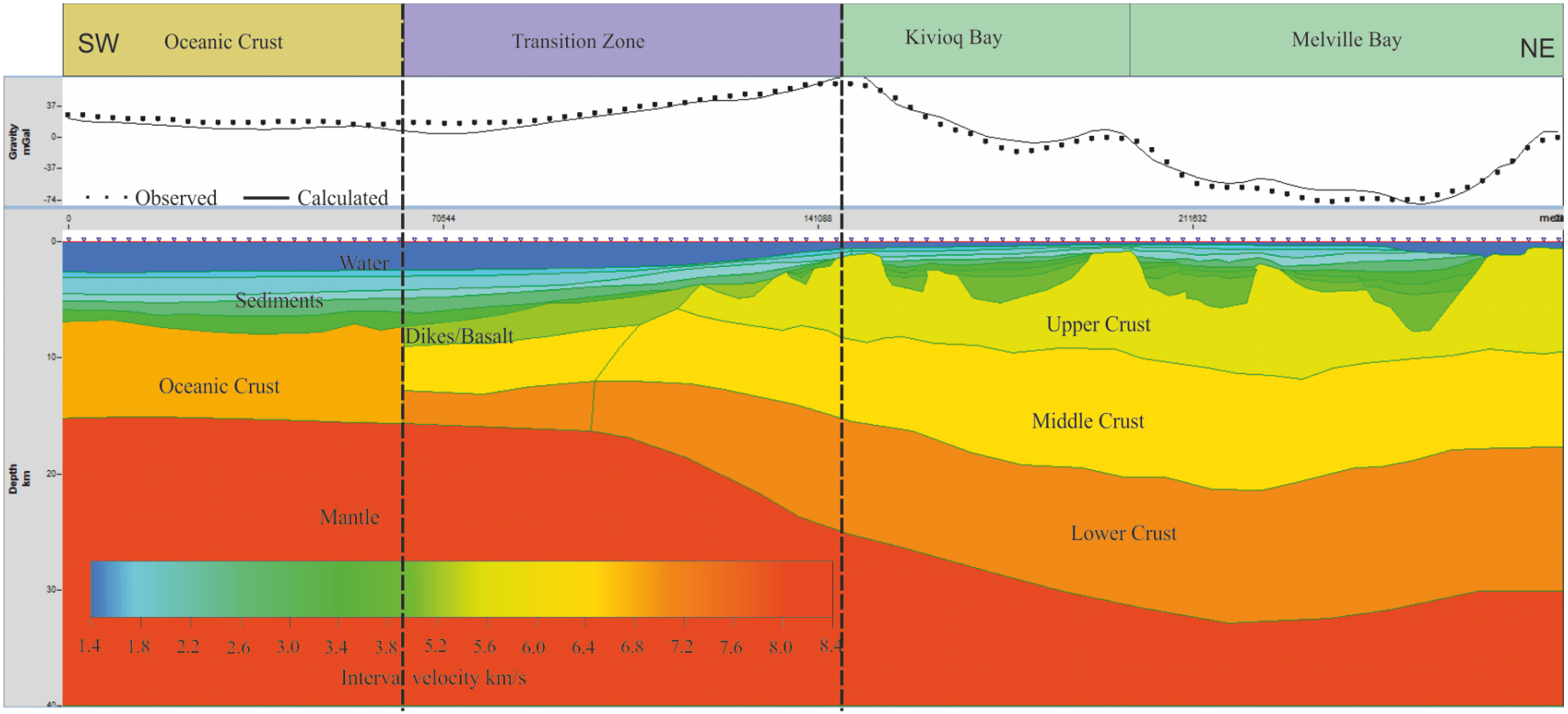

Figure 5.12: Interval velocity of rocks in Baffin Bay and its sub-basins. There is step in velocity value from the continental crust and the mantle.

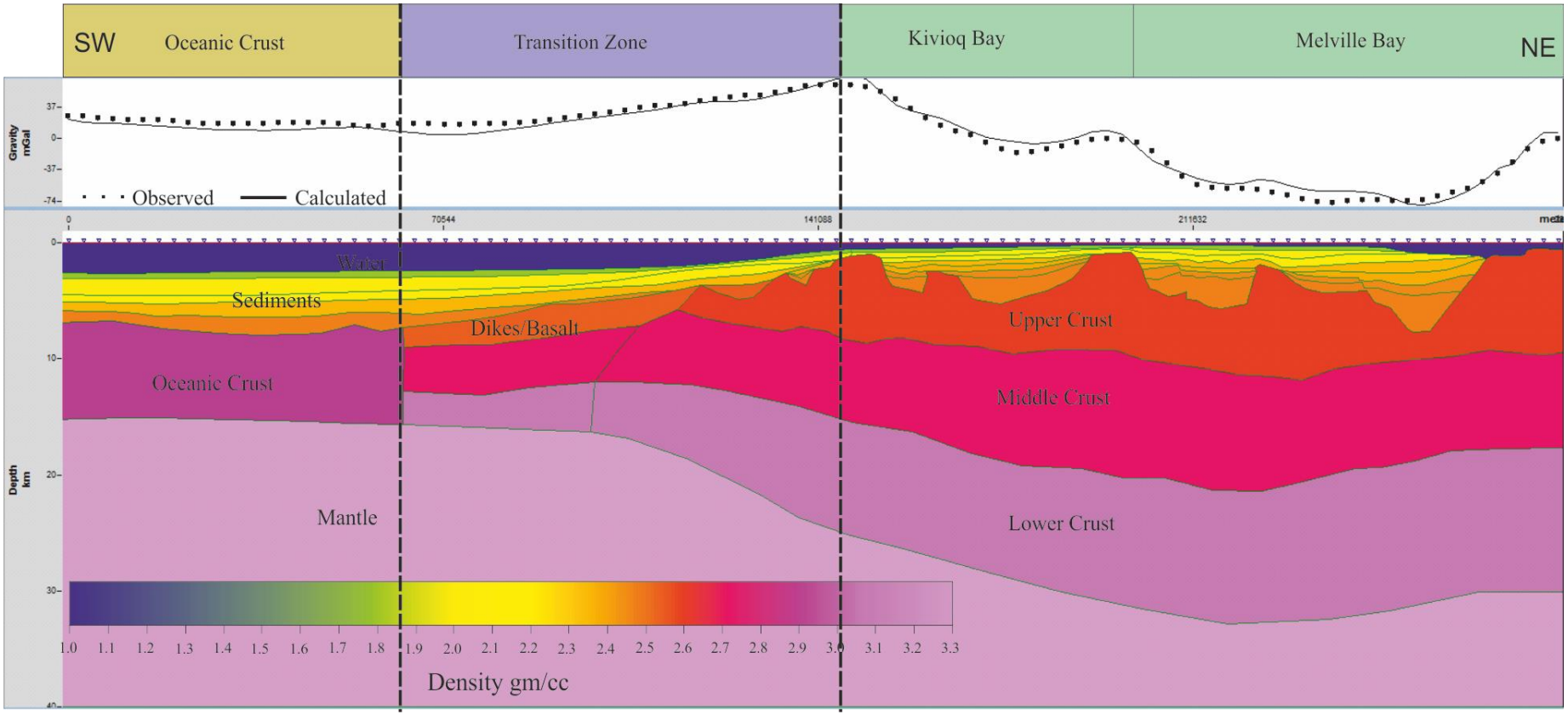

Figure 5.13: Modeled structure and crustal density of rocks in Baffin Bay and its sub-basins. There is a good match between the observed and calculated gravity anomaly.

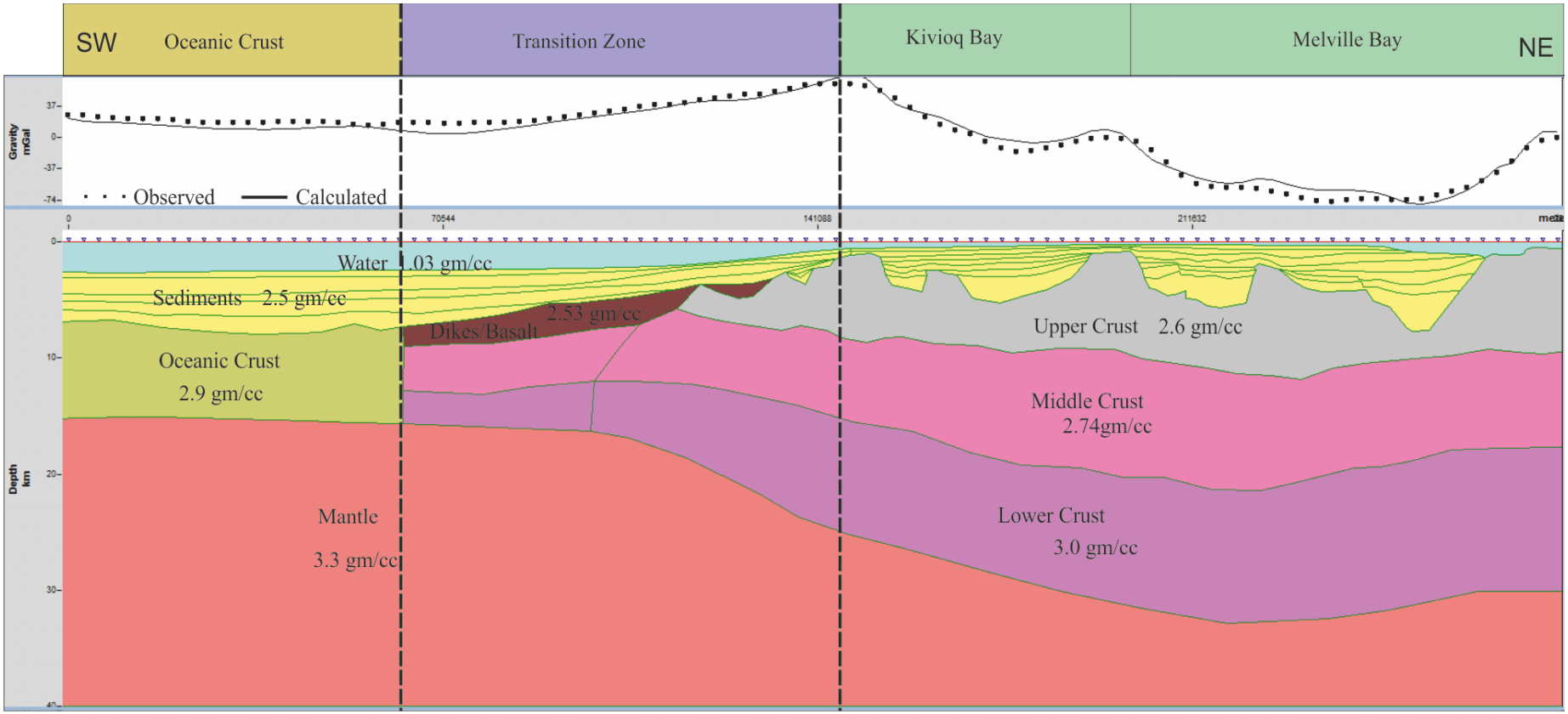

Figure 5.14: Modelled 2D gravity for Baffin Bay and its sub-basins.

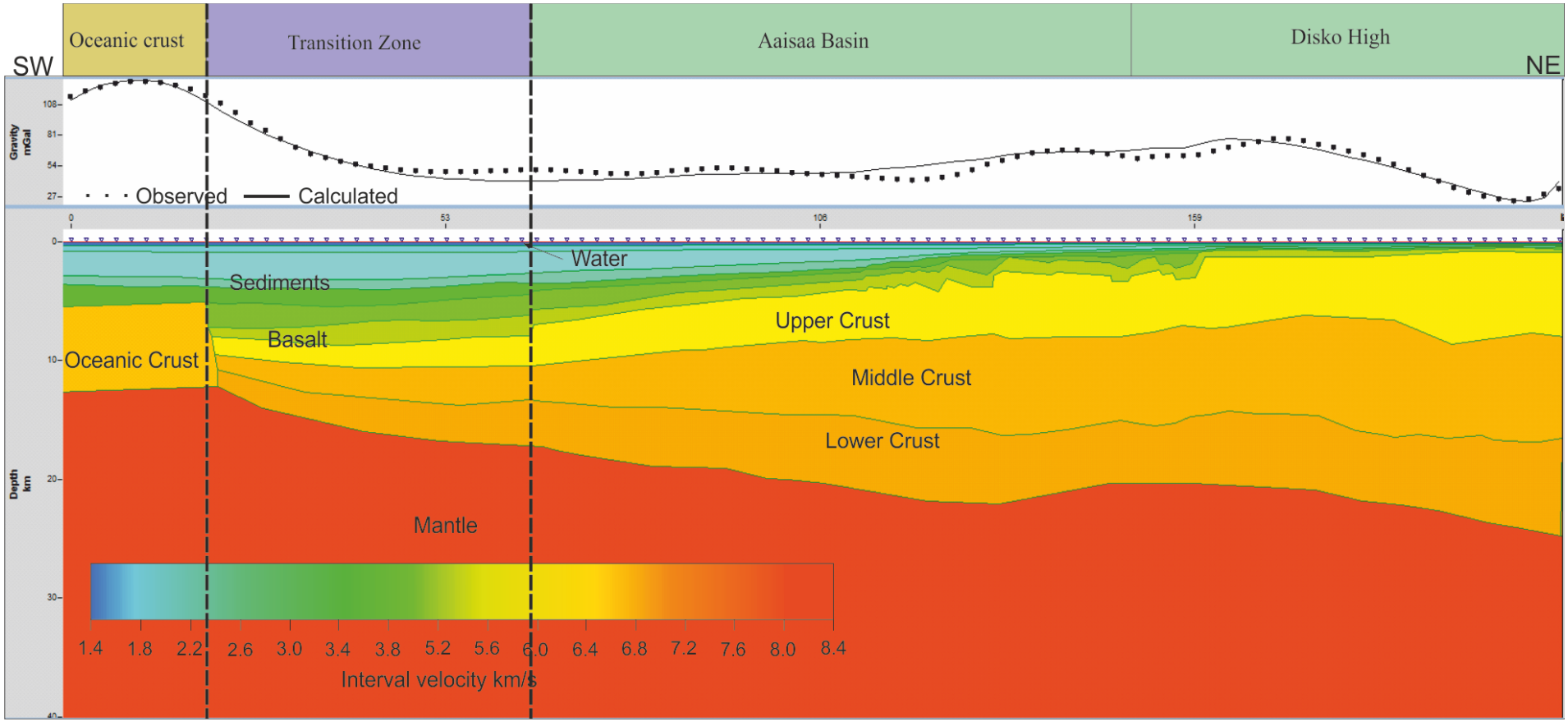

Figure 5.15: Interval velocity of rocks in Davis Strait and its sub-basins. There is a hop in velocity value from the continental crust and the mantle.

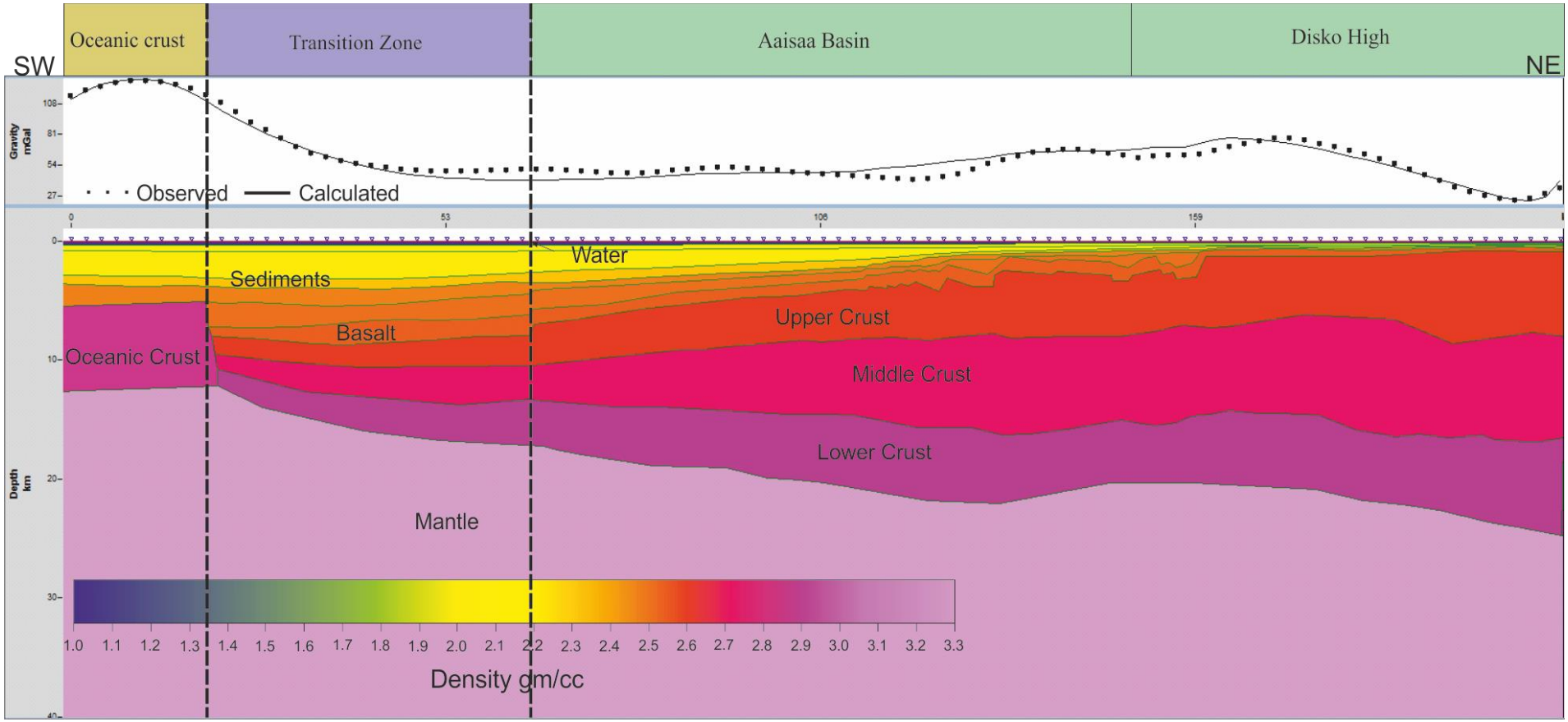

Figure 5.16: Modeled structure and crustal density of rocks in Davis Strait including Aaisaa Basin and Disko high. There is a perfect match between the observed and calculated gravity anomaly.

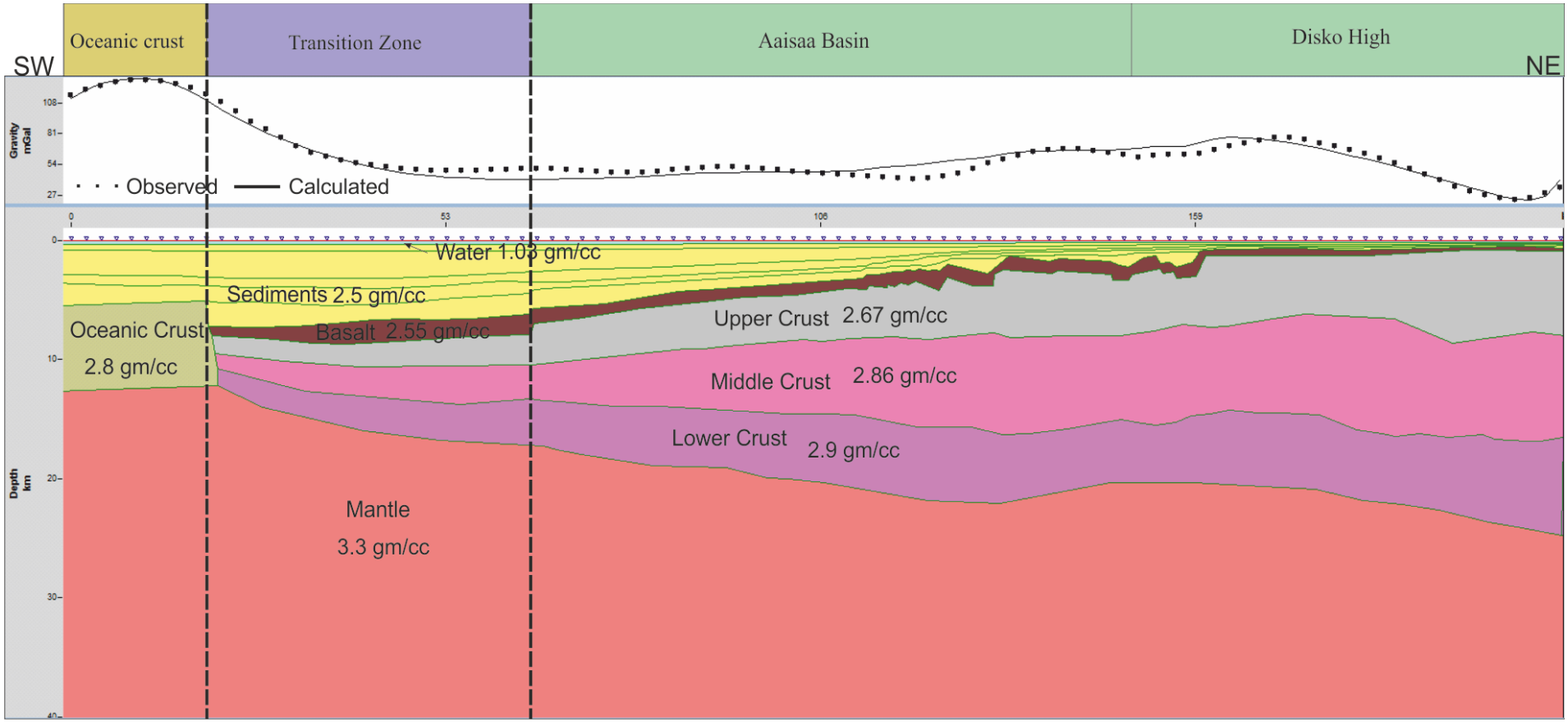

Figure 5.17: Modelled 2D gravity for Davis Strait and its sub-basins.

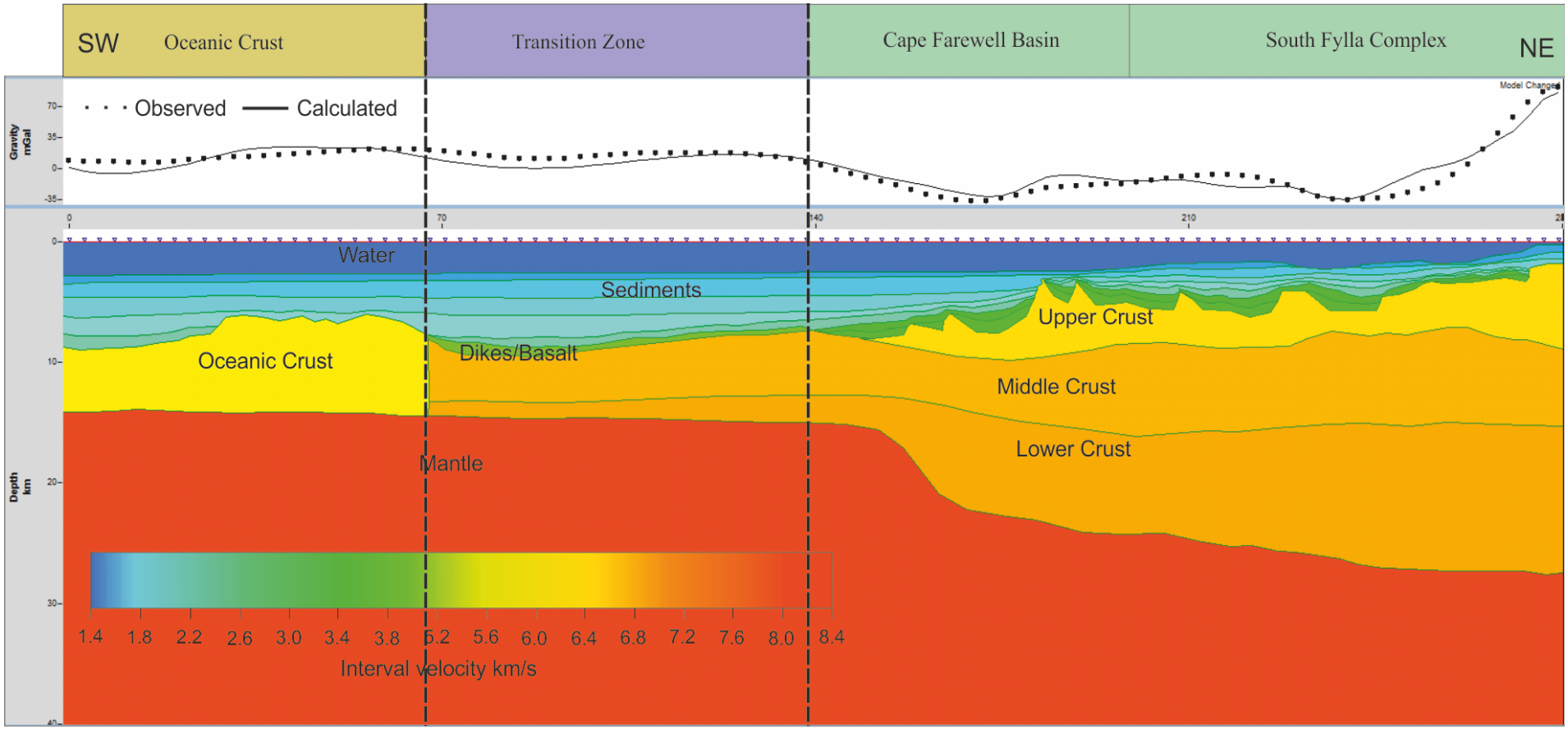

Figure 5.18: Interval velocity of rocks in Labrador Sea. There is step in velocity value from the continental crust and the mantle.

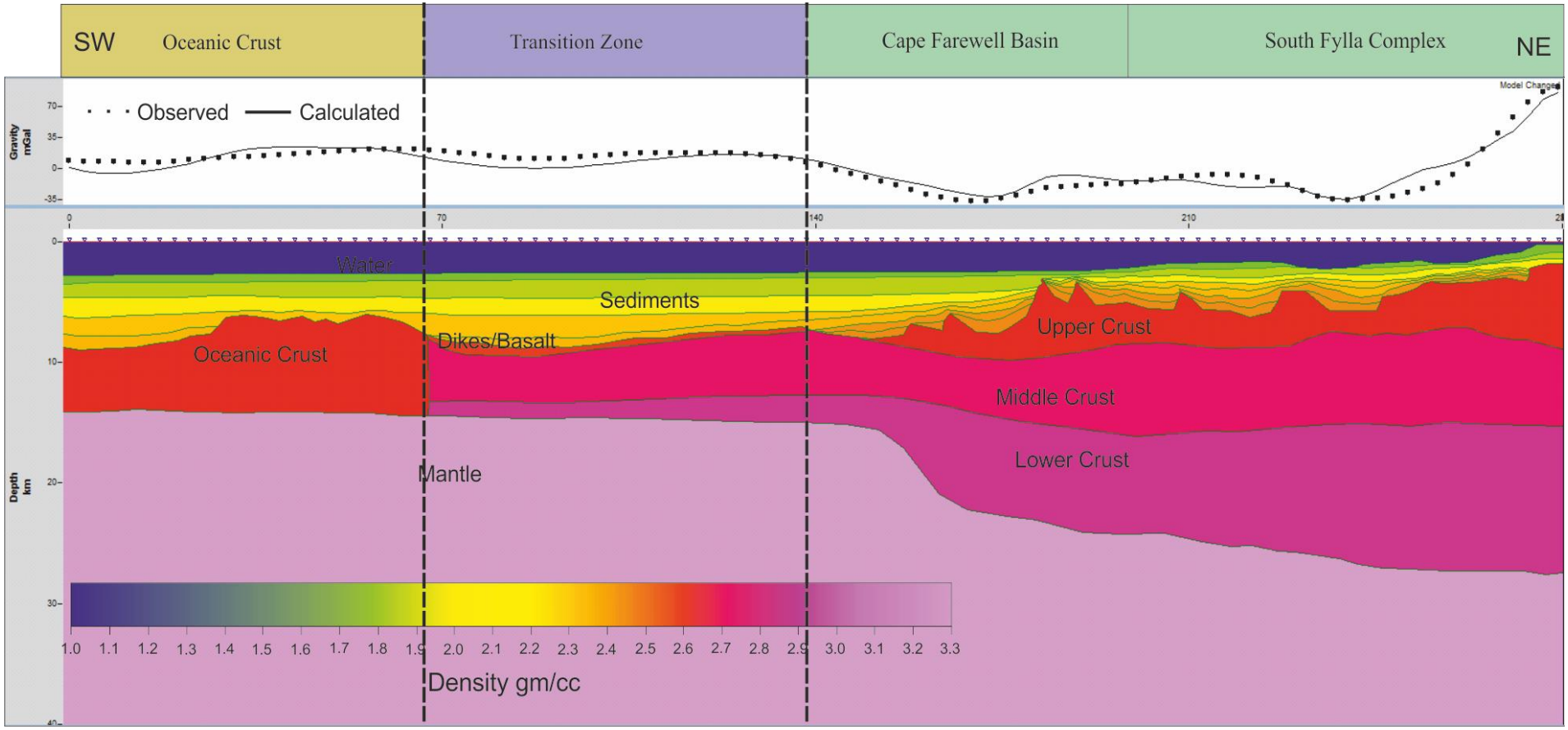

Figure 5.19: Modeled structure and crustal density of rocks in Labrador Sea. Contrast in anomalies are recorded in South Fylla complex and the transition zone between the oceanic and continental crust.

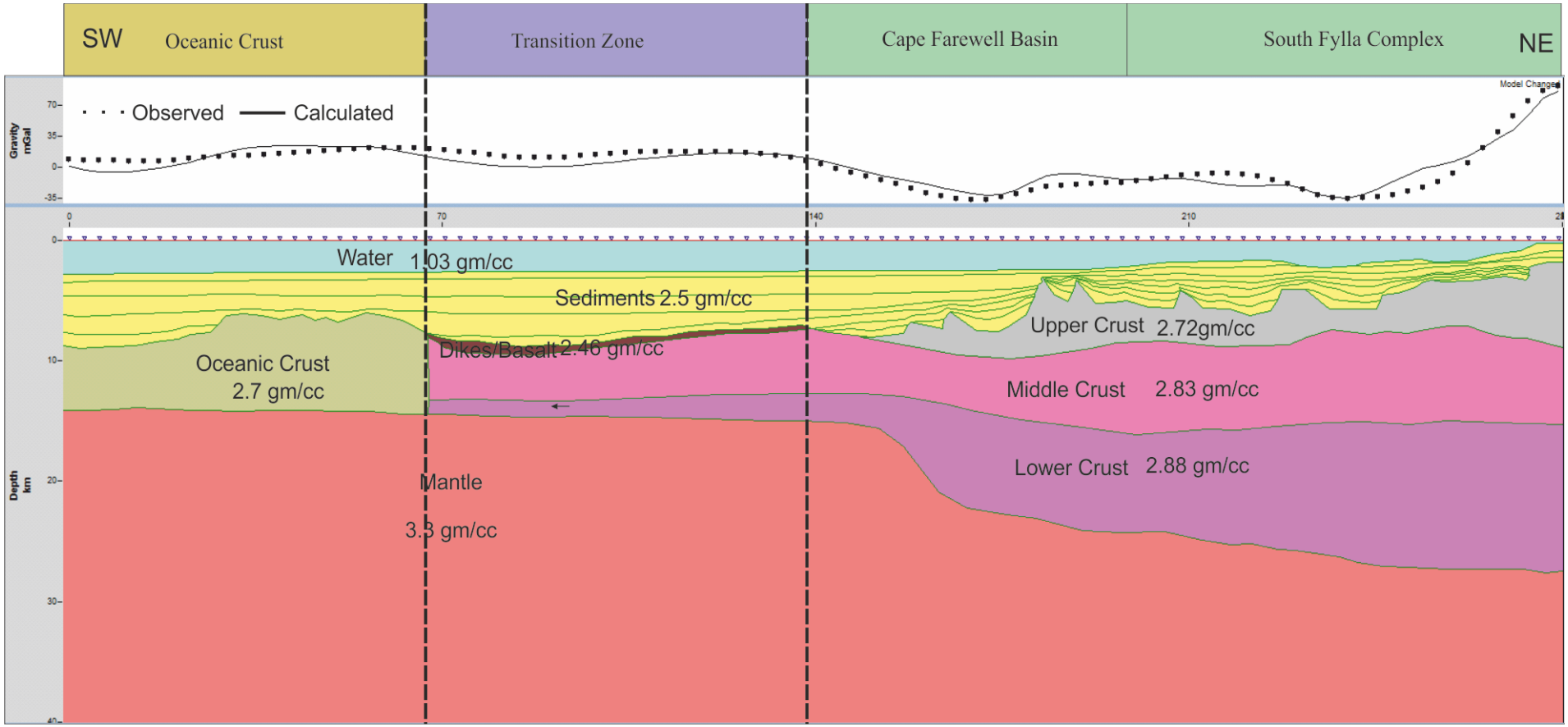

Figure 5.20: Modelled 2D gravity for Labrador Sea and its sub-basins.

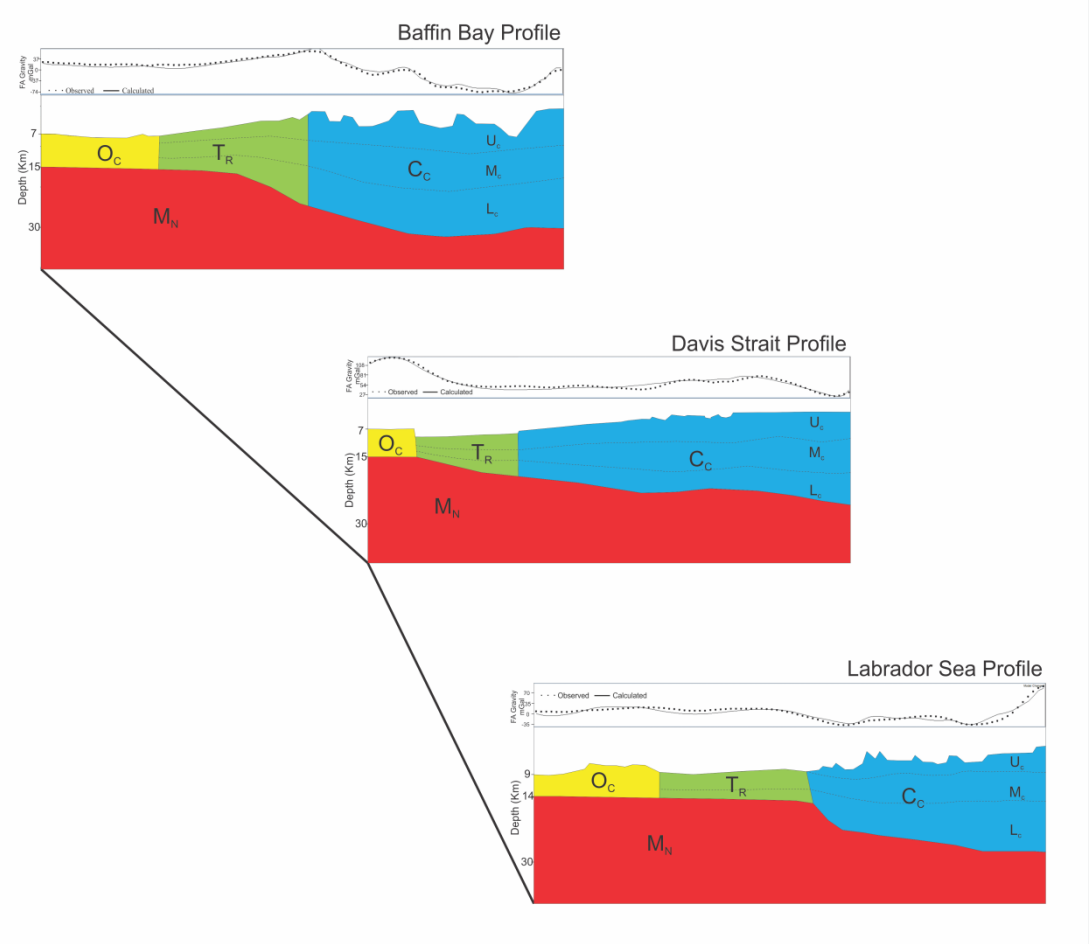

Figure 5.21: 3D sketch showing variation of the crustal structure from Baffin Bay to Labrador Sea. The continental crust thickens north towards Baffin Bay.

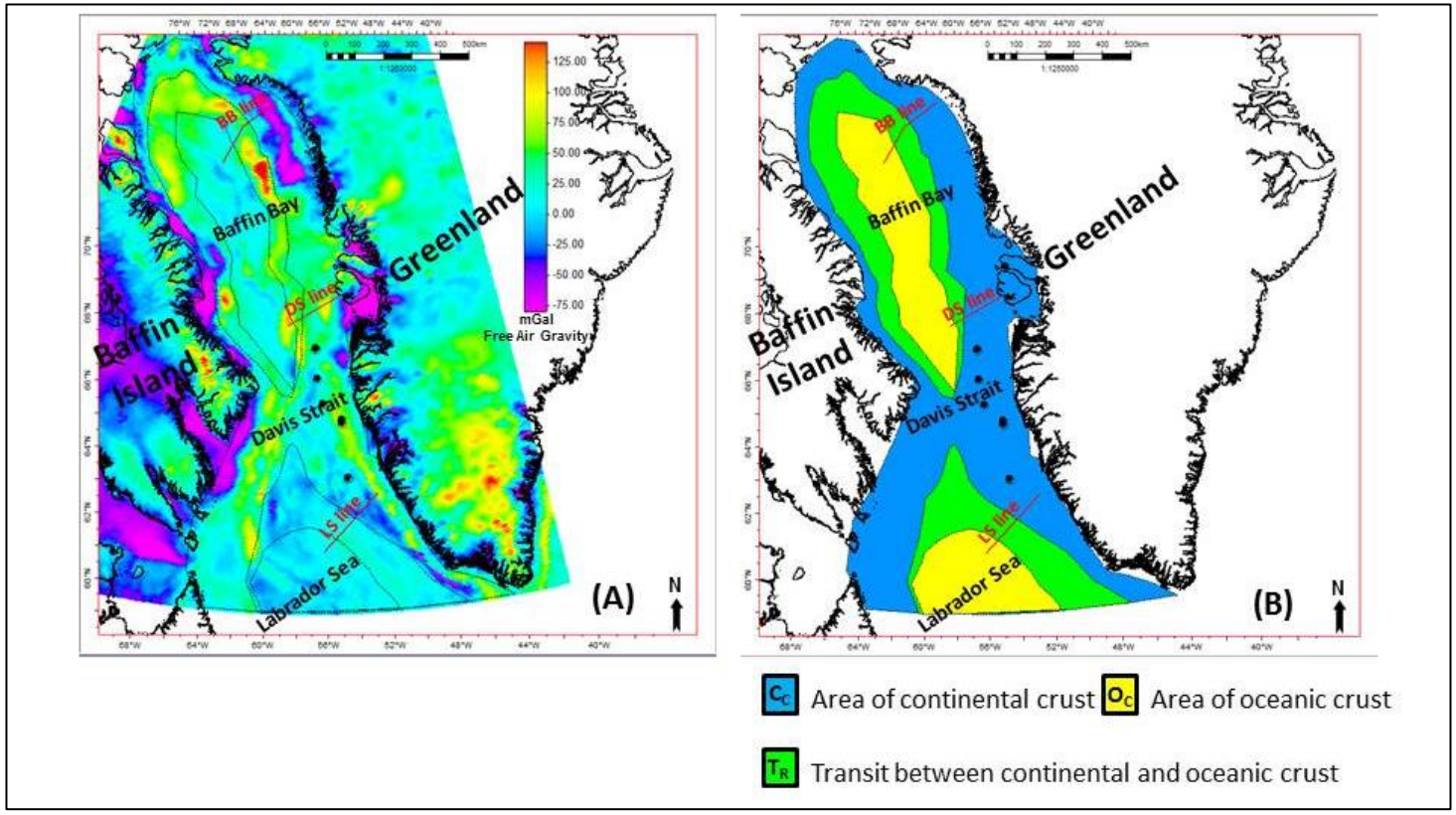

Figure 5.22: Free Air gravity map (A). Annotated FA gravity map of the study area showing the continental, transition and oceanic crusts (B)

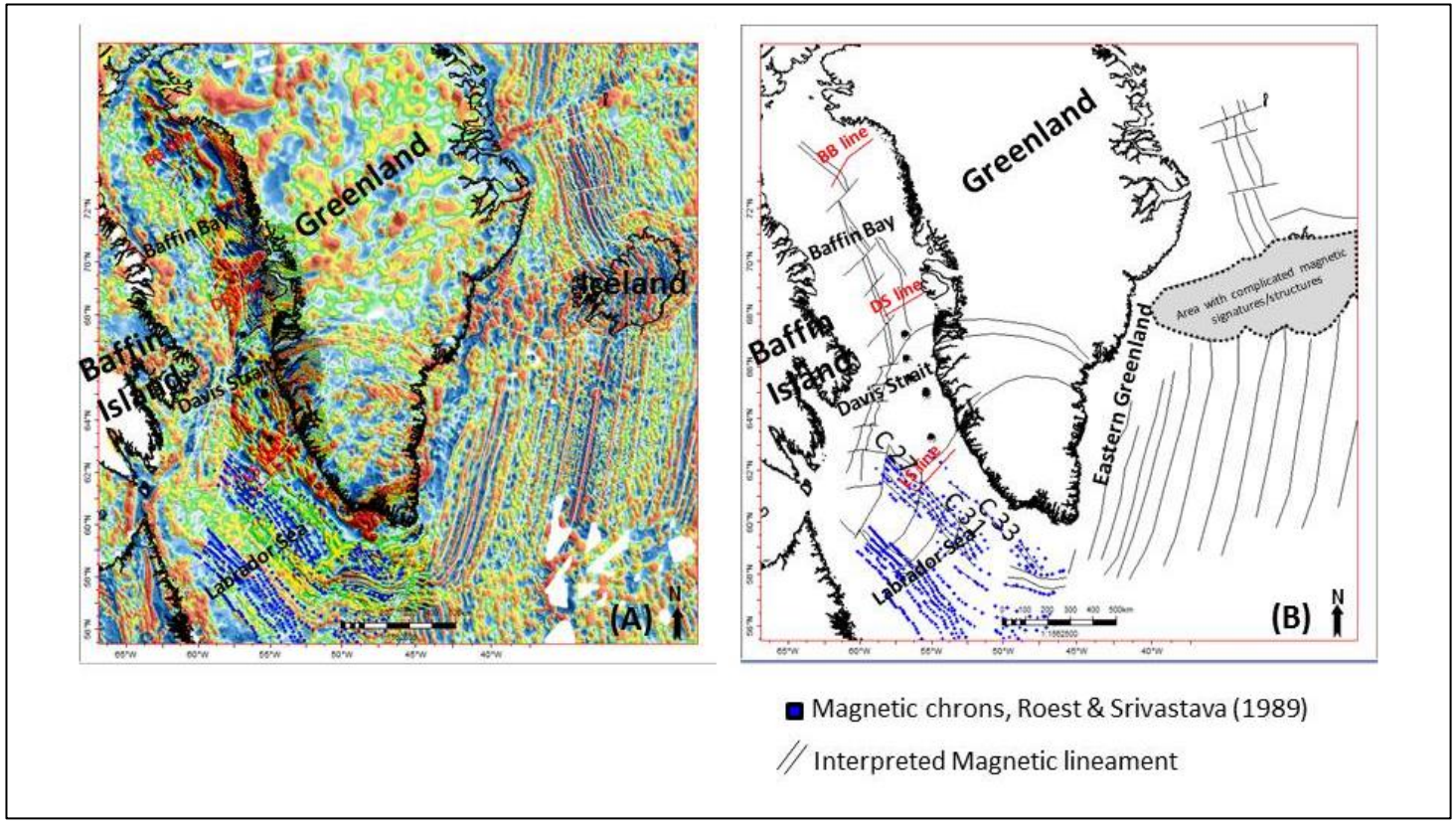

Figure 5.23: Aeromagnetic (TGS) map (A) of Western Greenland margins. Elongated stripe associated with low magnetic values are interpreted as structural lineaments. A sketch map (B) of interpreted lineament in the study area. The lineaments exhibit multiple orientations including NW-SE, N-S, NE-SW and the ENE- WSW.

5.4.4 Interpretation of Gravity Map

The FA Gravity maps reflect contrasting areas of high and low gravity (Figure 5.22). In the Baffin Bay, low gravity anomalies of 20 mGal were interpreted as oceanic crust, anomalies of 74-20 mGal were interpreted as the ocean-continent transition zone. Areas characterised by very low gravity anomaly (-74 mGal) are linked to the presence of low density strata, hence, the areas are interpreted as continental crust (Figure 5.22).

In the Davis Strait, there is no presence of negative anomalies. Instead, positive anomalies were lowest on the northeast side (27 mGal) and highest in southwest (135 mGal). The presence of anomaly 135 mGal is correlated with the presence of oceanic crust. Contrasting anomalies observed towards the Northeast are interpreted as representing ocean-continent transition zone (80 mGal) and continental crust (27 mGal; Figure 5.22).

In the Labrador Sea, the FA gravity signature has no strong contrast to differentiate between oceanic and transitional crust. The gradual transition from moderately high anomalies of 20 mGal to -35 mGal is correlated to the presence of the continental crust Northeast of the ocean-continent transition zone.

5.4.5 Interpretation of Aeromagnetic Map

Seventy one (71) magnetic lineaments were extracted from aeromagnetic data (Figure 5.23). The length and orientation of each lineament was extracted and their cross cutting relationship used to relatively date them. The magnetic lineaments were shown as continuous stripes that contrast to the background magnetic signal. In addition, magnetic anomalies were traceable over considerable distances. The longest and shortest lineaments are 71 km and 250 km, respectively (Figure 5.23).

The principal orientation of the magnetic lineaments is NW-SE across western Greenland margin. Other lineaments are oriented in the N-S, NE-SW and the ENE- WSW directions. Hence the lineaments that trend in similar direction were presumably produced by same tectonic process or stress regime. Alternatively, they reflect an inherited basement fabric, or a major structure (such as a suture zone, or pre-existing lineament). Using their intersection geometries, the NW-SE lineaments are cross-cut by the other interpreted lineaments. Notably, the ENE-WSW lineaments are abutted against the NW-SE lineaments (Figure 5.24). Using these cross-cutting relationship, the NW-SE lineaments are as dated the oldest and are presumed parallel to an extinct spreading axis between Canada and Greenland. Previous studies in the Labrador Sea revealed the NNW-SSE lineaments as being the oldest in the region; they are dated as coinciding with the 27 Chron (*cf*. Chalmers et al 1995). This study shows that the ENE-WSW lineaments traceable into onshore areas are presumably younger, and approaching the 20 Chron (Figure 5.24).

5.5 Discussion

The result from the forward modelling shows that the width of the oceanic crust varies significantly from North to South. The width of oceanic crust decreases with increasing width of the continental crust. The continental crust is thickest in Baffin Bay. The thickness of the crust varies with the depth of the Moho discontinuity (Figure 5.21). Where the mantle or Moho boundary is buried to depth of 14 to 15 km, the thickness of the oceanic crust is 7.5 to 8 km. This is not surprising as the Moho defines the base of the crust.

Specifically in the Davis Strait, thickness of the oceanic crust is 8 km and is also associated with positive gravity anomaly (Figure 5.21). The positive anomalies to the Southwest of the Aaisaa Basin are linked to the presence of oceanic crust. However, Funck et al (2012) interpreted oceanic crust thickness in the Davis Strait to be 9 km which is 1 km thicker than observed in this Chapter. The thicker oceanic crust interpreted here implies an ample magma supply, possibly related to melt extracted from a mantle plume (Funck et al 2012). Furthermore, in Labrador Sea, a clear magnetic anomaly of mid-ocean ridge stripes is observed and interpreted as oceanic crust 70 km long and 7.5 km thick. This interpreted zone corroborates the findings of earlier worker such as Chalmers 1991; Chalmers et al 1995. These workers interpreted the stripes as oceanic crust emplaced at Chron 27.

The crustal geometry interpreted from this chapter are in good agreement with seismic interpretation presented in Chapter 4. Figures 5.2 to 5.4 shows that there is a close match between the interpreted seismic Moho of Funck

et al (2012) and Suckro et al (2013) and those of gravity and magnetic modelling derived from this work. The geometry of the crust is revealed by both magnetic and gravity anomalies. Thick continental crust associated with large variations between observed and estimated magnetic susceptibility. In the Davis Strait, the continental crust is thin and characterised by both negative gravity and magnetic anomalies.

The geometry and location of the continental crust in the entire region provide hints on the nature of rifting during the breakup of North America from Europe in the Late Cretaceous and Early Tertiary. Since the widest area of continental crust is noted in Baffin Bay and the widest oceanic crust is located South, a northward propagation of continental rifting is implied- corroborating the work of Nielsen et al., 2002. Hence, sea-floor spreading started in the South (Labrador Sea) where the widest oceanic crust was formed and propagated North. The propagation direction is proposed to be ENE during Palaeogene by Chalmers (1991). The absence of clear cut magnetic anomalies in the Baffin Bay region may indicate the existence of serpentinised mantle underneath the continental crust and possibly ultraslow seafloor spreading in this region.

The Paleocene volcanic activity in the West Greenland margin are characterised by a positive difference between observed and calculated FA gravity anomalies (see also Larsen and Pulvertaft, 2000; Pedersen and Larsen, 2006) which were correlated to regional eruption of plume-related volcanic rocks (Schenk, 2011). This is further justified by the difference in

observed and calculated magnetic susceptibility values in Figures 5.9 to 5.11. Volcanics rocks have greater magnetic susceptibility compared to their sedimentary rocks.

The differences in observed and modelled anomalies are not mere coincidence. Naturally, it is possible to imagine that the values of the velocities and densities used in the model are short of the actual values from the margin. However, the seismic interpretation provided constraint on the nature of the crust and from their reflection character, their likely lithology composition. The variations noted in the anomalies are not coincidental but a reflection of the complex geology of the area.

5.6 Conclusions

Forward modelling of gravity and magnetic data were used to reconstruct the crustal structure of the Western Greenland margin. The conclusions from this chapter are as follows:

- There is a positive correlation between the seismic and gravity Moho discontinuity. The mantle-crust boundary is characterised by a jump in interval velocities and densities of rocks.
- The transition from continental to oceanic crust is marked by SDRs on seismic and accordingly notable contrast in gravity and magnetic anomalies from the model.
- Contrasts between observed and calculated FA gravity anomalies are associated with the presence of sub-basins along the western

Greenland margin such as Kivioq Bay, Melville Bay, South Fylla complex, Aasiaa basin, Cape Farewell and Disko high.

- The oceanic crust was interpreted at depth of *c*.7 to *c*.8 km from Baffin Bay to Labrador Sea. The mantle-crust boundary occur at depth of *c.*12.5 to *c*.13 km.
- Observed magnetic lineaments are interpreted as regional fault systems which are characterised by complex architecture in the Labrador Sea. The present Chapter interprets basement lineaments as striking towards Labrador Sea. The NW-SE magnetic lineaments are presumably parallel to an extinct spreading axis between Canada and Greenland.
- The length of the continental and oceanic crust provided hint on the mode of rifting and seafloor spreading on the margin. The western Greenland witnessed a northward propagation of rifting and seafloor spreading during the breakup of North America from Europe. In addition, the gravity and magnetic modelling provided additional constraints on the geometry of basins along West Greenland.

Chapter 6

Depth-Dependent Lithospheric Thinning of the West Greenland Continental Margin

6.1 Abstract

The aim of this Chapter is to investigate whether a simple or a pure shear depth-dependent model can explain the evolution of the West Greenland margin. We measured the magnitude of extension by estimating stretching factors (β) from upper-crustal faults and whole lithosphere extension using three depth-converted seismic profiles. The profiles sample three key locations that together represent structural variability along the West Greenland continental margin, from South to North.

The results in this Chapter show a clear and consistent difference in β_C and β_L for the entire West Greenland margin. Rifting in West Greenland started before the Palaeocene with a northeast shift in the rift axis from the Labrador Sea to the Baffin Bay. The largest amount of lithospheric thinning occurred in Baffin Bay. Based on our analyses, the thinning factor (β_c) from upper crust faulting (typically c.1.1 to 1.4) is less than (β_L) from the whole lithosphere (from c.1.5 to >10).

The whole lithosphere has extended more than the upper crust along the margin. Depth-dependent thinning in the West Greenland area occurred during early sea floor spreading rather than during early pre-break-up rifting. Furthermore, our interpretations suggest that the Labrador Sea and Davis Strait margins display evidence of more symmetric stretching in contrast to the Baffin Bay area that appears to be more asymmetric.

6.2 Introduction

Rifted continental margins form by crustal extension and thinning of continental lithosphere, which often lead to the initiation of seafloor spreading at high stretching factors (Le Pichon and Sibuet 1981). Despite the multiple published models on the evolution of extensional basins, the mechanisms driving the formation of rifted continental margins remain contentious to date. The simple 1D model of McKenzie (1978) was the first to explain that margins could form by uniform lithospheric thinning. Conversely, depth-dependent stretching model of Davis and Kusznir (2004) estimated stretching independently from upper-crust faulting, crustal thinning and post-rift lithosphere thermal subsidence. The depth-dependent stretching model of Davis and Kusznir (2004) shows that extension increases with depth within 150 km of the continent-ocean boundary (COB) such that crustal and lithosphere extension are significantly greater than upper- crustal extension (Roberts et al., 1997; Driscoll and Karner, 1998; Davis and Kusznir, 2004; Huisman and Beaumont, 2011).

The breakup stage and formation of the oceanic crust in West Greenland is firstly characterised by opening and northwards spreading of the oceanic crust in the Davis Strait and Baffin Bay, and by a major pulse of volcanism associated with the Icelandic plume (Chalmers, 1991; Larsen and Saunders, 1998, Roest and Srivastava, 1989). The evolution of West Greenland during continental breakup is controversial. Diverse opinions centre on the timing of uplift, on the number of phases of extrusive volcanism, on the initiation of rifting, sea-floor spreading and geotectonic development of the region during the continental breakup (Korstgärd and Nielsen, 1989; Storey et al., 1998; Larsen et al., 2009; Funck et al., 2012; Oakey and Chalmers 2012; Suckro et al., 2013).

The aim of this Chapter is to investigate whether a simple 1D pure shear model (McKenzie, 1978) or a pure shear depth-dependent thinning model (Davis and Kusznir, 2004) is appropriate to describe the development of the West Greenland margin by comparing the magnitude of :a) lithospheric thinning; and b) upper crustal thinning. We estimate the stretching factor (β) from measurements of upper-crustal faulting and use flexural backstripping, decompaction and reverse post-rift subsidence modelling of depth-converted seismic cross-sections to derive lithospheric extension along the West Greenland continental margin.

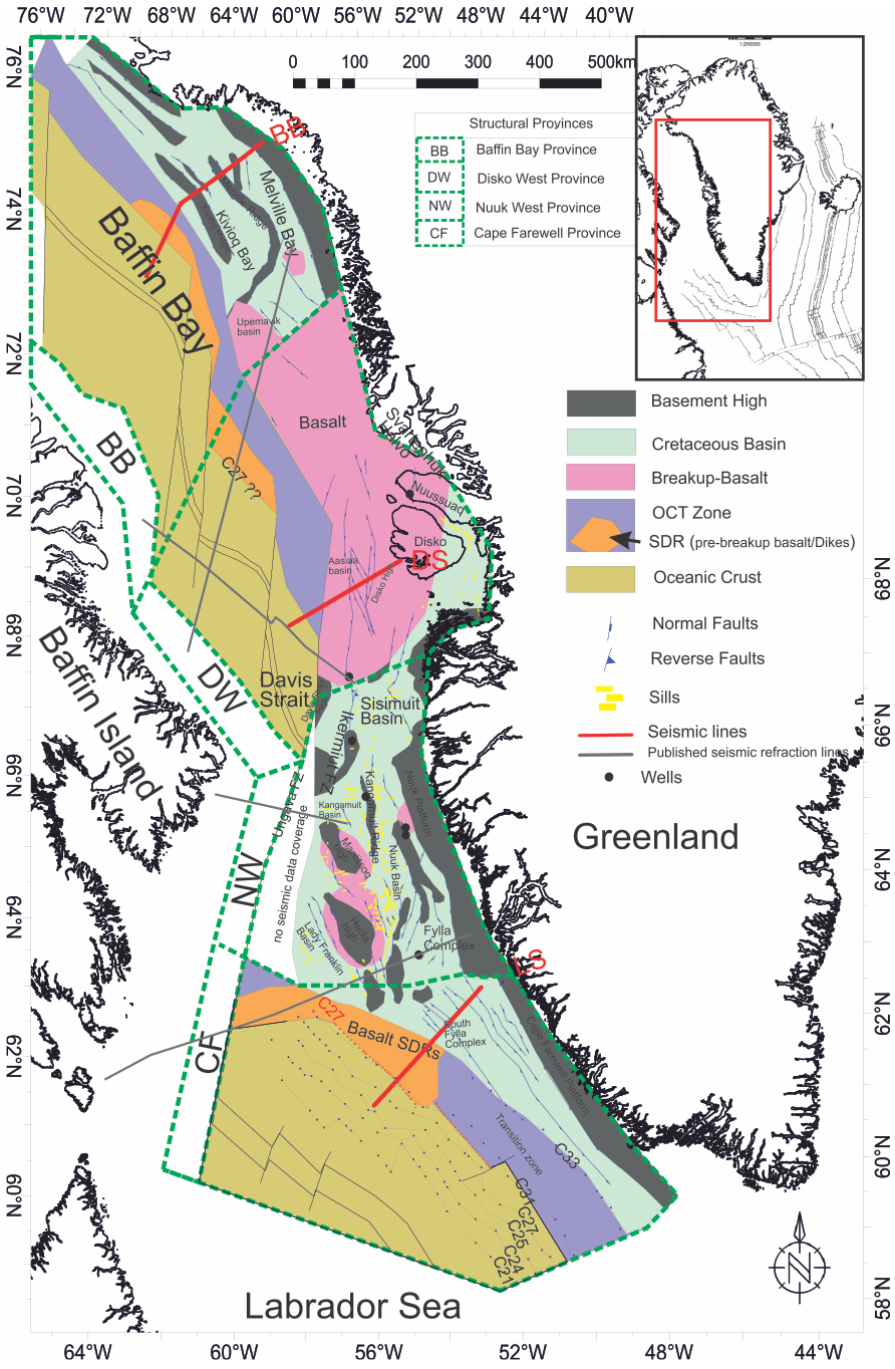

Figure 6.1: Regional tectonic framework of the west Greenland area generated by data integration of 2D seismic data (GEUS), structural provinces after Knutsen et al., (2012), seafloor data from Müller 2008, Global Seafloor Fabric and Magnetic chrons from Roest and Srivastava 1989; and Chalmers and Laursen (1995). BB=Baffin Bay line; DS=Davis Strait Line; LS=Labrador Sea line.

The study area comprises the Labrador Sea, Davis Strait and Baffin Bay regions (Figure 6.1). The basins and sub-basins of the West Greenland margin were formed by crustal extension and thinning of the lithosphere during the Early Cretaceous. The approximate position of the ocean-continent transition of the West Greenland margin is constrained using the age of seafloor bedrock defined by Müller, 2008. We choose representative seismic sections of the three major basins along the West Greenland margin and present them along with interpreted and modelled depth-converted cross-sections. In this paper, we demonstrate evidence for depth-dependent stretching along the West Greenland margin and discuss the implications of this result in terms of evolution of the margin and basins.

6.3 Methods

6.3.1 The Depth Dependent Stretching Modelling

The depth-dependent stretching model predicts greather thinning of the whole-lithosphere compare to the upper crust (Davis and Kusznir, 2004; Figure 6.2). The flexural backstripping, decompaction, and reverse post breakup thermal subsidence modelling produces a series of palaeo cross sections by back stripping a present-day section. The location of the backstripped cross-section and the estimated stretching factors for the three representative sections are shown in Figure 6.1.

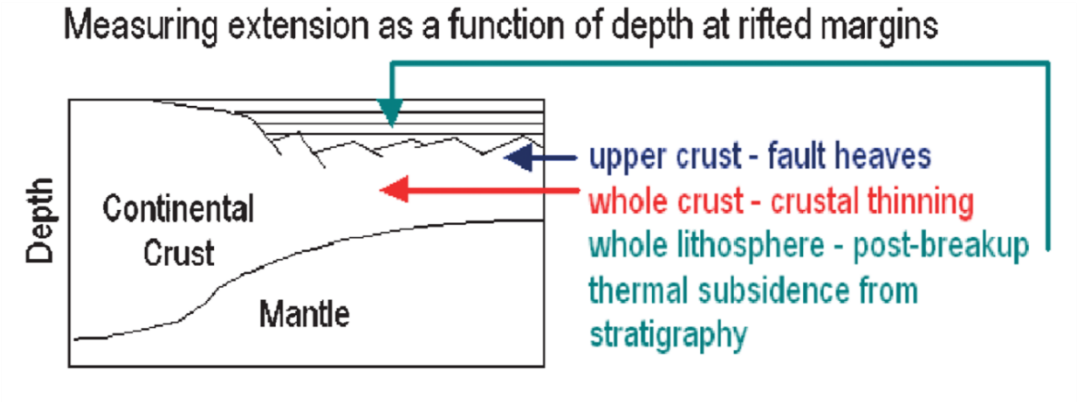

Figure 6.2: Estimation of continental margin extension and thinning at the level of the upper crust, the whole crust and the lithosphere using three discrete datasets and/or techniques (Davis and Kusznir, 2004; Kusznir et al., 2005).

6.3.2 Modelling Parameterization

We performed the depth-dependent modelling following work by Kusznir et al. 1991, 1995; Kusznir and Ziegler 1992; Roberts et al. 1993. However, we note the following:

1. When true dip section profiles were used, crustal thinning is influenced by the dip-slip component of faults (Kusznir et al., 2004). Hence, faults with slip directions that are not coincident with the two-dimensional depth profiles were ignored for the study.

2. We may have narrowly overestimated fault-related extension bearing in mind that block rotation were ignored. Faults are more likely to deform by vertical shear than as rigid “dominoes” (Westaway and Kusznir, 1993).

3. Tilt blocks are considered as consistent palaeobathymetric markers since their tips are eroded and were therefore used to constrain sea level in the reverse post breakup thermal subsidence modelling.

4. We used compaction parameters given by Sclater and Christie (1980) that include initial porosity, matrix density and compaction (See Table 6.1)

5. The break-up unconformity is assumed to be the top Palaeocene (c. 55Ma). See Table 6.2 and appendixes of (forward and reverse modelling input parameters)

Furthermore, a list of the parameters used for the modelling are provided in Table 6.1 and appendices.

3.3.3 Uncertainties in depth dependent stretching modelling

The lack of appropriate well control increases the uncertainties in interpreting the horizons in the study area. The deeper horizons (Moho and Basement) have poor reflection characteristics hence may create some errors when picked. The input parameters (density, porosity and palaeobathymetry) may also have significant uncertainties. The fault angle, location and heave estimations were manually derived, therefore the results and figures are prone to errors. Sub-seismic faults were not considered in the study, these faults are thought to account for minor errors in estimating the overall upper crust extension. In addition, the forward limits the analysis to a single rift episode.

3.3.4 Forward modelling (upper crust stretching (β_c) estimation)

The forward modelling is determined individually from upper-crustal faulting (fault heave calculation) for a single rifting episodes. In this study, the Rift 1 (Early Cretaceous) is modelled. The model was built up based on parameters that reflect the tectonic history of the study area as illustrated previously (see Chapters 4 and 5 for details). The tectonic times including pre-rift of > 150 Ma, rifting of 145 to 150 Ma and post-rift of 70 to 60 Ma. In addition to the default beta of 1, other parameters used are shown in table 6.1 and appendices.

3.3.5 Backstripping modelling (whole lithosphere stretching (β_L) estimation)

The post-breakup subsidence may be reverse modelled to estimate palaeo-bathymetry and beta (Roberts et al.,1998) The palaeobathymetries of the restored cross sections are dependent on the magnitude of the lithosphere-stretching factor used in the reverse post-breakup thermal modelling (McKenzie 1978; Roberts et al.,1998) and therefore β_L is estimated along each section. Individual horizons were backstripped with high degree of confidence using paleobathymetric control. The three seismic sections were restored using the post-breakup horizon (Top Palaeocene) at 55 Ma. The paleobathymetric of top Paleocene for three profiles was controlled by published drilled wells cutting samples and well logs deposition environment description, paleobathymetric maps and seismic interpretation. The Davis Strait profile (Figure 6.3) was restored to the seabed as it was in the

Hellefisk-1 well (130 km). Well log information indicate the top Palaeocene to have been in a shallow environment at this time (Dalhoff et al., 2003). In the Baffin Bay, Melville and Kivioq Ridges were restored to seabed as these ridges remain structurally high during drifting time (Palaeocene to Eocene; Whittaker et al. (1997). In the Labrador Sea, the profile was restored to the seabed at NE side of the section where the Qulleq-1 well is located. At thic section, Christiansen et al., (200) interpreted an unconformity between the lower Paleocene and Early Eocene unit. In addition, the southwestern side towards the oceanic crust showed paleobathymetry was 2 km below sea level (Srivastava and Arthur, 1989).

The workflow for restoring flexural backstripping and reverse post-rift modelling (Figure 6.3) includes: (1) the removal of the topmost stratigraphic unit; (2) the computation of the flexural isostatic response to the removed sediment matrix and water (3) the application of the flexural isostatic response to the remaining sedimentary section and basement (4) the sequential repetition of the above processes until all post-rift stratigraphic units have been removed.

Table 6.1 Modelling parameters for depth-dependent modelling in the West Greenland margin

Parameter	**Value**
Uniform previous beta	1.0
Depth to base crust	32.0 km
Compactable pre-rift	3.0 km
Asthenosphere temperature	1333°c
Density of asthenosphere	3.3 gm/cc
Crust density	2.8 gm/cc
Sediment matrix density	2.68 gm/cc
Water density	1.0 gm/cc
Sediment porosity	0.56
Beginning of rifting	145 Ma
Initiation of sea floor spreading	60
Brittle layer thickness	10.0 km

Table 6.2: Stratigraphic units, ages and compaction parameters used in reverse post-rift modelling (thermal subsidence).

	Initial Porosity	Compaction Constant (Km^{-1})	Matrix Density ($gm\ cm^{-3}$)	Age (Ma)	
Seabed	0	0	2.68	0	
Base Quaternary	56	0.44	2.68	2	
Mid Miocene	56	0.44	2.68	14	
Mid Eocene	56	0.44	2.68	49	
Top Palaeocene	56	0.44	2.68	55	Post-breakup
Top Basalt	0	0.01	2.68	61	
Top Cretaceous	56	0.44	2.68	65	
Mid Cretaceous	56	0.44	2.68	99	
Basement/DR	56	0.44	2.68	145	

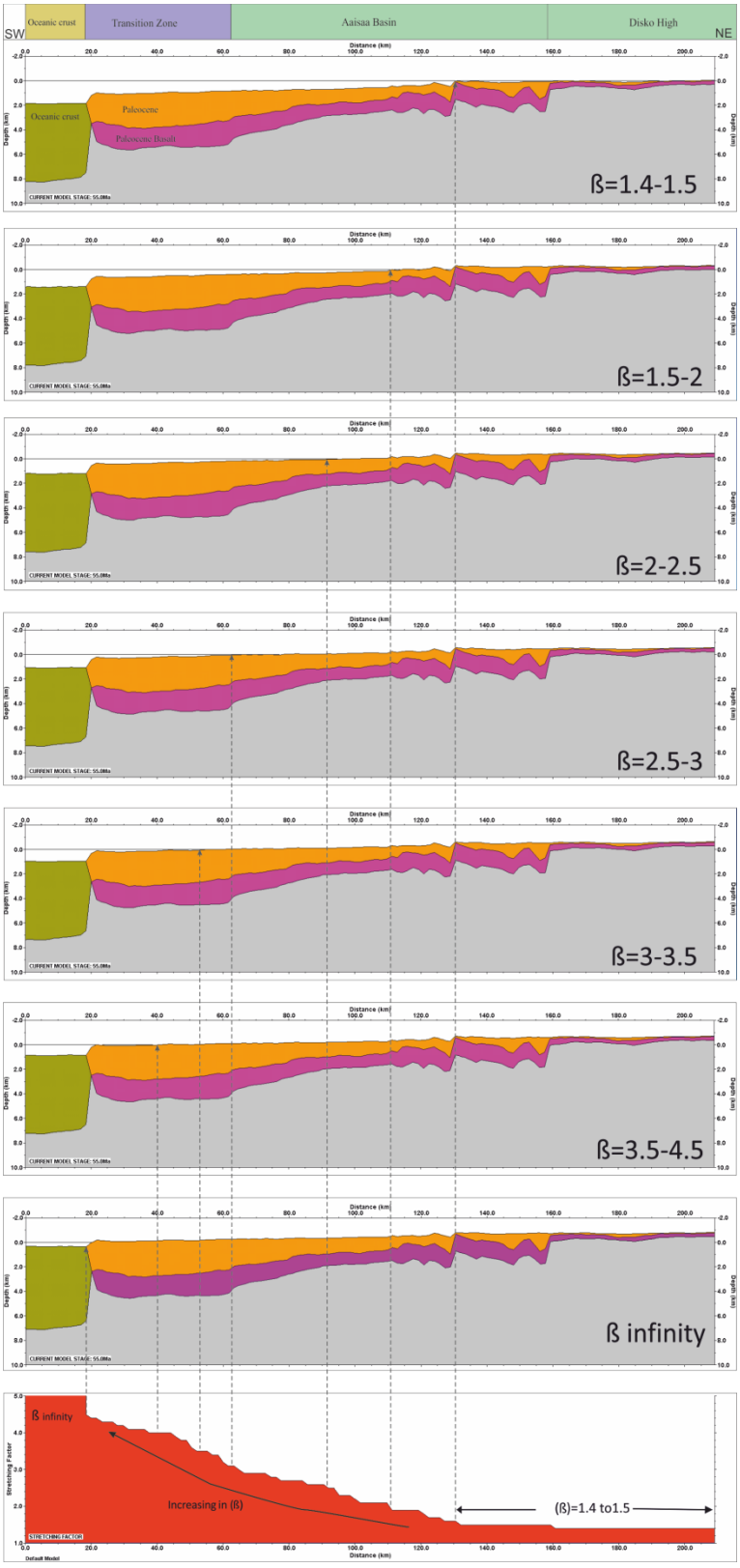

Figure 6.3: An example of Flexural Backstripping and Reverse Post-rift Modeling for Davis Strait line restoration Process.

6.4 Results

6.4.1 Overview of the seismic stratigraphy

Nine (9) seismic-stratigraphic surfaces were interpreted based on their seismic reflection character and position. The sea bed is a high-amplitude and continuous reflection. Hence, it was interpreted using the 2D autotrack tool. Other high amplitude and continuous peaks include Mid-Miocene Unconformity (MMU), Mid-Eocene unconformity (MEU), top Palaeocene (TP) and Early Cretaceous (EC). These horizons were consistently interpreted with a high degree of confidence using both the manual and guided autotrack tools. The base Quaternary (BQ); Palaeocene basalt (PB); top Cretaceous (TC) and Basement (Bs) are moderate amplitude and discontinuous reflections.

The acoustic basement is displayed as chaotic, low amplitude reflections associated with seaward dipping reflections (SDRs) in the Baffin Bay and Labrador Sea. SDRs are remarkable suites of accurate reflections, dipping seaward to form a wedge-shaped structure on seismic reflection profiles, their general characteristics and velocity structure is suggestive of a volcanic nature (Ajay et al., 2010; Mutter, 1985, Okay and Chalmers 2012). Notably, the acoustic basement, Cretaceous and top Cretaceous reflections were not mapped in Disko West as they have been masked by the overlying Palaeocene basalt (See chapter 5; Figure 5.2).

6.4.2 Seismic Stratigraphy of the Baffin Bay

Syn-rift packages in the Baffin Bay Province (See chapter 5; Figure 5.1) include Lower Cretaceous to top Palaeocene units. They are characterized by presenting significant thickness variations especially in graben structures within the Kivioq Bay and Melville Platform. The oldest and lowermost unit is 4 km thick, and comprises strata of Lower Cretaceous age. This unit displays high-amplitude reflection on the seismic profile (see Chapter 5; Figure 5.1) and thins to the Southwest onlapping a bounding fault. Pre-rift packages were not identified in this region. Contrastingly, the post-rift units presents a constant thickness draping the syn-rift topography and the tips of the faults mapped in the area. Fault observed to the North and South of the Baffin Bay basin are isolated, unlinked and segmented. The dominant dip of the fault is Southwest and Northeast. Fault geometry includes titled blocks on the boundary of Kivioq and Melville ridges (see Chapter 5; Figure 5.1). In the central part of Baffin Bay, sedimentary packages deposited in graben structures are strata of the Kivioq and Melville basins.

Extensional basins are bounded by major normal faults formed by Early Cretaceous rifting in the Baffin Bay region. The lowest unit is 4 km thick, consisting of Lower Cretaceous age sediments and characterized by low amplitude reflection. The unit thin towards the Southwest and is interpreted to show a syn-rift geometry as sediments. Whittaker et al., (1997) interpreted this unit as evidence for thermal subsidence using a seismic line parallel to this section. The top Cretaceous to top Paleocene unit does not contain basaltic rocks overlapping the top Cretaceous in the Northeastern region but

instead basalt is inferred in the transition zone from high amplitude reflections, some of which may represent seaward dipping reflections (SDRs). An oceanic crust approximately 8 to 7.5 km thick is interpreted in Southwest part of this section, at this same stratigraphic level. The unit is overlain by top Paleocene to mid-Eocene rocks and is characterized by a strong amplitude reflection at the mid-Eocene horizon. Both units are cut by normal faults and generally thin towards the southwest, they are therefore interpreted to be syn-rift. Above the syn-rift units, we interpret mid-Eocene to mid-Miocene; mid-Miocene to base Quaternary; base Quaternary to Sea bed horizons that are not cut by the observed normal faults and therefore are interpreted to be post-rift.

6.4.3 Seismic Stratigraphy of the Davis Strait

Cretaceous units are not present in the Davis Strait (see Chapter 5; Figure 5.2). Seismic data quality in the Davis Strait is otherwise poor below 6 km depth. The interprete d basalt layer is 2 to 3 km thick. The faults terminate at the interpreted top Paleocene and below the Mid-Eocene reflections. The basalt is most likely associated with breakup in Labrador Sea (Larsen and Saunders, 1998) (see Chapter 5; Figure 5.3) during Paleocene (61 Ma). Two types of faults are recognized in the upper crust in this section; normal faults to the Northeast and strike-slip to the Southwest. Units from mid-Eocene to the seabed are not affected by faulting and are likely to be post-rift.

6.4.4 Seismic Stratigraphy of the Labrador Sea

The oldest sedimentary unit in the Labrador Sea thins out significantly at the middle of the section (see Chapter 5; Figure 5.3). The post-rift sediments are Mid-Eocene to Recent in age and they are the thickest adjacently to the Fylla Complex and Cape Farewell. The Early Cretaceous units in the Labrador Sea are high-amplitude reflections. In the Cape Farewell region, the oceanic crust is interpreted at c.6000 m (TVD) (See chapter 5; Figure 5.3). It is flanked by Seaward Dipping Reflections (SDRs) that separate the transition zone between the oceanic and continental crust. The interpreted breakup basalt is capping the transition zone and is characterised by high-amplitude reflections on seismic data. The basalt separates regions of rotated fault blocks/dominoes from region of interpreted oceanic crust (See chapter 5; Figure 5.3).

Tilted blocks in stretched upper crust were observed on the shelf region to the northeast of the section. Cretaceous units grow onto active faults and are thus interpreted as syn-rift. The Cretaceous units thin towards the southwest and faded out in the middle of the section. High-amplitude reflections above the top Cretaceous are interpreted as extrusive basalts. This basalt layer thickens towards the southwest where it overlies high-amplitude SDRs. Oceanic crust up to 7.5 km thick is interpreted in the southWest section from the chaotic character/ lack of internal reflection of the packages. Late Paleocene sediments likely overlie the oceanic crust to the south.

6.5 Estimated stretching factor from upper-crustal faulting (βC)

The stretching factor upper-crustal faulting (β_C) for the Baffin Bay section approaches 1.4 (Figure 6.4) and the restored Moho at a depth of c.32 km. This area also coincides with the region where the greatest thickness (5 to 7 km) of syn-rift strata is observed. The combined thickness of the syn-rift and post-rift packages is approximately 7.5 km (Figure 6.4). The estimated stretching factor is 1.1 (Figure 6.5) for the Davis Strait profile. The modelled Moho is restored to a depth of 32 km in the Davis Strait.

The Labrador Sea profile shows upper crust stretching factor β_C approaching 1.2 (Figure 6.6). The modelled Moho is at a depth of c.32 km. Master faults dips towards the southwestern part of Labrador Sea. The crust is thinner at the central part of the Labrador Sea, corresponding to an area with the largest thickness (4 km) of syn-rift strata. For all of the restored cross sections, the crust (upper and lower) is approximately 15 km thick.

6.6 Thermal Subsidence

Whole lithosphere stretching factors (β_L) were calculated using the palaeo-bathymetry restoration of the post-breakup horizon (top Palaeocene). The oceanic crust was restored to 1.6 km depth at the southwestern section of the Baffin Bay. The syn-rift packages are thickest (7 km) within the restored depocentres (Figure 6.7), whereas the thickness of post rift strata is relatively constant in the Baffin Bay.

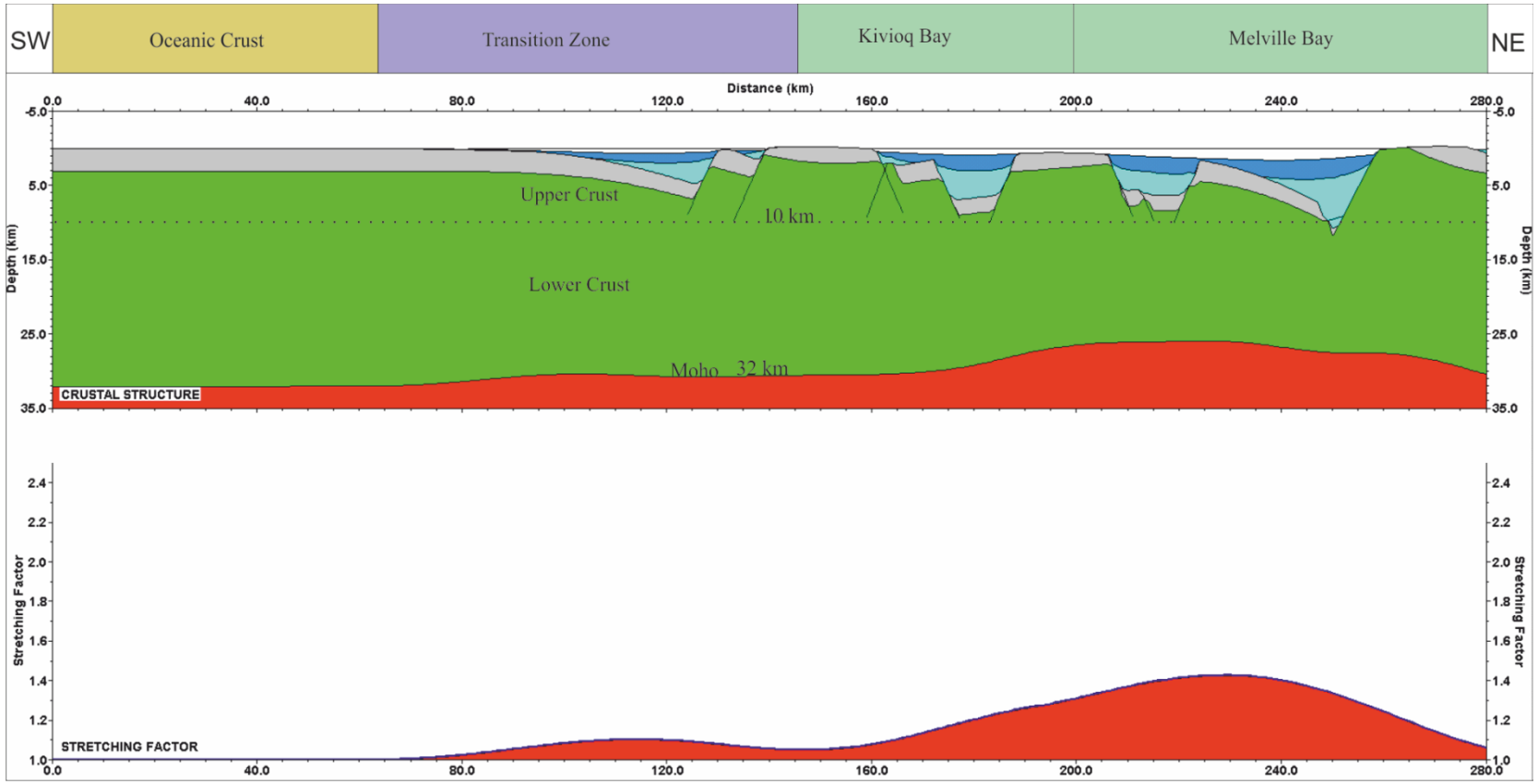

Figure 6.4: Estimated upper crust stretching factor (β_c) for Baffin Bay. High β_c values are associated with deeply buried horst and graben structures in Kivioq and Melville Bay respectively. Top panel shows 32 km modelled depth for Moho and 10 km between upper and lower crust as faults terminated from seismic reflection interpretation and seismic refraction (see text for published seismic refraction details, Suckro 2012 , 2013 and Funck 2007, 2012)

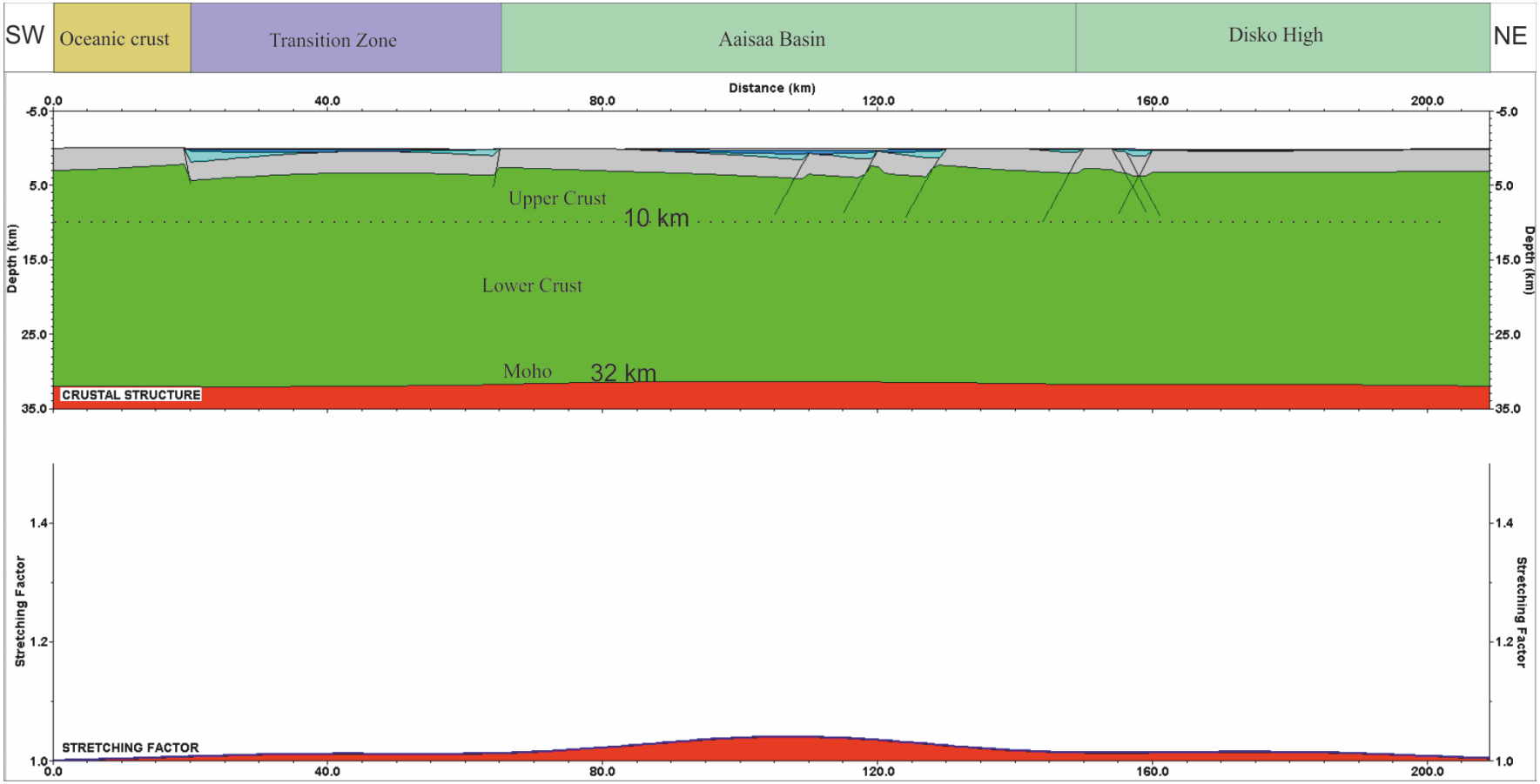

Figure 6.5: Estimated upper crust stretching factor (β_C) for Davis Strait. The highest upper crust faulting factor is recorded in the Aasiaa basin, NE of the OCB. Top panel shows 32 km modelled depth for Moho and 10 km between upper and lower crust as faults terminated from seismic reflection interpretation and seismic refraction (see text for published seismic refraction details, Suckro 2012 , 2013 and Funck 2007, 2012

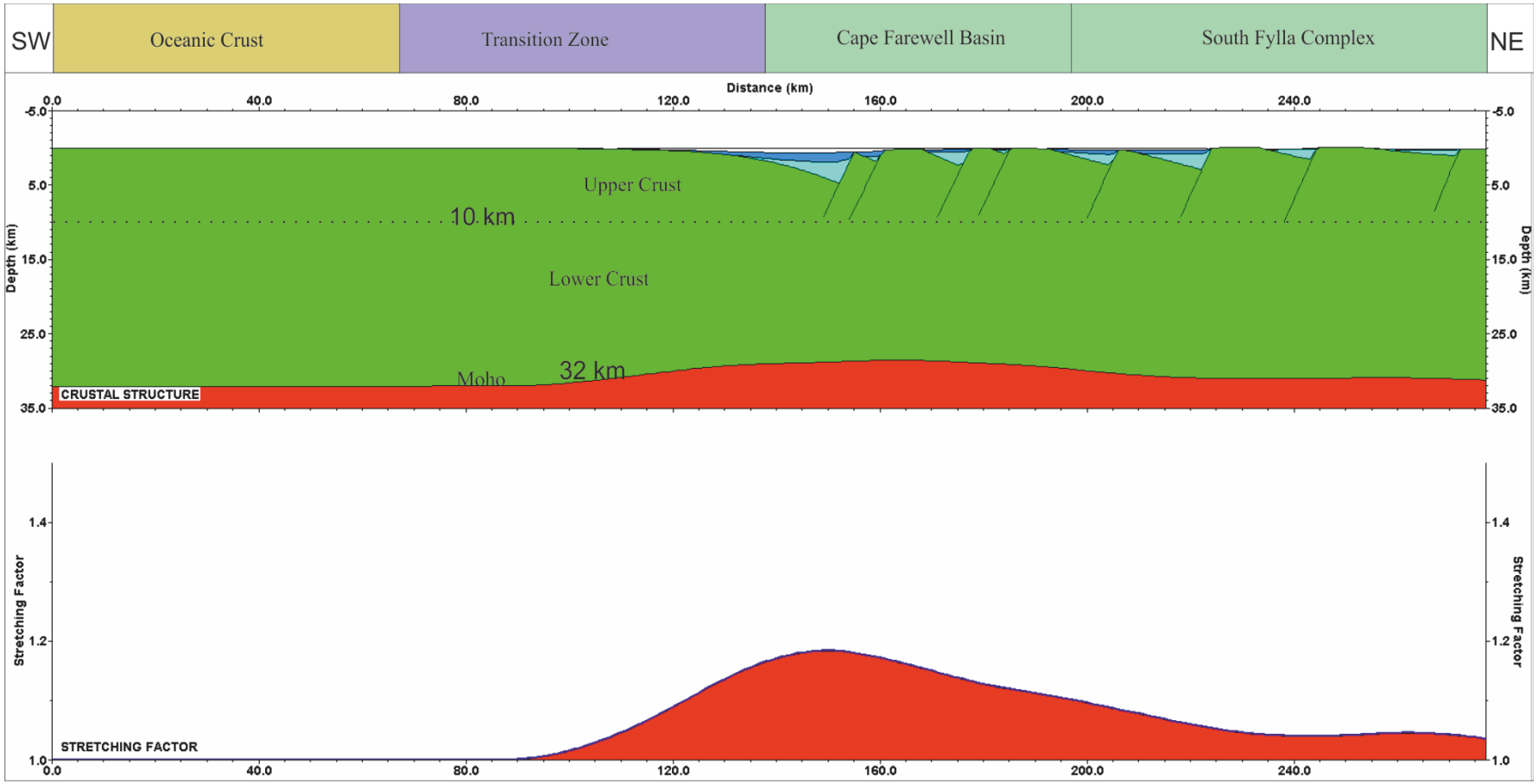

Figure 6.6: Estimated upper crust stretching factor (β_c) for Labrador Sea. The highest value of β_c was noted at the OCB in Cape Farewell basin. Top panel shows 32 km modelled depth for Moho and 10 km between upper and lower crust as faults terminated from seismic reflection interpretation and seismic refraction (see text for published seismic refraction details, Suckro 2012 , 2013 and Funck 2007, 2012)

The estimated lithosphere stretching factor (β_L) is greater than 5.0 in the southwestern part of the profile, where oceanic crust is expected. The Baffin Bay section required a β_L of 1.4 in the depocentre region, which is characterized by thick (7 km) syn-rift strata. The β_L is 2.4 at the eastern end of the section. Hence, there is an asymmetric pattern of whole lithosphere stretching in Baffin Bay. For the Davis Strait, the β_L value reaches infinity in the area of oceanic crust. In contrast, values of <5.0 were recorded in the adjacent areas of transition zone (Figure 6.8). βL decreases to 1.6 on the easternmost section (Figure 6.9). This area shows evidence of non-faulting to negligible faulting and less variability in the thickness of syn-rift strata. We interpret this as evidence that the greatest Lithospheric thinning occurred centrally beneath the rift axis or that the area are thermally uplifted, intensely eroded, and hence the syn-rift units are expected to be thicker on continental crust just inland of the region of thermal uplift.

The profile across the Labrador Sea margin requires a whole lithosphere β_L of 1.8 to restore the platform (c.3 km) to its paleobathymetry at the eastern side of the section of the profile (Figure 6.9). The β_L values increased from β=5 for over (c.134 km) of the margin to β_L=8 in the (75 km) of hyperextension zone and then βL value of infinity are found where we interpret the oceanic crust, 65 km wide in the southwest side of the section, possibly indicating a greater thinning of mantle lithosphere than of the crust in this region.

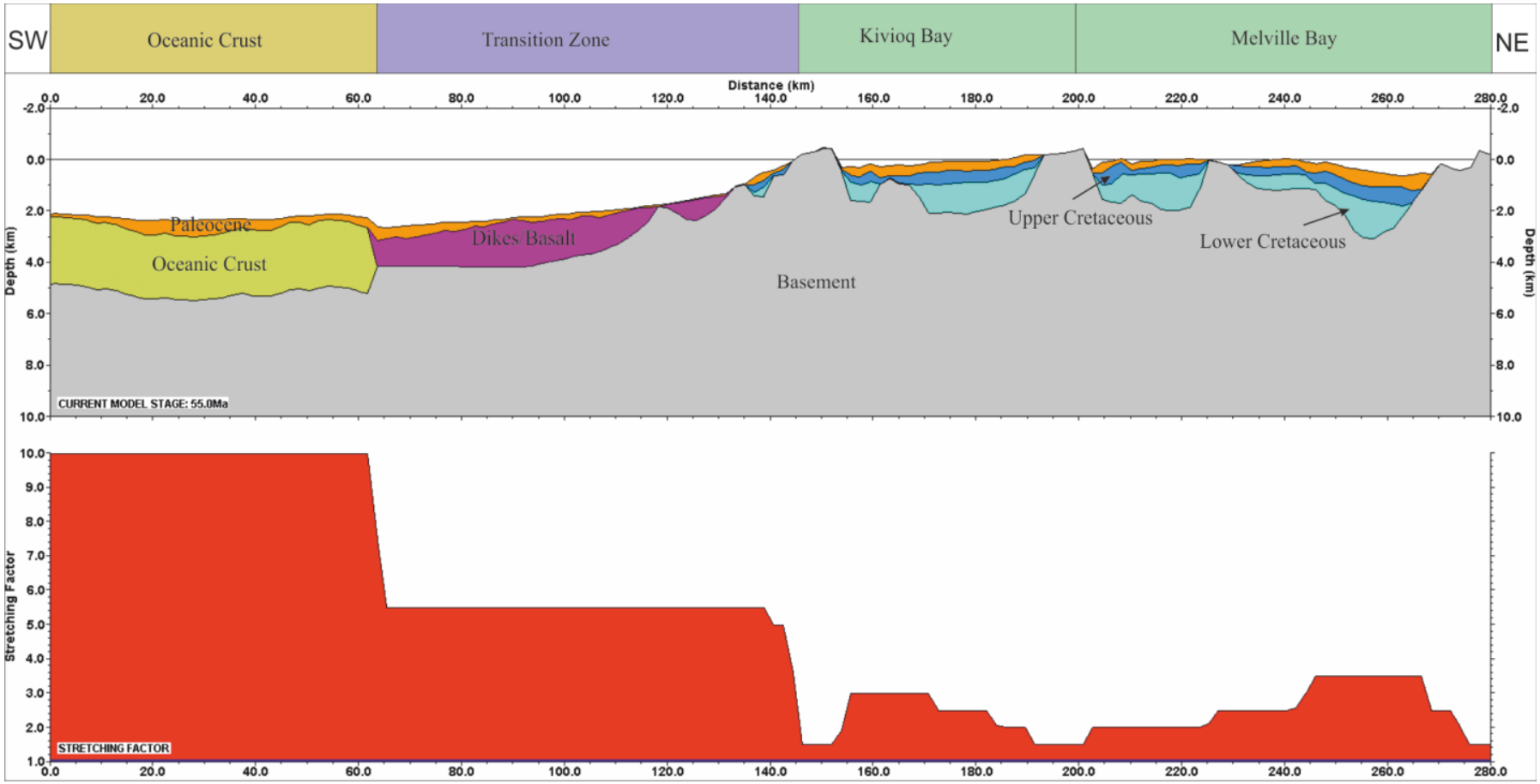

Figure 6.7: Estimated whole lithosphere stretching factor (β_L) for Baffin Bay. Uplifted section of Baffin Bay is characterized by very low β_L values in contrast to subsided section of Melville Bay.

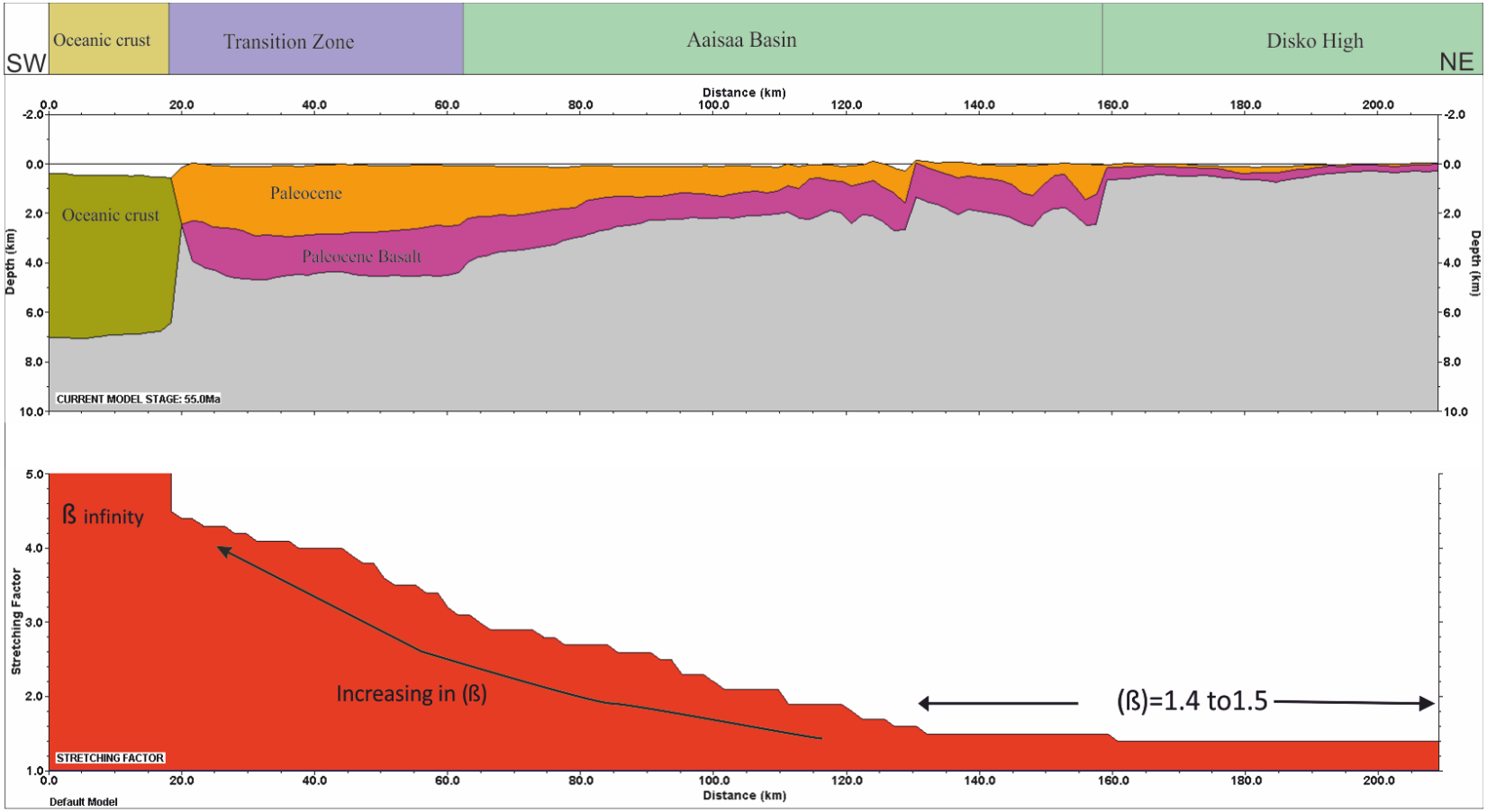

Figure 6.8: Estimated whole lithosphere stretching factor (β_L) for Davis Strait. The highest stretching factor is recorded SW of Davis Strait, there is a steep decrease in the β_L from the oceanic crust to the continental crust

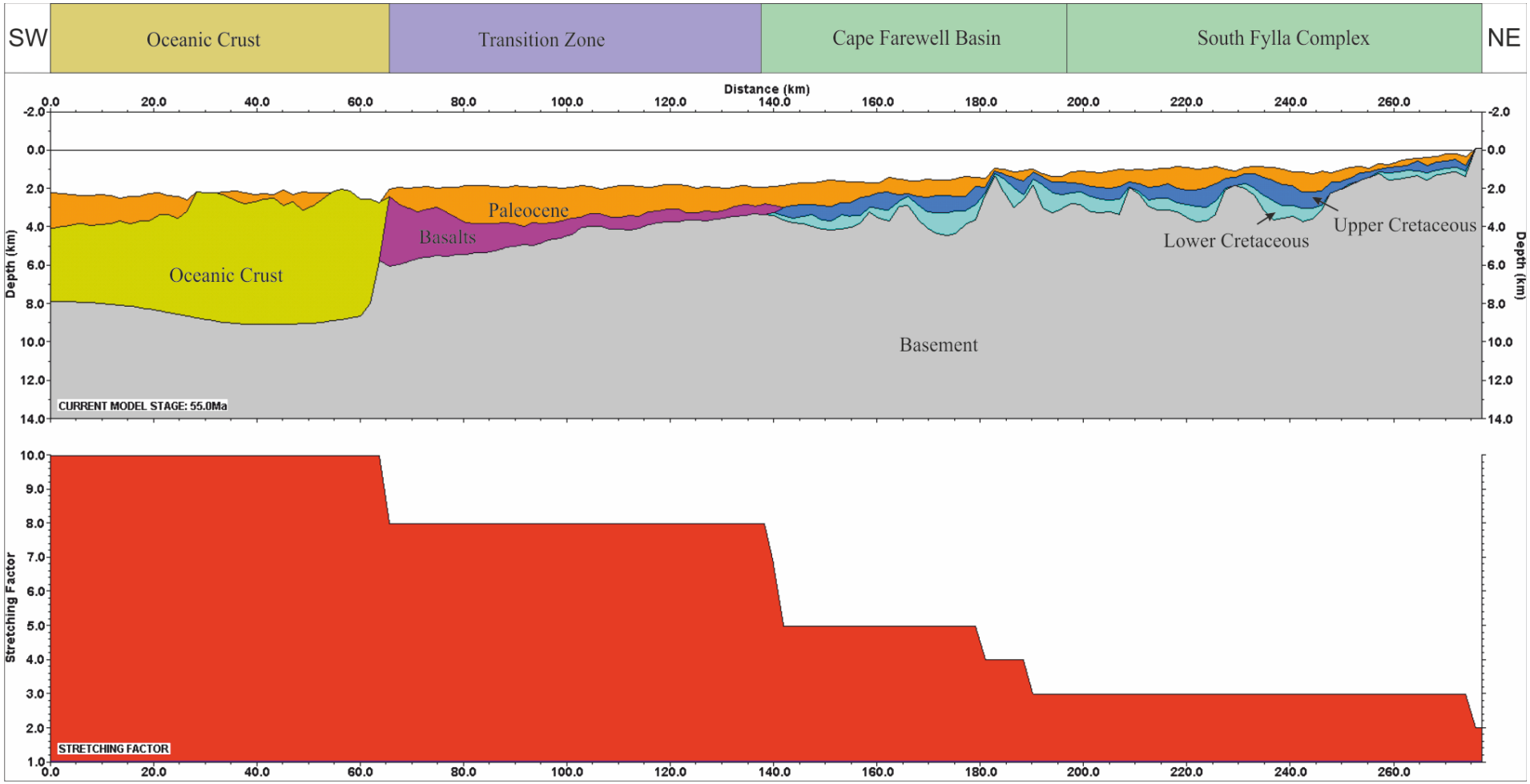

Figure 6.9: Estimated whole lithosphere stretching factor (β_L) for Labrador Sea. The highest β_L is noted in SW part of Labrador Sea where the oceanic crust is interpreted. Approximately *c.* 2 km were successfully restored on the northeast of this profile by β=*c.*2.

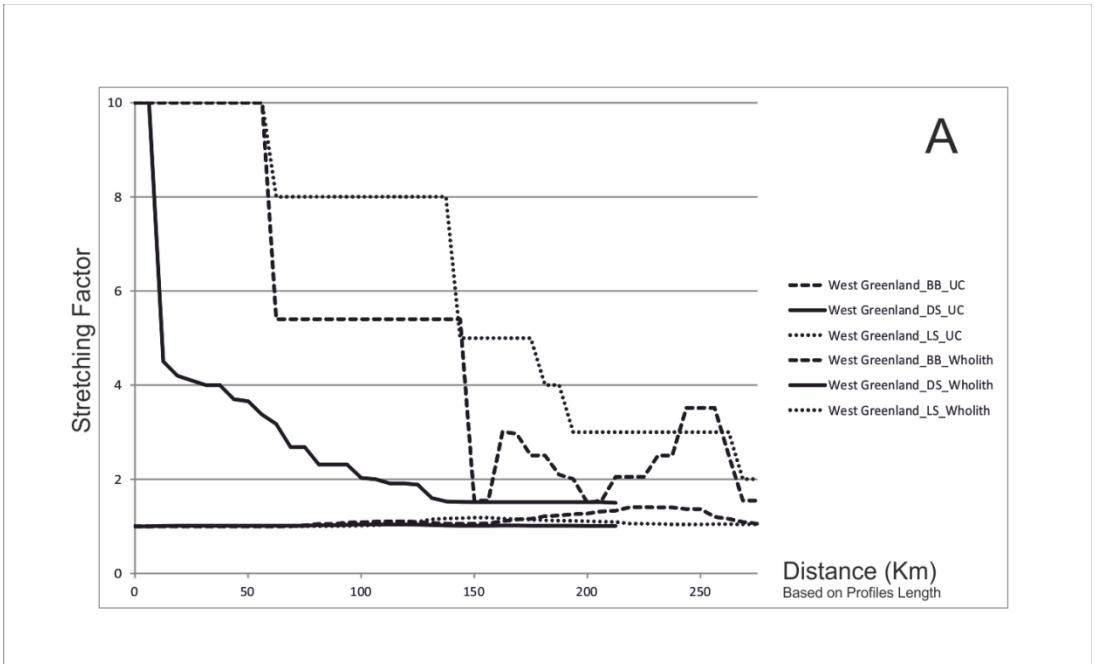

Figure 6.10: Comparison of (A) upper crust faulting versus whole lithosphere estimated (β) factor of West Greenland Continental margin.

6.7 Comparison of β_C and β_L along the three sections

Our data provides an opportunity to estimate variation in βc and β_L along West Greenland. The estimated upper crust stretching factors (β_C) for all of the profiles are low with maximum value of $\beta_C < 2.0$ (Figures. 6.4, 6.5 and 6.5). The profiles for the lithosphere stretching (β_L) are variable from $\beta_L < 2.0$ to infinity (Figures. 6.7, 6.8 and 6.9). The βc profile is asymmetric in Baffin Bay and Labrador Sea (Figure 6.10). The asymmetry of these profiles is defined as contrasting low values of β_C at the edges of a basin compared to the high values estimated at the centre of the profiles. The profiles for the lithosphere stretching (β_L) in Baffin Bay (Figure 6.10) showed very high values at the boundaries and low values of β_L at the centre. The β_L pattern at Labrador Sea displayed increasing beta geometry depicted by β_L values of >8.0, 8.0 - 2 and <2.0. An asymmetrical profile was obtained for the Davis

Strait (Figure 6.10); with β_L decreasing from infinity at the southwest part to very low at the northeast part of the Strait.

Consequently, there is significant variation in the values of β_L and β_C in the specific basins. This difference is in the order of 9.0 to 1.0 from the southwest part of all the sections, in comparison to their NE boundaries. Hence, there is a clear and consistent difference in β_C and β_L for the entire West Greenland margin. This implies that lithospheric stretching along the West Greenland is not a simple 1D pure shear model (McKenzie, 1978). Though, there is significant difference in the values obtained for β_C and β_L along West Greenland. We hypothesise that the lithosphere formed by variable depth-dependent stretching in Baffin Bay, Davis Strait and Labrador respectively. Asymmetric stretching factor profile deduced in the study area may be related to asymmetric rifting processes. As most rifted margins form through a long period of extension, the locus of rifting may change with time, resulting in asymmetric continental margins (Tucholke et al., 2007, Reston, 2009). Systematic differences between the patterns of upper crustal and lower crustal thinning may indicate an asymmetric rifting process (Reston, 2009). However, asymmetric rift can develop through the occurrence of two or more symmetric phases of rifting at different locations (e.g. Kusznir and Park, 1988; Bassi, 1995). We favour asymmetric rifting process for West Greenland.

Furthermore, we compare the thinning factors in the West Greenland profiles with those of Norwegian and West Australian margins in order to see if it is possible to develop a model for all depth-dependent rifts. The kinematic

continental lithosphere stretching of Davis Strait (this study) is similar with the Møre margins (Kusznir and Karner, 2007) (Figure 6.11). Both are classified to be volcanic margins that experience similar rifting, magmatism and breakup history. At the Møre margins, there is evidence of high velocity zones (HVZ) or lower crustal bodies (LCB) (Faleide et al., 2008; Reynisson et al., 2010). High velocity zones (HVZ) or lower crustal bodies (LCB) have also been observed in the Davis Strait (Funck et al, 2007, 2012; Suckro et al., 2013)

Here we present the remarkable depth-dependent stretching best match comparison (Figure 6.10), indicating both margins required lithosphere stretching factor higher than that of upper crust to restore paleo-water depth marker to sea level at and post breakup. Davis Strait (this study) and Møre margin (Kusznir and Karner., 2007) have similar upper crust stretching factor of 1.1 (Figure 6.11) and whole lithosphere stretching factor increased gradually from 1.6 to infinity.

The upper crust thinning factor for Baffin Bay is c.0.28 (Figure 6.12A). For West Australia, Labrador Sea and North Vøring, the β factor is c.0.33, c.0.16 and c.0.08 accordingly (Figure 6.12A). For whole lithosphere thinning factor (Figure 6.12B), there is different trend and value of β. However, West Australia (Roberts et al., 2013) has similar trend and β factor compared to the Baffin Bay and the Labrador Sea. Conversely, the timing and magnitude of depth-dependent lithosphere stretching on the southern Lofoten and northern Vøring continental margins offshore mid-Norway (Kusznir et al.,

2004, 2005) showed less match compare to west Greenland and West Australian margin respectively.

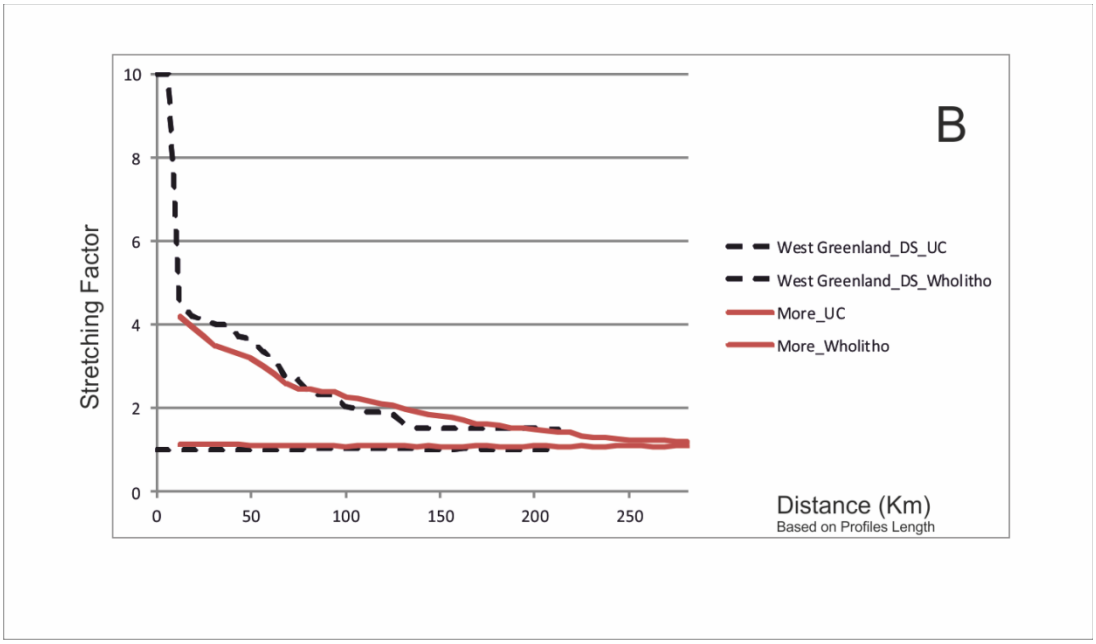

Figure 6.11: Comparison of Upper Crust faulting (β_c) versus whole lithosphere stretching factor (β_L) for (Norwegian margin (Møre) and West Greenland Margin (Davis Strait)

Table 6.3: Lithospheric stretching and thinning factors across the entire West Greenland margin and crustal zonation from this study , similar to Roberts et al. 2013; McKenzie & Bickle, 1988

Crustal Z**onation**	**Lithosphere Stretching Factor**	**Lithosphere** T**hinning Factor**
Thinned continental crust	0-4.5	0-0.7
Very high thinned continental crust (attenuated zone)	4.5-5.5	0.7-8.1
Transition zone	5.5-8	8.1-8.8
Oceanic crust	8-infinity	8.8-1

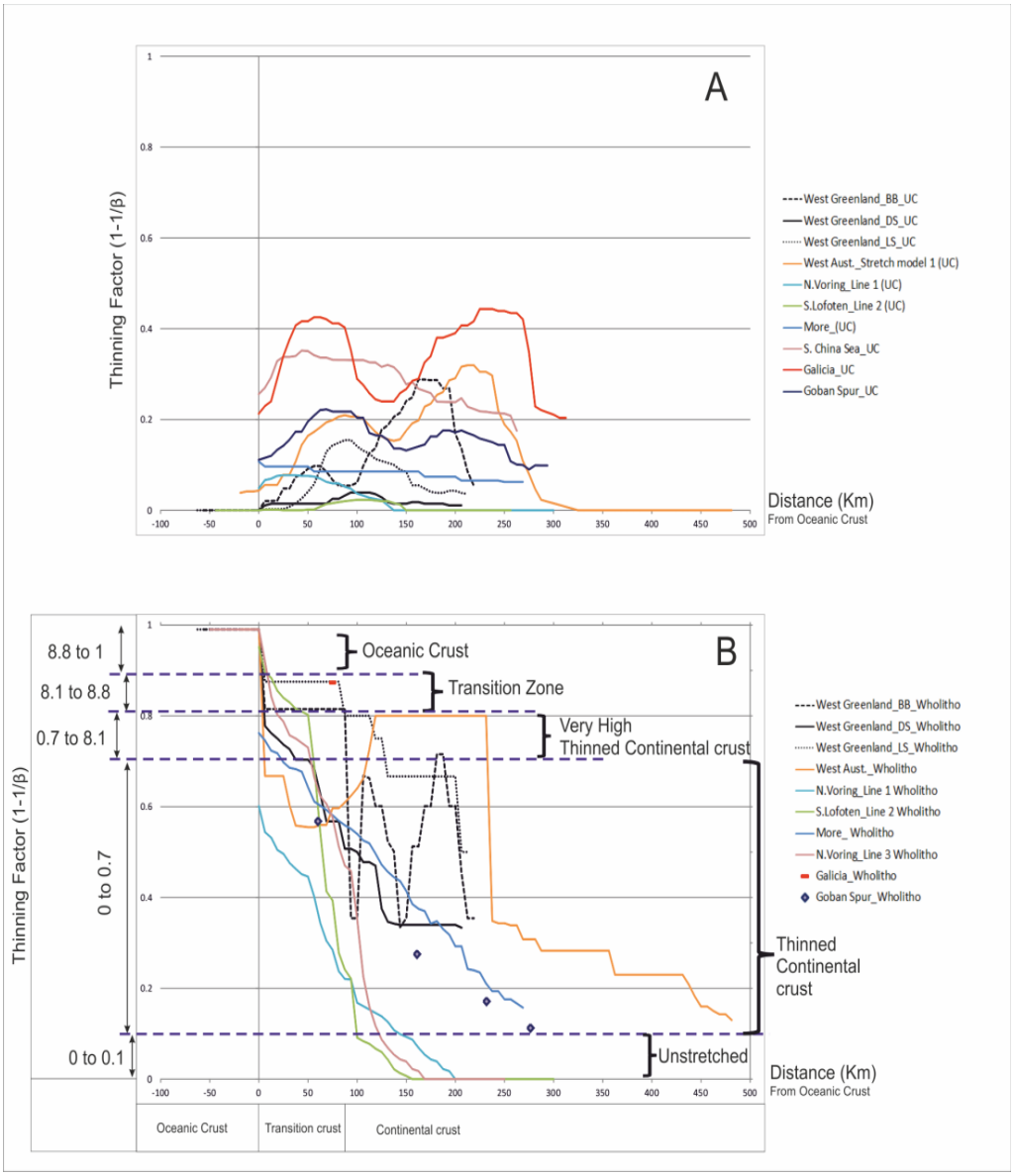

Figure 6.12: Comparison of (A) Upper crust stretching and (B) whole lithosphere stretching factor for West Greenland (this study) area, West Australia and Norwegian margins *Note: UC-Upper Crust, Wholelitho-Whole lithosphere, BB-Baffin Bay, DS-Davis Strait, LS-Labrador Sea.*

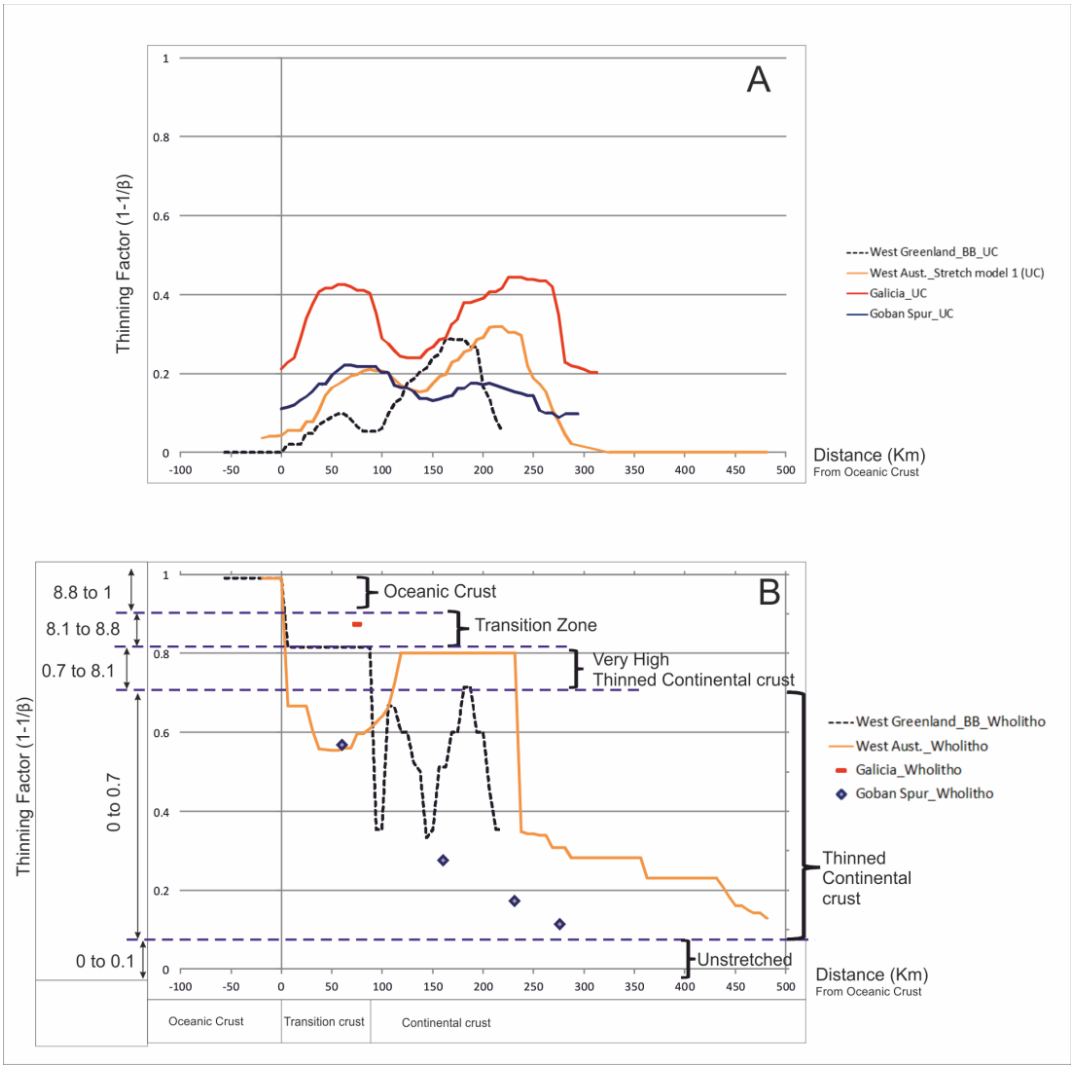

Figure 6.13: Comparison of Baffin Bay thinning factor versus other margins (e.g west aust, Galicia; Iberian and Gabor spur ;UK). A) Upper crust thinning and B) whole lithosphere thinning factor

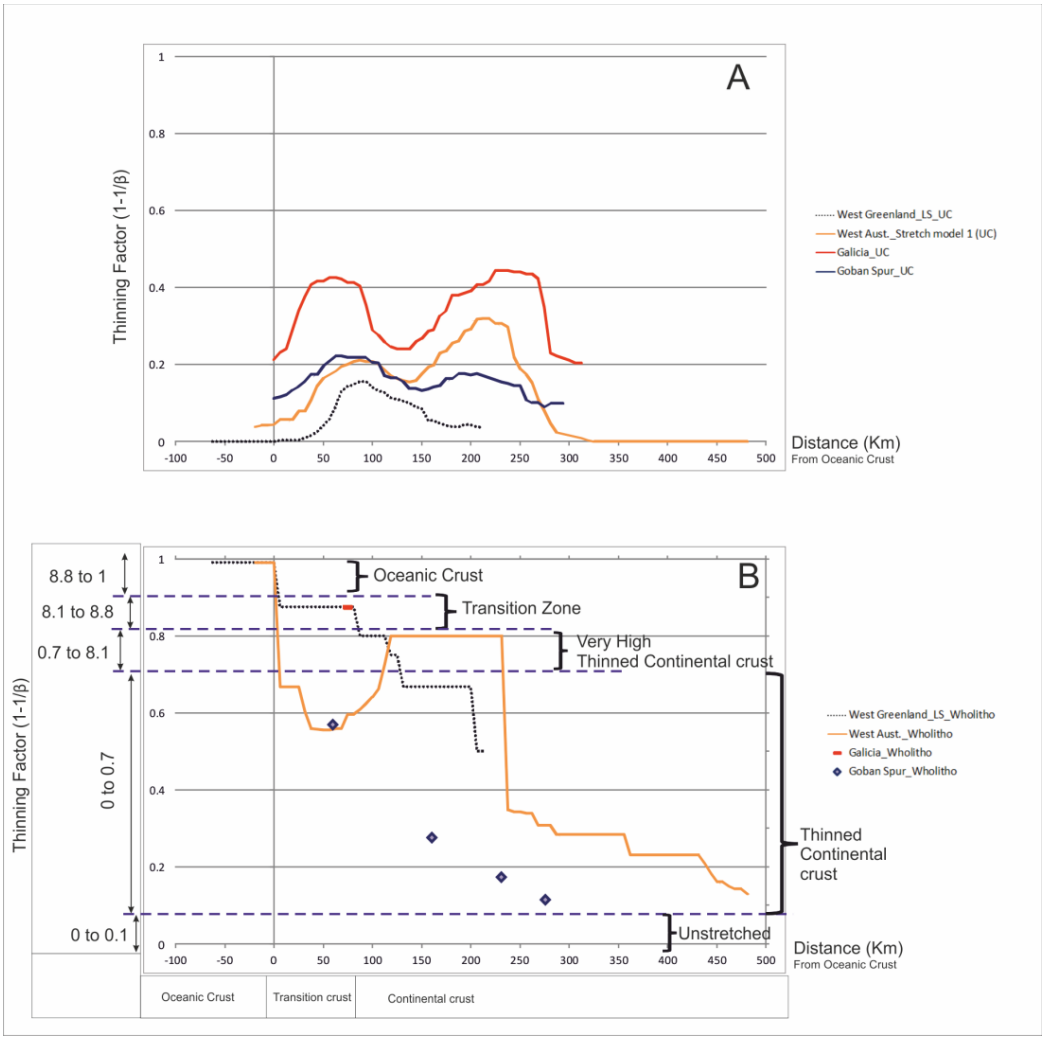

Figure 6.14: Comparison of Labrador Sea thinning factor versus other margins (e.g west aust, Galicia; Iberian and Gabor spur ;UK). A) Upper crust thinning and B) whole lithosphere thinning factor

6.8 Discussion

A key application of depth-dependent stretching is the establishment the timing of stretching either at breakup intercontinental rifting or during sea floor spreading initiation (Kusznir et al., 2005). Large variations between upper crust extension and whole lithosphere thinning are generally attributed to sub-seismic resolution faults, which often accounts for 30% of the missing extension in the upper crust (Walsh et al., 1991). The high variation in beta

ratio of the stretching factor for upper crust extension and whole lithosphere provides evidence that depth-dependent stretching in the West Greenland area occurred during early sea floor spreading rather than during early pre-break-up rifting (e.g. Kusznir et al., 2004). Furthermore, the higher difference for the stretching factors is apparently related to the presence of plume-related magma in Labrador Sea. This study shows that subsidence in the West Greenland margin is thermal-dependent and controlled to less extent by fault activity and extension.

Asymmetric β_L along the profile for the Baffin Bay region is attributed to non-volcanic rifting in contrast to the symmetrical profiles of the Labrador Sea and Davis Strait. The latter margin shows evidence for the presence of oceanic from seismic character and from the modelling of whole lithosphere stretching where β_L value tends to infinity. Baffin Bay region also has the highest value of βc in the entire West Greenland area suggesting lesser crustal thickening relative to Labrador Sea and Davis Strait. The post breakup sediments above the fault blocks are thickest (5-6 km) in the Baffin Bay region in contrast to very low thickness (1-3 km) on the fault blocks near the inferred ocean-continental boundary (OCB). All point to the relevance of depth-dependent stretching occurred during early seafloor spreading in the West Greenland margin.

In comparison with other margins, it was shown that the stretching factor due to whole lithosphere is similar between West Australia, Baffin Bay and Labrador Sea and between Møre and Davis Strait margins while upper crust

stretching factor for Møre and Davis Strait are the same. It should be noted that the Norwegian margin is affected by a complex history of stretching and igneous volcanic activity. These activities resulted in the emplacement of SDRs, sill intrusions, high velocity and density bodies, and extrusive lavas (White and McKenzie, 1989). These igneous activities and high velocity zones were also noted in Davis Strait (Funck et al, 2007), however clear-cut SDRs were not observed in Davis Strait from Greenland side but observed in Canadian side (Skaarup et al., 2006). This is in addition to volcanic sills and SDRs interpreted in Baffin Bay and Labrador Sea. If Møre and Davis Strait do have similar upper crust and whole lithosphere stretching factors, it is not a coincidence but rather a pointer to history of rifting on both margins.

Most basins in northeastern Atlantic experience regional Palaeocene uplift and accelerated Eocene subsidence. The Eocene subsidence anomaly is generated by the decay of Palaeocene regional uplift event associated with the initiation of the Iceland plume (Bertram and Milton 1988; Nadin and Kusznir 1996). Hence, Davis Strait in a similar fashion with Møre has protracted history of rifting. Evidence for this is provided by the inference of two stages of rifting along the West Greenland margins. First episode of rifting was recorded by Cretaceous units while sedimentary units associated with second phase of rifting are top Palaeocene strata. Lithosphere stretching in West Australia, Baffin Bay and Labrador Sea shows that the margins are very highly to moderately stretched.

6.9 Conclusions

- Based on our analyses we conclude that the stretching factor (βc) from the upper crust faulting (typically *c.*1.1 to 1.4) is less than the stretching factor (β_L) from the whole lithosphere (from *c.*1.5 to >10). This is evidence that the whole lithosphere has extended more than the upper crust and, therefore, a depth-dependent thinning model may be valid when considering the break-up evolution of the west Greenland margin.

- Rifting in West Greenland started in pre Palaeocene times. The rift axis changed from north to northeast from Labrador Sea to Baffin Bay during rifting along the margin. Maximum thinning of the lithosphere are proportionate with high values of β_L and onset of magmatism. In addition, the breakup stage is signified by the presence of voluminous Palaeocene basalt in the Davis Strait and Labrador Sea, respectively. The Ocean-Continent boundary is inferred in the Labrador Sea supporting the hypothesis for a northward propagation of rifting and sea floor spreading in the West Greenland margin.

- Furthermore, the Labrador Sea and Davis Strait margins display evidence of a more symmetric stretching pattern in contrast to the Baffin Bay area that appears to be more asymmetric. We believe that the depth-dependent stretching in West Greenland occurred as a result of whole lithosphere stretching and variations along the margin are probably caused by presence of second generation faulting of

Post Cretaceous units in Baffin Bay and Davis Strait regions and plume-related magma in Davis Strait.

- The upper crust thinning factors for Baffin Bay and Labrador Sea Figures 6.13 and 6.14, are similar to the other margins (e.g, West Australia, Galicia, west Iberia and Gabor spur ;United Kingdom) . The whole lithosphere thinning factor of Baffin Bay is similar to West Australia while the whole lithosphere thinning factor for the Labrador Sea is similar to Galicia, west Iberia, while Davis strait has whole lithosphere thinning factor comparable to Vøring margin (Figure 6.11).

Chapter 7

Hydrocarbon Prospectivity of the West Greenland margin

7.1 Abstract

The implications of the new tectonic model (Chapter 4) on the hydrocarbon prospectivity of West Greenland margin is assessed using 1D and 2D petroleum modelling techniques. The petroleum system modelling input utilises the seismic interpretation of nine regional megasequences (Chapter 4) and heat flow analysis that come from the depth-dependent stretching modelling along the margin (Chapter 6)

The margin of West Greenland has potential for hydrocarbon generation. The source rocks which are organic-rich upper Cretaceous and Neogene rocks are in places thermally mature. These source rocks are deposited in rift-depressions where maximum heat flow is estimated. Thermal maturation of the source rocks commenced in Eocene with the oil window reached post Miocene time. The greatest heat flows were modelled in Eocene times, ~46 mW/m^2, 55 mW/m^2 and 49 mW/m^2 for Baffin Bay, Davis Strait and Labrador Sea respectively.

As a consequence, viable hydrocarbons are predicted within two distinct syn-rift packages that are located at shallow and deeper stratigraphic positions. Hydrocarbon migration predicted is through fault systems produced during the rift phase. We predicted hydrodynamic migration mechanism for Cretaceous source rocks. Hydrocarbon types include oil, wet and dry gas. Younger stratigraphic units along the margin are devoid of hydrocarbon suggesting that migration of hydrocarbon is restricted to deeper strata.

7.2 Introduction

The West Greenland margin remains under explored with respect to both hydrocarbon and scientific studies (Balkwill et al., 1990; Chalmers, 1991, 2000, 2012; Chalmers and Pulvertaft, 2001; Chalmers et al., 1993; Nielsen et al., 2002; Roest and Srivastava, 1989; Rowley and Lottes, 1988; Schenk, 2011). The crustal structures, their evolution and their impact on hydrocarbon generation remain the subject of debate and ongoing research. Much of this is a consequence of the sparse data coverage and the complex tectonic evolution of the margin (e.g. Chalmers et al., 1993). The revised evolutionary model of Greenland margin presented in Chapter 4, revealed that it is not a simple rift to drift formation. Therefore, it is important to consider the impact of this uncertainty on the hydrocarbon potential of the West Greenland basins. A preamble on historical hydrocarbon exploration on the margin is given in section 7.3. Having described the architecture of Cretaceous and Tertiary sediments in the study area and their potential as

viable petroleum systems will be considered. This chapter will focus on heat flow and the influence of depth-dependent stretching (DDS) on the hydrocarbon potential of the margin.

To understand the process driving hydrocarbon accumulation on any margin, it requires an understanding of the petroleum system, tectonic and sedimentation interaction (e.g. Iliffe et al., 1991). Adequate data including high resolution seismic, well and stratigraphic information are required (Al-Hajeri et al., 2009). A petroleum system modelling approach has been applied in various research studies (e.g. Burrus et al., 1991; Johannesen et al., 2002; Kubala et al., 2003; Paton et al 2007). Where sufficient data are available, thermal and petroleum systems models are useful in predicting the hydrocarbon potential of a basin. The maturation of hydrocarbon reservoirs is dependent on paleo-temperatures, which are influenced by heat production in the basement (Nadeau et al., 2005). Therefore, a good knowledge of the basement rock and its associated structure is critical information for estimating the thermal condition in any sedimentary basin.

The aim of this chapter is to model the hydrocarbon potential of the West Greenland. This will be achieved by a) assessing the thermal maturity of the syn-rift strata and their capability to generate hydrocarbon, b) estimating the burial history of the source rocks, and c) determining the migration mechanisms from source to reservoir rock. To achieve these objectives, we used the 3D tectonic model derived from the seismic interpretation (Chapter

4) and integrate that with published data to constrain the ages of lithology for each interval.

7.3 Previous works

Exploration for hydrocarbons in West Greenland began in the early to mid-1970s and was focussed on areas where water-depths are less than 500m (Rolle, 1985)**.** Five exploratory wells were drilled in 1976 and 1977 respectively (Rolle, 1985); Hellefisk-1, Ikermiut-1, Kangâmiut-1, Nukik-1, and Nukik-2 (See Chapter 3; Figure 3.1). Unfortunately, none of the five wells showed evidence for hydrocarbon accumulations and all were declared dry at the time (GEUS, 2014). However, slight gas show were recorded in the lowermost part of the sedimentary sequence in Kangâmiut-1 well (Rolle, 1985). In the 1980s and early 1990s, two breakthroughs in prospectivity along the West Greenland margin were that (a) an improved understanding whereby the sedimentary basins that could contain oil and gas were much larger than earlier thought and (b) the discovery of extensive oil seeps onshore in the Nuussuaq Basin (Chalmers & Laursen 1995, Chalmers *et al.* 1993; Bojesen-Koefoed *et al.* 1999). At the end of the century, Qulleq-1 well was drilled in 2000 (Pegrum, 2001) by the Statoil group as part of their commitments in the eastern sub-area of the Fylla licence. The main target of the well was the cross-cutting reflection (CCR) that were interpreted to be bright spots related to hydrocarbon. The well, however, encountered only mudstones in this interval and no gas or oil (Christiansen et al, 2001). In Table 7.1, further information is provided on the previous hydrocarbon

exploration and discovery on the margin (Gregersen and Bidstrup, 2008; Bojesen-Koefoed et al., 2004; Sønderholm et al., 2003; Bojesen-Kofoed et al., 1999; Dam, et al., 1998 and Núñez-Betelu et al., 1993).

A number of deep basins with Cretaceous and Cenozoic sedimentary successions have been recognised offshore West Greenland since the 1970s (e.g. Chalmers and Pulvertaft, 2001). During the Early to mid-Cretaceous times, major structural complexes and basins developed in the region mainly as a result of extensional faulting (See Chapter 5; Figure 5.2; 5.3 and 5.4). These include the Kivioq and Melville Bays and the Upernavik basin in Baffin; Bay province, the Aaisaa basin in the Disko west province; the Lady Franklin, Kangamuit, Sisimuit and Fylla complex Basins in Nuuk West province; the south Fylla complex basin and the Cape Farewell basin in Cape Farewell province.

Ordovician carbonate strata are noted on the Davis Strait High. Together with reworked Jurassic or older palynomorphs observed in the Qulleq-1 well farther south suggests the possibility of pre-Cretaceous strata in the deepest parts of these basins (Dalhoff et al., 2006). Based on outcrop studies, regional Cretaceous sand-prone units are expected to be present in the offshore region as deltaic and shallow-marine and turbidite deposits.

In Chapter 4, it is shown that new rifting was initiated in the Late Cretaceous and was characterised by normal faulting, subsidence and syn-rift sedimentation including deposition of a thick mudstone succession of

Campanian–Maastrichtian age (Dam et al. 2000). This phase lasted into Early Palaeocene times resulting in repeated erosion and filling of sub-aerial valley and submarine canyons and formation of regional unconformities (Dam and Sønderholm, 1994, 1998; Dam et al. 2000).

A major episode of volcanic eruption occurred during the Palaeocene–Eocene and hundreds of metres of thick basalts cover part of the offshore region (Bojesen-Koefoed et al., 2004; Sønderholm et al., 2003; Dam, et al., 1998, see Chapter 4, Figure 4.4 for further details). The basalts may reach thicknesses of more than 2 km in the north-eastern offshore part of the study area. However, the current interpretation from Chapter 4 suggests that the volcanic succession is thinner and less widely distributed than suggested in previous publications and maps (e.g. Chalmers et al. 1993; Chalmers and Pulvertaft 2001; Skaarup 2002).

Strike-slip movements during Late Palaeocene and Early Eocene caused local transpression of structures primarily along the Ikermiut Fault Zone, and locally in the basins and structures farther north, contemporaneous with subsidence in the Ikermiut Basin region (Chalmers et al. 1993; Chalmers and Pulvertaft 2001). Transtensional and extensional movements farther to the north-east, subsequent to the extrusion of the Paleocene basalts, resulted in the development of more than 200 km long Ilulissat Graben (Chalmers and Pulvertaft 2001).

During the Eocene, and especially during the late Miocene to Pliocene, the offshore basins subsided rapidly, and large sedimentary wedges prograded towards the west and south, possibly as a consequence of Neogene uplift in the present onshore areas to the east (Dalhoff et al. 2003; Japsen et al. 2005, 2010; Bonow et al. 2006).

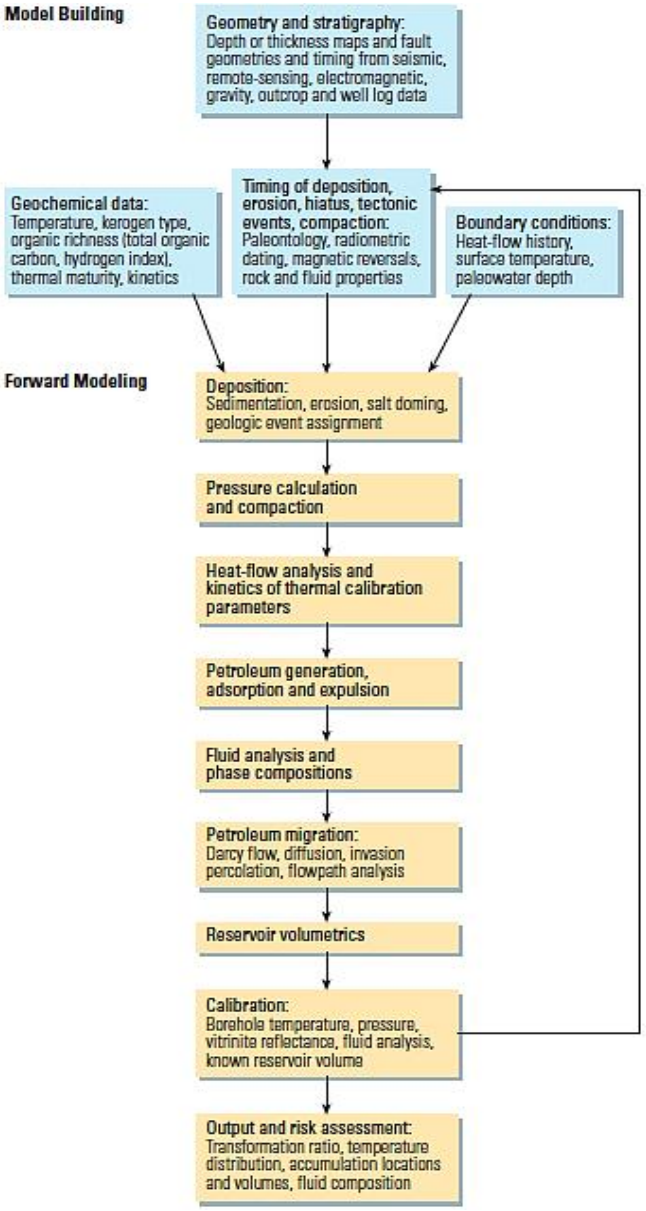

Figure 7.1: Flowchart for basin modelling as proposed by Al- Hajeri et al. (2009).

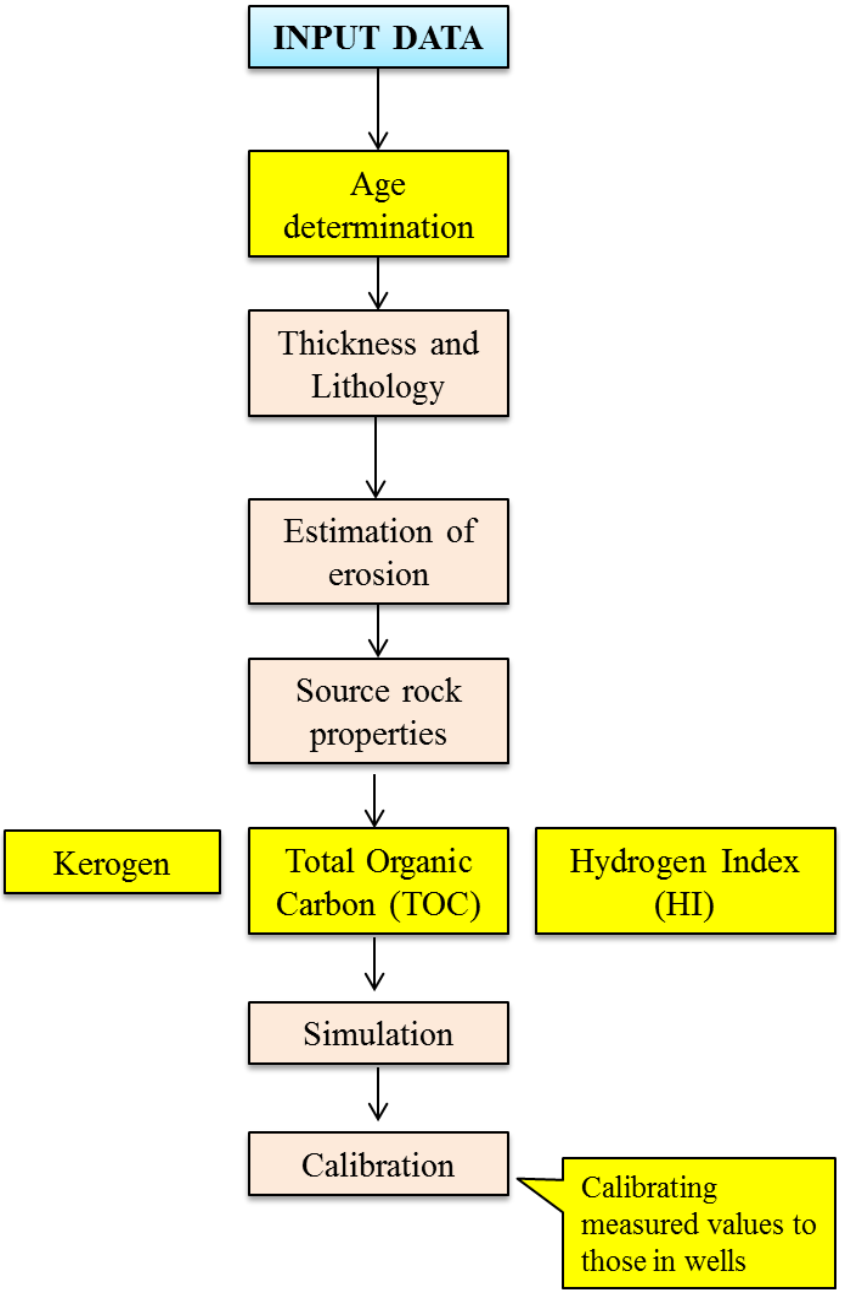

Figure 7.2: Workflow for basin and heat flow modelling in the study area (Modified after Al-Hajeri et al., 2009).

7.4 Methods

Representative lines were selected from each of the structural provinces to conduct 1D and 2D Basin analysis and Petroleum system modelling using PETROMOD (Schlumberger, Petrel trade mark software). Nuuk west province is the main region that consists of wells drilled. In order to evaluate its hydrocarbon prospectivity, a reprocessed 2D seismic line by TGS is used for this province. The line intersects the main wells and while the others were projected. The seismic data is tied to the four existing offshore exploration wells (Hellefisk-1, Ikermiut-1, Kangâmiut-1, and Qulleq-1). Nine seismic horizons ranging from acoustic basement, mid-Cretaceous, top-Cretaceous, Top Palaeocene, mid-Eocene, mid-Miocene, Base Quaternary and Seabed (See Appendix IV; Figure 7) have been interpreted regionally from depth-converted seismic profiles using pre-stack interval velocities provide by GEUS and interval velocities (Chapter 4 and 5).

The workflow chart for the hydrocarbon modelling is provided in Figure 7.1 and 7.2. An integrated basin modelling approach was used to define the hydrocarbon potential of the margin. This is used to reconstruct and quantify the geological and thermal evolution of a sedimentary basin, and hence to derive the history of generation, migration and accumulation of petroleum (Welte and Yalcin, 1988). The first stage is the construction of a geo model, and involves constructing a structural model populated with sequence and sedimentologic properties of the stratigraphic units. The

input parameter of the model include a) Formation names, ages, thicknesses and lithology type b) Vitrinite reflectance, temperature, geothermal gradient c) Source rock properties d) Erosion and e) Heat flow, palaeowater temperature. The general workflow and required input parameters for both 1D and 2D basin and heat flow modelling are summarised in Figure 7.2. The input parameters for the hydrocarbon modelling are presented in Tables AII:1 to 5. For details of the methods and parameter used in the modelling are provided in Appendix V.

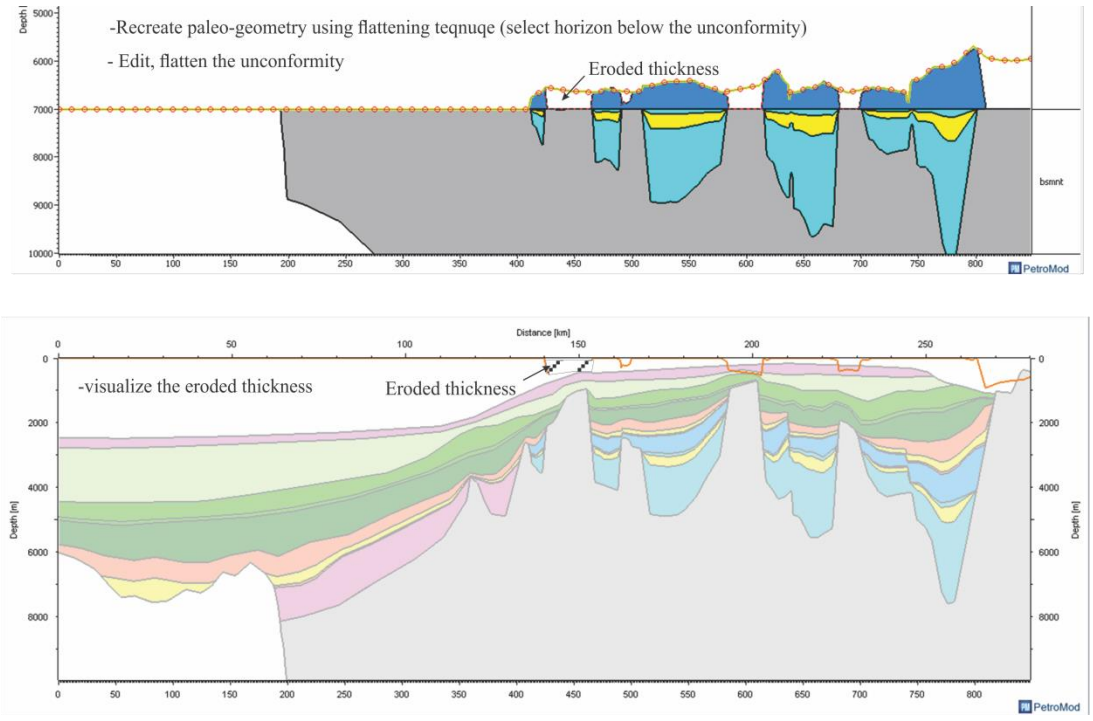

Figure 7.3: Comparison of reconstructed eroded cross section to the interpreted seismic section. The figure shows the amount of strata eroded at Cretaceous along West Greenland margins.

7.5 Results

7.5.1 Heat flow (1D Modelling)

One dimensional (1D) heat flow modelling of the Nuuk West from the four wells shows that the highest heat flow are estimated in the Ikermiut well (See Appendix IV; Figure 4). Heat flow maxima are estimated in Eocene units of all the wells except Kangamiut well (See Appendix IV; Figure 5). In the latter, the heat flow maximum value was estimated in Lower Miocene Strata. Heat flow curves of Hellefisk-1, Ikermiut -1 and Qulleq -1 are similar. These curves exhibit very steep gradients above the upper Cretaceous units and shallow gradients with depth. The Kangamiut well displays a variable gradient (See Appendix IV; Figure 5). In this well, minimum heat flow values were estimated above the basement rock, in addition to skeps in the curve observed at the upper, mid Eocene boundaries.

There is close match between observed and modelled temperature and average geothermal gradient for all the wells. However, Qulleq-1 and Ikermiut-1 wells showed an excellent calibration between Vr observed and modelled (See Appendix IV; Figure 4 and 5). Good calibration between Vr observed and modelled indicated (See Appendix IV; Figure 4 and 5) from Kangamiut-1 and Hellefisk-1 wells which are probably due to large faults interpreted near the wells (See Appendix IV; Figure 7).

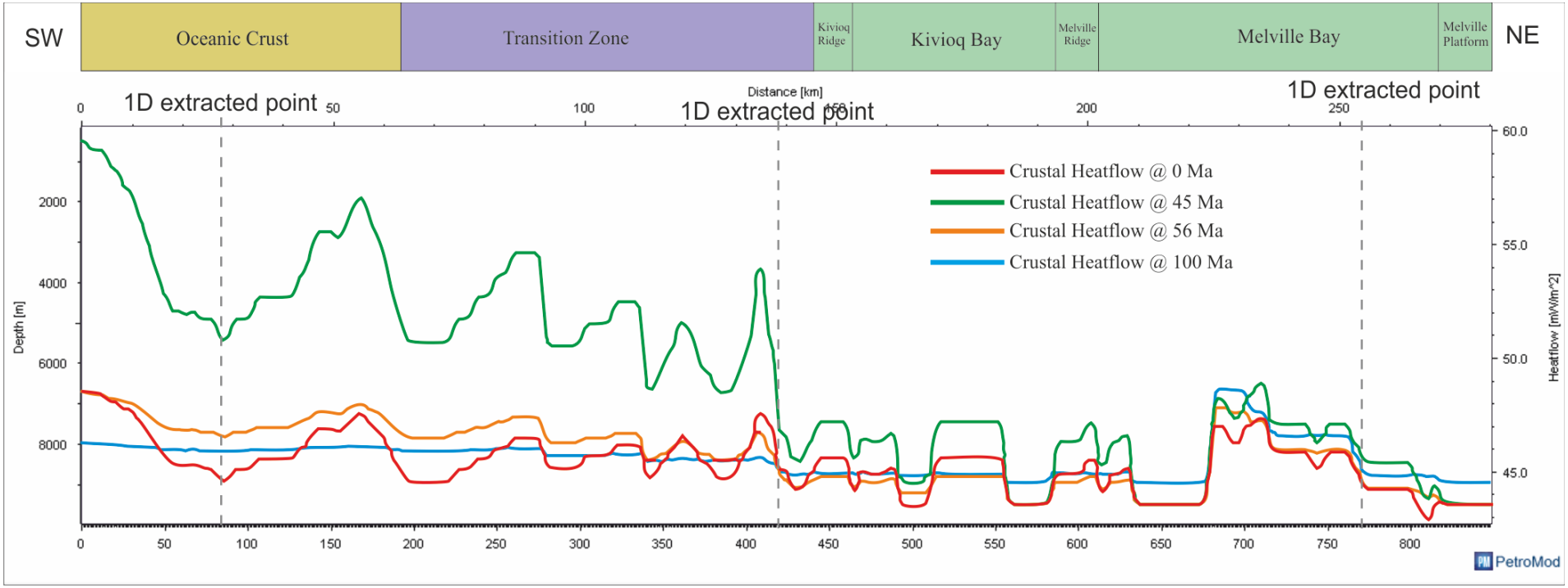

Figure 7.4: 2D modelled heat flow along Baffin Bay province. N.B: The yellow line represents heat flow of top palaeocene that matched and calibrated with DDS beta. Location of seismic line is shown in Figure 7.10.

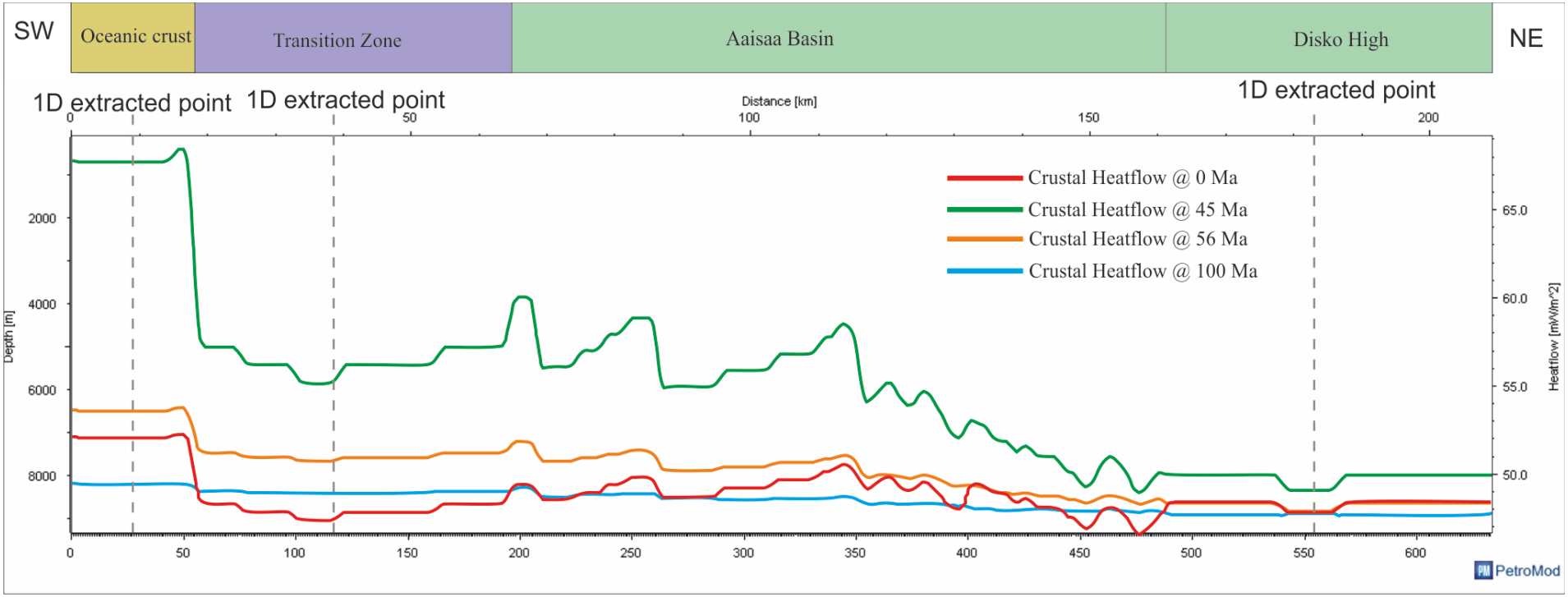

Figure 7.5: 2D modelled heat flow along Disko West Province. N.B: The yellow line represents heat flow of top palaeocene that matched and calibrated with depth-dependent stretching (DDS) beta. Location of seismic line is shown in Figure 7.10.

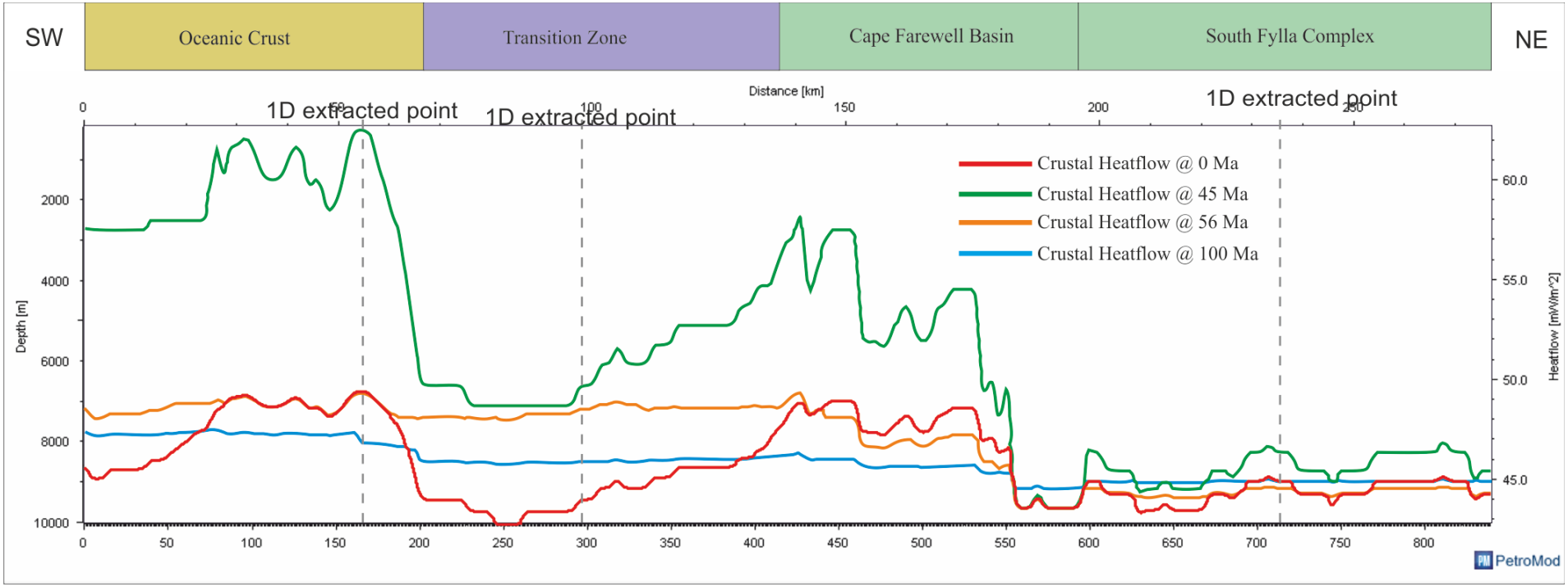

Figure 7.6: 2D modelled heat flow along Labrador Sea. N.B: The yellow line represents heat flow of top palaeocene that matched and calibrated with depth-dependent stretching (DDS) beta. Location of seismic line is shown in Figure 7.10.

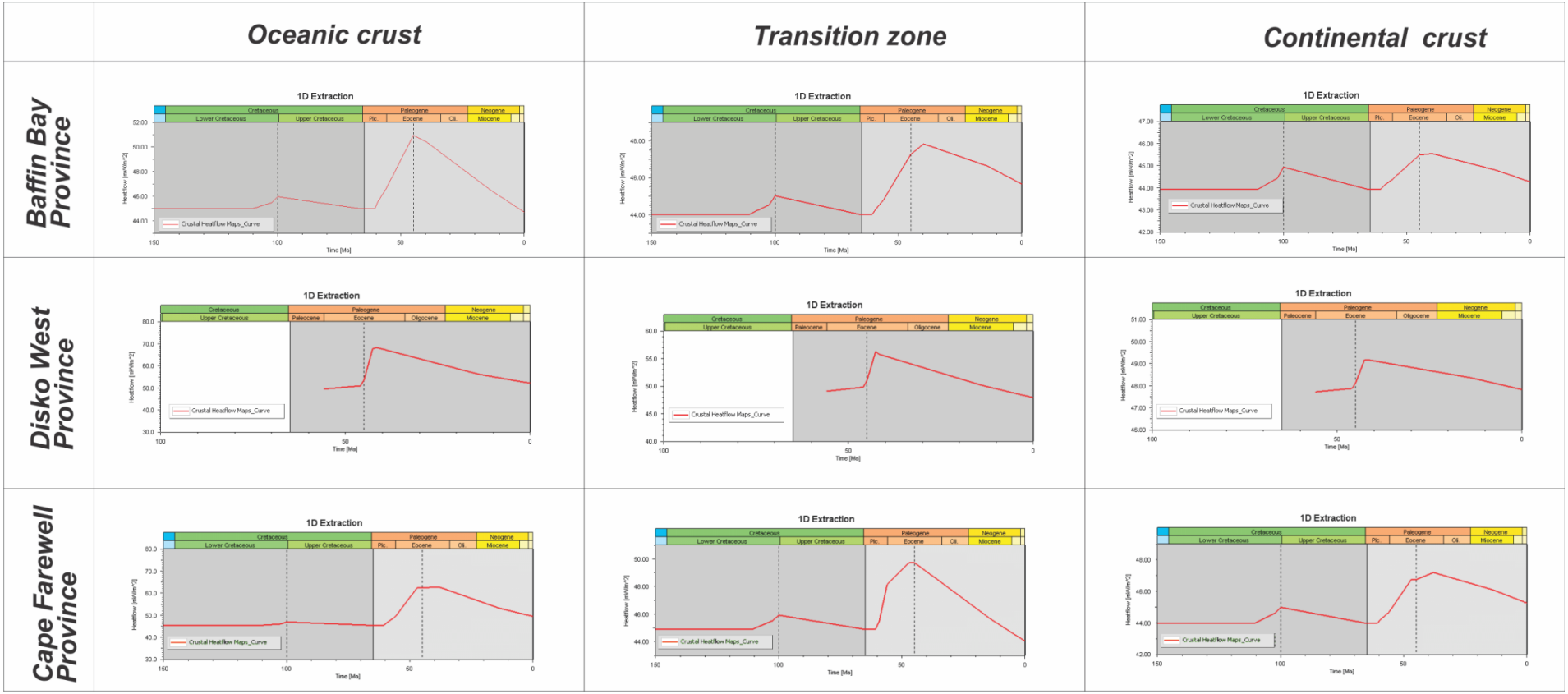

Figure 7.7: 1D heat flow model extreacted points for the oceanic crust, transitional zone and continental crust in Baffin Bay, Disko West, and Cape Farewell respectively. Location of points are showen in figures 7.13, 7.14 and 7.15)

7.5.2 Hydrocarbon potential (1D Modelling)

Temperature, Vitrinite reflectance and porosity of potential source and reservoir rocks are modelled in one-dimension from the wells intersecting the Nuuk West section. The physical properties of the rocks as noted from the wells are summarised as follows:

- Quilleq-1: potential reservoir rocks are below 3150 m which is similar to the works of Christiansen, et al., (2001) (Figure 7.10). Potential source rocks include upper Cretaceous to Palaeocene rocks. Ro values of 0.450 to 0.50 were recorded in these rocks (See Appendix IV; Figure 5). Potential reservoirs rocks are post-Palaeocene strata where porosity values of 50% were modelled.

- Hellefisk -1: potential hydrocarbon reservoir rock is below the basalt (Figure 7. 10). Temperature of the basaltic units ~75^0 C at depth of 3000 m (See Appendix IV; Figure 4). The highest geothermal gradient was noted in the Upper Cretaceous strata. Potential source rocks include Lower Eocene, Mid Eocene and Upper Eocene rocks with Ro of 0.5, 0.05 and 0.04% respectively (See Appendix IV; Figure 4).

- Ikermiut -1 and Kangamiut-1 showed potential early hydrocarbon generation at the bottom of the wells (Figure 7.10). This is in accord with the works of Rolle, (1985) and Chalmers et al., (1993). In Ikermiut – 1, Ro of 1% are interpreted in Upper Cretaceous rocks, though, maximum geothermal heat was predicted in the Lower Miocene sediments (See Appendix IV; Figure 4).

Potential source rocks in this well include Lower Eocene to Upper Cretaceous rocks (Figure 7. 14). For Kangamiut-1, Lower Eocene to Lower Miocene strata has Ro of < 0.5 % while Upper Cretaceous to Lower Eocene rocks have Ro > 0.5%. The highest geothermal heat was noted in Miocene and Quaternary rocks (See Appendix IV; Figure 5).

7.5.3 Heat flow (2D Modelling)

The result of 2D heat flow modelling across West Greenland basins are discussed below. Estimated heat flows in Baffin Bay include 51 mW/m^2, 47 mW/m^2 and 46 mW/m^2 along the interpreted oceanic crust, transitional zone and continental crust respectively (Figure 7.4 and 7.7). Heat flow is generally constant, with value of 45 mW/m^2 in Cretaceous strata. There is a drastic change in gradient in heat flow within Paleogene rocks (Figure 7.4). The highest heat flow value was noted within Eocene units. After this period, there is a sharp decrease in gradient in younger stratigraphic units. However, the modeled heat flow value is greater than those of Cretaceous rocks. For example, heat flow of Miocene age rocks at the oceanic, transitional and continental zones are 47, 46.5 and 45 mW/m^2 compared to 44 mW/m^2 recorded in Cretaceous age unit (Figure 7. 4).

Similarly, the highest heat flow was estimated in Eocene strata (~ 45 Ma) along the Disko West province. The heat flow values ranges from 67, 52 and 49 mW/m^2 from the oceanic to continental crust accordingly (Figure 7.5 and

7.7). However, heat flow within the Cretaceous units of the Disko West could not be constrained (Figure 7.5).

In Cape Farewell province, heat flow maxima are in the Eocene unit. From the oceanic, transition zone to continental crust, the heat flow varies from 62, 49.5 and 47 mW/m^2 (Figure 7.6 and 7.7). The curve showed within Cretaceous rock variable heat flow along the province within Cretaceous rocks.

Heat flow curves from all provinces dramatically change through time. The heat flow curves show similar trends with values of backstripped beta from thermal subsidence modelling. For example, the heat flow curve of top Paleocene in Cape Farewell, Baffin Bay and Disko West provinces gradually increases from northeast (continental) side to southwest (oceanic) side which is similar to the trend of thermal subsidence Beta observed and modelled for these same 2D lines (Figures 7.4 to 7.6).

7.5.4 Hydrocarbon potential (2D Modelling)

Predicted hydrocarbon types from the 2D modelling include wet gases within Cretaceous units in Baffin Bay. Early and main oil are restricted to younger stratigraphic intervals (Figure 7.8). The Cretaceous packages in In Baffin Bay are characterized by significant thickness variation in Kivioq Bay and southwest of the Melville Platform. Average thickness of the Cretaceous unit is c.4 km (See chapter5; Figure 5.1).

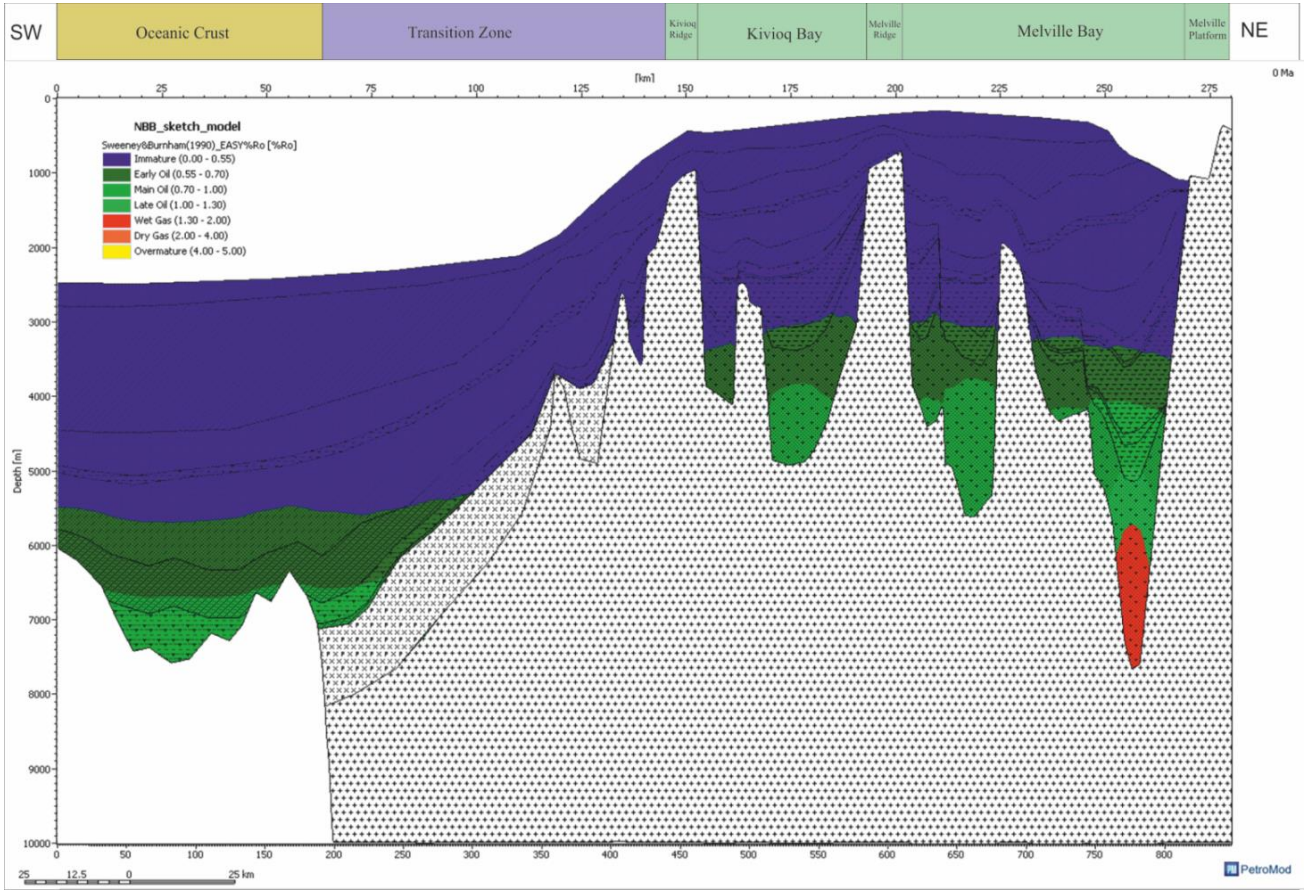

Figure 7.8: Hydrocarbon potential and maturation model for Baffin Bay**.**

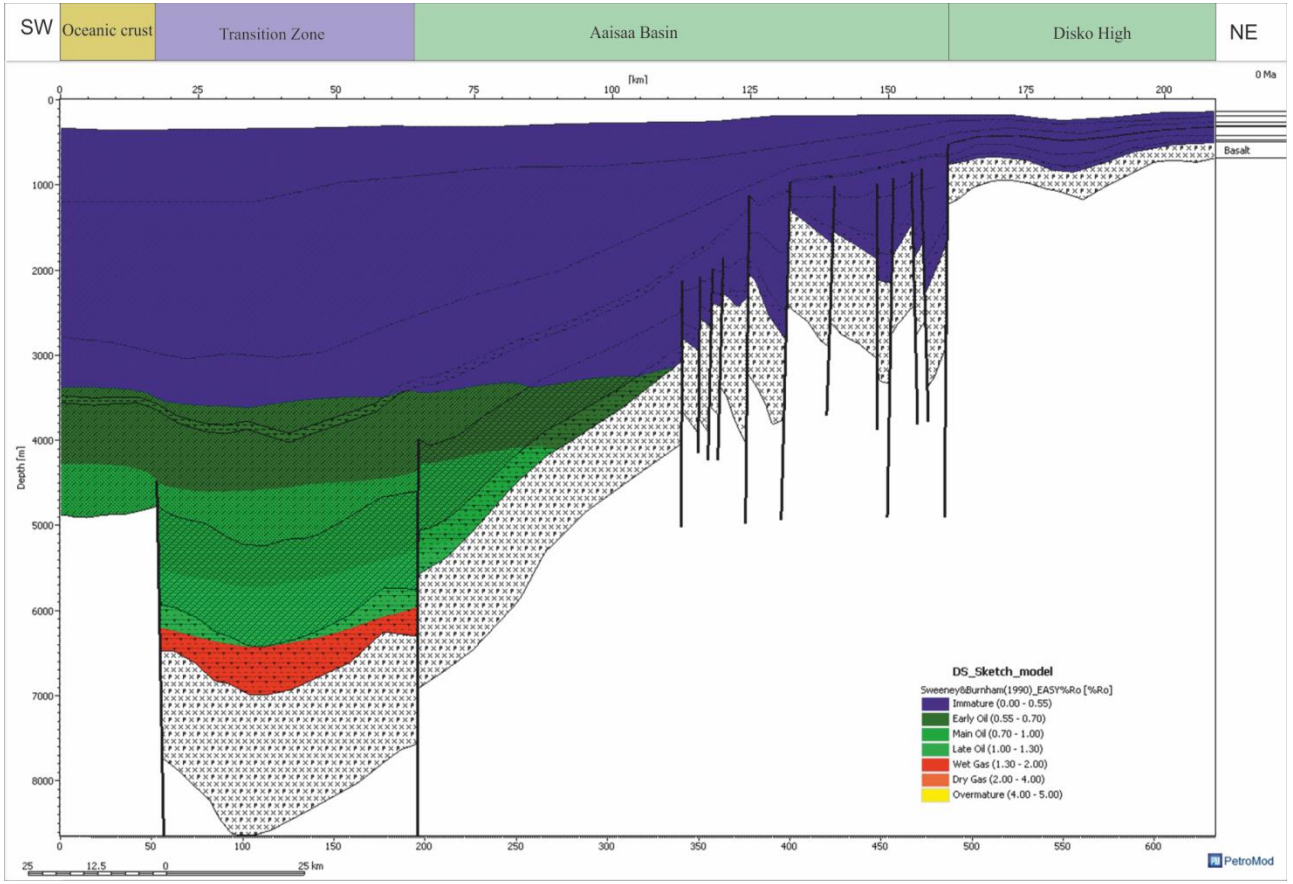

Figure 7.9: Hydrocarbon potential and maturation model for Disko West**.**

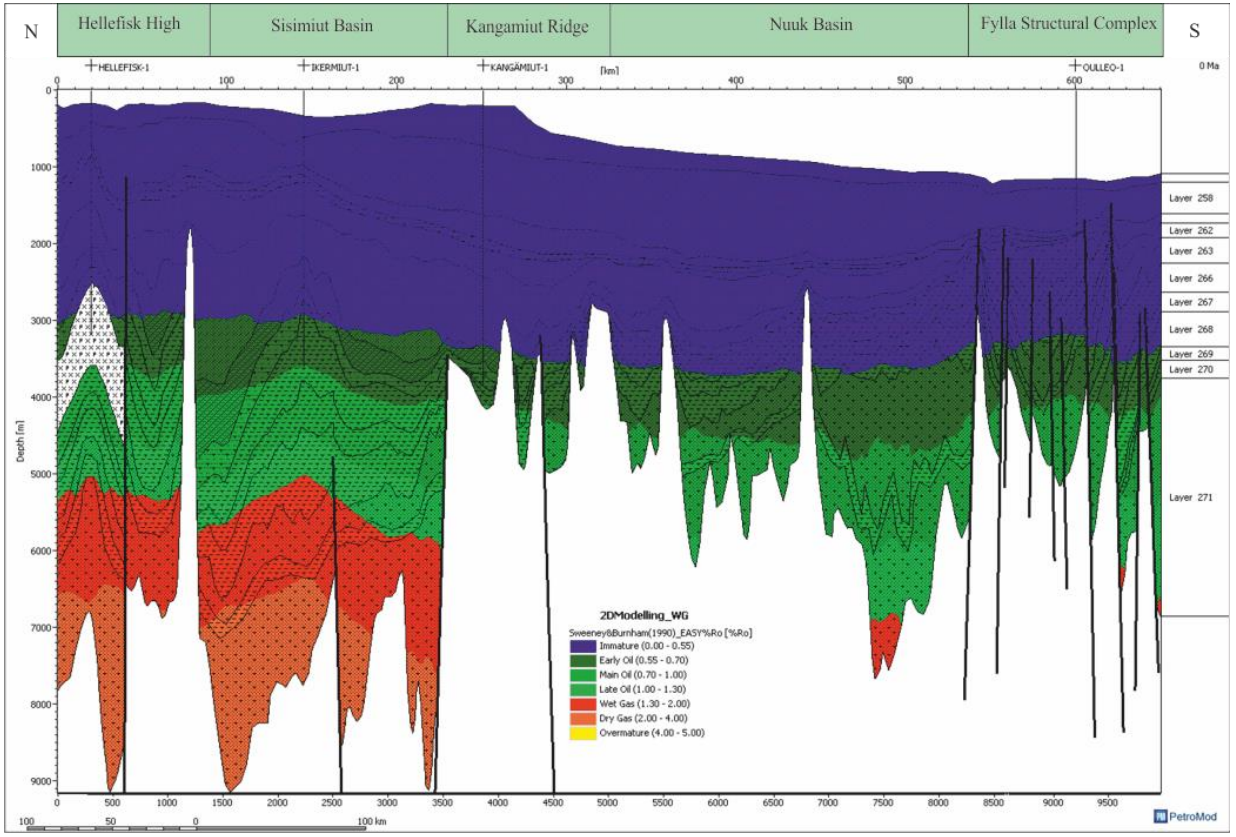

Figure 7.10: Hydrocarbon potential and maturation model for Nuuk West**.**

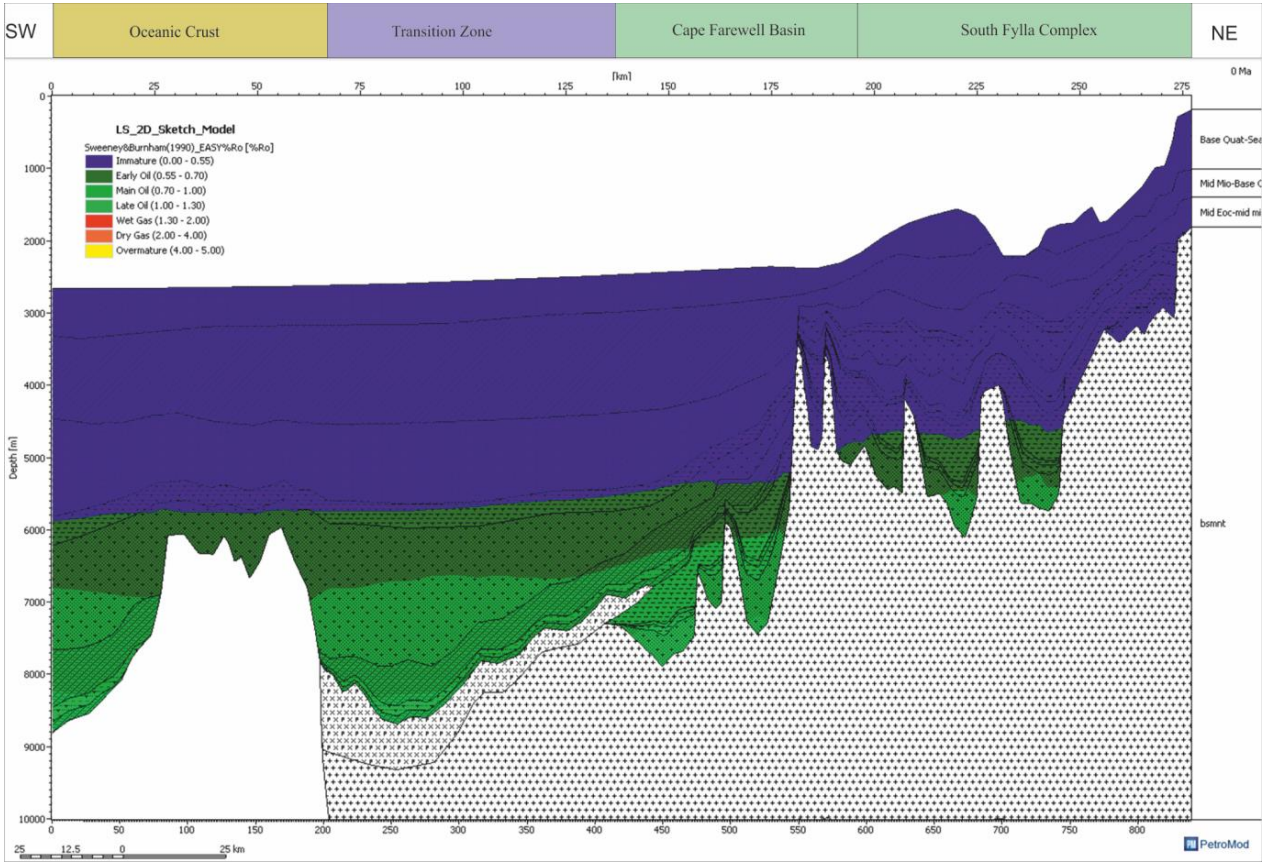

Figure 7.11: Hydrocarbon potential and maturation model for Cape Farewell**.**

Faults associated with the interval where hydrocarbon are predicted in Baffin Bay basin have their upper tips terminated by post rift strata of Mid Miocene to Base Quaternary age. These faults were produced during Late Jurassic – Early Cretaceous rifting in the Baffin Bay region. Furthemore, oil types modelled in Disko West include oils that are predicted within Mid-Eocene to Base Quaternary strata and wet gas estimated in Top Palaeocene sandstone above the basalt (Figure 7. 9). The basalt in Disko West cover an area of c.150,000 km^2. Mid-Eocene to Base Quaternary strata were deposited during the second rifting event proposed in chapter 4 (Figure 4.5) and (Figure 7.8).

In contrast to Disko West, hydrocarbon types of Nuuk West include oil, wet and dry gas. The oldest Cretaceous strata contain dry gas while oil is predicted in post-Palaeocene units (Figure 7.10). Cretaceous strata in Nuuk West include Syn-rift I and Post-rift I packages deposited in a series of isolated wide (> 7 km) rift basins (Figures 4.5and 7.10). Post Palaeocene units are syn-rift II sediments downlapping onto the basalt and top Cretaceous sediments (Figure 7.10). Faults in Nuuk West include NE-SW strike-slip and flower structures associated with the Ungava transform fault. In Cape Farewell province, hydrocarbon types include early and main oil predicted within Mid-Cretaceous rocks (Figure 7. 11). These rocks are associated with syn- and post-rift I sediments deposited in narrow continental margin. Apart from this, the Cape Farewell province is characterised by long faults up to 200 to 400 km in length, some of these faults were reactivated during the second phase of rifting.

In terms of thermal maturity, early and main oil in Baffin Bay are immature (Figure 7.8). In Disko West, oils of Mid-Eocene to Base Quaternary are immature (Figure 7. 18). On the contrary, the oil of Nuuk West ranges from immature to late oil (Figure 7.10) while Cape Farewall comprises immature oils within sediments with Ro values of < 0.55%. Generally, it is noticed that the viable hydrocarbon types were predicted within syn-rift packages.

7.6 Discussion

7.6.1 Hydrocarbon accumulation and Petroleum system of West Greenland Basins

The reliability of both 1D and 2D modeling used in this study is dependent on the quality and validity of the input parameters. Despite uncertainty in the input model, this chapter provides a useful estimation of the hydrocarbon potential of the margin. Most of the parameters are well constrained having come from high resolution seismic and well data. In addition to data coming from reliable literature works on the margin. However, the greatest uncertainty is the extrapolation of well information across the area. This is a common proble in any frontier exploration setting.

The petroleum system is composed of source rocks, reservoirs rocks and seals. Source rocks identified in this Chapter include thermally-mature and organic-rich rocks of Upper Cretaceous, Lower Eocene, Mid Miocene and Palaeocene ages (Figures 7.12 to 7.15). Our prediction of source rocks in

Upper Cretaceous and Tertiary rocks agree with the works of Rolle, 1985 and Laier, 2012.

As for the timing of thermal maturation, the 2D dimensional heat flow models revealed a significant jump in heat flow during Eocene times in Baffin Bay, Davis Strait and Labrador Sea respectively. Hence, thermal maturation of the source rocks is likely to have been after Eocene. Gregersen and Skaarup (2007); Gregersen et al., (2013) showed that source rock intervals along West Greenland margin possibly came into the oil window after mid-Miocene time.

Furthermore, reservoir rocks are found at both shallow and deeper stratigraphic positions. The hydrocarbon migration or/and charge are not full understood. Was hydrocarbon migrating from deeper source rocks or shallow stratigraphic levels? It is imperative to understand the migration system for the hydrocarbon charge. A starting point is to imagine that faults produced during the rift phase acted as pathways for fluid from the source rock into shallow reservoir rocks. This situation will be suitable for upward fluid migration as suggested and modelled in Figures 7.17 to 7.20. However, if the deeper reservoir are charged from shallow stratigraphic intervals, it implies that hydrodynamic mechanisms could be responsible for migration of hydrocarbons from shallow sources. A reservoir rock was interpreted beneath the basalt. Since basalt is crystalline and characterised by low permeability, the basalt could act as a seal to this reservoir (Figure 2..17). Hydrocarbon traps for include stratrigraphic pinch-outs, four-way and three-way dip closures (Figures 7.12 to 7.16).

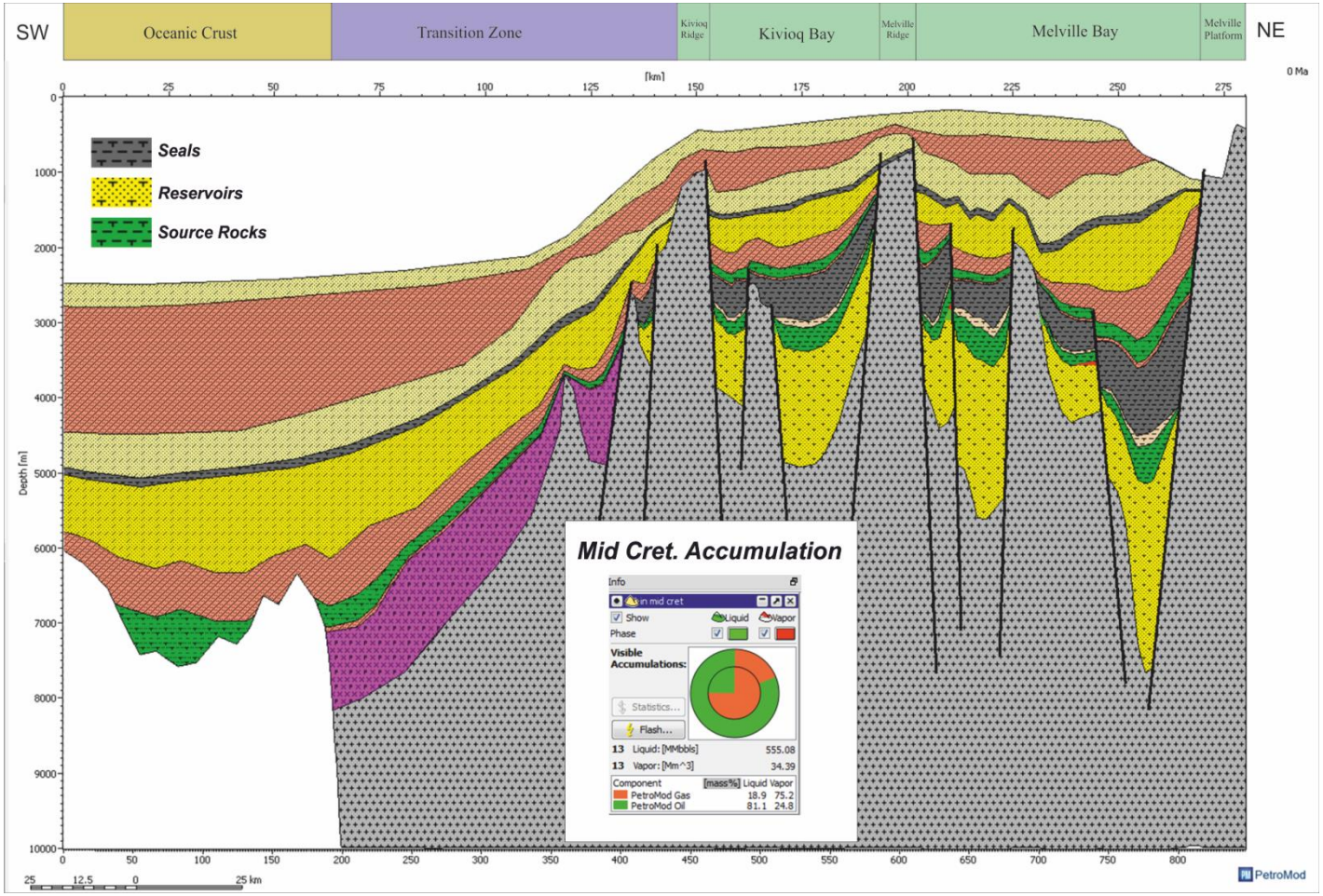

Figure 7.12: Modelled hydrocarbon accumulation in Mid Cretaceous reservoir of Baffin Bay province

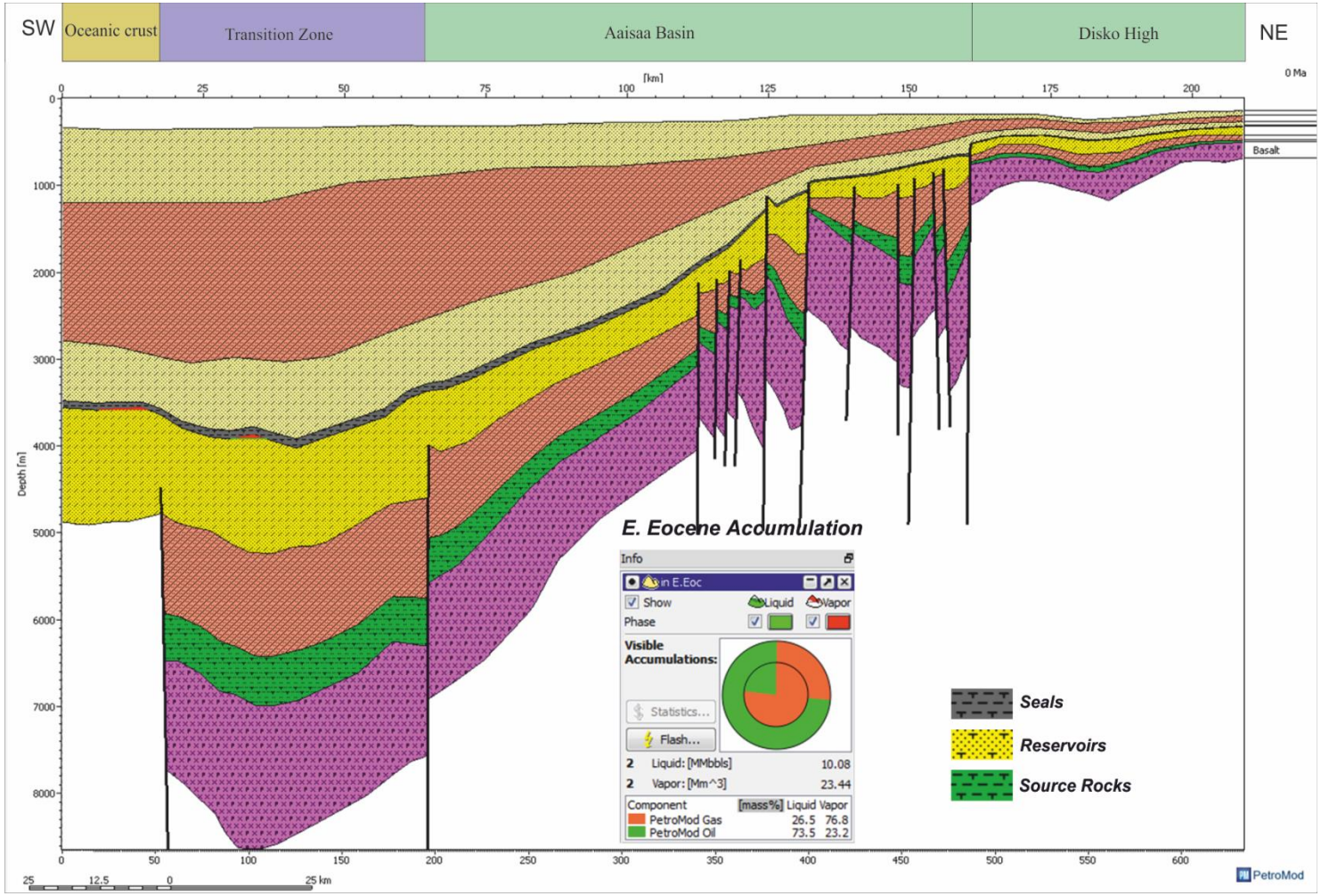

Figure 7.13: Modelled hydrocarbon accumulation in Early Eocene reservoir Cretaceous reservoir of Disko West province

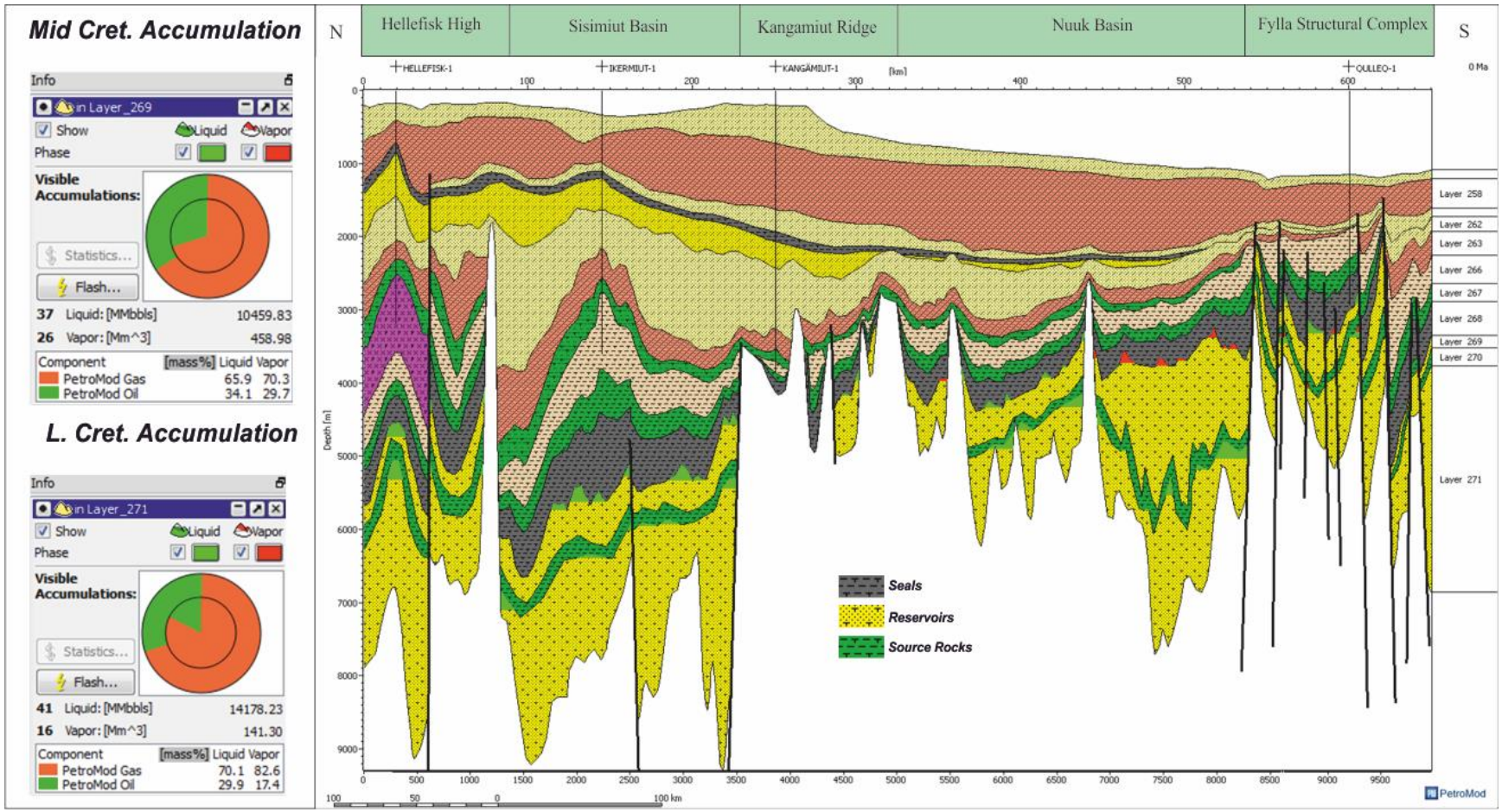

Figure 7.14: Modelled hydrocarbon accumulation in Lower and Middle Cretaceous reservoirs of Nuuk West province

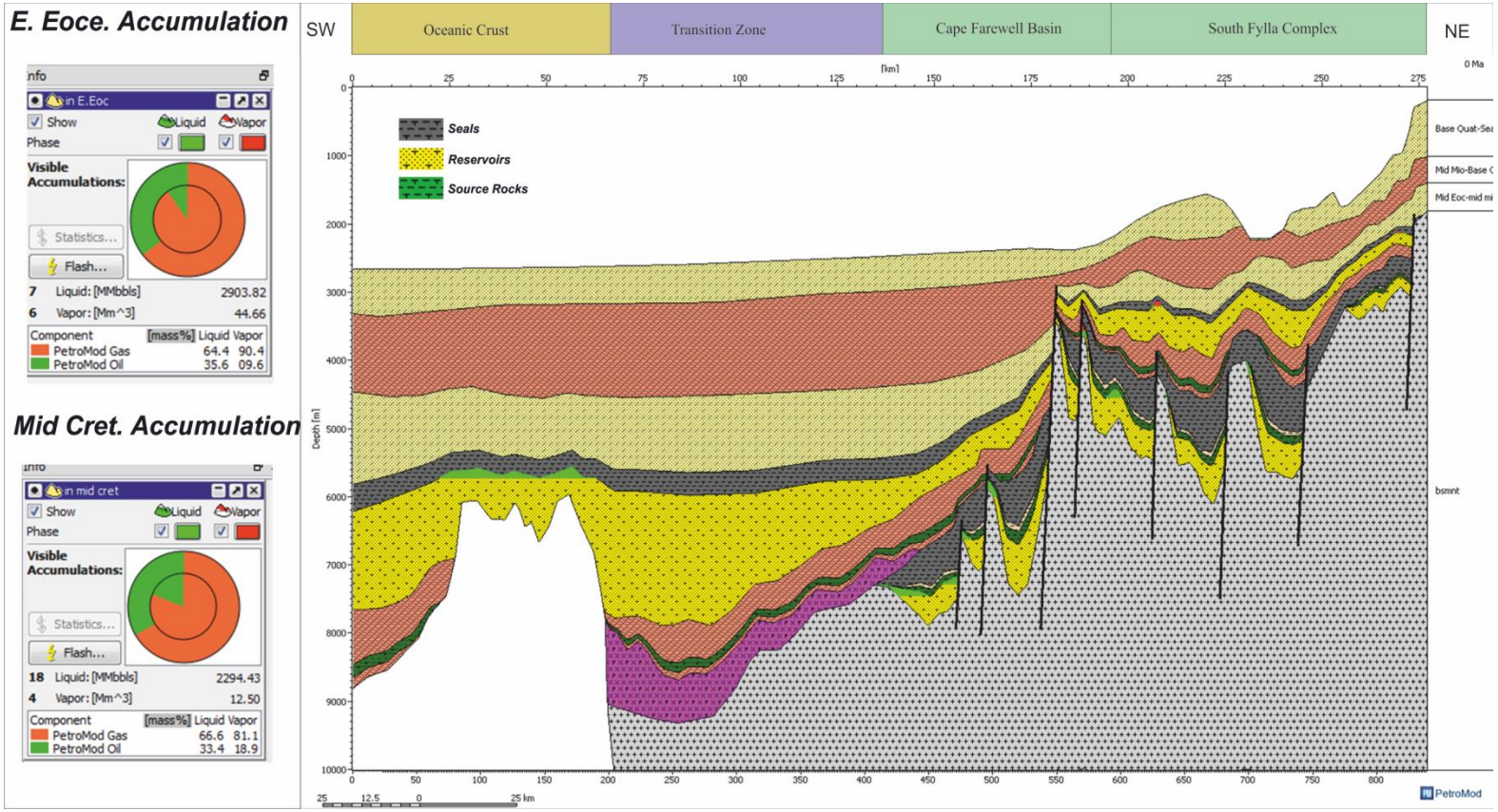

Figure 7.15: Modelled hydrocarbon accumulation in mid Cretaceous and Early Eocene reservoirs of Cape Farewell province

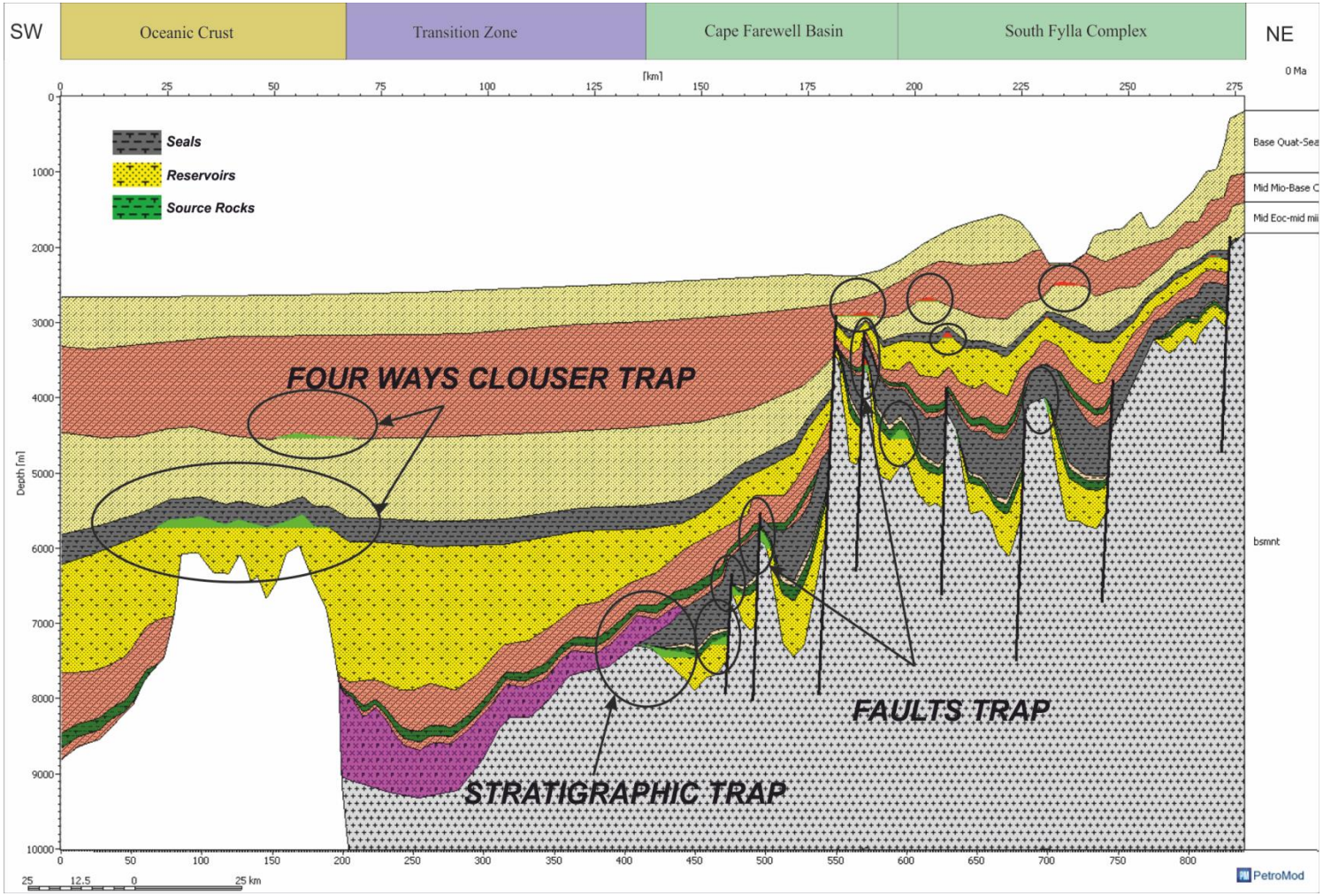

Figure 7.16: Hydrocarbon accumulation and trap types modelled along the margin.

7.6.2 Implication of Lithospheric stretching for Hydrocarbon potential of the West Greenland basins

Lithospheric stretching is an important process of continental break-up (Royden and Keen 1980; Kusznir and Karner 2007). In Chapter 6, we have shown that Depth-dependent stretching (DSS) model is applicable to the breakup of West Greenland. The whole lithosphere on West Greenland has undergone more extension than the upper Crust. The natural consequences of depth-dependent stretching is that as the heat flow field propagates upwards from depth, the mantle and lower crust are thinned more than the upper crust (*cf.* Roberts et al., 2013). The asymmetrical thinning/stretching observed in Baffin Bay, Labrador Sea and Davis Strait implies the margins of the West Greenland will be characterized by narrow sub-basins and short transition zones between the continental and oceanic crust (*cf.* Roberts et al., 2013). On the other hand, margins where symmetrical thinning is experienced were formed through Mc Kenzie's 1D pure shear. At such margins, lithospheric stretching is time-dependent, creating broad basins characterized by wide transition between the crusts. Hence, broader basins have more accommodation space for sediments and higher potential for hydrocarbon accumulation than their narrow counterparts.

This study shows that there is lateral heat flow variation along West Greenland margin. Heat flow influences subsidence, chemical reactions and controls

related fluid transport (Royden and Keen 1980; Kusznir and Karner 2007). Temparature distribution and its evolution through time is the result of heat transfer from the mantle and heat derived from radiogenic elements within the lithosphere itself (Kusznir et al., 2005) Variation of heat flow along the West margin is correlated with values of the predicted Beta factor. We hypothesise that there is direct proportionality between the beta values, heat flow and hydrocarbon accumulation along the margin. For example, assymmetric stretching predicted in the three localities is reflected also as asymmetric heat flow trend. Heat flow maxima are estimated in area of oceanic crust where high Beta factors were applied, and minima in areas of continental crusts that are characterised by very low beta values. The applicability of depth-dependent stretching along the margins implies that heat flow is can not be justified using pure shear model of Mc Kenzie 1978.

This is further corroborated by thermal-maturity against depth of predicted hydrocarbon types. For the study area, no overmature hydrocarbon was predicted. The maturity of the hydrocarbon decreases with depth, immature hydrocarbon were predicted at shallow depths, and mature and dry gases were modelled at deeper depth. The dry gases are surmised as thermogenic gases.

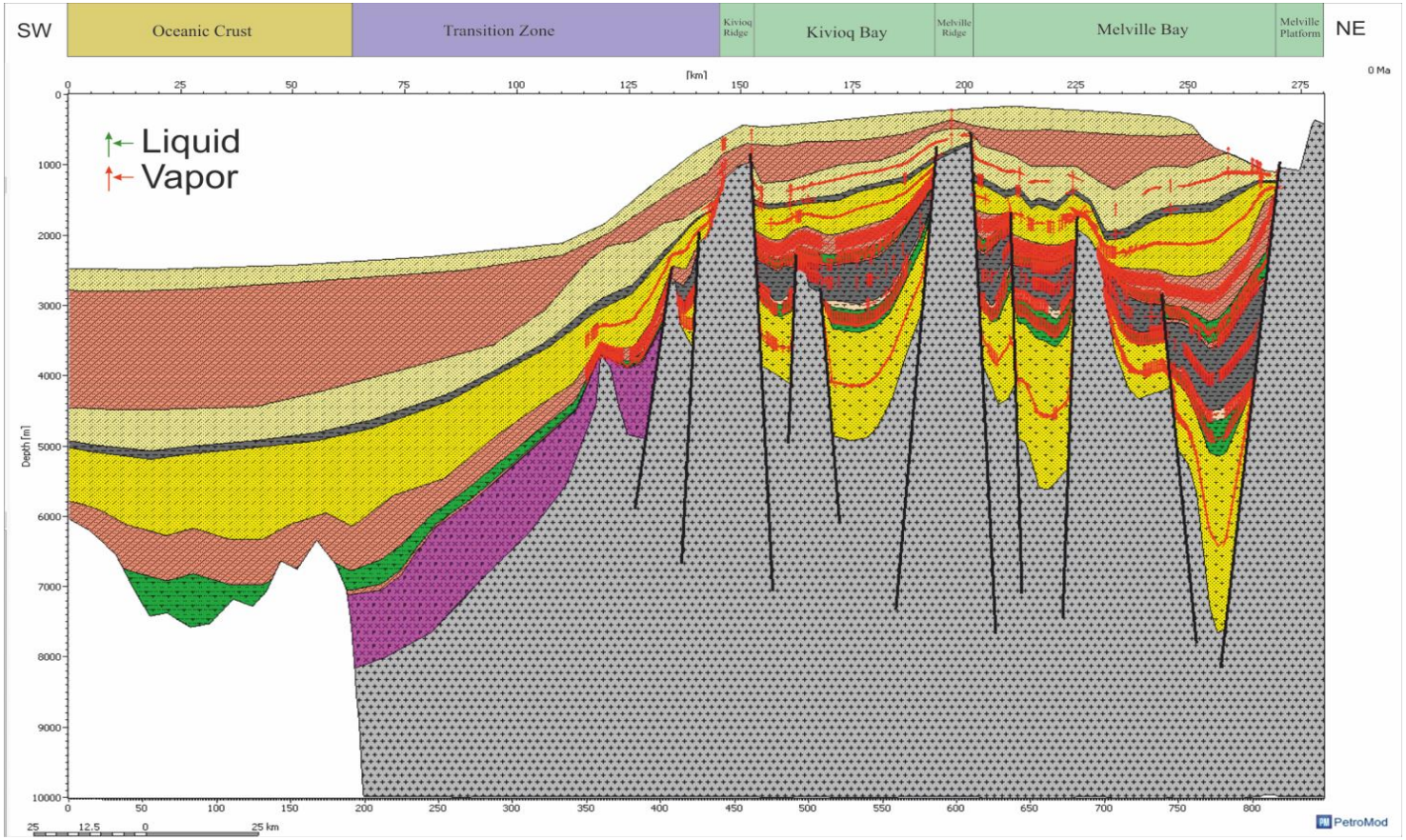

Figure 7.17: Modelled hydrocarbon migration pathway of Baffin Bay province

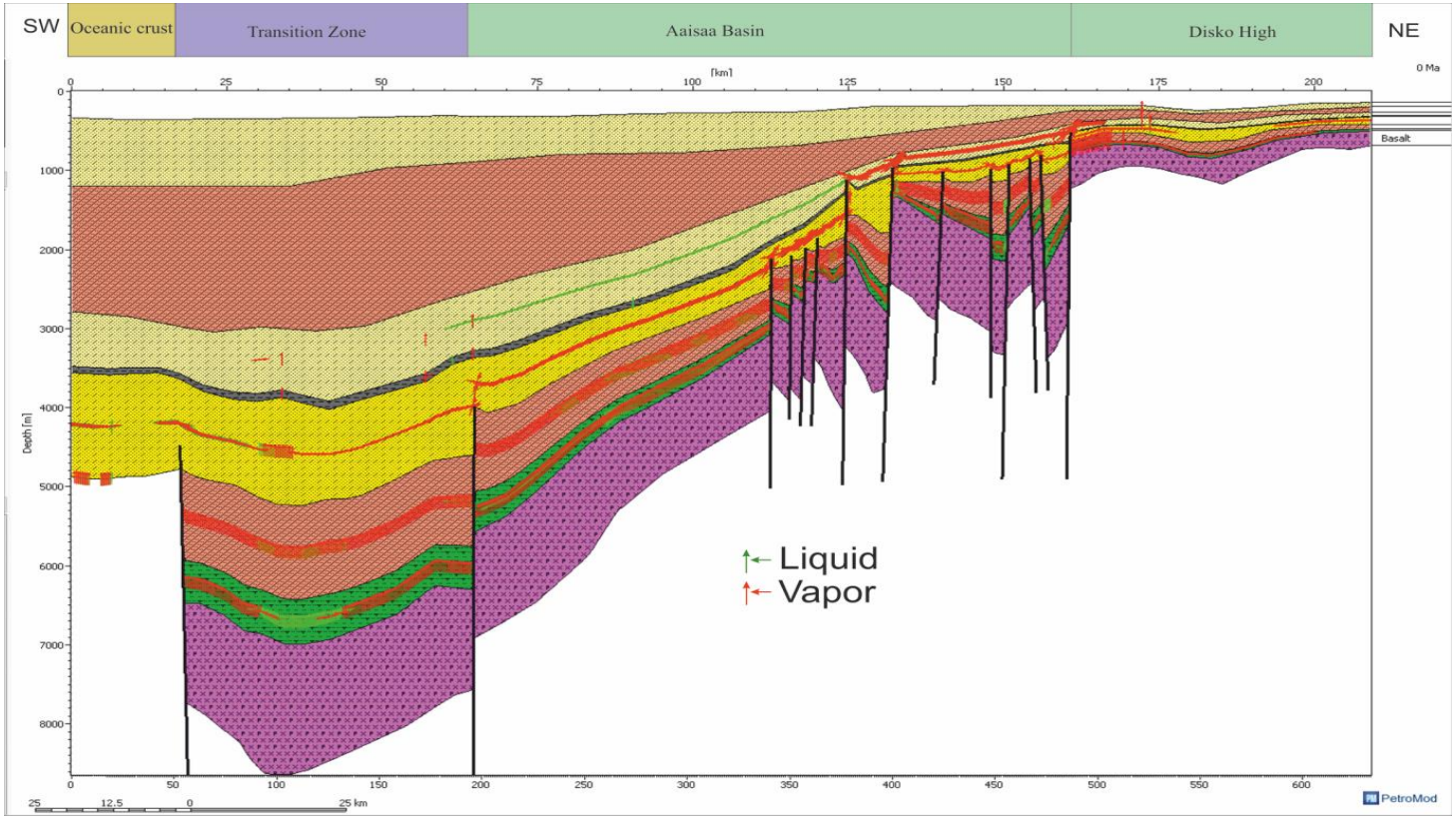

Figure 7.18: Modelled hydrocarbon migration pathway of Disko West province

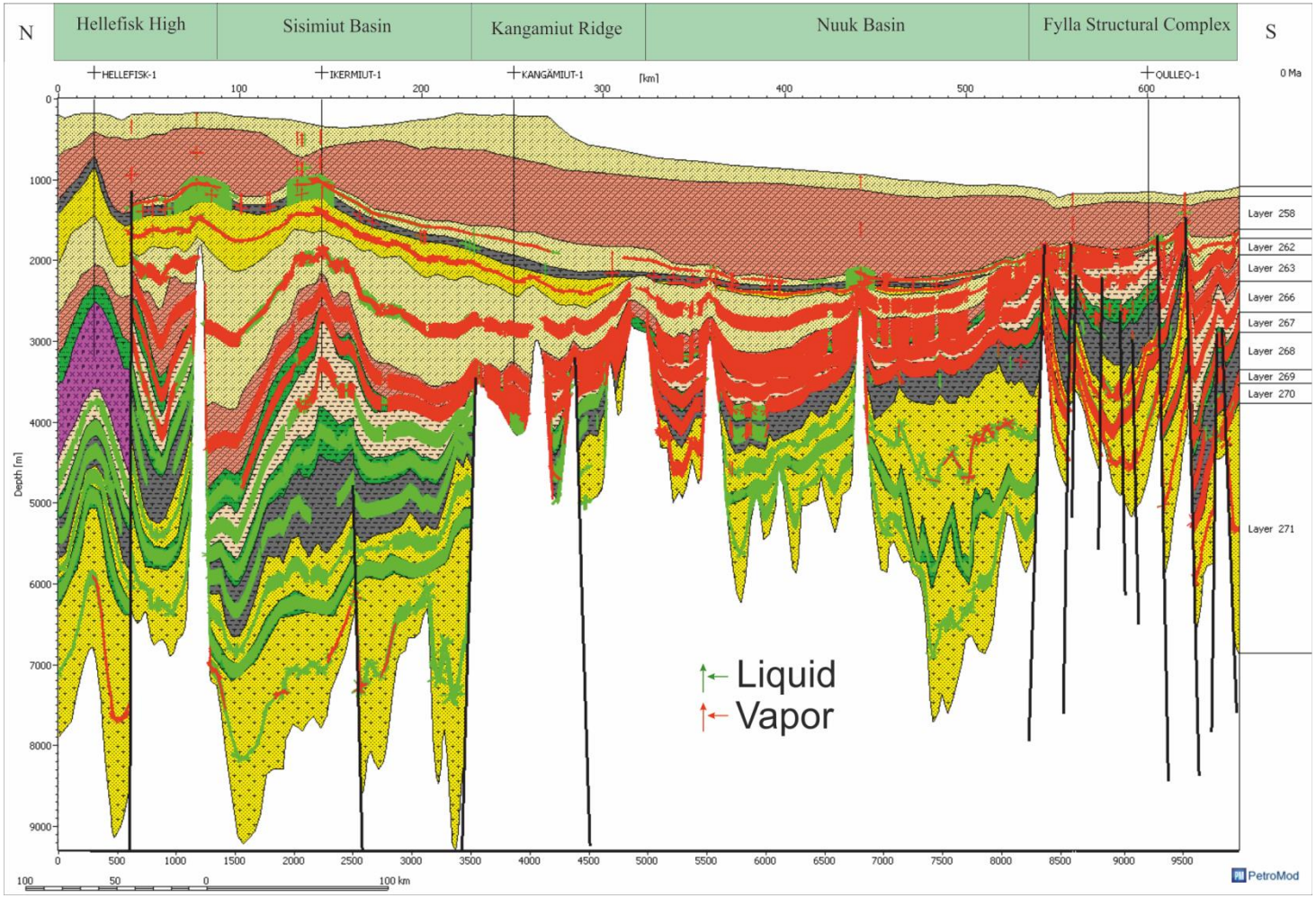

Figure 7.19: Modelled hydrocarbon migration pathway of Nuuk West province

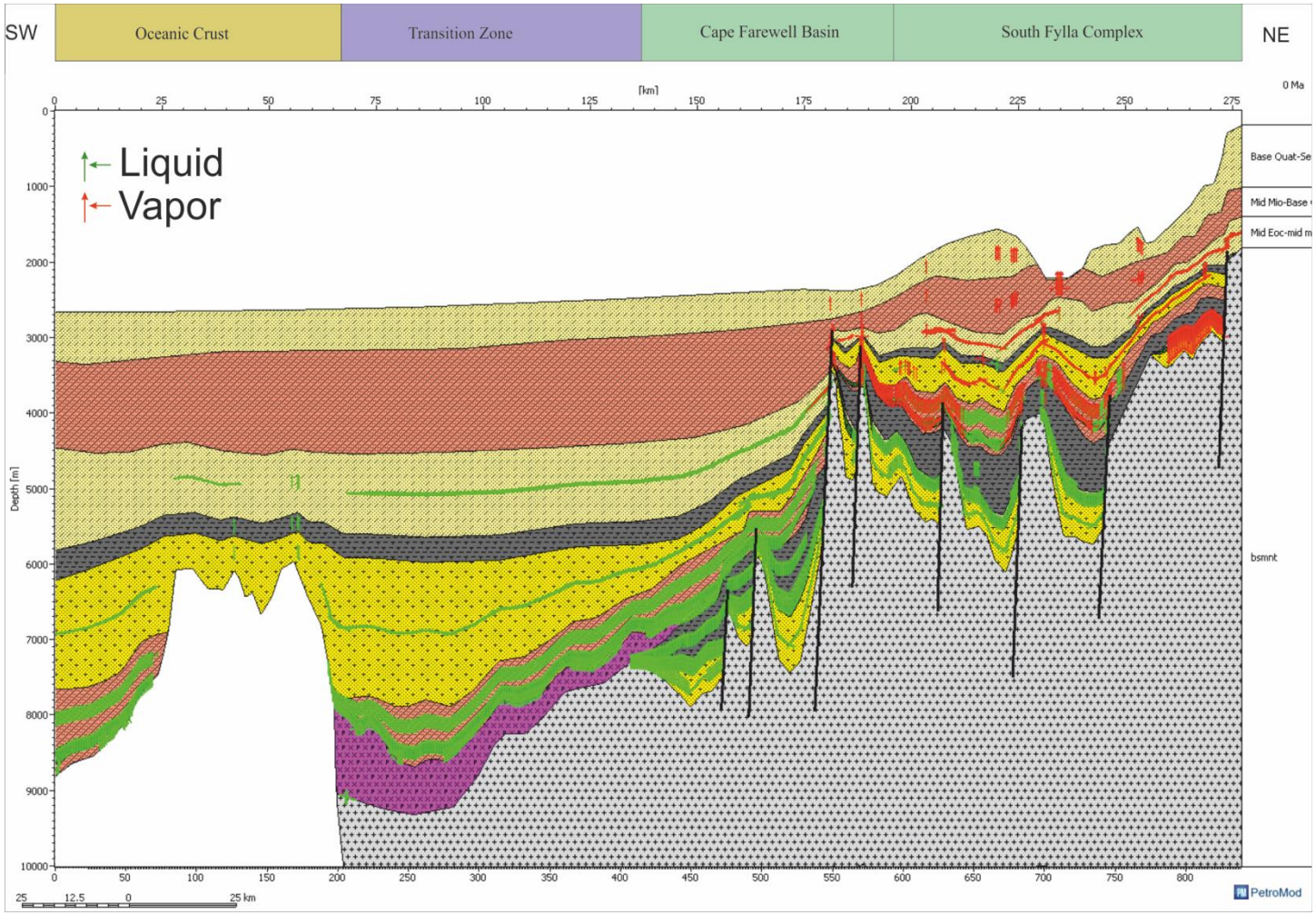

Figure 7.20: Modelled hydrocarbon migration pathway of Cape Farewell province

7.7 Conclusions

The conclusions from this Chapter include:

- The West Greenland has a significant potential for hydrocarbon generation. It's tectonic evolution resulted in concomitant deposition of two distinct syn-rift and post rift packages.
- The lithosphere in West Greenland records more extension than the upper crust. Importantly, heat flow along the margin is associated with stretching factors, high beta factors were correlated with heat flow maxima.
- Petroleum systems of the west Greenland are composed of thick syn-rift reservoir rocks, source rocks, extrusive and seal rocks.
- The greatest heat flows were estimated in Eocene times, ~46 mW/m^2, 55 mW/m^2 and 49 mW/m^2 for Baffin Bay, Davis Strait and Labrador Sea respectively. The highest heat flow was recorded in the ocean-continent transition zones.
- Mature source rock intervals (mid-Cretaceous and Lower Palaeocene). Mid Cretaceous source rocks have % TOC of 6. Campanian and Early Palaeocene source rocks have average % TOC values of 3 respectively. These rocks reached the oil window in post-Eocene times
- Reservoir rocks are buried at both shallow and deeper levels. Hydrocarbons are restricted to Cretaceous deposits. Hydrocarbon types include oil, wet and dry gas. Younger stratigraphic units in the

predicted model are devoid of hydrocarbons. Hence, the migration and trapping of hydrocarbons are restricted to deeper strata in the studied area of West Greenland

Chapter 8

Discussion and Conclusions

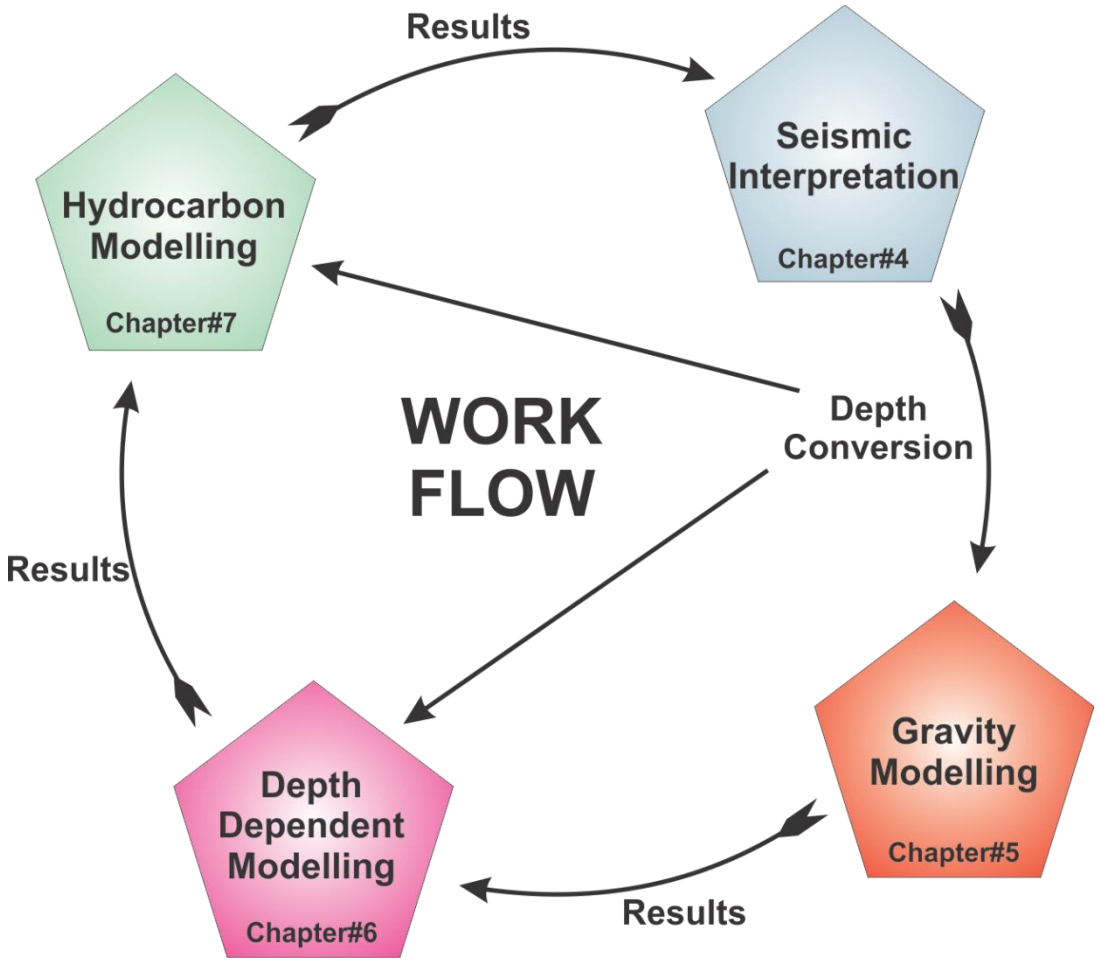

Figure 8.1: Summary of the workflow and major findings from this thesis.

8.1 Discussion

8.1.1 Integration of techniques

This section integrate the results obtained from the different techniques and data chapters. The importance, shortcoming, and overall contribution of each of the methods to a new tectonic model for West Greenland margin and global understanding of lithospheric stretching are highlighted. A summary of the entire study is provided Figure 8.1.

The starting models were dependent on the initial interpretation of several 2-D seismic lines which are regional lines through Baffin Bay to Labrador Sea. Seismic stratigraphic units defined from the lines are consistent with previous stratigraphic classification of the margin (*cf*. Schenk, 2011). In general, the transition from rift to drift is marked by the breakup unconformity, BU (*cf*. Franke, 2013). The BU in this study is the mid-Miocene horizon. Angular unconformities with top lap truncations on seismic profiles were interpreted as the rift onset unconformity (ROU) in line with the definition of Falvey, 1974. In the study area, the ROU is the top Cretaceous Horizon. The position of the ocean-continent transition (OCT) is marked by presence of seaward dipping reflections (SDRs).

Despite the interpretation of faults in the time domain, the results are realistic and are robust when compared in depth-converted seismic profiles. Faults interpreted in time domain have similar geometries but

different shapes to those interpreted in depth-domain (Tvedt et al., 2013). The interpretation of the Ungava Fault along the margin provides evidence for the Eurekan orogeny. Compressional and inversion structures accompanied by strike-slip faulting and local transtensional faults and flexures are evidence for the Eurekan orogeny (Gregersen et al., 2013). The orogeny developed as a result of northward and possible counter-clockwise rotation of Greenland relative to the North American plate (Gregersen et al., 2013). The initial crustal structure from seismic provided adequate hint on the sedimentary and tectonic composition of West Greenland. However, pitfalls in the seismic interpretation are related to velocity models and age constraints. The lack of adequate well control in Baffin Bay and Labrador means the parameters and units were extrapolated over these two regions.

No single method on its own can provide adequate or independent information on the tectonic evolution of a margin (Roberts et al., 2013). Wide-angle refraction data or deep-seismic reflection can offer deep imaging and velocity control; however, they are not readily accessible. The gravity and magnetic field combined with simple stratigraphic information provide constraints on present-day crustal structure (see also Teng et al., 2012; Kilaru et al., 2013; Døssing et al., 2011, 2013). The gravity modeling was undertaken to understand the deeper structure of the igneous bodies observed in the seismic reflection data and their relationship with the

overall crustal structures of the margin. The Moho discontinuity in the study area is marked by a significant step in both interval velocities and densities of rocks. In addition, the ocean-continent transition (OCT) recorded notable gravity and magnetic anomalies. This is consistent with interpretation of positive gravity anomalies at the transition to oceanic crust at the West rim of the Kivioq ridge (Whittaker et al., 1997). Hence, there is a positive correlation between mantle-crust boundary from gravity and magnetic methods.

8.1.2 Estimates of extension

The determination of Moho depth, crustal thickness and thinning factor is important at rifted continental margins for understanding the structure and location of the ocean–continent transition (Chappell and Kusznir, 2008). The major conclusion from Chapter six is that the whole lithosphere has extended more than the upper crust along the margin. The amount of extension observed on upper-crustal faults is known to be less than the extension of the whole crust or whole lithosphere (c*f*. Davis and Kusznir, 2004; Kusznir and Karner, 2007). High values of whole lithosphere stretching factors were recorded from the oceanic crust to areas classified as thinned-continental crust from both seismic and gravity methods. There is an inverse relationship between the β for whole lithosphere and distance to continental crust. Expectedly, high β for upper crust faulting were recorded on the continental margins along West Greenland. Depth-

dependent stretching of the lithosphere is an inexorable result of the process of break-up on continental margins (Royden and Keen 1980; Kusznir and Karner 2007). Continental margins where depth-dependent stretching are characterized by highly extended lithosphere compared to their non-depth dependent counterparts. The natural consequences of depth-dependent stretching along West Greenland is that as the flow field propagates upwards from depth, the mantle and lower crust are thinned more than the upper crust (*cf.* Roberts et al., 2013). It should however be remembered that at a lithospheric scale the margin (and its conjugate) should balance. Such an analysis requires further study.

8.1.3 Application to explanation of frontier areas

Depth-dependent stretching is also essential to studies of tectonics along margins and in the context of oil exploration. For example, the main radiogenic contribution to top-basement heat flow comes from upper-crustal basement rather than the lower crust. If the lower crust and mantle are preferentially thinned by comparison with the upper crust then upper-crustal radiogenic heat productivity may still be preserved, providing higher heat-flow estimates than would be made from the application of a depth-uniform thinning model (Kusznir et al., 2005). This piece of information is essential to understanding hydrocarbon prospectivity on West Greenland margins. Our study shows that there is a direct

relationship between heat flow, thermal maturation of source rocks, hydrocarbon types and beta factors along West Greenland margin.

As for hydrocarbon modeling parameters, all the wells were located in Davis Strait. Hence, interpolation of parameters across the margin was representative for Davis Strait and relatively applicable to Baffin Bay and Labrador Sea. It is not a coincident that hydrocarbon potential was modeled in deeper and syn- rift packages where faults were interpreted on seismic. Post-rift and younger sediments are devoid of hydrocarbon and were modelled immature source rocks.

8.1.4 Interaction of volcanic margin evolution

Our model offer Supporting evidence for the occurrence of passive continental margin comprised of both volcanic and magma-poor lithospheric extension. Since most passive margins develop in response to lithospheric extension driven by far-field stresses, passive margins can be classified into two end-members depending on the volume of extension-related magmatism (Franke 2013). Volcanic margins are characterized by extensive extrusive magmatism manifested as Seaward Dipping Reflections (SDRs) on seismic data (Franke, 2013; Torsvik et al., 2001). Baffin Bay and Labrador Sea are volcanic margins characterized by SDRs at their ocean-continent transition. This is agreement with the classification of Funck et al (2007), Gerlings et al (2009) and Keen et al

(2012). These authors showed that Labrador Sea is exemplified by the presence of excess magmatism, SDRs, volcanic plateau and thick igneous crust. However, Skaarup et al (2000) proposed that a non-volcanic margin occupies the Labrador Sea area. Similar volcanic margins characterized by SDRs include the British Isles (Watts and Fairhead, 1997), Offshore Norway (Eldholm et al., 1989), East Greenland and West India (Roberts and Bally, 2012). On the other hand, magma-rifted margins are rich in wide domains of extended crust but with limited magmatism that are sometimes delayed to post-breakup (Franke, 2013). This description is characteristic of sub-basin in Davis Strait. The margin is defined by a wide area of highly attenuated crust where the upper crust is deformed by planar faults. Unlike other magma-poor passive margins, the detachment over which the fault soles was not observed. Between these extremes lies the South China Sea which is an intermediate between the two end members (Franke, 2013). Therefore, the West Greenland to the north and south are volcanic margins while centrally it is magma-poor margin. As a whole, we considered the West Greenland has an intermediary passive margin.

Furthermore, in our model the mantle plume is suspected at the transfer zone where the Ungava transform fault is located and we further propose that the mantle was inactive during rifting possibly causing cessation of the latter. The role of the mantle plume in the evolution of volcanic- passive

margins has been a subject of controversy. Rifting can evolve in conjunction with a plume head as a) where the plume head triggers the rift evolution by a circular uplift in which the earliest and widest rift is expected close to the plume head and the width of the rift decreases away from the plume and b) where the rift starts farther from the plume with a consistently decreasing width of the rift toward the plume (Franke, 2013; Nestola et al., 2013). Like Iberia–Newfoundland, the Equatorial Atlantic Ocean, and East Antarctica–Australia, our models fit more into the second Franke's scenario. We have shown that extension along the West Greenland was less dependent on the mantle plume and that continental extension and break-up is not always associated with large amounts of volcanism. In addition, we have demonstrated that the evolution of passive margins is also dependent on and ultimately on the mode of rift propagation and its associated barriers (*cf.* Franke, 2013).

8.2 Conclusions

The major conclusions and findings from this thesis are:

- Rifting in West Greenland margins occurred during different geological times. Rifting was intiatited in the southern part of the Labrador Sea and propagated northwards through the Davis Strait to the Baffin Bay.

- Two episodes of rifting are interpreted in this study: Early Cretaceous and Palaeocene to Mid-Miocene. As a consequence, sedimentary packages on the West Greenland margin are divided into pre-rift, syn-rift, and post-rift packages reflecting the different phases of basin development. These sedimentary packages were differentiated based on thickness variations, their internal geometry, and their relationship to active rift-related faults.

- Cretaceous syn-rift packages are intercalated with volcanic sills. The Palaeocene basalt is observed in the Disko West, South Baffin Bay and the North Cape Farewell provinces. Extrusive rock are associated with the continental breakup stage of NE Canada and West Greenland margin.

- The architecture of faults in the Davis Strait High provided hints on the relationship between faults of Labrador Sea and Baffin Bay. Strike-slip faults in the Davis Strait presumably acted as transfer zones during sea floor spreading. The cessation of strike-slip movement is characterized by extension and subsequent rifting in the southern part of Baffin Bay. In addition, observed magnetic lineaments are interpreted as regional fault systems showing complex architectures. These basement lineaments trends towards the Labrador Sea. Conversely, NW-SE magnetic lineaments are

presumably parallel to an extinct spreading axis between Canada and Greenland.

- Seafloor spreading started in the Cape Farewell, propagated North West and into the Baffin Bay region where the underlying continental crust was markedly extended over a probable serpentinised mantle. The mantle-crust boundary is characterised by a jump in interval velocities and densities of rocks. The transition from continental to oceanic crust is marked by SDRs on seismic and remarkable contrast in gravity and magnetic anomalies. As for lithospheric extension, our analyses show that the stretching factor (β_C) from the upper crust faulting is less than the stretching factor (β_L) from the whole lithosphere along West Greenland margin.

- The West Greenland has potential for hydrocarbon generation. Heat flow along the margin is depth-dependent. The greatest heat flows were recorded in Eocene times. Mature source rocks are defined in Campanian to lower Palaeocene rift-depressions where heat flow maxima are noted. These rocks presumably reached the oil window in post-Miocene times.

References

ABDELMALAK, M. M., GEOFFROY, L., ANGELIER, J., BONIN, B., CALLOT, J. P., GÉLARD, J. P. & AUBOURG, C. 2012. Stress fields acting during lithosphere breakup above a melting mantle: A case example in West Greenland. Tectonophysics, 581, 132-143.

AJAY, K., CHAUBEY, A., KRISHNA, K., RAO, D. G. & SAR, D. 2010. Seaward dipping reflections along the SW continental margin of India: Evidence for volcanic passive margin. Journal of earth system science, 119, 803-813.

ALVES, T. M., MOITA, C., CUNHA, T., ULLNAESS, M., MYKLEBUST, R., MONTEIRO, J. H. & MANUPPELLA, G. 2009. Diachronous evolution of Late Jurassic–Cretaceous continental rifting in the northeast Atlantic (west Iberian margin). Tectonics, 28, TC4003.

AL-HAJERI, M. M., AL SAEED, M., DERKS, J., FUCHS, T., HANTSCHEL, T., KAUERAUF, A. & PETERS, K. 2009. Basin and petroleum system modeling. Oilfield Review, 21, 14-29.

ASLANIAN, D., MOULIN, M., OLIVET, J.-L., UNTERNEHR, P., MATIAS, L., BACHE, F., RABINEAU, M., NOUZÉ, H., KLINGELHEOFER, F., CONTRUCCI, I. & LABAILS, C. 2009. Brazilian and African passive margins of the Central Segment of the South Atlantic Ocean: Kinematic constraints. Tectonophysics, 468, 98-112.

BADLEY, M. E. 1985. Practical seismic interpretation, Medium: X; Size: Pages: 265 p.

BALKWILL, H. R., MCMILLAN, N. J., MACLEAN, B., WILLIAMS, G. L. & SRIVASTAVA, S. P. 1990. Geology of the continental margin of Eastern Canada / edited by M.J. Keen and G.L. Williams, Ottawa :, Canadian Government Publishing Center.

BALLY, A. W. & OLDOW 1983. Plate tectonics, structural styles, and the evolution of sedimentary basins. Houston Geological Society, short course manual.

BASSI, G. 1995. Relative importance of strain rate and rheology for the mode of continental extension. Geophysical Journal International 122, 195–210

BERTRAM, G. T. & MILTON, N. J. 1988. Reconstructing basin evolution from sedimentary thickness; the importance of palaeobathymetric control, with reference to the North Sea. Basin Research, 1, 247-257.

BOJESEN-KOEFOED, J. A., BIDSTRUP, T., CHRISTIANSEN, F. G., DALHOFF, F., GREGERSEN, U., NYTOFT, H. P., NØHR-HANSEN, H., PEDERSEN, A. K. & SØNDERHOLM, M. 2007. PETROLEUM SEEPAGES AT ASUK, DISKO, WEST GREENLAND: IMPLICATIONS FOR REGIONAL PETROLEUM EXPLORATION. Journal of Petroleum Geology, 30, 219-236.

BOJESEN-KOEFOED, J. A., CHRISTIANSEN, F. G., NYTOFT, H. P. & PEDERSEN, A. K. 1999. Oil seepage onshore West Greenland:

evidence of multiple source rocks and oil mixing. Geological Society, London, Petroleum Geology Conference series, 5, 305-314.

BOJESEN-KOEFOED, J. A., NYTOFT, H. P. & CHRISTIANSEN, F. G. 2004. Age of oils in West Greenland: Was there a Mesozoic seaway between Greenland and Canada. Geological Survey of Denmark and Greenland Bulletin, 4, 49-52.

BONOW, J. M., JAPSEN, P., LIDMAR-BERGSTRÖM, K., CHALMERS, J. A. & PEDERSEN, A. K. 2006. Cenozoic uplift of Nuussuaq and Disko, West Greenland—elevated erosion surfaces as uplift markers of a passive margin. Geomorphology, 80, 325-337.

BROCHER, T. M. 2005. Empirical Relations between Elastic Wavespeeds and Density in the Earth's Crust. Bulletin of the Seismological Society of America, 95, 2081-2092.

BRUN, J. P. 1999. Narrow rifts versus wide rifts: inferences for the mechanics of rifting from laboratory experiments. Series A 357, 695–712. Philosophical Transactions of the Royal Society of London., 357, 695-712.

BURDEN, E. T. & LANGILLE, A. B. 1990. Stratigraphy and sedimentology of Cretaceous and Paleocene strata in half-grabens on the southeast coast of Baffin Island, Northwest Territories. Bulletin of Canadian Petroleum Geology, 38, 185-196.

BURKE, K. & DEWEY, J. F. 1973. Plume generated triple junctions: key indicators in applying plate tectonics to old rock. Journal of Geology, 81, 406-433.

BURRUS, M., CHANABE, C., ALIBERT, G. & BIDNEY, D. 1991. Regeneration of fertile plants from protoplasts of sunflower (Helianthus annuus L.). Plant cell reports, 10, 161-166.

CHALMERS, J. A. 1991. New evidence on the structure of the Labrador Sea/Greenland continental margin. Journal of the Geological Society, 148, 899-908.

CHALMERS, J. A. 1997. The continental margin off southern Greenland: along-strike transition from an amagmatic to a volcanic margin. Journal of the Geological Society, 154, 571-576.

CHALMERS, J. A. 2000. Offshore evidence for Neogene uplift in central West Greenland. Global and Planetary Change, 24, 311-318.

CHALMERS, J. A. 2012. Labrador Sea, Davis Strait, and Baffin Bay. In: ROBERTS, D. G. & BALLY, A. W. (eds.) Regional Geology and Tectonics: Phanerozoic Passive Margins, Cratonic Basins and Global Tectonic Maps. Boston: Elsevier.

CHALMERS, J. A., LARSEN, L. M. & PEDERSEN, A. K. 1995. Widespread Palaeocene volcanism around the northern North Atlantic and Labrador Sea: evidence for a large, hot, early plume head. Journal of the Geological Society, 152, 965-969.

CHALMERS, J. A. & LAURSEN, K. H. 1995. Labrador Sea: the extent of continental and oceanic crust and the timing of the onset of seafloor spreading. Marine and Petroleum Geology, 12, 205-206.

CHALMERS, J. A. & PULVERTAFT, T. C. R. 2001. Development of the continental margins of the Labrador Sea: a review. Geological Society, London, Special Publications, 187, 77-105.

CHALMERS, J. A., PULVERTAFT, T. C. R., CHRISTIANSEN, F. G., LARSEN, H. C., LAURSEN, K. H. & OTTESEN, T. G. 1993. The southern West Greenland continental margin: rifting history, basin development, and petroleum potential. Geological Society, London, Petroleum Geology Conference series, 4, 915-931.

CHALMERS, J. A., PULVERTAFT, T. C. R., MARCUSSEN, C. & PEDERSEN, A. K. 1999. New insight into the structure of the Nuussuaq Basin, central West Greenland. Marine and Petroleum Geology, 16, 197-211, 213-224.

CHAPPELL, A. R. & KUSZNIR, N. J. 2008. Three-dimensional gravity inversion for Moho depth at rifted continental margins incorporating a lithosphere thermal gravity anomaly correction. Geophysical Journal International, 174, 1-13.

CHIAN, D. & LOUDEN, K. E. 1994. The continent-ocean crustal transition across the southwest Greenland margin. J. Geophys. Res., 99, 9117-9135.

CHRISTENSEN, N. I. & MOONEY, W. D. 1995. Seismic velocity structure and composition of the continental crust: A global view. Journal of Geophysical Research: Solid Earth, 100, 9761-9788.

CHRISTIANSEN, F. G. 2011. Chapter 42 Greenland petroleum exploration: history, breakthroughs in understanding and future challenges. Geological Society, London, Memoirs, 35, 647-661.

CHRISTIANSEN, F. G., BOJESEN-KOEFOED, J., DAM, G., NYTOFT, H. P., LARSEN, L. M., PEDERSEN, A. K. & PULVERTAFT, T. C. R. 1996. The Marraat oil discovery on Nuussuaq, West Greenland: evidence for a latest Cretaceous-earliest Tertiary oil prone source rock in the Labrador Sea-Melville Bay region. Bulletin of Canadian Petroleum Geology, 44, 39-54.

CHRISTIANSEN, F. G., BOJESEN-KOEFOED, J. A., CHALMERS, J. A., DALHOFF, F., MATHIESEN, A., SØNDERHOLM, M., DAM, G., GREGERSEN, U., MARCUSSEN, C. & NØHR-HANSEN, H. 2001. Petroleum geological activities in West Greenland in 2000. Geology of Greenland Survey Bulletin, 189, 24-33.

CLIFT, P. D. & TURNER, J. 1995. Dynamic support by the Icelandic plume and vertical tectonics of the northeast Atlantic continental margins. Journal of Geophysical Research: Solid Earth, 100, 24473-24486.

CLOETINGH, S., BUROV, E. & FRANCOIS, T. 2013. Thermo-mechanical controls on intra-plate deformation and the role of plume-folding

interactions in continental topography. Gondwana Research, 24, 3, 815-837.

CONDIE, K. C. 1982. Plate Tectonics and Continental Drifts, Pergamon Press, Oxford.

CORTI, G. 2003. Analogue modelling of continental extension: a review focused on the relations between the patterns of deformation and the presence of magma. Earth-Science Reviews, 63, 169-247.

CORTI, G. 2009. Continental rift evolution: From rift initiation to incipient break-up in the Main Ethiopian Rift, East Africa. Earth-Science Reviews, 96, 1-53.

DALHOFF, F., CHALMERS, J. A., GREGERSEN, U., NØHR-HANSEN, H., AUDUN RASMUSSEN, J. & SHELDON, E. 2003. Mapping and facies analysis of Paleocene–Mid-Eocene seismic sequences, offshore southern West Greenland. Marine and Petroleum Geology, 20, 935-986.

DALHOFF, F., LARSEN, L. M., INESON, J. R., STOUGE, S., BOJESEN-KOEFOED, J. A., LASSEN, S., KUIJPERS, A., RASMUSSEN, J. A. & NØHR-HANSEN, H. 2006. Continental crust in the Davis Strait: new evidence from seabed sampling.

DAM, G., LARSEN, M. & SØNDERHOLM, M. 1998. Sedimentary response to mantle plumes: implications from Paleocene onshore successions, West and East Greenland. Geology, 26, 207-210.

DAM, G., NØHR-HANSEN, H., PEDERSEN, G. K. & SØNDERHOLM, M. 2000. Sedimentary and structural evidence of a new early Campanian rift

phase in the Nuussuaq Basin, West Greenland. Cretaceous Research, 21, 127-154.

DAM, G., PEDERSEN, G. K., SØNDERHOLM, M., MIDTGAARD, H. H., LARSEN, L. M., NØHR-HANSEN, H. & PEDERSEN, A. K. 2009. Lithostratigraphy of the Cretaceous–Paleocene Nuussuaq Group, Nuussuaq Basin, West Greenland. Geological Survey of Denmark and Greenland Bulletin, 19, 1-171.

DAM, G. & SØNDERHOLM, M. 1994. Lowstand slope channels of the Itilli succession (Maastrichtian-Lower Paleocene), Nuussuaq, West Greenland. Sedimentary Geology, 94, 49-71.

DAM, G. & SØNDERHOLM, M. 1998. SEDIMENTOLOGICAL EVOLUTION OF A FAULT-CONTROLLED EARLY PALEOCENE INCISED-VALLEY SYSTEM, NUUSSUAQ BASIN, WEST GREENLAND. Relative Role of Eustasy, Climate, and Tectonism in Continental Rocks. SEPM (Society for Sedimentary Geology).

DAVIES, G. 1998. A channelled plume under Africa. Nature, 395, 743-744.

DAVIS, M. & KUSZNIR, N. J. 2004. Depth-dependent lithospheric stretching at rifted continental margins. In: Karner, G. D. (ed.) Proceedings of NSF Rifted Margins Theoretical Institute. Columbia University Press, 92–136.

DAVISON, I. 2005. Central Atlantic margin basins of North West Africa: Geology and hydrocarbon potential (Morocco to Guinea). Journal of African Earth Sciences, 43, 254-274.

DILLON, W. P., PAULL, C. K., BUFFLER, J. P. & FAIL 1979. Structure and development of the southeast Georgia embayment and northern Blake plateau: Preliminary analysis. Geological and Geophysical Investigations of Continental Margins, ed. J. S. Watkins, L. Montadert, and P. W. Dickerson. AAPG Memoir.

DIX 1955. Seismic velocities from surface measurements. Geophysics, 20, 68–86.

DORÉ, A. G., LUNDIN, E. R., JENSEN, L. N., BIRKELAND, Ø., ELIASSEN, P. E. & FICHLER, C. 1999. Principal tectonic events in the evolution of the northwest European Atlantic margin. Geological Society, London, Petroleum Geology Conference series, 5, 41-61.

DØSSING, A. 2011. Fylla Bank: structure and evolution of a normal-to-shear rifted margin in the northern Labrador Sea. Geophysical Journal International, 187, 655-676.

DØSSING, A., HOPPER, J. R., OLESEN, A. V., RASMUSSEN, T. M. & HALPENNY, J. 2013. New aero-gravity results from the Arctic: Linking the latest Cretaceous-early Cenozoic plate kinematics of the North Atlantic and Arctic Ocean. Geochemistry, Geophysics, Geosystems, 14, 4044-4065.

DRISCOLL, N. W. & KARNER, G. D. 1998. Lower crustal extension across the Northern Carnarvon basin, Australia: Evidence for an eastward dipping detachment. Journal of Geophysical Research: Solid Earth, 103, 4975-4991.

DURRHEIM, R. J. & COOPER, G. R. J. 1998. EULDEP: a program for the Euler deconvolution of magnetic and gravity data. Computers & geosciences, 24(6), 545-550.

ELDHOLM, O., THIEDE, J. & TAYLOR, E. 1989. The Norwegian continental margin: Tectonic, volcanic, and paleoenvironmental framework. Proceedings of the ocean drilling program, scientific results,5-26.

FALEIDE, J. I., TSIKALAS, F., BREIVIK, A. J., MJELDE, R., RITZMANN, O., ENGEN, O., WILSON, J. & ELDHOLM, O. 2008. Structure and evolution of the continental margin off Norway and the Barents Sea. Episodes, 31, 82.

FALVEY, D. A. 1974. The development of continental margins in plate tectonic theory. APEA J, 14, 95-106.

FLETCHER, R., KUSZNIR, N., ROBERTS, A. & HUNSDALE, R. 2013. The formation of a failed continental breakup basin: The Cenozoic development of the Faroe-Shetland Basin. Basin Research, 25, 532-553

FRANKE, D. 2013. Rifting, lithosphere breakup and volcanism: Comparison of magma-poor and volcanic rifted margins. Marine and Petroleum Geology, 43, 63-87.

FUNCK, T., GOHL, K., DAMM, V. & HEYDE, I. 2012. Tectonic evolution of southern Baffin Bay and Davis Strait: Results from a seismic refraction transect between Canada and Greenland. J. Geophys. Res., 117, B04107.

FUNCK, T., JACKSON, H. R., LOUDEN, K. E. & KLINGELHÖFER, F. 2007. Seismic study of the transform-rifted margin in Davis Strait between Baffin Island (Canada) and Greenland: What happens when a plume meets a transform. Journal of Geophysical Research: Solid Earth, 112, n/a-n/a.

GAC, S. & GEOFFROY, L. 2009. 3D Thermo-mechanical modelling of a stretched continental lithosphere containing localized low-viscosity anomalies (the soft-point theory of plate break-up). Tectonophysics, 468, 158-168.

GARDNER, G., GARDNER, L. & GREGORY, A. 1974. FORMATION VELOCITY AND DENSITY—THE DIAGNOSTIC BASICS FOR STRATIGRAPHIC TRAPS. Geophysics, 39, 770-780.

GEUS website. Greenland Hydrocarbon Exploration Information Service. [online] avilable at: http://www.geus.dk/ghexis/index.htm , Accessed, July 1, 2014.

GILL, R. C. O., HOLM, P. M. & NIELSEN, T. F. D. 1995. Was a short-lived Baffin Bay plume active prior to initiation of the present Icelandic plume? Clues from the high-Mg picrites of West Greenland. Lithos, 34, 27-39.

GODFREY, N., BEAUDOIN, B. & KLEMPERER, S. 1997. Ophiolitic basement to the Great Valley forearc basin, California, from seismic and gravity data: Implications for crustal growth at the North American continental margin. Geological Society of America Bulletin, 109, 1536-1562.

GRADSTEIN, F. M. & SRIVASTAVA, S. P. 1980. Aspects of Cenozoic stratigraphy and paleoceanography of the labrador sea and baffin bay. Palaeogeography, Palaeoclimatology, Palaeoecology, 30, 261-295.

GREEN, P. F., JAPSEN, P., CHALMERS, J. A. & BONOW, J. M. 2011. Thermochronology, erosion surfaces and missing section in West Greenland. Journal of the Geological Society, 168, 817-830.

GREGERSEN, U. & BIDSTRUP, T. 2008. Structures and hydrocarbon prospectivity in the northern Davis Strait area, offshore West Greenland. Petroleum Geoscience, 14, 151-166.

GREGERSEN, U., HOPPER, J. R. & KNUTZ, P. C. 2013. Basin seismic stratigraphy and aspects of prospectivity in the NE Baffin Bay, Northwest Greenland. Marine and Petroleum Geology, 46, 1-18.

GREGERSEN, U. & SKAARUP, N. 2007. A mid-Cretaceous prograding sedimentary complex in the Sisimiut Basin, offshore West Greenland—stratigraphy and hydrocarbon potential. Marine and Petroleum Geology, 24, 15-28.

GRIFFITHS, R. W. & CAMPBELL, I. H. 1990. Stirring and structure in mantle starting plumes. Earth and Planetary Science Letters, 99, 66-78.

HALL, B. D. & WHITE, N. 1994. Origin of anomalous Tertiary subsidence adjacent to North Atlantic continental margins. Marine and Petroleum Geology, 11, 702-714.

HARRIS, P. T. & WHITEWAY, T. 2011. Global distribution of large submarine canyons: Geomorphic differences between active and passive continental margins. Marine Geology, 285, 69-86.

HARRISON, J. C., BRENT, T. A. & OAKEY, G. N. 2011. Chapter 40 Baffin Fan and its inverted rift system of Arctic eastern Canada: stratigraphy, tectonics and petroleum resource potential. Geological Society, London, Memoirs, 35, 595-626.

HARRISON, J. C., MAYR, U., MCNEIL, D. H., SWEET, A. R., EBERLE, J. J., MCINTYRE, D. J., HARINGTON, C. R., CHALMERS, J. A., DAM, G. & NOHR-HANSEN, H. 1999. Correlation of Cenozoic sequences of the Canadian Arctic region and Greenland; implications for the tectonic history of northern North America. Bulletin of Canadian Petroleum Geology, 47, 223-254.

HEAD, M.J., NORRIS, G. & MUDIE, P.J. 1989. Palynology and dinocyst stratigraphy of the Miocene in ODP Leg 105, Hole 645E, Baffin Bay. In Srivastava, S.P., Arthur, M.A., Clement, B., et al., Proc. ODP, Sci. Results, 105: College Station, TX (Ocean Drilling Program), 467–514.sr.105.137.1989

HOFFMAN, P. F. 1988. United Plates of America, The Birth of a Craton: Early Proterozoic Assembly and Growth of Laurentia. Annual Review of Earth and Planetary Sciences, 16, 543-603.

HOLLIGER, K. & KLEMPERER, S. L. 1989. A comparison of the Moho interpreted from gravity data and from deep seismic reflection data in the northern North Sea. Geophysical Journal International, 97, 247-258.

HOLM, P. M., GILL, R. C. O., PEDERSEN, A. K., LARSEN, J. G., HALD, N., NIELSEN, T. F. D. & THIRLWALL, M. F. 1993. THE TERTIARY PICRITES OF WEST GREENLAND - CONTRIBUTIONS FROM ICELANDIC AND OTHER SOURCES. Earth and Planetary Science Letters, 115, 227-244.

HSU, H.-J., WEN, S. & CHEN, C.-H. 2011. 3D topography of the Moho discontinuity in the Taiwan area as extracted from travel time inversion of PmP phases. Journal of Asian Earth Sciences, 41, 335-343.

HUISMANS, R. & BEAUMONT, C. 2011. Depth-dependent extension, two-stage breakup and cratonic underplating at rifted margins. Nature, 473, 74-78.

HUISMANS, R. S. & BEAUMONT, C. 2007. Roles of lithospheric strain softening and heterogeneity in determining the geometry of rifts and continental margins. Geological Society, London, Special Publications, 282, 111-138.

ILIFFE, J. E., LERCHE, I. & DEBUYL, M. 1991. Basin analysis and hydrocarbon generation of the South Mozambique graben using extensional models of heat flow. Marine and Petroleum Geology, 8, 152-162.

ISSLER, D. R. & BEAUMONT, C. 1987. Thermal and subsidence history of the Labrador and West Greenland continental margins.

JAPSEN, P., BONOW, J. M., GREEN, P. F., CHALMERS, J. A. & LIDMAR-BERGSTRÖM, K. 2006. Elevated, passive continental margins: Long-term highs or Neogene uplifts? New evidence from West Greenland. Earth and Planetary Science Letters, 248, 330-339.

JAPSEN, P. & CHALMERS, J. A. 2000. Neogene uplift and tectonics around the North Atlantic: overview. Global and Planetary Change, 24, 165-173.

JAPSEN, P., CHALMERS, J. A., GREEN, P. F. & BONOW, J. M. 2012. Elevated, passive continental margins: Not rift shoulders, but expressions of episodic, post-rift burial and exhumation. Global and Planetary Change, 90–91, 73-86.

JAPSEN, P., GREEN, P. F., BONOW, J. M., RASMUSSEN, E. S., CHALMERS, J. A. & KJENNERUD, T. 2010. Episodic uplift and exhumation along North Atlantic passive margins: implications for hydrocarbon prospectivity. Geological Society, London, Petroleum Geology Conference series, 7, 979-1004.

JAPSEN, P., GREEN, P. F. & CHALMERS, J. A. 2005. Separation of Palaeogene and Neogene uplift on Nuussuaq, West Greenland. Journal of the Geological Society, 162, 299-314.

JOHANNESEN, J., HAY, S. J., MILNE, J. K., JEBSEN, C., GUNNESDAL, S. C. & VAYSSAIRE, A. 2002. 3D oil migration modelling of the Jurassic

petroleum system of the Statfjord area, Norwegian North Sea. Petroleum Geoscience, 8, 37-50.

KEEN, C. E., DICKIE, K. & DEHLER, S. A. 2012. The volcanic margins of the northern Labrador Sea: Insights to the rifting process. Tectonics, 31, n/a-n/a.

KILARU, S., GOUD, B. K. & RAO, V. K. 2013. Crustal structure of the western Indian shield: Model based on regional gravity and magnetic data. Geoscience Frontiers.

KNUTSEN, S. M., ARENDT, N. P., RUNGE, M. K., STILLING, J. & BRANDT, M. P. 2012. Structural provinces offshore West Greenland and key geological variations influencing play assessment. First Break 30, 43-55.

KORSTGÄRD, J.A. & NIELSEN, O.B. 1989. Provenance of dropstones in Baffin Bay and Labrador Sea, Leg 105. In Srivastava, S.P., Arthur, M.A., Clement, B., et al., Proc. ODP, Sci. Results, 105: College Station, TX (Ocean Drilling Program), 65–69. sr.105.200.1989.

KUBALA, M., BASTOW, M., THOMPSON, S., SCOTCHMAN, I. & ØYGARD, K. 2003. Geothermal regime, petroleum generation and migration. In: The Millennium Atlas: Petroleum Geology of the Central and Northern North Sea (D. Evans, A. Armour, P. Bathurst, J. Gammage, J. Swallow, C. Graham and H. Stewart, eds), Geological Society London, 289–315.

KUSZNIR, N. J., HUNSDALE, R. & ROBERTS, A. M. 2004. Timing of depth-dependent lithosphere stretching on the S. Lofoten rifted margin offshore

mid-Norway: pre-breakup or post-breakup? Basin Research, 16, 279-296.

KUSZNIR, N. J., HUNSDALE, R., ROBERTS, A. M. & TEAM, I. 2005. Timing and magnitude of depth-dependent lithosphere stretching on the southern Lofoten and northern Vøring continental margins offshore mid-Norway: implications for subsidence and hydrocarbon maturation at volcanic rifted margins. Geological Society, London, Petroleum Geology Conference series, 6, 767-783.

KUSZNIR, N. J. & KARNER, G. D. 2007. Continental lithospheric thinning and breakup in response to upwelling divergent mantle flow: application to the Woodlark, Newfoundland and Iberia margins. Geological Society, London, Special Publications, 282, 389-419.

KUSZNIR, N. J., MARSDEN, G. & EGAN, S. S. 1991. A flexural-cantilever simple-shear/pure-shear model of continental lithosphere extension: applications to the Jeanne d'Arc Basin, Grand Banks and Viking Graben, North Sea. Geological Society, London, Special Publications, 56, 41-60.

KUSZNIR, N. J., ROBERTS, A. M. & MORLEY, C. K. 1995. Forward and reverse modelling of rift basin formation. Geological Society, London, Special Publications, 80, 33-56.

KUSZNIR, N. & PARK, R.G. 1987. The extensional strength of continental lithosphere: its dependence on geothermal gradient, and crustal composition and thickness. In: Coward, M.P., Dewey, J.F., Hancock, P.L.

(Eds.), Continental Extensional tectonics. Geological Society of London, Special Publication, vol. 28, pp. 35–52

KUSZNIR, N. J. & ZIEGLER P. A. 1992. The mechanics of continental extension and sedimentary basin formation: A simple-shear/pure-shear flexural cantilever model: Tectonophysics, v. 215, p. 117-131.

LAIER, T. & NYTOFT, H. P. 2012. New evidence for possible generation of oil off south-western Greenland. Geological Survey of Denmark and Greenland Bulletin, 26, 65-68.

LARSEN & SAUNDERS 1998. Tectonism and volcanism at the southeastGreenlandriftedmargin: A record of plume impact and later continental rupture. Proc. ODP, 152, 503–533.

LARSEN, J. G. & PULVERTAFT, T. C. R. 2000. The structure of the Cretaceous-Palaeogene sedimentary-volcanic area of Svartenhuk Halvø, central West Greenland, Geological Survey of Denmark and Greenland, Ministry of Environment and Energy.

LARSEN, L. M. 2006. Mesozoic to Palaeogene dyke swarms in West Greenland and their significance for the formation of the Labrador Sea and the Davis Strait, GEUS, Geological Survey of Denmark and Greenland.

LARSEN, L. M., HEAMAN, L. M., CREASER, R. A., DUNCAN, R. A., FREI, R. & HUTCHISON, M. 2009. Tectonomagmatic events during stretching and basin formation in the Labrador Sea and the Davis Strait: evidence

from age and composition of Mesozoic to Palaeogene dyke swarms in West Greenland. Journal of the Geological Society, 166, 999-1012.

LARSEN, T. B., YUEN, D. A. & STOREY, M. 1999. Ultrafast mantle plumes and implications for flood basalt volcanism in the Northern Atlantic Region. Tectonophysics, 311, 31-43.

LAURENT, G. 2005. Volcanic passive margins. Comptes Rendus Geoscience, 337, 1395-1408.

LE PICHON, X. & SIBUET, J. C. 1981. Passive margins: a model of formation. Journal of Geophysical Research: Solid Earth (1978–2012), 86, 3708-3720.

LISTER, G. S., ETHERIDGE, M. A. & SYMONDS, P. A. 1986. Detachment faulting and the evolution of passive continental margins. Geology, 14, 246-250.

LOUDEN, K., 2002, Tectonic Evolution of the East Coast of Canada: CSEG Recorder, p. pp. 37-48.

LUDWIG, J. W., NAFE, J. E. & DRAKE, C. L. 1970. Seismic refraction, in The Sea, New York, Wiley.

LUNDIN, E. R. & DORÉ, A. G. 2011. Hyperextension, serpentinization, and weakening: A new paradigm for rifted margin compressional deformation. Geology, 39, 347-350.

MACLEAN, B., WILLIAMS, G. & ZHANG, S. 2011. Cretaceous strata on the Baffin Island Shelf. AAPG Search and Discovery Article, 90130, 2011.

MCGREGOR, E. D., NIELSEN, S. B., STEPHENSON, R. A., CLAUSEN, O. R., PETERSEN, K. D. & MACDONALD, D. I. M. 2012. Evolution of the west Greenland margin: offshore thermostratigraphic data and modelling. Journal of the Geological Society, 169, 515-530.

MCKENZIE, D. 1978. SOME REMARKS ON DEVELOPMENT OF SEDIMENTARY BASINS. Earth and Planetary Science Letters, 40, 25-32.

MCKENZIE, D. & BICKLE, M. J. 1988. The Volume and Composition of Melt Generated by Extension of the Lithosphere. Journal of Petrology, 29, 625-679.

MERLE, O. 2011. A simple continental rift classification. Tectonophysics, 513, 88-95.

MITCHUM JR, R. M., P. R. VAIL & SANGREE, J. B. 1977. Seismic stratigraphy and global changes of sea level, part 11:Stratigraphic Interpretation of Seismic Reflection Patterns in Depositional Sequences. AAPG Bulletin, Memoir 26, 117-133.

MÜLLER, R. D., SDROLIAS, M., GAINA, C. & ROEST, W. R. 2008. Age, spreading rates, and spreading asymmetry of the world's ocean crust. Geochem. Geophys. Geosyst., 9, Q04006.

MUTTER, J. C. 1985. Seaward dipping reflections and the continent-ocean boundary at passive continental margins. Tectonophysics, 114, 117-131.

NADEAU, P.H., BJØRKUM, P.A. & WALDERHAUG, O. 2005. Petroleum system analysis: Impact of shale diagenesis on reservoir fluid pressure,

hydrocarbon migration and biodegradation risks. In: A.G. Doré & B. Vining (eds.), Petroleum Geology: North-West Europe and Global Perspectives – Proceedings of the 6th Petroleum Geology Conference, Petroleum Geology Conferences Ltd., Published by the Geological Society, London, 1267-1274.

NADIN, P. A. & KUSZNIR, N. J. 1996. Forward and reverse stratigraphic modelling of Cretaceous-Tertiary post-rift subsidence and Paleogene uplift in the Outer Moray Firth Basin, central North Sea. Geological Society, London, Special Publications, 101, 43-62.

NESTOLA, Y., STORTI, F., BEDOGNI, E. & CAVOZZI, C. 2013. Shape evolution and finite deformation pattern in analog experiments of lithosphere necking. Geophysical Research Letters, 40, 2013GL057618.

NIELSEN, T. K., LARSEN, H. C. & HOPPER, J. R. 2002. Contrasting rifted margin styles south of Greenland: implications for mantle plume dynamics. Earth and Planetary Science Letters, 200, 271-286.

NØHR-HANSEN, H. 2003. Dinoflagellate cyst stratigraphy of the Palaeogene strata from the Hellefisk-1, Ikermiut-1, Kangâmiut-1, Nukik-1, Nukik-2 and Qulleq-1 wells, offshore West Greenland. Marine and Petroleum Geology, 20, 987-1016.

NØHR-HANSEN, H. & DAM, G. 1997. Palynology and sedimentology across a new marine Cretaceous-Tertiary boundary section on Nuussuaq, West Greenland. Geology, 25, 851-854.

NØTTVEDT, A., GABRIELSEN, R. H. & Steel, R.J. 1995. Tectonostratigraphy and sedimentary architecture of rift basins with reference to the northern North Sea. Mar. Petrol. Geol., 12, 881–901.

NØTTVEDT, A., BERGE, A. M., DAWERS, N. H., FÆRSETH, R. B., HAGER, K. O., MANGERUD, G. & PUIGDEFABREGAS, C. 2000. Syn-rift evolution and resulting play models in the Snorre-H area, northern North Sea. In: Dynamics of the Norwegian Margin. (Ed. A. Nøttvedt), Geol. Soc. Spec. Publ., 167, 179–218.

NÚÑEZ-BETELU, L.K. 1993. Rock-Eval/TOC pyrolysis data from the Kanguk Formation (Upper Cretaceous), Axel Hieberg and Ellesmere Islands, Canadian Arctic; Geological Survey of Canada Open File Report #2727, 29p

OAKEY, G. N. & CHALMERS, J. A. 2012. A new model for the Paleogene motion of Greenland relative to North America: Plate reconstructions of the Davis Strait and Nares Strait regions between Canada and Greenland. J. Geophys. Res., 117, B10401.

OAKEY, G. N. & STEPHENSON, R. 2008. Crustal structure of the Innuitian region of Arctic Canada and Greenland from gravity modelling: implications for the Palaeogene Eurekan orogen. Geophysical Journal International, 173, 1039-1063.

PARK, R. G. 1988. Geological Structures and Moving Plates, Glasgow.

PARKIN, C. J., LUNNON, Z. C., WHITE, R. S. & CHRISTIE, P. A. F. 2007. Imaging the pulsing Iceland mantle plume through the Eocene. Geology, 35, 93-96.

PATON, D. A., DI PRIMIO, R., KUHLMANN, G., VAN DER SPUY, D., & HORSFIELD, B. 2007. Insights into the petroleum system evolution of the southern Orange Basin, South Africa. South African Journal of Geology, 110, 261-274.

PEDERSEN, A. K. & LARSEN, L. M. 2006. The Ilugissoq graphite andesite volcano, Nuussuaq, central West Greenland. Lithos, 92, 1-19.

PEDERSEN, A. K., LARSEN, L. M., RIISAGER, P. & DUEHOLM, K. S. 2002. Rates of volcanic deposition, facies changes and movements in a dynamic basin: the Nuussuaq Basin, West Greenland, around the C27n-C26r transition. Geological Society, London, Special Publications, 197, 157-181.

PEGRUM, R. M., ØDEGÅRD, T., BONDE, K. & HAMANN, N. E. Exploration in the Fylla area, SW Greenland. Proceedings of AAPG Regional Conference, 2001. 15-18.

PEREIRA, R. & ALVES, T. M. 2011. Margin segmentation prior to continental break-up: A seismic-stratigraphic record of multiphased rifting in the North Atlantic (Southwest Iberia). Tectonophysics, 505, 17-34.

PÉREZ-GUSSINYÉ, M., MORGAN, J. P., RESTON, T. J. & RANERO, C. R. 2006. The rift to drift transition at non-volcanic margins: Insights from numerical modelling. Earth and Planetary Science Letters, 244, 458-473.

PHILIPPON, M., CORTI, G., SANI, F., BONINI, M., BALESTRIERI, M.-L., MOLIN, P., WILLINGSHOFER, E., SOKOUTIS, D. & CLOETINGH, S. 2014. Evolution, distribution, and characteristics of rifting in southern Ethiopia. Tectonics, 33, 2013TC003430.

PIK, R., MARTY, B. & HILTON, D. R. 2006. How many mantle plumes in Africa? The geochemical point of view. Chemical Geology, 226, 100-114.

PROSSER, S. 1993. Rift-related linked depositional systems and their seismic expression. In: Tectonics and seismic sequence stratigraphy (Eds G.D. Williams and A. Dobb), Geol. Soc. Spec. Publ., 71, 35–66.

RANALLI, G. & ADAMS, M. (2013). Rheological contrast at the continental Moho: Effects of composition, temperature, deformation mechanism, and tectonic regime. Tectonophysics, 609, 480-490.

RASMUSSEN, J. A. & SHELDON, E. 2003. Microfossil biostratigraphy of the Palaeogene succession in the Davis Strait, offshore West Greenland. Marine and petroleum geology, 20, 1017-1030.

RAVNÅS, R. & STEEL. R. J. 1998. Architecture of Marine Rift-Basin Successions AAPG Bulletin, V. 82, No. 1. P. 110-146.

REID, A., ALLSOP, J., GRANSER, H., MILLETT, A. & SOMERTON, I. 1990. Magnetic interpretation in three dimensions using Euler deconvolution. Geophysics, 55, 80-91.

REID, I. & JACKSON, H. R. 1997. Crustal structure of northern Baffin Bay: Seismic refraction results and tectonic implications. J. Geophys. Res., 102, 523-542.

REYNISSON, R.F., EBBING, J., LUNDIN, E. & OSMUNDSEN, P. T. 2010. Properties and distribution of lower crustal bodies on the mid-Norwegian margin. In Geological Society, London, Petroleum Geology Conference series (Vol. 7, pp. 843-854).

RESTON, T.J. 2009. The structure, evolution and symmetry of the magma-poor rifted margins of the North and Central Atlantic: A synthesis. Tectonophysics 468, 6–27. doi:10.1016/j.tecto.2008.09.002

RESTON, T & PÉREZ GUSSINYÉ M. 2007. Lithospheric extension from rifting to continental break-up at magma-poor margins: rheology, serpentinization and symmetry. International Journal of Earth Sciences , 96, 6, 1033-1046

ROBERTS, A. M., KUSZNIR, N. J., CORFIELD, R. I., THOMPSON, M. & WOODFINE, R. 2013. Integrated tectonic basin modelling as an aid to understanding deep-water rifted continental margin structure and location. Petroleum Geoscience, 19, 65-88.

ROBERTS, A. M., KUSZNIR, N. J., YIELDING, G. & STYLES, P. 1998. 2D flexural backstripping of extensional basins; the need for a sideways glance. Petroleum Geoscience, 4, 327-338.

ROBERTS, A. M., LUNDIN, E. R. & KUSZNIR, N. J. 1997. Subsidence of the Vøring Basin and the influence of the Atlantic continental margin. Journal of the Geological Society, 154, 551-557.

ROBERTS, A. M., YIELDING, G., KUSZNIR, N. J., WALKER, I. & DORN-LOPEZ, D. 1993. Mesozoic extension in the North Sea: constraints from

flexural backstripping, forward modelling and fault populations. Geological Society, London, Petroleum Geology Conference series, 4, 1123-1136.

ROBERTS, D. G. & BALLY, A. 2012. Regional Geology and Tectonics: Three-Volume Set, Newnes.

ROBINSON & DURRANI 1986. Geophysical Signal Processing. Englewood Cliffs, Prentice-Hall.

ROEST, W. R. & SRIVASTAVA, S. P. 1989. Sea-floor spreading in the Labrador Sea: A new reconstruction. Geology, 17, 1000-1003.

ROLLE, F. 1985. Late Cretaceous – Tertiary sediments offshore central West Greenland: lithostratigraphy, sedimentary evolution, and petroleum potential. Canadian Journal of Earth Sciences, 22, 1001-1019.

ROSENBAUM, G., WEINBERG, R. F. & REGENAUER-LIEB, K. 2008. The geodynamics of lithospheric extension. Tectonophysics, 458, 1-8.

ROWLEY, D. B. & LOTTES, A. L. 1988. Plate-kinematic reconstructions of the North Atlantic and Arctic: Late Jurassic to Present. Tectonophysics, 155, 73-120.

ROYDEN, L. & KEEN, C. E. 1980. Rifting process and thermal evolution of the continental margin of Eastern Canada determined from subsidence curves. Earth and Planetary Science Letters, 51, 343-361.

SCHENK, C. J. 2011. Chapter 41 Geology and petroleum potential of the West Greenland–East Canada Province. Geological Society, London, Memoirs, 35, 627-645.

SCOTCHMAN, I. C., GILCHRIST, G., KUSZNIR, N.J., ROBERTS, A. M. & FLETCHER, R. 2010. The breakup of the South Atlantic Ocean: formation of failed spreading axes and blocks of thinned continental crust in the Santos Basin, Brazil and its consequences for petroleum system development, in: Petroleum Geology: From Mature Basins to New Frontiers—Proceedings of the 7th Petroleum Geology Conference. Geological Society of London, pp. 855–866.

SCLATER, J. G. & CHRISTIE, P. 1980. Continental stretching: An explanation of the Post-Mid-Cretaceous subsidence of the central North Sea Basin. Journal of Geophysical Research: Solid Earth (1978–2012), 85(B7), 3711-3739.

SENGÖR, A. M. C. & BURKE, K. 1978. Relative timing of rifting and volcanism on Earth and its tectonic implications. Geophysical Research Letters, 5, 419-421.

SHERIFF & GELDART 1995. Exploration Seismology. Cambridge University Press, 2nd ed.

SKAARUP, N. 2002. Evidence for continental crust in the offshore Palaeogene volcanic province, central West Greenland. Geology of Greenland Survey Bulletin, 191, 97-102.

SKAARUP, N., CHALMERS, J. A. & WHITE, D. 2000. An AVO study of a possible new hydrocarbon play, offshore central West Greenland. AAPG Bulletin, 84, 174-182.

SKAARUP, N., JACKSON, H. & OAKEY, G. 2006. Margin segmentation of Baffin Bay/Davis Strait, eastern Canada based on seismic reflection and potential field data. Marine and Petroleum Geology, 23, 127-144.

SOARES, D. M., ALVES, T. M. & TERRINHA, P. 2012. The breakup sequence and associated lithospheric breakup surface: Their significance in the context of rifted continental margins (West Iberia and Newfoundland margins, North Atlantic). Earth and Planetary Science Letters, 355–356, 311-326.

SØNDERHOLM, M., NØHR-HANSEN, H., BOJESEN-KOEFOED, J., DALHOFF, F. & RASMUSSEN, J. A. 2003. Regional correlation of Mesozoic-Palaeogene sequences across the Greenland-Canada boundary, GEUS, Geological Survey of Denmark and Greenland.

SØRENSEN, A. B. 2006. Stratigraphy, structure and petroleum potential of the Lady Franklin and Maniitsoq Basins, offshore southern West Greenland. Petroleum Geoscience, 12, 221-234.

SRIVASTAVA, S.P. & ARTHUR, M.A. 1989. Tectonic evolution of the Labrador Sea and Baffin Bay: constraints imposed by regional geophysics and drilling results from Leg 105. In Srivastava, S.P., Arthur, M.A., Clement, B., et al., Proc. ODP, Sci. Results, 105: College Station, TX (Ocean Drilling Program), 989–1009. doi:10.2973/odp.proc.sr.105.163.1989

SRIVASTAVA, S. P. & ROEST, W. R. 1999. Extent of oceanic crust in the Labrador Sea1. Marine and Petroleum Geology, 16, 65-84.

SRIVASTAVA, S. P., VERHOEF, J. & MACNAB, R. 1988. Results from a detailed aeromagnetic survey across the northeast Newfoundland margin, Part II: Early opening of the North Atlantic between the British Isles and Newfoundland. Marine and Petroleum Geology, 5, 324-336, in1-in8, 337.

STEEL, R. J. 1993. Triassic-Jurassic megasequence stratigraphy in the northern North Sea: rift to post-rift evolution, in J. R. Parker, ed., Petroleum geology of northwest Europe: Proceedings of the 4th Conference: London, The Geological Society, p. 299-315.

STOREY, M., DUNCAN, R. A., PEDERSEN, A. K., LARSEN, L. M. & LARSEN, H. C. 1998. 40Ar/39Ar geochronology of the West Greenland Tertiary volcanic province. Earth and Planetary Science Letters, 160, 569-586.

SUCKRO, S. K., GOHL, K., FUNCK, T., HEYDE, I., EHRHARDT, A., SCHRECKENBERGER, B., GERLINGS, J., DAMM, V. & JOKAT, W. 2012. The crustal structure of southern Baffin Bay: implications from a seismic refraction experiment. Geophysical Journal International.

SUCKRO, S. K., GOHL, K., FUNCK, T., HEYDE, I., SCHRECKENBERGER, B., GERLINGS, J. & DAMM, V. 2013. The Davis Strait crust—a transform margin between two oceanic basins. Geophysical Journal International.

TENG, J., ZHANG, Z., ZHANG, X., WANG, C., GAO, R., YANG, B., QIAO, Y. & DENG, Y. 2012. Investigation of the Moho discontinuity beneath the Chinese mainland using deep seismic sounding profiles. Tectonophysics.

TORSVIK, T. H., MOSAR, J. & EIDE, E. A. 2001. Cretaceous-Tertiary geodynamics: a North Atlantic exercise. Geophysical Journal International, 146, 850-866.

TORSVIK, T. H., STEINBERGER, B., GURNIS, M. & GAINA, C. 2010. Plate tectonics and net lithosphere rotation over the past 150My. Earth and Planetary Science Letters, 291, 106-112.

TUCHOLKE, B. E. & FRY, V. A. 1985. Basement structure and sediment distribution in Northwest Atlantic Ocean. AAPG Bulletin, 69, 2077-2097.

TUCHOLKE, B.E., SAWYER, D.S., SIBUET, J.-C., 2007. Breakup of the Newfoundland–Iberia Rift. Geological Society of London, Special Publication 282, 9–46.

TVEDT, A. B. M., ROTEVATN, A., JACKSON, C. A. L., FOSSEN, H. & GAWTHORPE, R. L. 2013. Growth of normal faults in multilayer sequences: A 3D seismic case study from the Egersund Basin, Norwegian North Sea. Journal of Structural Geology, 55, 1-20.

UMPLEBY, D. C. 1979. Geology of the Labrador Shelf, Geological Survey of Canada.

WALSH, J., WATTERSON, J. & YIELDING, G. 1991. The importance of small-scale faulting in regional extension. Nature, 351, 391-393.

WATTS, A. B. & FAIRHEAD, J. D. 1997. Gravity anomalies and magmatism along the western continental margin of the British Isles. Journal of the Geological Society, 154(3), 523-529.

WATTS, A. B., ZHONG, S. J. & HUNTER, J. 2013. The Behavior of the Lithosphere on Seismic to Geologic Timescales. Annual Review of Earth and Planetary Sciences, 41, 443-468.

WELTE, D. H. & YALCIN, M. N. 1988. Basin modelling—a new comprehensive method in petroleum geology. Organic Geochemistry, 13, 141-151.

WERNICKE, B. 1985. Uniform-Sense Normal Simple Shear of the Continental Lithosphere. Canadian Journal of Earth Sciences, 22, 108-125.

WERNICKE, B. & BURCHFIEL, B. C. 1982. MODES OF EXTENSIONAL TECTONICS. Journal of Structural Geology, 4, 105-115.

WESTAWAY, R. & KUSZNIR, N. 1993. Fault and bed 'rotation' during continental extension: block rotation or vertical shear? Journal of Structural Geology, 15, 753-770.

WHITE, N. J., JACKSON, J. A. & MCKENZIE, D. P. 1986. The relationship between the geometry of normal faults and that of the sedimentary layers in their hanging walls. Journal of Structural Geology, 8, 897-909.

WHITE, R. & MCKENZIE, D. 1989. Magmatism at Rift Zones: The Generation of Volcanic Continental Margins and Flood Basalts. J. Geophys. Res., 94, 7685-7729.

WHITTAKER, R. C., HAMANN, N. E. & PULVERTAFT, T. C. R. 1997. A new frontier province offshore northwest Greenland: Structure, basin development, and petroleum potential of the Melville Bay area. Aapg Bulletin-American Association of Petroleum Geologists, 81, 978-998.

ZIEGLER, P. A. 1992. Plate tectonics, plate moving mechanisms and rifting. Tectonophysics, 215, 9-34.

ZIEGLER, P. A. & CLOETINGH, S. 2004. Dynamic processes controlling evolution of rifted basins. Earth-Science Reviews, 64, 1-50.

Appendices

Appendix I : Description of seismic lines

Table A I-1: Seismic dataset

	GEUS DATA			TGS DATA
Surveys	**Loaded, Petrel**	**Loaded in KS, Nav data added**	**Reloaded, Petrel**	**New data loaded, Petrel**
1		BGR1977-R01	BGR1977-R01	
2		BMP2000	BMP2000	
3	FN1998			
4	FYLLA1994			
5	FYLLA2001			
6	GGU1990			
7	GGU1991			
8		GGU1992	GGU1992	
9		GGU1995	GGU1995	
10	HGS1990			
11	KAN1992W			
12		NFE1997	NFE1997	
13		NSI1998	NSI1998	
14		NU9804	NU9804	
15	PH2000G			
16	PH9901			
17	TGS-GR2000			
18	TGS-GREEN1999			
19				GRC01, GRC01 A, GRC01B, GRC02
20				SW2000
21				BB07RE11
22				BB08RE11
23				DW02, DW05
24				Reprocessed (TGS) DN12RE-T-117-PRCMIG DN12RE-T-202-PRCMIG DN12RE-T-214-PRCMIG

Appendix II: Velocity models and depth conversion

A II-1: Velocity models - Stacking velocities along west Greenland margin and 2D seismic data coverage

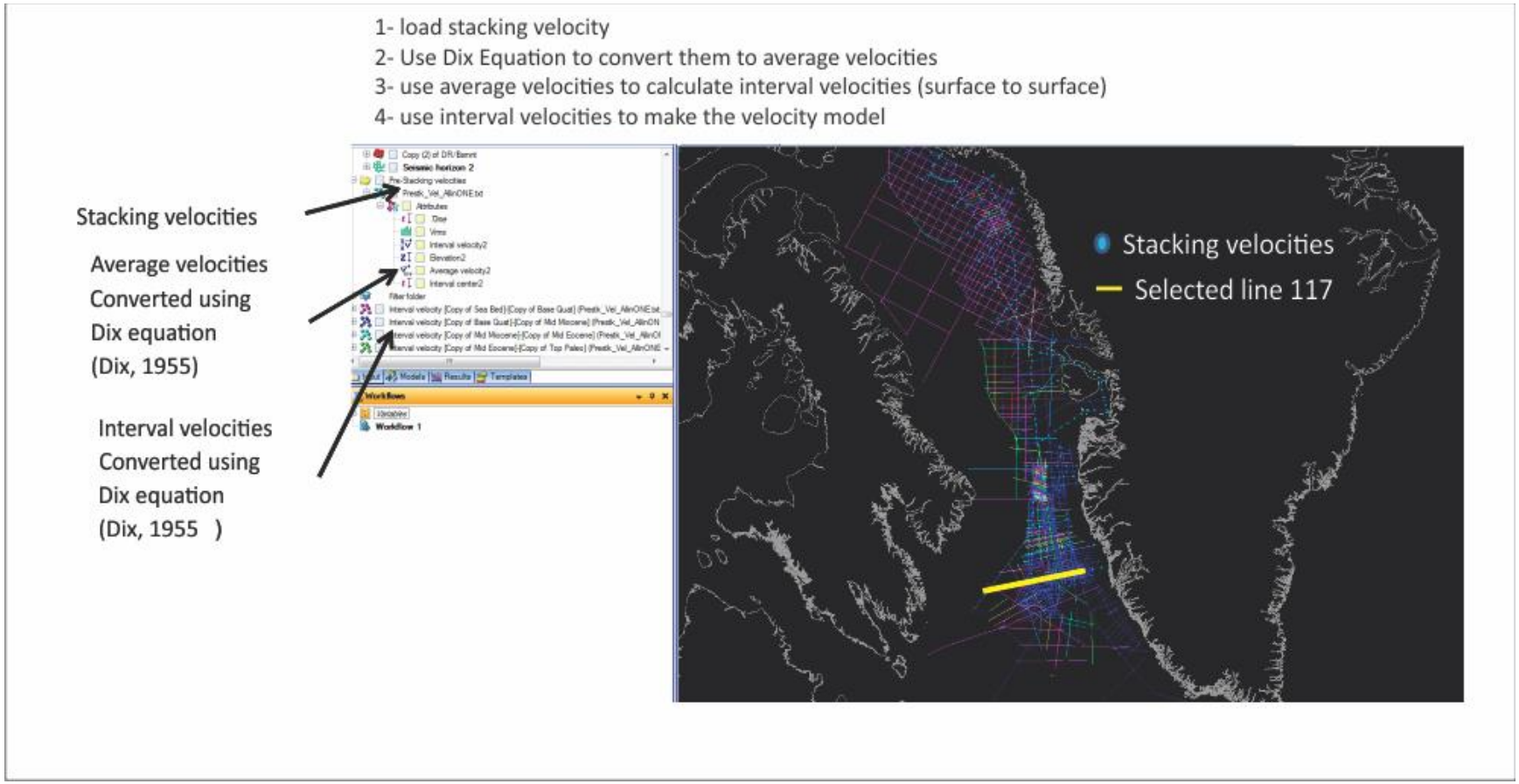

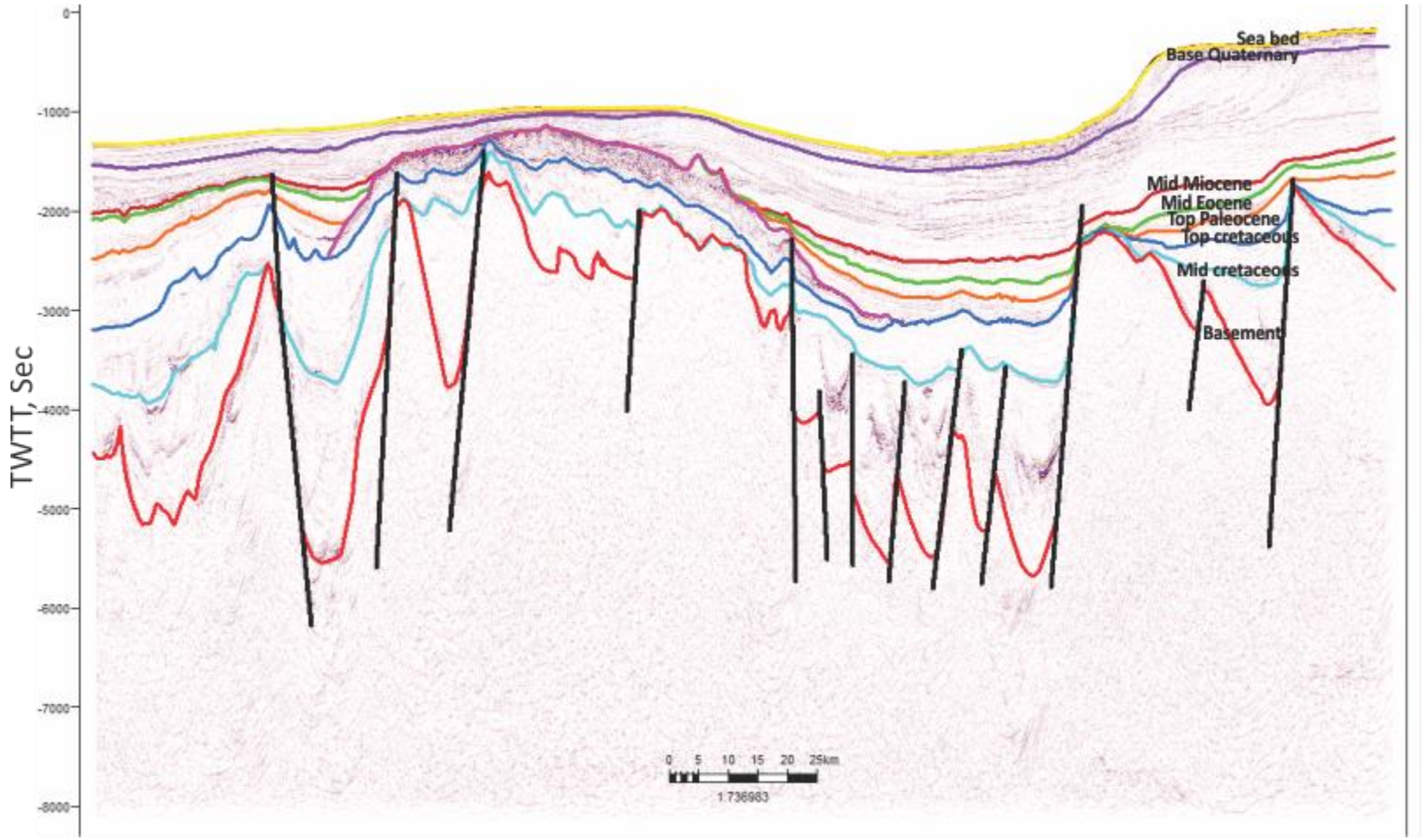

A II-2: Selected line 117 (Time)

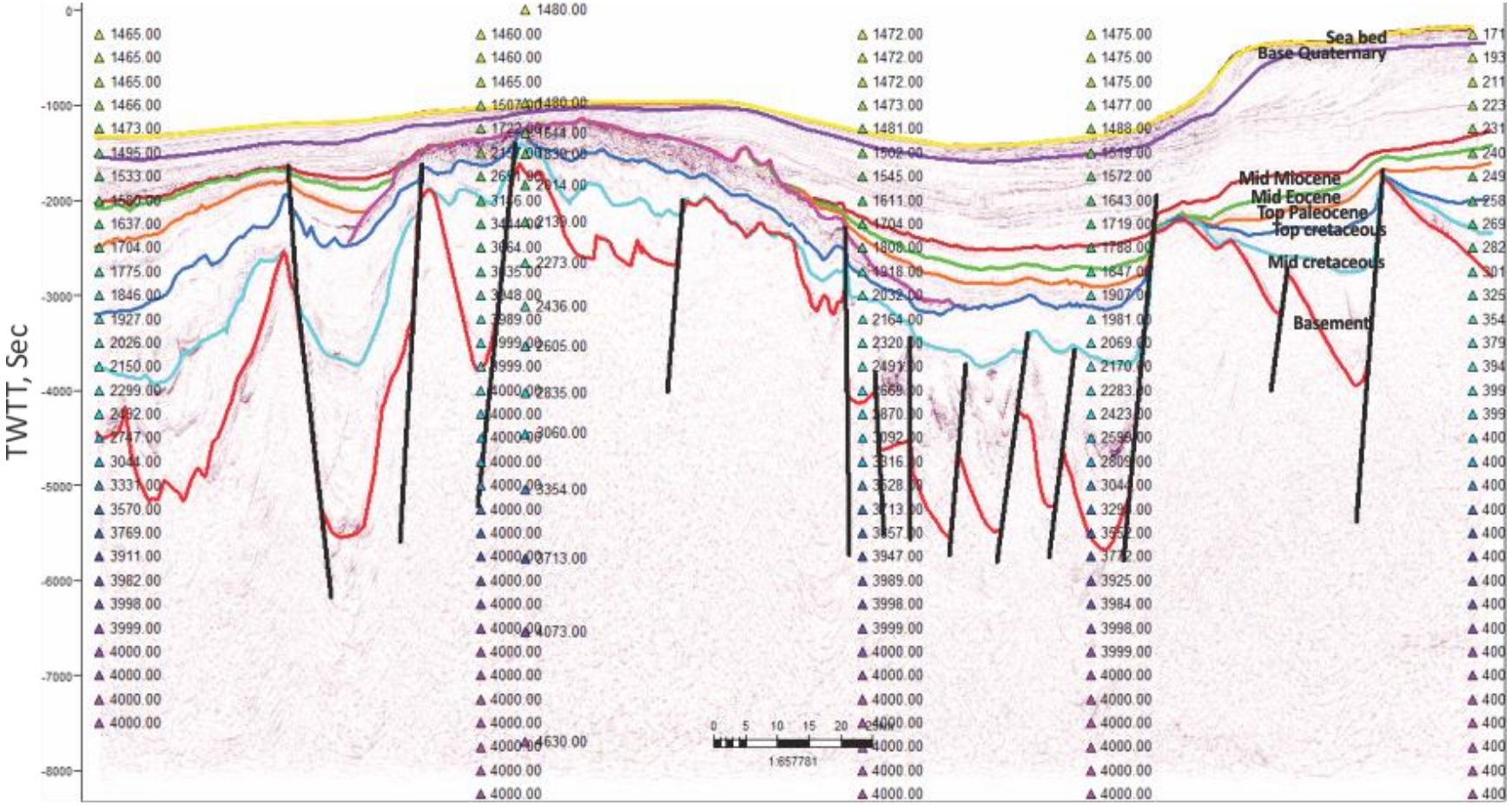

A II-3: Stacking velocities

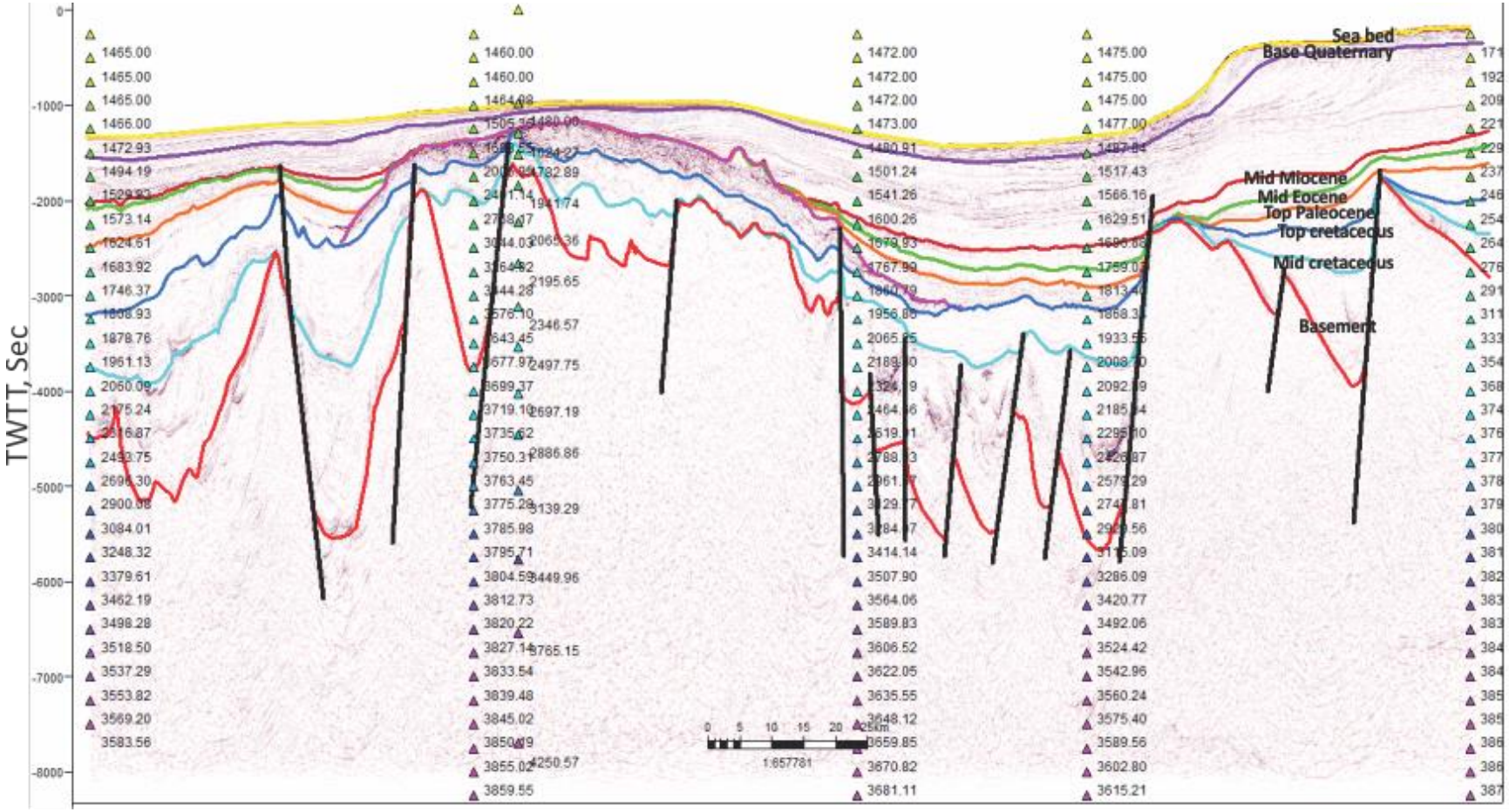

A II-4: Average velocities

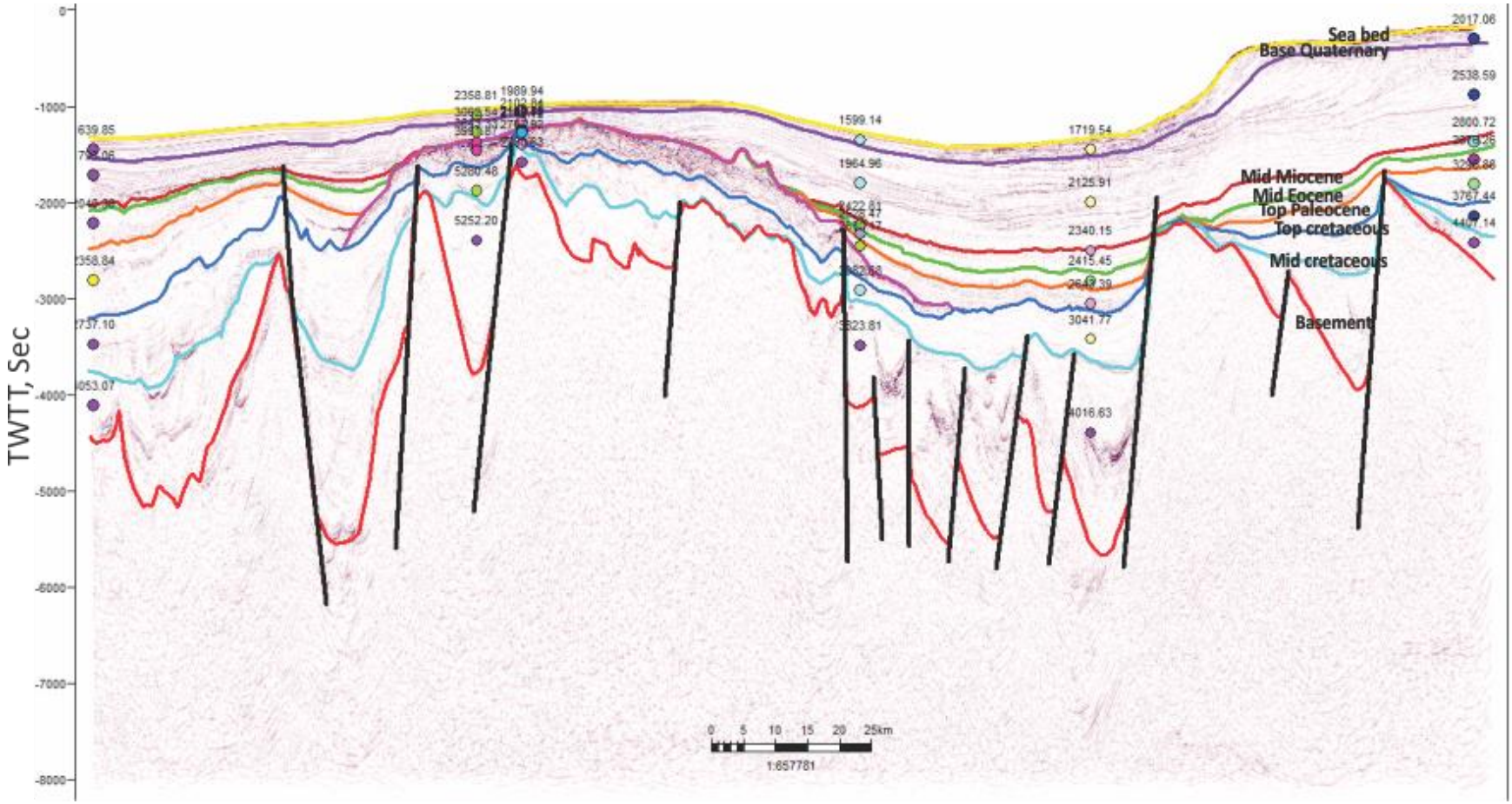
TWTT, Sec
0
-1000
-2000
-3000
-4000
-5000
-6000
-7000
-8000
Sea bed
Base Quaternary
Mid Miocene
Mid Eocene
Top Paleocene
Top cretaceous
Mid cretaceous
Basement
2017.06
2538.59
2800.72
3236.88
3767.44
4497.14
639.85
2358.84
1737.10
4053.07
2358.81
1989.94
5280.48
5252.20
1599.14
1964.96
5523.81
1719.54
2125.91
2340.15
2415.45
3041.77
4016.63
0 5 10 15 20 25km
1:657781

A II-5: Interval velocities

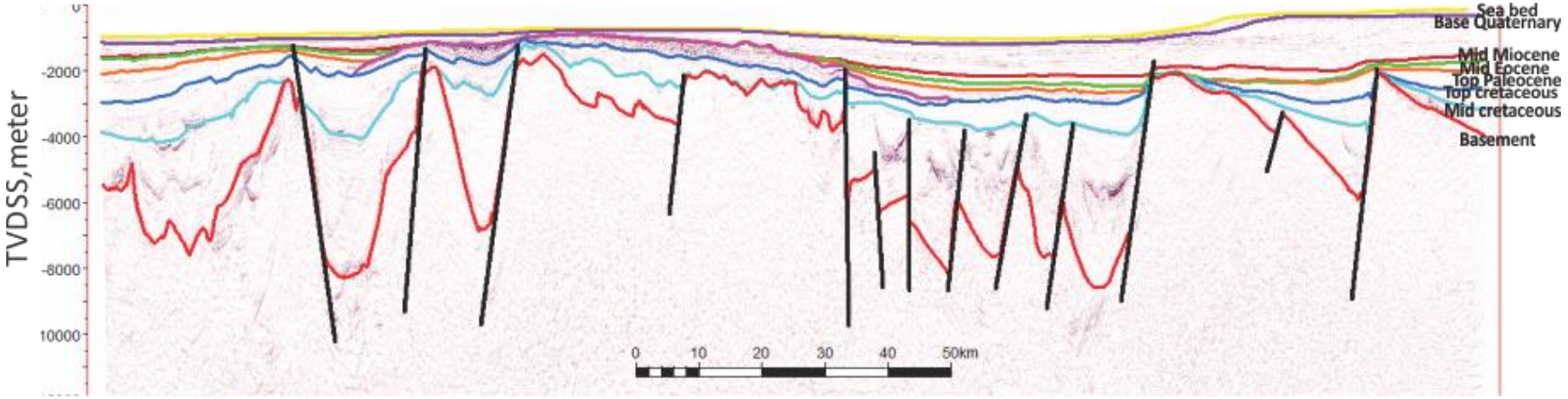

A II-6: Depth-converted Line 117

Appendix III: Parameters for depth-dependent stretching models in Chapter 6

A III-1: Faults distance and heave parameters used in forward modelling (upper crust) for Baffin Bay profile

Distance (km)	Extension (km)	Dip (degree)	P-S width (km)	P-S offset (km)	Dip Direction
130	3	60	100	-70	L
140.5	2	60	100	-70	L
160	3	60	100	-30	R
163	1	60	100	-70	L
172	3	60	100	-30	R
188.5	3	60	100	-70	L
205	3.4	60	100	-30	R
212	0.5	60	100	-30	R
224	2.4	60	100	-70	L
247	1.5	60	100	-30	R
262	11	60	100	-70	L

A III-2:Stratigraphic units, ages and compaction parameters used in reverse post-rift modelling (thermal subsidence) for Baffin Bay profile

Layers	Initial Porosity (%)	Compaction Constant (km^{-1})	Matrix Density ($gm\ cm^{-3}$)	Age (Ma)
Sea bed	0	0	2.6800001	0
Base Quaternary	56	0.44	2.6800001	2
Mid Miocene	56	0.44	2.6800001	14
Mid Eocene	56	0.44	2.6800001	49
Top Paleocene	56	0.44	2.6800001	55
Oceanic crust	56	0.44	2.6800001	60
Basalt	0	0.01	2.6800001	61
Top Cretaceous	56	0.44	2.6800001	65
Mid Cretaceous	56	0.44	2.6800001	99
Acoustic Basement/DR	56	0.44	2.6800001	145

A III-3:Faults distance and heave parameters used in forward modelling (upper crust) for Davis Strait profile

Distance (km)	Extension (km)	Dip (degree)	P-S width (km)	P-S offset (km)	Dip Direction
19	0.4	60	100	-30	R
65	0.2	60	100	-70	L
110	0.4	60	100	-70	L
120	0.5	60	100	-70	L
130	1	60	100	-70	L
150	0.4	60	100	-70	L
154	0.25	60	100	-30	R
156	0.2	60	100	-30	R
160	0.3	60	100	-70	L

A III-4:Stratigraphic units, ages and compaction parameters used in reverse post-rift modelling (thermal subsidence) Davis Strait profile

Layers	Initial Porosity (%)	Compaction Constant (Km^{-1})	Matrix Density ($gm\ cm^{-3}$)	Age (Ma)
Sea bed	0	0	2.6800001	0
Base Quaternary	56	0.44	2.6800001	2
Mid Miocene	56	0.44	2.6800001	14
Mid Eocene	56	0.44	2.6800001	49
Top Paleocene	56	0.44	2.6800001	55
Oceanic crust	56	0.44	2.6800001	60
Basalt	0	0.01	2.6800001	61
Deeper Reflection	56	0.44	2.6800001	145

A III-5:Faults distance and heave parameters used in forward modelling (upper crust) for Labrador Sea profile

Distance (km)	Extension (km)	Dip (degree)	P-S width (km)	P-S offset (km)	Dip Direction
155	2.9	60	100	-70	L
162	2.6	60	100	-70	L
178	2.3	60	100	-70	L
186	1.5	60	100	-70	L
206	1.5	60	100	-70	L
225	2.9	60	100	-70	L
245	1.7	60	100	-70	L
272	0.6	60	100	-70	L

A III-6:Stratigraphic units, ages and compaction parameters used in reverse post-rift modelling (thermal subsidence) for Labrador Sea profile

Layers	Initial Porosity (%)	Compaction Constant (Km^{-1})	Matrix Density (gm cm^{-3})	Age (Ma)
Sea bed	0	0	2.6800001	0
Base Quaternary	56	0.44	2.6800001	2
Mid Miocene	56	0.44	2.6800001	14
Mid Eocene	56	0.44	2.6800001	49
Top Paleocene	56	0.44	2.6800001	55
Oceanic crust	56	0.44	2.6800001	60
Basalt	0	0.01	2.6800001	61
Top Cretaceous	56	0.44	2.6800001	65
Mid Cretaceous	56	0.44	2.6800001	99
Acoustic Basement/DR	56	0.44	2.6800001	145

Appendix IV: Petroleum system of West Greenland: Previous works and parameters for heat flow modelling in Chapter 7

A IV-1: Source rock

The discovery of numerous oil seeps in the onshore Nuussuaq Basin changed the general opinion that the West Greenland basins contained at best only gas-prone source rocks (Bojesen-Koefoed et al. 1999). Five different types of oil have been recognised and other non-marine and marine source rocks of presumed local importance (Bojesen-Koefoed et al. 1999). Marine shales of Cenomanian-Santonian age have not been penetrated in any of the offshore wells; only two of the wells from the 1970s penetrated the Campanian-Maastrichtian shales. Potential petroleum source rocks (See Chapter 7; Figures 7.12 to 7.15) are present in the Upper Cretaceous to Palaeocene mudstone (Rolle, 1985). Mature source rock intervals include the mid-Cretaceous and Lower Paleocene which show no evidence for hydrocarbon in Quileq-1 well (Gregersen and Skaarup, 2007; Christiansen, 2011). The oil seepages in Nuussuaq are found in Tertiary plateau basalts overlying Cretaceous and Tertiary age sediments, some of which are potential marine source rocks (Laier, 2012; Bojesen-Koefoed et al. 1999, 2004, 2007). In contrast to the Nuussuaq region, no potential source rock for hydrocarbons has been reported in South Greenland (Laier, 2012). The hydrocarbons in the Ilimaussaq intrusion were largely ignored in the context of offshore exploration. The Maraat oil is one of the oils that have been discovered seeping to the surface in the Nuussuaq Basin (Bojesen-Koefoed et al. 1999). Pre-Cretaceous source rocks offshore southern West Greenland may also exist, especially within a Lower Paleozoic or Jurassic succession (Chalmers et al., 1993).

Non-marine oil-prone source rocks of Cretaceous age may be present as lacustrine shales or hydrogen-rich coals within the Appat sequence, which is a possible equivalent to the upper member of the Bjarni Formation of the Labrador Shelf and the Kome, Upernivik Naes (Chalmers et al 1993). Onshore West, Atane formations, coal source rock with some hydrogen-rich coals (Total organic content of c. 40% and Hydrogen index of *c.* 250) were discovered recently on the north coast of Disko (Chalmers et al., 1993). Outcrops on Svartenhuk, Neither top nor base of this succession on Svartenhuk is well exposed but the thickness is estimated to be a few hundred metres. The few old unpublished data indicate TOC values between 5% and 10%. This succession is one of the main targets for GGU's shallow (Chalmers et al., 1993).

A IV-2: Reservoirs

From the drilled wells no reservoir rocks were encountered in the deeper parts of the sedimentary sequences (Rolle, 1985). Only Kangamiut-1 showed potential reservoir in the Campanian sandstones underlying thick Paleocene shales with TOC values > 2% (Chalmers et al., 1993). A Santonian sand interval in Quileq well is a probable reservoir; the sandstone has porosity of ~ 23% (See Chapter 7; Figure 7.14). However, there is no evidence for hydrocarbon in the Santonian sandstone (Pegrum, 2001).

A IV-3: Traps

The Melville and Kivioq areas in Baffin Bay are believed to consist of Cretaceous tilted-fault blocks and anticlinal structures forming potential traps

(Whittaker et al, 1997). Gentle folds and hanging wall anticlines as well as tilted-fault blocks are identified as viable structural traps in the other provinces (See Chapter7; Figure 7.7).

A IV-4: Seals

The shallow sandstone sequence may be an appropriate seal (Rolle, 1985) while Santonian reservoirs can be sealed by Cretaceous marine mudstone sediments of Campanian age (See Chapter7; Figures 7.12 to 7.15). The marine mudstone is interbedded with dolomite and siltstone. At the cross-cutting reflection (CCR), no hydrocarbon shows were recorded on the mudlog (Pegrum, 2001).

A summary of the existing hydrocarbon potential of the West Greenland is provided in Table A IV-1 and A IV-2

Table A IV-1: Summary and chronological description of petroleum system of West Greenland margins from previous works

Component	Age	Example	Reference
Source Rock	Cretaceous source rocks	Nuussuaq Basin	Bojesen-Koefoed *et al*. (1999)
	Early–Middle Cretaceous or even Late Jurassic age		Bojesen-Koefoed et al. (1999) Sørensen, (2006)

	Cenomanian to Turonian marine source rocks	Kanguk Formation on Ellesmere Island	Núñez-Betulu, 1993
	Upper Cretaceous	This oil may be related to the Greenland oil seeps	(MacLean et al., 2011) Gregersen et al., 2013.
	Palaeozoic		Sørensen, 2006 Gregersen et al., 2013
Reservoir rocks	Cretaceous and Palaeogene Successions	Baffin Bay, Melville Bay Graben and Kivioq Basins	Sørensen, (2006)
	Lower Cretaceous	Appat and Kitsissut sequences in lady Franklin and all west Greenland	Gregersen et al., 2013.
	Upper Cretaceous Source rock	Fylla complex Labrador Sea Baffin Bay	Christiansen et al. 2001 Christiansen et al. 1996
Seals:	Cretaceous or Palaeozoic source rocks	Appat Sequence are sealed for Kangeq mudstone	Sørensen, (2006)
	Lower–mid-Cretaceous or Paleocene		Sørensen, (2006)
Traps	Precambrian fault blocks Lower Cretaceous lithologies	Types rift blocks, compressional ridges and drapes	Gregersen et al., 2013, Sørensen, (2006)

Table A IV-2: Historical Hydrocarbon Prospectivity along the West Greenland margin

Location & Reference	**Well**	**Modelling**	**Source, vitrinite reflectance values (Ro)**	**Age**	**Geothermal gradient**
Labrador Sea (Issler and Beaumont, 1987)		1D			Predicted heat flow ranges from 40 to 50mW/m^2 for the Labrador Shelf and 50 to 60mW/m^2 for the northern Labrador Sea-Davis Strait region

Disko West (Kwiecinska, and Petersen, 2004)	GRO-3		Random vitrinite reflectance range: app. 0.35–0.5%Ro to app. 1.2%Ro).	Cretaceous	
NUUK West	Kangâmiut -1 and Nukik-1 wells		Offshore West Greenland. Vitrinite reflectance is 0.5%.		
Disko West (Japsen et al., 2005)	Gro-3			Neogene	Gro-3 and Gane-1 boreholes were buried 1500–2000 m deeper than at the present day, and the palaeo geothermal gradient was 40–48 °C km^{-1}.
Canyon South Helca high (Dalhoff - 2006)			Hydrogen Index ~400, Total Organic Carbon = 1.3–4%	Upper Ordovician mudstone	
Svartenhuk			5% and 10%.	Marine shales of Cenomanian-Santonian age	
NUUK West (Rolle 1985 and Chalmers et al, 1993)	Hellefisk-1		(0.5-2.0%)	Late Paleo-early Eoc	24.1
	Ikermiut		1.5 to 3% organic carbon	Early Palaeocene	28.9
	Kangamiut		1.5 to 3% organic carbon	Early Palaeocene	28.5
	Nuuk 1		0.5 and 1.5%	Early Eocene	21.1
	Nuuk 2		0.5 and 1.5%	Early Eocene	19.3
Fylla Complex (Christiansen et al, 2001)	Quileq		3-7%	Lower Campanian marine mudstones	

Table A IV-3: Paleobathymetry data along the West Greenland margins from previous research works.

	E CRET.	L CRET.	E PALEOCENE	E EOCENE	E OLIGOCENE	PRESENT	References
KANGAMIUT-1	0	200	600	700	450	200	Gradstein and Srivastava, (1980), Rolle (1985)
IKERMIUT-1	0	400	450	200	400	330	Rasmussen and Sheldon, 2003, Rolle (1985)
HELLEFISK-1	0	120	100	80	40	170	Dalhoff et al., (2003), Rolle (1985)
QULLEQ-1	0	150	0	20	100	1140	Christiansen et al., (2001)
Labrador Sea	0	800	2000	2300	2000	2197.296	Gradstein and Srivastava, (1980), Srivastava and Arthur, (1989)
Davis Strait	0	500	100	600	1200	1018.2	Head et al., (1989), Srivastava and Arthur, (1989)
Baffin Bay	0	800	1000	1300	1800	2018.2	Head et al., (1989), Srivastava and Arthur, (1989)

A IV-5: Erosion applied to both 1D and 2D modelling

The erosion values were calculated by restoring the sections to syn-depositional geometry and reconstructing the missing structure through a flattening technique (See Chapter7; Figure 7.3). The steps for estimating erosion are summarized as follows:

1- Present day layers geometry is digitized
2- Age assigned for these layers
3- Add Unconformities
4- Recreate paleo-geometry using flattening technique (select horizon below the unconformity)
5- Edit, flatten the unconformity then visualize the eroded thickness
6- Restoration and simulation preview

The erosional events along the west Greenland margins from published data were interpreted as major unconformities surfaces on the seismic profiles (See an example in Chapter7; Figure 7.3). These unconformities include:

1. An erosional event between Cretaceous - Paleocene (Nøhr-Hansen *et al*. 2003).
2. Paleocene–Eocene Unconformity (Christiansen et al. 2001)
3. Uppermost Eocene to uppermost Miocene erosional event (Christiansen et al., 2001).

A IV-6: 1D modelling

The main purpose of 1D modelling is calibration of simulated heat flow against the observed vitrinite reflectance (Vr), bottom-hole temperature and geothermal gradient (Table A IV-4 and A IV-5; Figures 1 to 5).

1D Modelling Calibration

The 1D modelling was calibrated with available well data, calibration was done for physical properties such as vitrinite reflectance, temperature and average geothermal gradient for Ikermiut-1 Kangamiut-1 and Hellefisk-1 wells (Figures 4 and 5). Qulleq-1 well was calibrated with only Vitrinite reflectance (Figure 5).

Table A IV-4: Information on the four wells used for the Hydrocarbon modeling

Well Name	Start elevation (JB or DF) (m)	Total Drill Depth (m)	True Vertical depth (m)	PetroMod start elevation (m)	PetroMod Total Drill Depth (m)	PetroMod True Vertical depth (m)
HELLEFISK-1	12	3201	3201	-12	3189	3189
IKERMIUT-1	12	3619	3619	-12	3607	3607
KANGAMIUT-1	12	3874	3874	-12	3862	3862
QULLEQ-1	36	2973	2973	-36	2937	2937

Table A IV-5: Creating heat flow trend from (depth dependent stretching beta)

Rift Phases	Syn-Rift From (Ma)	150	To	100	Post-Rift From (Ma)	100	To	0
Stretching Factors	Beta-Crust	1.01	Beta-Mantle	4				
Pre-Rift Thicknesses	Crust (M)	30000	Mantle	95000				

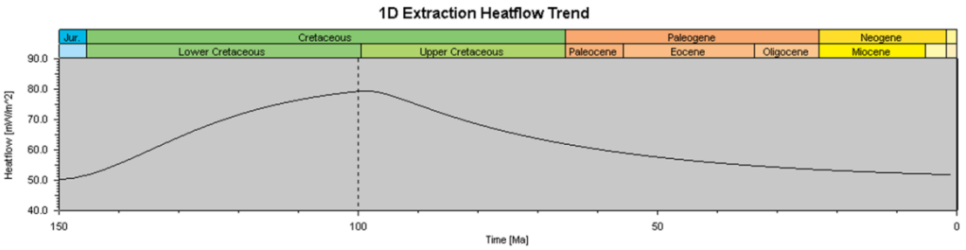

Figure (A IV-1): Heat flow trend was assigned using McKenzie 1978 model to fit observed Vr reflectance from the wells

Table A IV-6: Input parameters for the ID modeling

Layer	Top (m)	Base (m)	Thick. (m)	Eroded (m)	Depo. from (Ma)	Depo. to (Ma)	Eroded From (Ma)	Eroded to (Ma)	Lithology	PSE
Quat.	1143	1256	113		3.00	0.00			Shale	O. Rock
Plio	1256	1727	471		5.00	3.00			Shale	O. Rock
M-U Mio	1727	1860	133		15.00	5.00			Shale	O. Rock
L Eoc.	1860	1878	18	105	56.00	45.00	45.00	15.00	Sand silty	O. Rock
Palaeo	1878	1888	9	94	61.00	60.00	60.00	56.00	Silty sand	O. Rock
U. Cret.	1888	2193	305	97	76.00	75.00	75.00	61.00	Shale	O. Rock
U Cret SR	2193	2336	143		85.96	76.00			Shale (3% TOC)	S. Rock
U Cret	2336	3100	764		100.00	85.96			Shale	Sl Rock
Mid Cret.	3100	3312	212		110.00	100.00			Sandstone	R. Rock
Mid Cret SR	3312	3369	57		115.00	110.00			Shale (8% TOC)	S. Rock
Lower Cret	3369	4600	1231		145.00	115.00			Sandstone	R. Rock
Basement	4600	5600	1000		150.00	145.00			Basement	S. Rock
						150.00				

N.B: O. Rock = Overburden Rock, S. Rock = Source Rock, R. Rock = Reservoir Rock, Sl Rock = Seal Rock. TOC data are from Burnham, 1989.

Three main erosion events are highlighted in yellow

Figure (A IV-2): Palaeo-water depth SWIT and Heat flow Qulleq-1 well, West Greenland margins

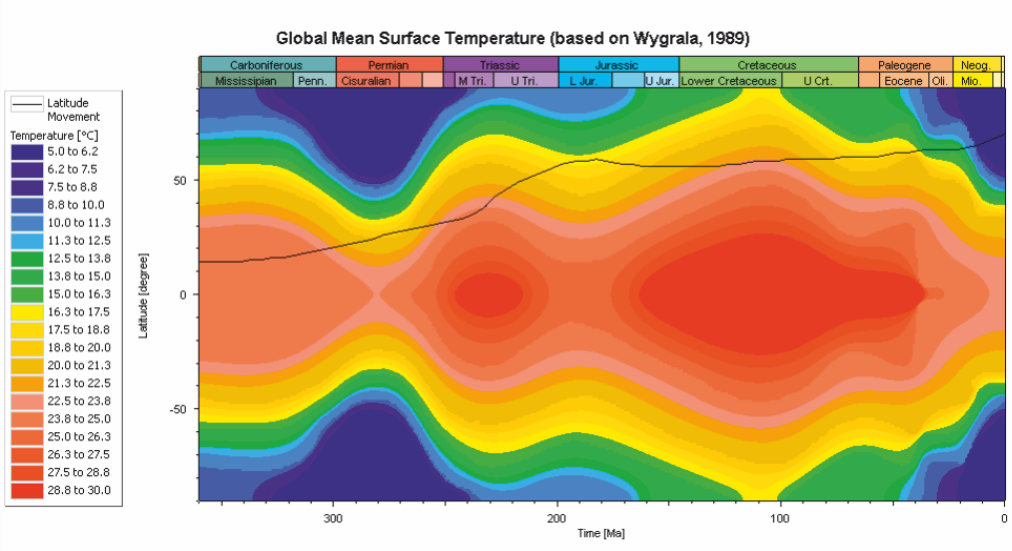

Figure (A IV-3): Sediment Water Interface Temperature (SWIT) values in this study are based on the global mean surface temperatures of Wygrala, 1989.

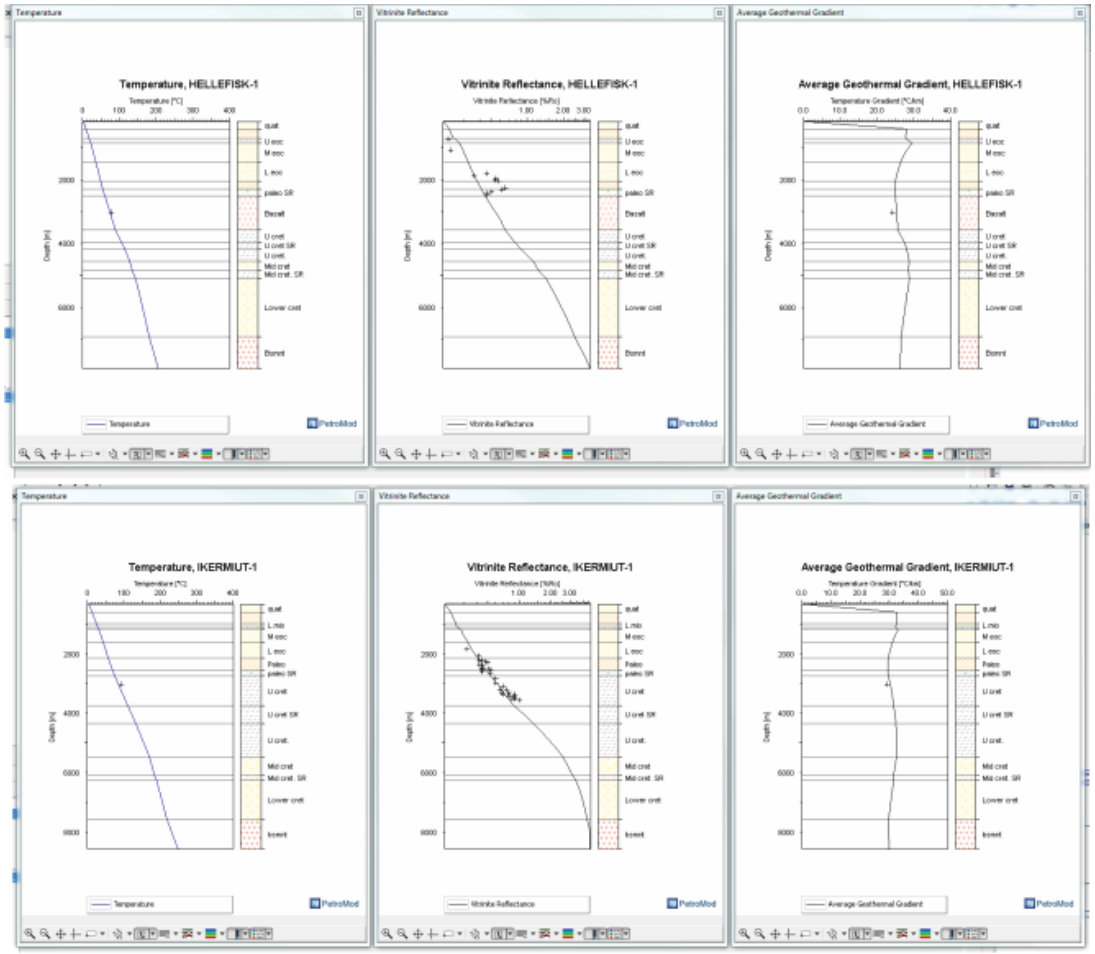

Figure (A IV-4): 1D modelling of Temperature, Vitrinite reflectance and average geothermal gradient for the Hellefisk-1 and Ikermiut-1

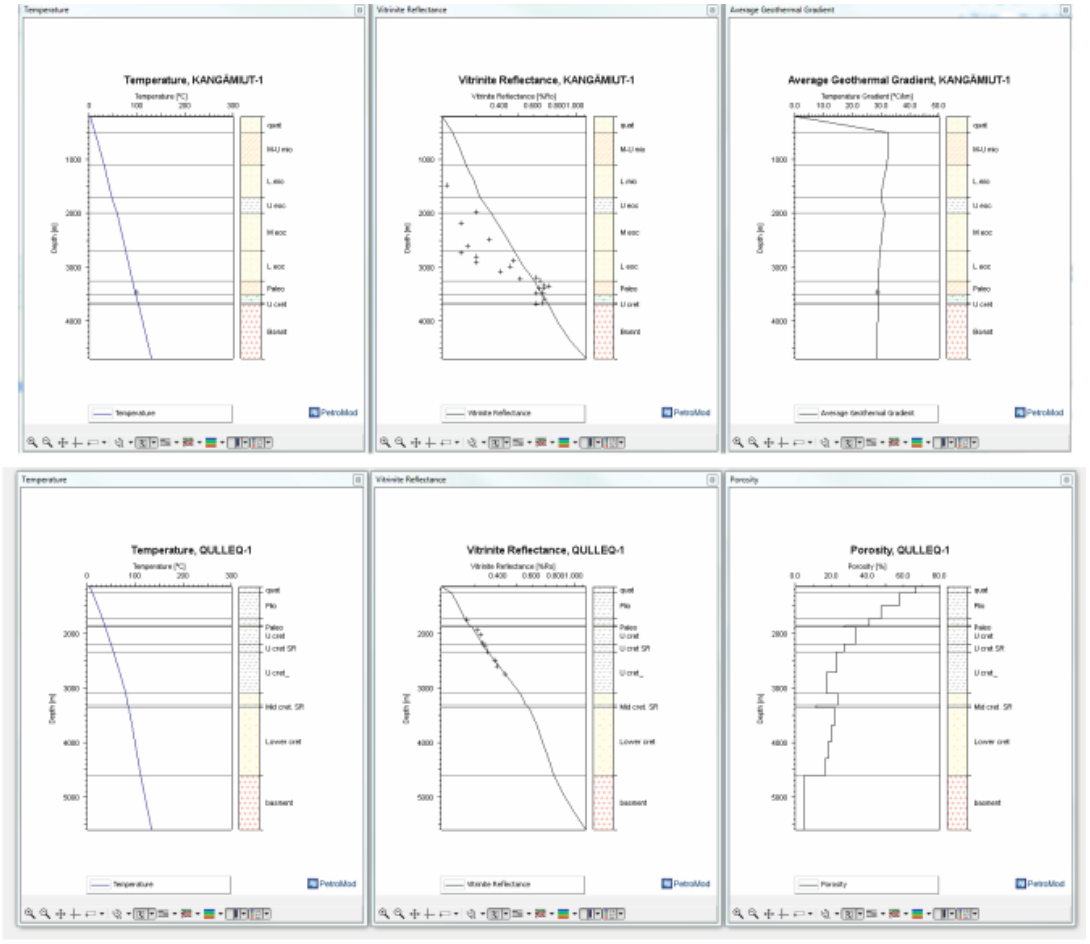

Figure (A IV-5): 1D modelling of Temperature, Vitrinite reflectance and average geothermal gradient for the Kangamiut-1 and Qulleq-1

A IV-7: 2D modelling

In Figure 6 the location of the four seismic profiles used for each of the provinces is shown. The 2D hydrocarbon modelling was done along strike of the wells (A IV-7 Figure 7) and diplines (See Chapter5; Figures 5.2; 5.3 and 5.4).

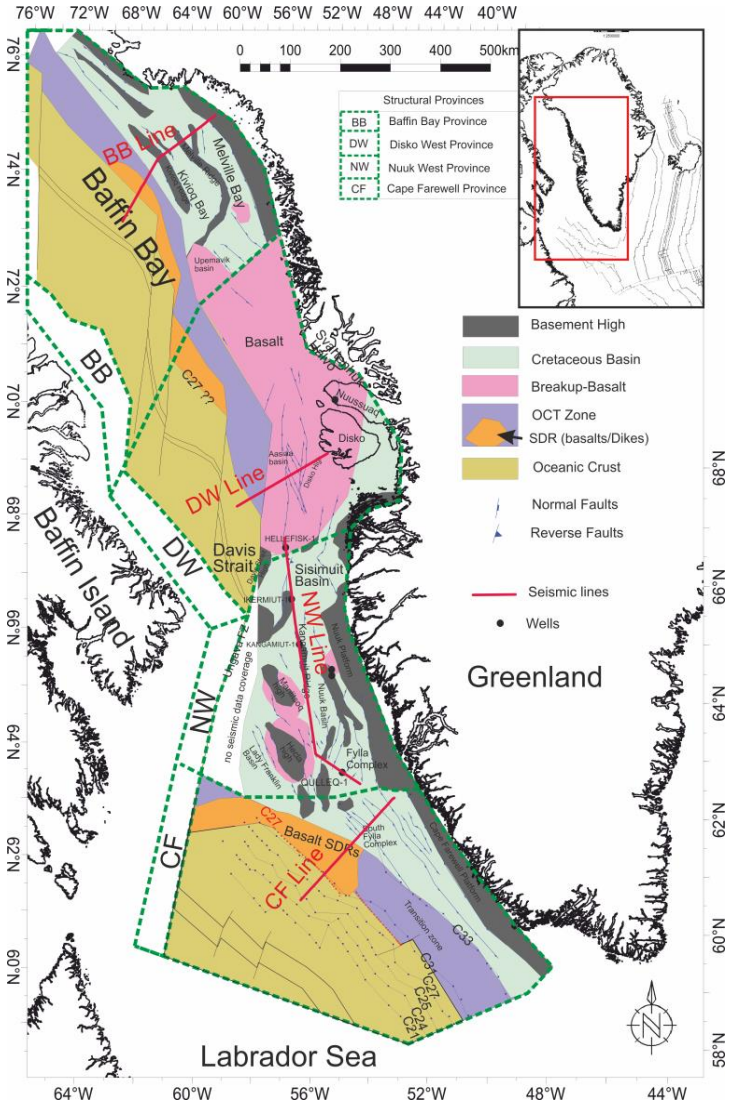

Figure (A IV-6): Base map showing location of selected lines for the 2D hydrocarbon modelling superimposed upon a tectonic framework map (chapter 4).

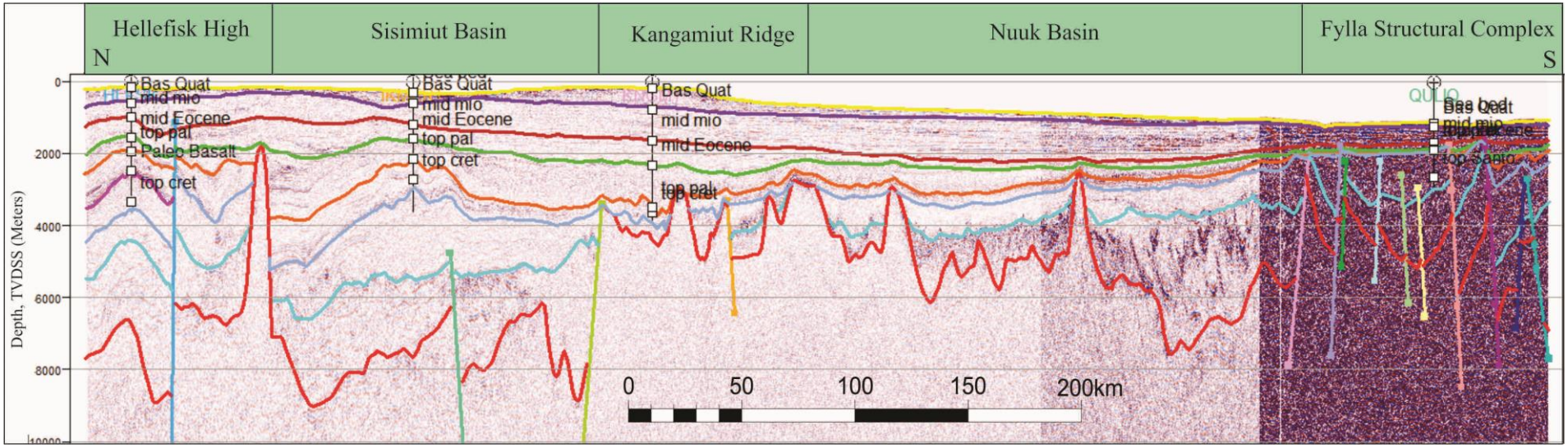

Figure (A IV-7): Depth-converted seismic line along the strike of the wells used in this study. The location of the seismic profile is shown in Figure (A IV-6).

Workflow for 2D modelling

Annotated cross sections were imported into Petrobuilder

1. Horizons and faults are digitized as pre grid (Table 7.7)
2. Boundary condition of Erosion, PWD and SWIFT (Discussed before in this chapter)
3. Age and Erosion chart (Table 7.7)
4. Facies types were assigned (Table 7.8)
5. Faults were assigned (Table 7.9)
6. Beta factors from depth-dependent stretching modelling were applied to define heat flow trend (See table 7.6). After that, the two phases of rifting were defined and model was inverted to calculate crustal heat flow maps (Table 7.10)
7. Heat flow calculation was done before simulation was run. This is necessary to ensure the crust and mantle beta from DDS were applied (A IV-7 Figure 8). All BB, DS and LS 2D lines were backstripped and Beta calculated to restore top Paleocene (post breakup). The Beta factors from whole lithosphere stretching were used as input. In Chapter 7; Figures 7.4, 7.5 and 7.6 shows that top Paleocene heat flow matches with DDS beta in Chapter six (Figures 6.5, 6.6, and 6.7).
8. Simulation
9. HC potential
10. Reservoir accumulation

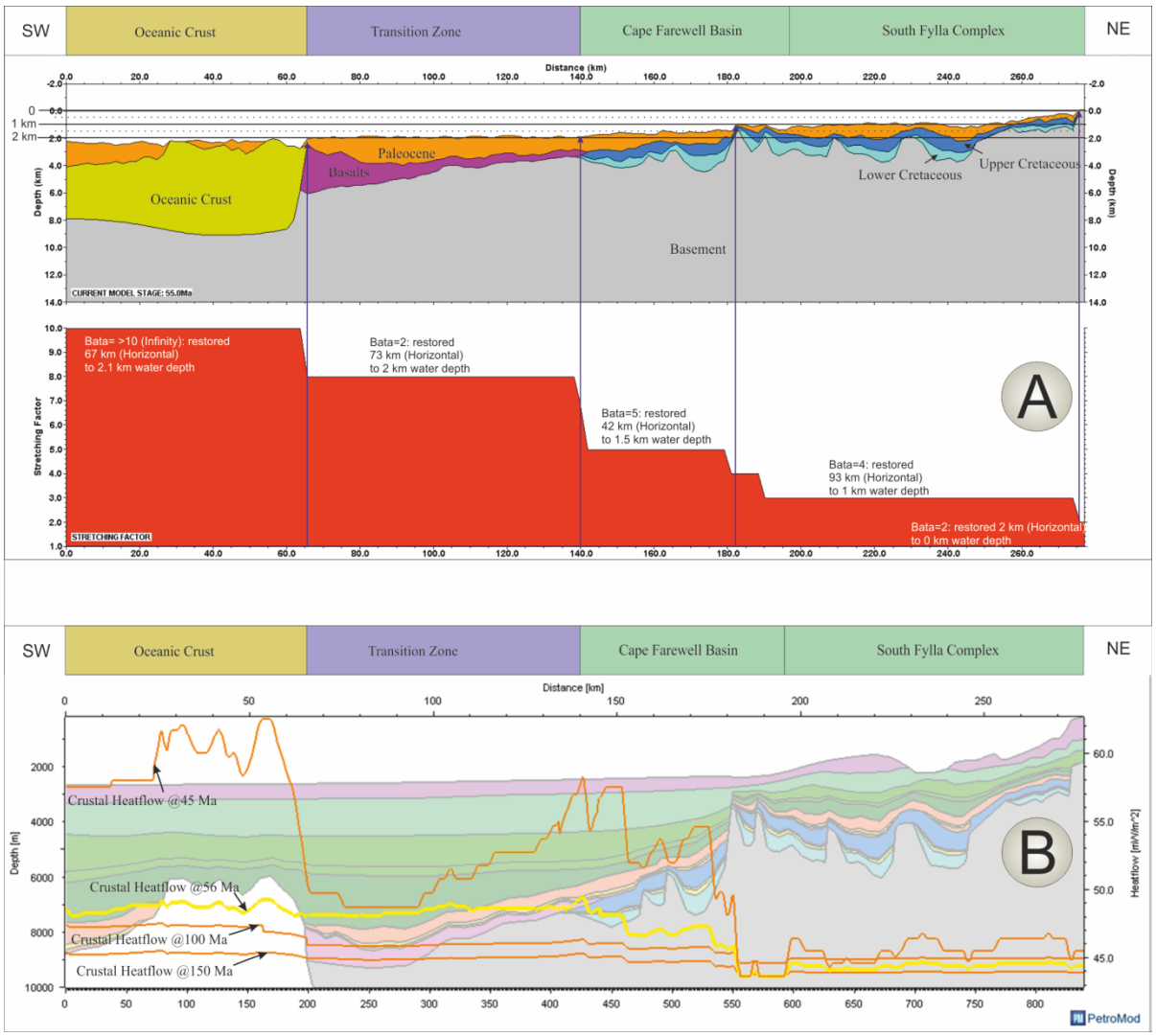

Figure (A IV-8): Stretching factors derived from backstripping (A) provides heat flow (B) Showing the Top Paleocene estimated heat flow is higher than Cretaceous and it changes laterally from northeast to southwest. This is in accordance with the DDS variation along the seismic line

Table A IV-7: Horizons are digitized as pre grid, age assigned, erosion and facies maps were assigned

Age (Ma)	Horizon	Pre-grid Horizon	Gridded Horizon	Erosion Map	Layer	Event Type	Facies Map	Maximum Time Step (Ma)
0	Seabed	Seabed	Seabed					
					Base Quat.-Seabed	Deposition	Base Quat.-Seabed_Facies_Map	10
3	Base Quat	Base Quat	Base Quat					
					Mid Mio-Base Quat.	Deposition	Mid Mio-Base Quat._Facies_Map	10
14	Mid Mio	Mid Mio	Mid Mio					
					Mid Eoc-Mid Mio	Deposition	Mid Eoc-Mid Mio._Facies_Map	10
39.79	Mid Mio Seal	Mid Mio Seal	Mid Mio Seal					
					Mid Mio Seal	Deposition	Mid Mio Seal._Facies_Map	10
40	Mid Eoc-Mid Mio Erosion	Mid Eoc-Mid Mio Erosion	Mid Eoc-Mid Mio Erosion	Mid Eoc-Mid Mio Erosion map				
					Mid Eoc-Mid Mio Erosion	Erosion		10
45	Mid Eoc	Mid Eoc	Mid Eoc					
					Mid Eoc	Deposition	Mid Eoc._Facies_Map	10
46	Top Paleo-Mid Eoc Erosion	Top Paleo-Mid Eoc Erosion	Top Paleo-Mid Eoc Erosion	Top Paleo-Mid Eoc Erosion map				
					Top Paleo-Mid Eoc Erosion	Erosion		10
56	Top Paleo	Top Paleo	Top Paleo					
					Top Paleo	Deposition	Top Paleo_Facies_Map	10
59	Top Paleo Source rock	Top Paleo Source rock	Top Paleo Source rock					
					Top Paleo Source rock	Deposition	Top Paleo Source rock_Facies_Map	10
60	lower Paleo	lower Paleo	lower Paleo					
					lower Paleo	Deposition	lower Paleo_Facies_Map	10
61	Basalt	Basalt	Basalt					
					Basalt	Deposition	Basalt_Facies_Map	10
62	Top Cret-lower Paleo Erosion	Top Cret-lower Paleo Erosion	Top Cret-lower Paleo Erosion	Top Cret-lower Paleo Erosion map				
					Top Cret-lower Paleo Erosion	Erosion		10
66	Top Cret	Top Cret	Top Cret					
					Top Cret	Deposition	Top Cret_Facies_Map	10
100	Mid Cret	Mid Cret	Mid Cret					
					Mid Cret	Deposition	Mid Cret_Facies_Map	10
102	Mid Cret Source rock	Mid Cret Source rock	Mid Cret Source rock					
					Mid Cret Source rock	Deposition	Mid Cret Source rock_Facies_Map	10
110	Lower Cret	Lower Cret	Lower Cret					
					Lower Cret	Deposition	Lower Cret_Facies_Map	10
150	Basement	Basement	Basement					
					Basement	Deposition	Basement_Facies_Map	10

Table A IV-8: Facies types were assigned, TOC, Kinetics and Petroleum system elements

Facies Name	Lithology Value	TOC Mode	TOC Value (%)	TOC	Kinetics	HI Mode	HI Value (mgHC/gTOC)	HI Map	Petroleum System Elements
Base Quat.-Seabed_Facies	SANDsilty								Underburden Rock
Mid Mio-Base Quat._Facies	SILTsandy								Underburden Rock
Mid Eoc-Mid Mio._Facies	SANDsilty								Underburden Rock
Mid Mio Seal._Facies	Shale (Typical)								Seal Rock
Mid Eoc._Facies	SANDsilty								Reservoir Rock
Top Paleo_Facies	SILTsandy								Underburden Rock
Top Paleo Source rock_Facies	Siltstone (Organic rich, 2-3% TOC)	Value	3		Burnham (1989)_TIII				Source Rock
lower Paleo_Facies	SILTsandy								Underburden Rock
Basalt_Facies	Basalt (normal)								None
Top Cret_Facies	Shale (Typical)								Seal Rock
Mid Cret_Facies	Shale (Typical)								Underburden Rock
Mid Cret Source rock_Facies	Shale (Organic rich, 6 % TOC)	Value	6		Burnham (1989)_TIII				Source Rock
Lower Cret_Facies	sandstone (Typical)								Reservoir Rock
Basement_Facies	Basement								Underburden Rock
Crust_Facies	Upper Crust (Continental, Granite)								None
Mantle_Facies	Upper Mantle (Peridotite)								None

Table A IV-9: Fault types and age were assigned

Fault Name	Period	Age from (Ma)	Age to (Ma)	Type
Fault_1	1	150	15	Closed
Fault_2	1	150	15	Closed
Fault_3	1	150	61	Closed
Fault_4	1	150	61	Closed
Fault_5	1	150	61	Closed
Fault_6	1	150	15	Closed
Fault_7	1	150	15	Closed
Fault_8	1	150	61	Closed
Fault_9	1	150	61	Closed
Fault_10	1	150	15	Closed
Fault_11	1	150	45	Closed
Fault_12	1	150	45	Closed

Table A IV-10: Crustal heat flow trend using McKenzie, 1978 was inverted for the two phases of rifting to calculate crustal heat flow maps

Syn-Rift From Mode	Syn-Rift From Value (Ma)	Syn-Rift From Map	Syn-Rift From Mode	Syn-Rift From Value (Ma)	Syn-Rift From Map	Post-Rift From Mode	Post-Rift From Value (Ma)	Post-Rift From Map	Post-Rift From Mode	Post-Rift From Value (Ma)	Post-Rift From Map
value	150		value	100		value	100		value	65	
value	65		value	45		value	45		value	0	